THE PALAEOMAGNETISM OF SOME SOUTH AUSTRALIAN AND VICTORIAN ROCKS.

by

W. G. Mumme.

- - - -

A THESIS
PRESENTED FOR THE DEGREE
OF DOCTOR OF PHILOSOPHY
IN THE
UNIVERSITY OF ADELAIDE
1962.

STATEMENT

This thesis contains no material which has been accepted for the award of any other degree or diploma in any University, and to the best of the candidate's knowledge and belief, the thesis contains no material previously published or written by another person except where due reference is made in the text of the thesis.

Signed ..

C O N T E N T S

		Page No.
	Acknowledgments	1
	Summary	2
1.	Introduction	3
2.	Apparatus	7
2.1	The measurement of the magnetic properties of rocks by means of the astatic magnetometer	7
2.1.1	Introduction	
2.1.2	Theory of design	
2.1.3	Construction of magnetometer	
2.1.4	Adjustment and calibration	
2.1.4.1	Adjustment of the coil system	
2.1.4.2	Astaticising the magnet system	
2.1.4.3	Centering the magnet system	
2.1.4.4	Centering the specimen holder	
2.1.4.5	Sensitivity	
2.1.5	The method of collecting samples and preparing specimens.	
2.1.6	Measurement of the direction of magnetization of rock specimens.	
2.1.7	Calculation of total moment of magnetization	
2.1.8	Measurement of susceptibility.	
2.2	Description of thermal demagnetization apparatus.	36
2.2.1	Introduction	
2.2.2	Apparatus	
2.2.3	Measurement of temperature	
2.2.4	Standard thermal demagnetization curves	

		Page No.
2.3	Description of a.c. magnetic field demagnetization apparatus ..	50
2.3.1	Introduction	
2.3.2	Description of apparatus	
2.3.2.1	Demagnetization coil	
2.3.2.2	Helmholtz coil system	
2.3.2.3	Spinning mechanism	
3.	Estimation of the Ancient Pole position	61
3.1	Calculation of mean direction of magnetization of a rock formation	61
3.2	Calculation of pole position ..	66
4.	Palaeomagnetism of Precambrian rocks from South Australia	68
4.1	Introduction	68
4.2	Description of apparatus	69
4.2.1	Introduction	
4.2.2	Measurement of the direction of magnetization	
4.3	Collection of samples	71
4.4	Discussion	78
5.	The palaeomagnetism of the Older Volcanic basalts of Victoria	80
5.1	Introduction	80
5.2	Geology of the Older Volcanic Basalts	80
5.3	Field work	83
5.4	Direction of magnetization after initial measurement ..	85
5.5	Remeasurement of direction of magnetization	87

		Page No.
5.6	Remarks on stability of magnetization	88
5.7	The a.c. magnetic field cleaning of the Older Volcanics	94
5.7.1	Introduction	
5.7.2	Mean direction of magnetization after cleaning	
5.7.3	Pole position after cleaning.	
6.	The origin of the magnetism of the Older Volcanic basalts	99
6.1	Introduction	99
6.2	Thermal demagnetization of rock specimens	99
6.2.1	Introduction	
6.2.2	Continuous thermal demagnetization in zero field.	
6.2.3	Discussion of continuous thermal demagnetization in zero field.	
6.2.4	Discontinuous thermal demagnetization in zero field.	
6.2.5	Discussion of discontinuous demagnetization in zero field.	
6.2.6	Discussion of results.	
6.3	X-ray investigation of magnetic minerals	125
6.3.1	Introduction	
6.3.2	Results of investigation	
6.4	Conclusions	128
7.	A.c. magnetic field experiments and thermal demagnetization experiments on specimens from Drouin-South	129
7.1	The investigation of the mixed polarity of magnetization at Drouin-South ..	129

Page No.

7.1.1	Introduction	
7.1.2	Field Work	
7.1.3	Results of measurements of direction of magnetization.	
7.1.4	Geology of the quarry at Drouin-South	
7.1.5	A.c. cleaning experiments	
7.1.5.1.	Introduction	
7.1.5.2.	A description of the experiments	
7.1.5.3.	Results and discussion.	
7.1.6	Thermal demagnetization experiments on specimens from Drouin-South.	
7.1.7	Petrology and mineragraphy of specimens from Drouin-South.	
7.1.8	Discussion of the reversed magnetization observed in the Older Volcanic basalts.	
8.	An investigation of the scatter of directions of magnetization of specimens from a single lava flow	172
8.1	Introduction	172
8.2	Field Work	172
8.3	The results of the measurement of the direction of magnetization from single flows at Merri Creek, and Abberfeldie Quarries	173
8.4	The direction of magnetization after a.c. magnetic field cleaning on specimens from Abberfeldie Quarry	176
8.5	Thermal demagnetization experiments on specimens from Merri Creek Quarry	181
9.	Experiments on the stability of magnetization in specimens, both natural and artificial, containing titano-magnetite	182

		Page No.
9.1	Introduction	182
9.2	Experiments on stability of magnetization	184
9.2.1	Experiment 1. An experiment showing the effect of minimum intensity of magnetization and the variation of directions of magnetization after magnetic field cleaning in basalt specimens containing both high and low Curie point titanomagnetites.	
9.2.2	Experiment 2. An experiment on the stability of T.R.M. in low and high Curie point titanomagnetites.	
9.2.3	Experiment 3. The effect of sustained heating on the stability of magnetization of basalt specimens.	
9.2.4	Experiment 4. Experiment on the stability of laboratory synthesized titanomagnetites.	
9.3	Conclusions	213
APPENDIX I	The determination of the correction factor to be applied to the direction of magnetization as measured in 2.1.6	216
	1. Introduction. 2. Evaluation of the correction factor 3. The correction factor 4. Experimental verification.	
APPENDIX II	The method of conversion of measured directions of magnetization.	226
	1. Introduction 2. Conversion formulae 3. Graphical methods.	

Page No.

APPENDIX III — Table giving the direction of magnetization of Older Volcanic basalts — 229

1. Introduction
2. Table of results
3. Calculation of mean direction of magnetization.

APPENDIX IV — Tables giving the results of the thermal demagnetization experiments — 247

APPENDIX V — Tables giving the directions of magnetization of Older Volcanic basalt specimens after a.c. cleaning. — 257

1. Results
2. Calculation of mean direction of magnetization.

APPENDIX VI — Tables showing directions of magnetization of the Precambrian rocks from South Australia. — 347

REFERENCES — 350

- - -

ACKNOWLEDGEMENT

I would like to take this opportunity to thank Dr. D. J. Sutton and Mr. E. Irving for helpful discussions during this investigation.

This work was started while the writer was in receipt of a C.S.I.R.O. studentship, and was completed during tenure of a G.M.H. Post-Graduate Research Fellowship.

- - - -

CONVENTION APPLICABLE TO STEREOGRAPHIC PROJECTIONS

Directions of magnetization are plotted on an equal angle stereographic projection. North seeking directions plotted on the upper hemisphere are indicated by open circles (normal) while those plotted on the lower hemisphere are indicated by dots (reversed).

In figures 21-25 however all the directions plotted are relative to the disc only and have not been corrected to take into account the orientation of the specimens from which they were removed. In these figures both open circles and full dots represent north seeking poles plotted on the upper hemisphere.

SUMMARY

A preliminary investigation of the palaeomagnetism of Proterozoic sedimentary rocks, and a reinvestigation of the palaeomagnetism of Cainozoic basalts is described. The investigation of the Proterozoic rocks produced baffling results and without measuring techniques available, little further work could be carried out on these rocks. The reinvestigation of the Older Cainozoic basalts of Victoria produced many interesting results. Although a mean direction of magnetization close to that obtained by Green and Irving (1958) was obtained, instability of magnetization, not reported by these authors, was found to be present in these rocks. For this reason thermal demagnetization and a.c. magnetic field demagnetization experiments were carried out on specimens from these basalts. The results of thermal demagnetization experiments revealed that the magnetic minerals in these basalts are titanomagnetites. A.c. magnetic field demagnetization experiments are described. Among these is a description of the a.c. cleaning of specimens from all the localities sampled, the result of which was to give a mean direction of magnetization of greater inclination than that originally obtained, and which was very close to that value obtained by Irving et al (1961) for other Tertiary basalts in N.S.W. Further a.c. demagnetization experiments on specimens from one of the sites of mixed polarity reported

by Green and Irving indicated that the natural magnetization in these rocks was caused by unstable components of magnetization superimposed on a stable reversed direction of magnetization which the rocks possess.

Thermal demagnetization experiments on these specimens from this site showed that instability was dependent on the composition of the titanomagnetite in the rocks. Titanomagnetites with the composition near to that of magnetite were stable, those with a high percentage of Ti were unstable.

1. INTRODUCTION

The writer began the investigation of the Older Cainozoic basalts of Victoria in 1959 after discussions with Mr. E. Irving of the Department of Geophysics A.N.U. Canberra. At that stage the University of Adelaide had an astatic magnetometer which had a sensitivity of 8×10^{-6} oersted /cm. scale deflection built by Dr. Sutton, and which therefore was quite suitable for measuring the magnetic properties of more magnetic rock types, such as basalts in particular. The department also had facilities for preparing cylindrical rock specimens in its work shops, previously set up by the writer.

Before commencing the investigation on the Older Volcanics, the writer, in October 1958, had spent time, some at Canberra, investigating the palaeomagnetism of some of the metamorphosed slates and quartzites of the Marinoan in the Adelaidean System of the Precambrian near Adelaide. The results of this investigation were baffling, and there could be no straightforward interpretation placed on them. Secondary components of magnetization were probably present and the area was quite complicated structurally, to make matters even more difficult.

There seemed to be three possibilities for future work:-

(1) Further work on the Adelaidean.

(2) An entirely new project, as for instance the study of the magnetic properties of granites.

(3) Work on special problems on a rock formation already studied - the Older Volcanics of Victoria.

It was thought that in view of the apparatus that the department at Adelaide had available, the last of the above suggestions would be the most sensible to consider. Several lines of investigation were available. These were:-

(1) Reversals are known to occur in some of the coast sections on Phillip Island. Transition zones are almost certainly present and could be found by careful sampling. No transition zones have yet been found in the Southern Hemisphere and information from them would be of the greatest interest for the theory of reversal of the earth's field. Knowledge of transition zones anywhere is in any case very rudimentary. The sites of mixed polarity reported in these basalts by Irving and Green (1958) might possibly represent such zones.

(2) Counting backwards in time the pole for the Older Volcanics is the first departure from the present geographic pole, and from results from other continents. It is therefore critical for polar wandering and drift, and it was thought that a closer study was necessary to date more accurately that rather startling event.

(3) Detailed studies of variation of intensity of initial susceptibility through a lava flow from top to bottom

can be done. There is practically no information on this matter. Flows are well exposed in shore sections.

(4) Detailed study of the scatter of directions in a lava flow is a matter on which little is known. The scatter apparently exceeds the experimental errors and there is no explanation for this. Magneto-strictive effects through jointing may be responsible, and a comparison of flows of different jointing patterns would be interesting.

The work commenced in April, 1959, when the writer with the help of Dr. Sutton, resampled the Older Volcanics for a palaeomagnetic survey. It was thought that the first step in the investigation should be to check Green and Irving's results of 1958.

Later, thermal demagnetization experiments were carried out, and also some considerable attention was given to the stability of the magnetization of the basalts. This of course entailed the construction of the thermal demagnetization and a.c. magnetic field demagnetization apparatus, which is described in 2.

During the investigation, papers which touched on problems that the writer was investigating or had investigated were published, and reference to these will be made at the appropriate time. For the moment it is sufficient to mention papers by Parry (1960), Irving et al (1961), and Khan (1960),

in which problems of thermal demagnetization and instability were discussed.

The results of experiments described in some of the following sections of the text are given in the following papers written by the author.

1. A note on the mixed polarity of magnetization in Cainozoic basalts in Victoria, Australia.
   Geophysical Journal (in press).

2. Stability of magnetization in Cainozoic basalts from Victoria, Australia.
   Phil. Mag. (in press)

3. Thermal and alternating magnetic field demagnetization experiments on Cainozoic basalts from Victoria, Australia.
   Communicated to the Geophysical Journal.

2. APPARATUS

2.1 Measurement of the magnetic properties of rocks by means of the astatic magnetometer

2.1.1 Introduction

Of the instruments which can be used to measure the small magnetic fields associated with the remanent magnetization of rocks only two have been developed to the high degree of sensitivity necessary for the measurement of the more weakly magnetic sediments. They are the rock generator and the astatic magnetometer. The astatic magnetometer has been used for measurement of weak static magnetic fields for nearly 100 years. The extension of its use to detect the magnetic properties of rock specimens, particularly of weakly magnetized sedimentary rocks, followed the development by Blackett (1952) of a very sensitive astatic magnetometer. The magnetometer at the Physics Department is an astatic magnetometer with a sensitivity of 8×10^{-6} oersted /cm. scale deflection, and is quite suited for the investigation of the magnetic properties of basic igneous rocks.

2.1.2 Theory of design

The astatic magnetometer is essentially a magnetic gradiometer which responds to horizontal fields possessing a vertical gradient. The magnetic system consists of two parallel and oppositely polarized

magnets which have nearly equal moments p. These two magnets are fixed at either end of a rigid perspex beam at a distance of L cm. apart. The beam is suspended vertically by a phosphor bronze suspension as shown diagramatically in figure 1.

If a small dipole is placed on the axis of the magnet system at a distance Z from the lower magnet and at right angles both to this axis and to the direction of magnetization of the magnets, it will produce magnetic fields H and H' at A and A' respectively, such that

$$H/H' = \frac{(L + Z)^3}{Z^3}$$

In the following discussion it is assumed that

$$H/H' >> 1$$

in which case the effect on the upper magnet can be neglected.

If I_0 and I_1 are the moments of inertia of a single magnet, and the mirror and the rod holding the mirror and the two magnets, then for an astatic system the total moment of inertia I is given by

$$I = 2I_0 + I_1$$

It is convenient to write

$I = \alpha I_0$, where α must be larger than 2 for an astatic system.

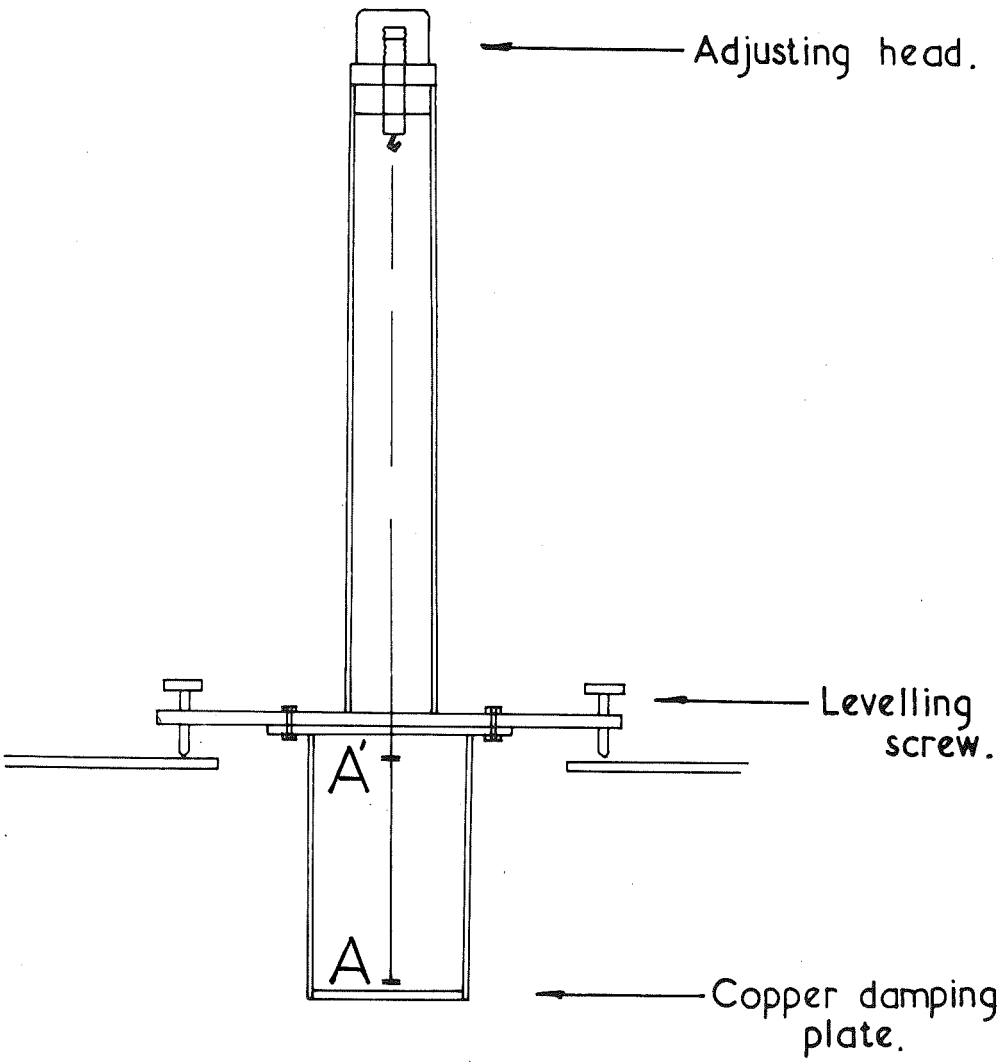

Diagram of magnetometer case showing suspension.

Figure 1.

If σ is the torsional constant of the fibre and T the undamped period of the system, we have

$$T^2 = 4\pi^2 \, I/\sigma$$

If a magnetic field H acts at right angles to the lower magnet of dipole moment p, a deflection θ_H is produced given by,

$$\theta_H = \frac{H.p}{\sigma}$$

The field acts at right angles to the magnets in the final position. Thus the sensitivity is given by

$$\frac{\theta_H}{H} = \frac{T^2 p}{4\pi^2 I}$$

Showing that the sensitivity is proportional to T^2 for a given value of p and I, and is proportional to p/I for given T.

Although the sensitivity is proportional to T^2, there are reasons why T should not be made too large. For example, sixteen deflections must be measured to determine the direction and intensity of the magnetic moment of a rock disc, thus it is desirable to acquire the required sensitivity with the minimum possible period.

To obtain high sensitivity in practice it is important that the control be purely torsional. The magnetic control due to the geomagnetic field is reduced by giving the system a high degree of astaticism (if the moments of the two magnets are very nearly equal, no resultant torque acts on the system) and also by reducing the horizontal

component of the geomagnetic field by means of a compensating coil system.

Actually it is possible to obtain full sensitivity almost without compensating the horizontal component of the earth's field if the astaticism is high. However, this compensation is desirable for other reasons, namely that the rock specimens should have no induced magnetization so that the effects of permanent and induced magnetization can be separated and measured.

2.1.3 The details of the construction of the magnetometer.

Plate 1 shows the Alcomax IV system which is used in the magnetometer. The beam is constructed out of perspex and the bearing shown allows the relative rotation of the magnets about the vertical axis. At the top of the holder is a hook to which is attached the suspension strip. Figure 1 shows the magnetometer case. The torsion head which carries the suspension strip is at the top of the case, the lower part of the case carries the viewing window. A copper damping plate screws into the base of the case so that its distance from the lower magnet can be adjusted.

The magnetometer case stands on its three levelling screws on a plate which is supported by a Müller suspension system. Plate 2 shows this suspension system, which has the effect of eliminating short period vibrations on the magnet system.

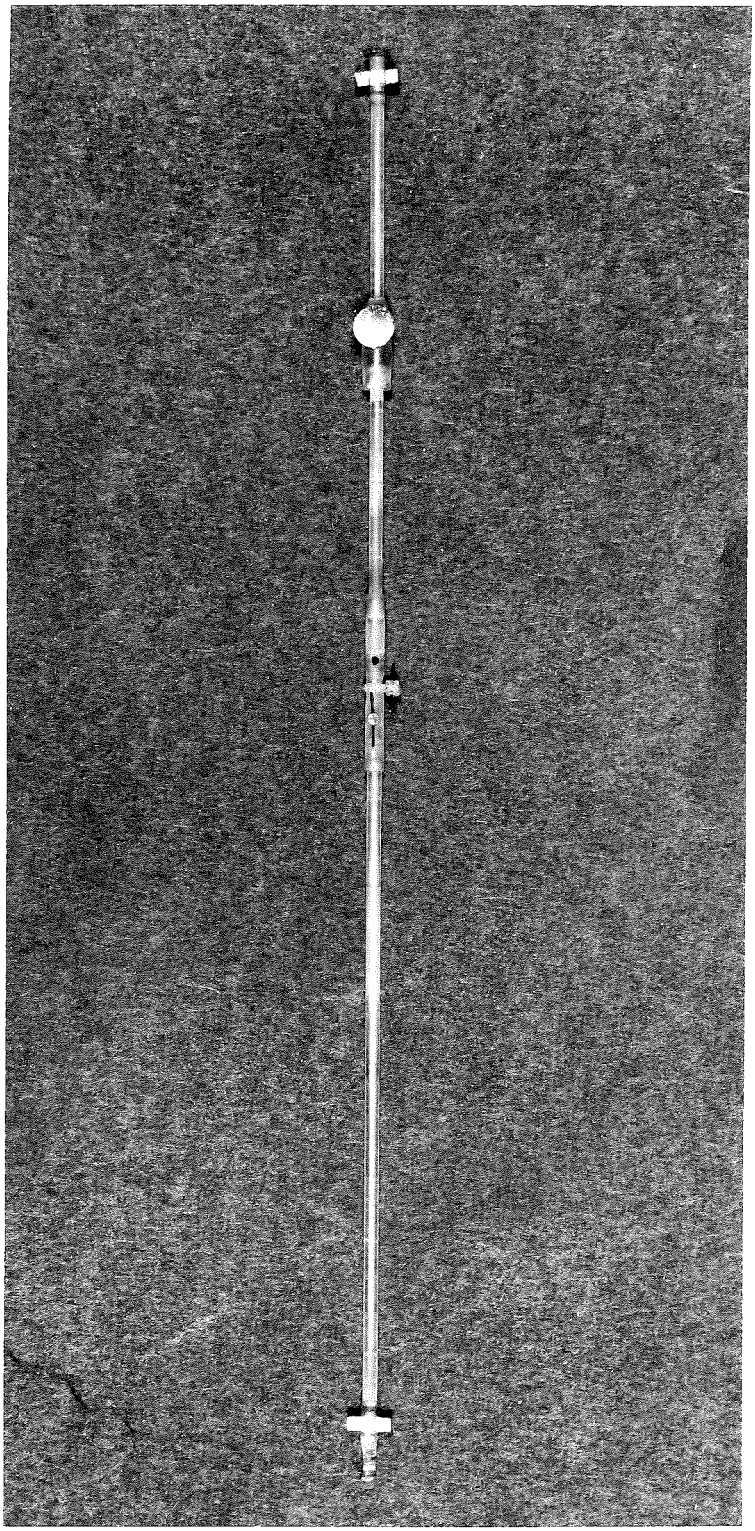

Plate.I.

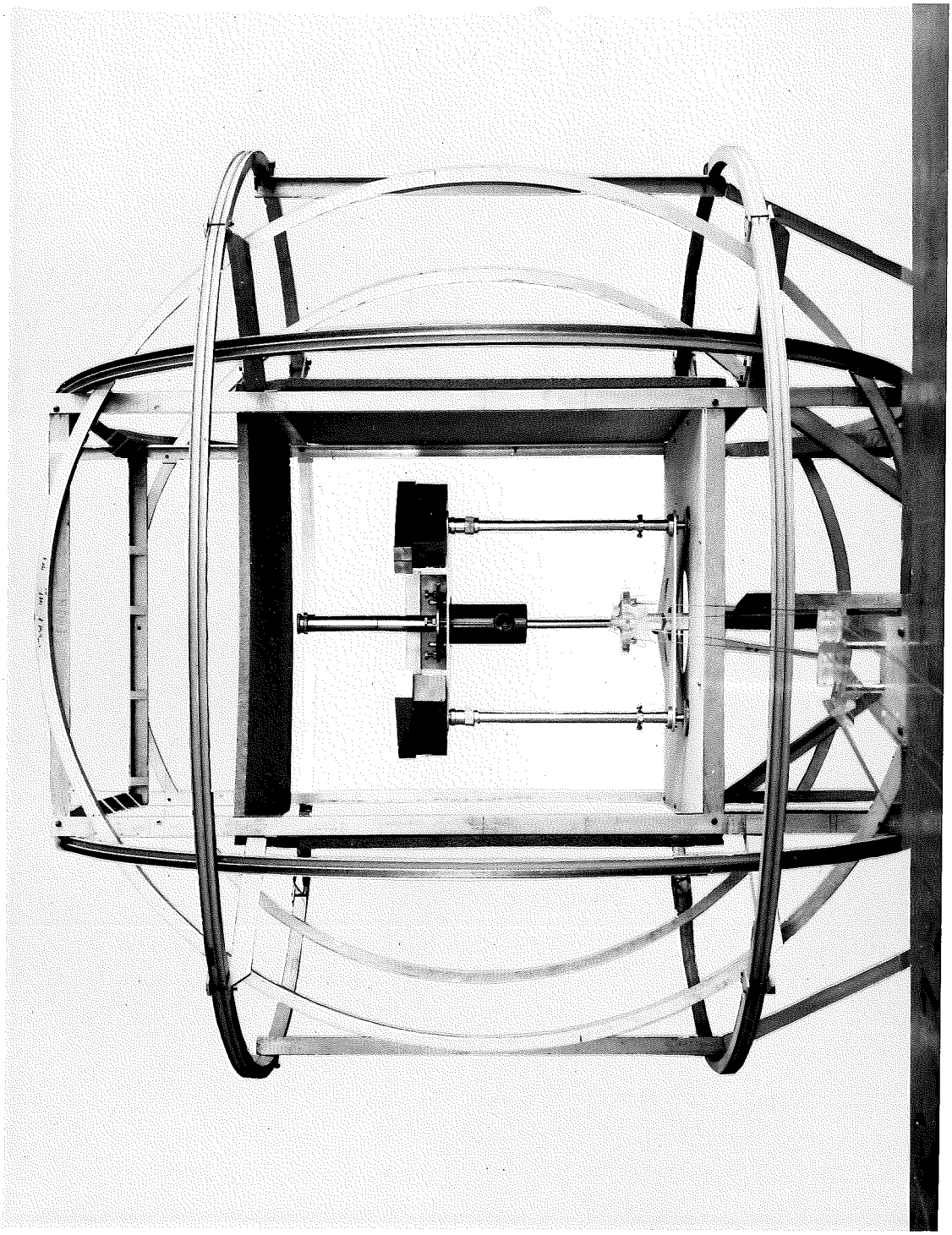

Plate. 2.

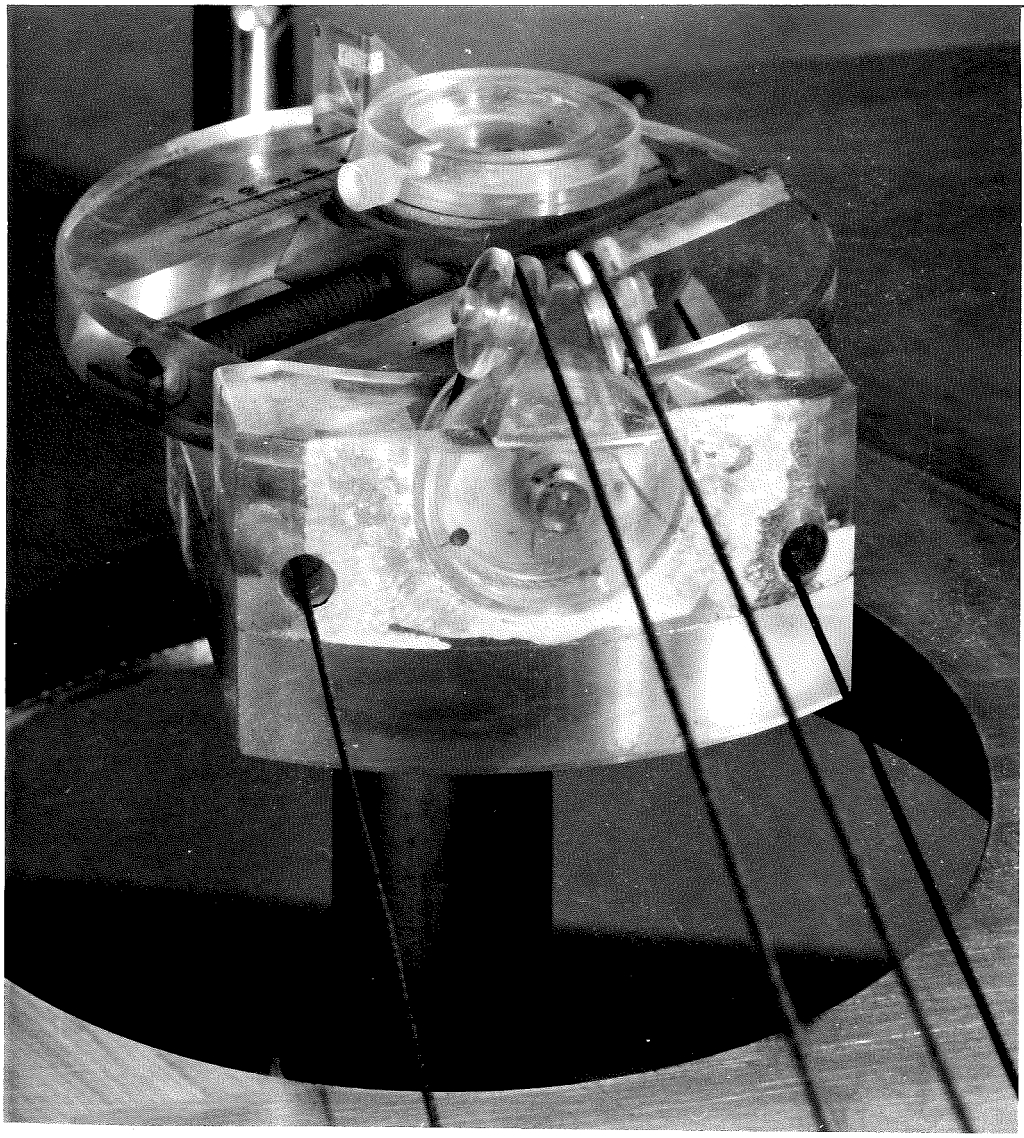

Plate. 3.

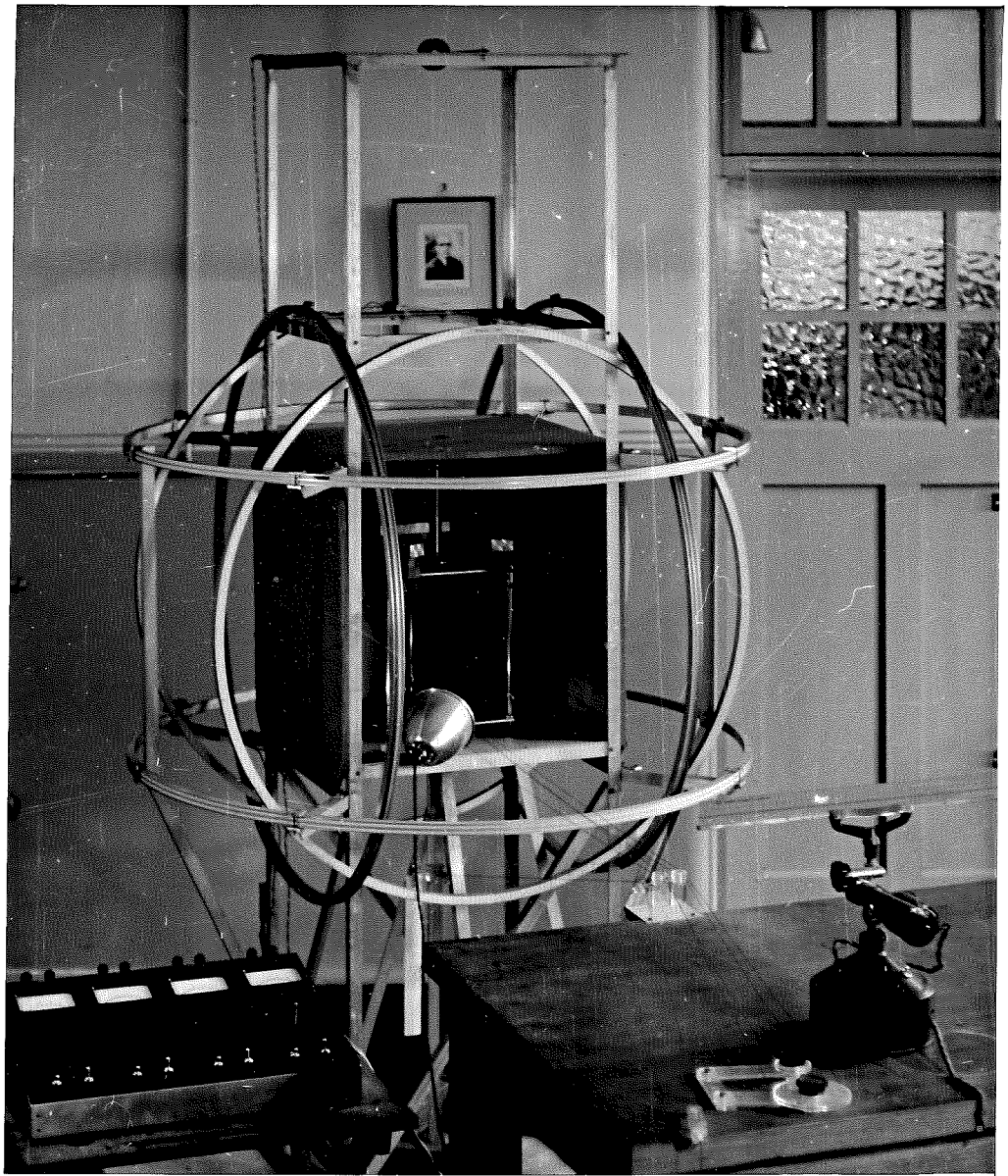

Plate.4.

During measurement, the specimen is raised and lowered below the magnet system, as well as being rotated to different azimuths and traversed horizontally (in an east-west direction). Because of disturbances produced when the apparatus is approached, all these movements are done by remote control. The specimen holder is mounted on top of a length of perspex rod which runs through vertical guides, and is raised and lowered by means of cords and pulleys. A stop on the perspex rod controls the height so that the distance of the specimen below the magnet system can be repeated accurately at each step in the measurement. The position in azimuth is determined by sighting through a telescope and reading the scale on the specimen holder. Traversing is also carried out by remote control. Plate 3 shows the specimen holder, piston and traversing mechanism. The general layout of the magnetometer is shown in Plate 4 .

2.1.4 Adjustments and calibration.

2.1.4.1. Adjustment of the Helmholtz coil system:

In order to be able to carry out experiments in a nearly field free space, three pairs of Helmholtz coils are placed around the magnetometer to compensate the horizontal component of the earth's field, and the vertical component.

Three pairs of coils are required, for the apparatus is not set exactly north-south.

The radii of these three pairs of coils are 58.13, 55.25 and 62.90 cm. respectively. Each coil contains 96 turns of wire, and currents of 135 and 5.7 M.A. are required to compensate for the earth's local horizontal component of .20 oersted, while a current of 420 M.A. compensates for the vertical component of .56 oersted.

If two coaxial circular coils of radius "a" are set a distance "a" apart, and the rectangular components of the field are Fx and Fy, x axial and y transverse, then at a point whose coordinates are x and y relative to the centre,

$$Fx = \frac{.899716}{a} \; ni \left(1 - 18 \left(8x^4 - 24\, x^2\, y^2 + 3y^4\right) \ldots\ldots \right.$$

n = no. of turns
i = current in amps.

This is the expression given by Chapman and Bartels (Geomagnetism Volume I).

Along the axis of the pair of coils then if they have a radius of approximately 50 cm., the value of the compensating field does not vary by more than $^1/_{500}$ of its value at the centre of the system for 10 cm. on either side of the centre point. Thus by using pairs of Helmholtz coils set at right angles to each other in the manner described above, it is possible to obtain

quite a uniformly field free space.

The Helmholtz field coils are adjusted by finding the currents which cause a small magnet suspended by nylon thread to swing freely at their centre.

The value of the currents through the horizontal coils when this condition was achieved were 135 M.A. and 5.7 M.A.

The value of the current which must be passed through the vertical field coils to produce the compensating field equal to the vertical component of the earth's field was found by placing a dip needle, aligned north-south, at their centre. A needle suspended in this way will swing freely about its horizontal axis when the required current is passed to compensate the vertical field. The value of this current was 420 M.A. giving the value of the vertical field as .56 oersted.

The currents to the coils are supplied by lead accumulators, and adjusted by variable resistances. They are read by milli-ammeters which with the variable resistances are placed in a control panel for convenience of operation.

2.1.4.2 Astaticizing the magnet system.

The system consists of two Alcomax IV magnets, .1 x .1 x .3 cm., with their centres 10 cm. apart.

The pair of magnets chosen were ground until their weights were nearly equal. The magnets were saturated and both were slightly demagnetized in an a.c. magnetic field and then were placed in the magnet system with

their moments parallel. The period T_1 was measured, the system being suspended from a nylon fibre. The period T_2 with the magnets anti-parallel was then measured. The lower magnet was rotated by means of the bearing until T_2 was a maximum. To improve the astaticism even further, the stronger magnet was demagnetized in stages using a small a.c. magnetic field.

If each magnet is of pole strength p, the astaticism

$$S = p/\Delta p$$

$$= \frac{1}{2} \frac{T_2^2}{T_1^2}$$

and equalled about 450 when this magnet system was first constructed.

To reach higher values of astaticism, trimming magnets of dipole moment p_1 and p_2, somewhat greater than the two horizontal components of the out of balance moment Δp can be rotated so as to compensate as nearly as possible the out of balance moment of the two main magnets.

2.1.4.3 Centering the magnet system.

The suspended system should be centered within the field coils as accurately as possible, or else some deflection will be given to the magnet system when the currents through the field coils are switched on and off. The system is positioned at the centre of the horizontal field coils by direct measurement.

When the magnet system lies along the magnetic axis of the vertical field coils, there is no deflection when the current is altered in these coils.

2.1.4.4 Centering the specimen holder.

The specimen holder is centred on the vertical axis of the magnet system by placing small coils, one a vertical coil of the same radius as the specimen disc, the other a small horizontal coil aligned east-west in the specimen holder. The first coil simulates a vertical dipole, the second a horizontal dipole. Figures 2,3 show the deflections obtained by traversing these coils from the west to east positions. Equal and opposite deflections are obtained at each end of the traverse for the vertical coil, and the deflection in the central position is zero. For the horizontal coil equal deflections are obtained at each end of the traverse and the deflection in the central position is maximum. These results indicate that the direction of traverse is east-west, and at right angles to the axis of the magnets, and that the magnet system is suspended directly above the specimen holder when this is in its central position.

2.1.4.5 Sensitivity

The sensitivity can be obtained with a small horizontal coil of known dimensions which when a current is passed through it can be used to simulate a horizontal dipole of known strength. The deflections obtained using this coil at various distances from the magnet system gives an

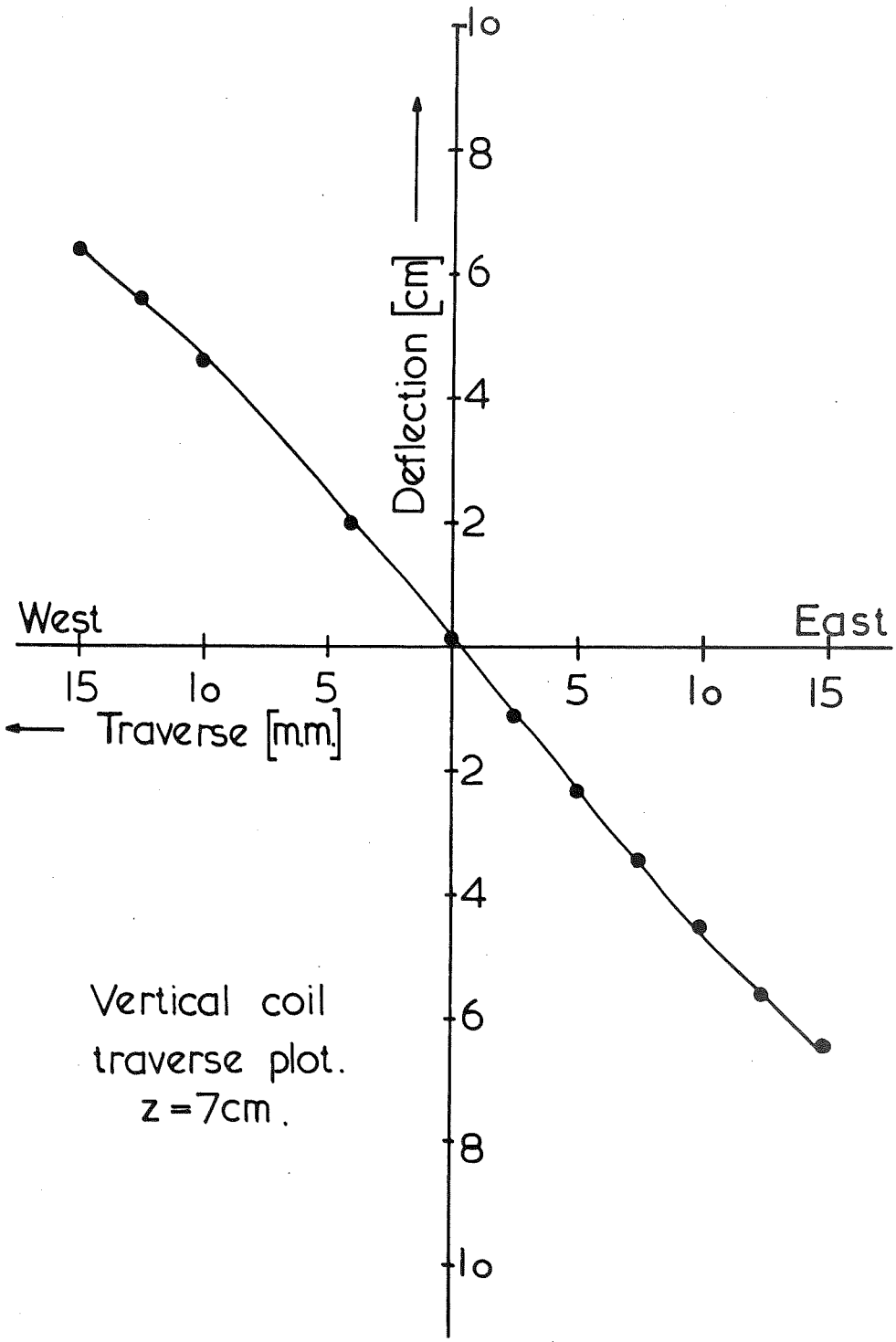
10
8
6
4
2
Deflection [cm]
West
East
15
10
5
5
10
15
Traverse [mm]
2
4
6
8
10
Vertical coil
traverse plot.
z = 7cm.

Figure.2.

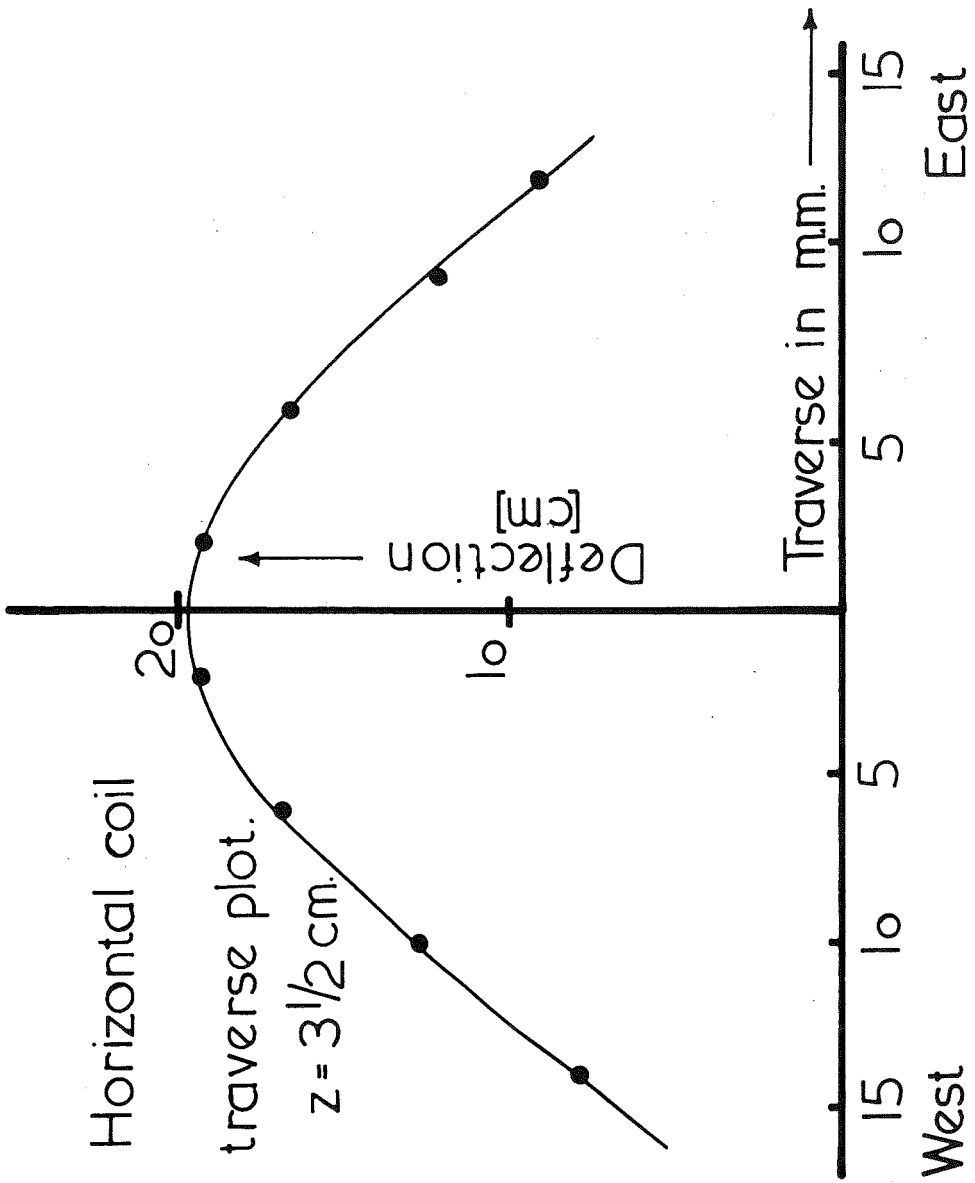
Horizontal coil
traverse plot.
z = 3 1/2 cm.
2o
1o
Deflection [cm]
Traverse in mm.
5
1o
15
East
15
1o
5
West

Figure 3.

estimation of the sensitivity.

The field acting at the lower magnet

= deflection x sensitivity

i.e. $^{p}/_{Z^3}$ = deflection x sensitivity

p = magnetic moment of calibration coil

$$= \frac{n.i.A}{10.1000}$$

Where,

n = no. of turns on the coil = 8

i = current in milli-amps = 60

A = area of cross section of the coil which has diameter 4.75 mm.

Z = distance of coil from lower magnet = 5.7 cm.

The deflection of the system measured on the scale was 5.8 cm.

$$\text{Thus} \quad p = \frac{60}{1000.10} \cdot \frac{4.75^2}{10} \cdot \frac{\pi .8}{4}$$

$$\text{Sensitivity} = \frac{60}{1000.10} \cdot \frac{4.75^2}{10} \frac{\pi}{4} \cdot \frac{8}{5.7^3 \cdot 5.8}$$

$$= 8.10^{-6} \text{ oersted /cm. scale deflection}$$

We see from line one above that the deflection $\propto {}^{1}/_{Z^3}$

Figure 4 shows the deflection plotted against $^{1}/_{Z^3}$ for the following points. The graph obtained indicates that scale height readings are correct.

Z	Deflection
3.7	11.1
4.7	5.2
5.7	2.9
6.7	1.8

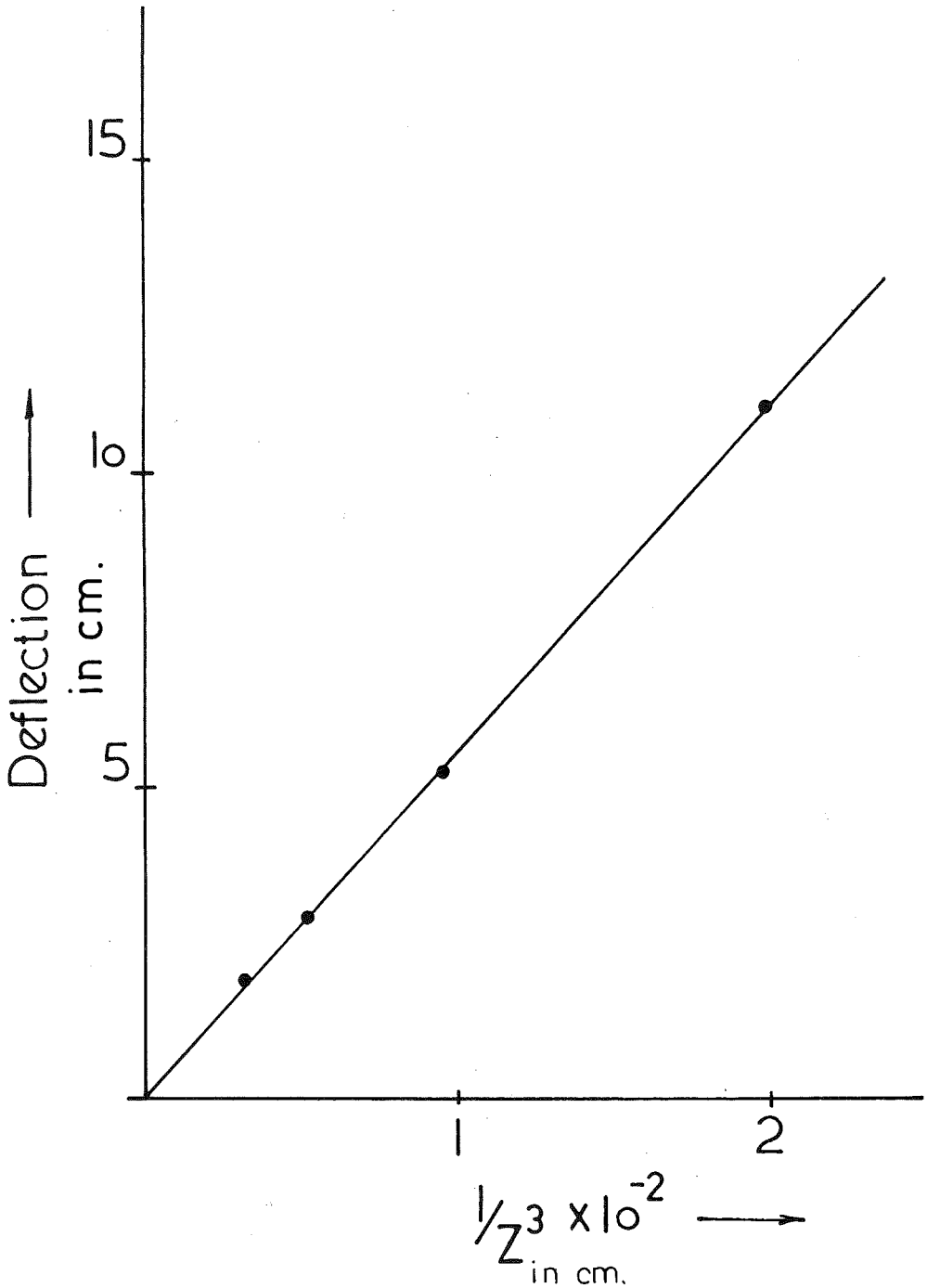

Figure 4.

2.1.5 The method of collecting and preparing the specimens.

Three points are marked on the surface of a rock where the three legs of a small threelegged level come into contact with the surface. This level is shown in plate 5 . If two of these points are arranged such that the line joining them is horizontal, then these two points (with the third) not only determine a plane, but also fix the strike of this plane. The attitude of the third point fixes the dip of this plane. Thus, the strike and dip of a plane determined by the three points marked on the rock can be measured and information can be recorded concerning the orientation of this plane, and therefore of the rock itself. With this level, it was possible to mark any rock thought suitable for collection as it was not necessary to select a sample having a flat surface (which was sometimes impossible to do).

All samples oriented in the manner outlined above were of course in situ at the time of collection.

For coring, the rock was set in plaster so that the plane determined by the three points mentioned above was horizontal. At least two cores of $1\frac{3}{8}$" diameter were removed from any one rock sample using a non-magnetic diamond coring bit.

These cores were sliced by means of a non-magnetic diamond impregnated saw. The coring machine and saw are shown in plates 6,7.

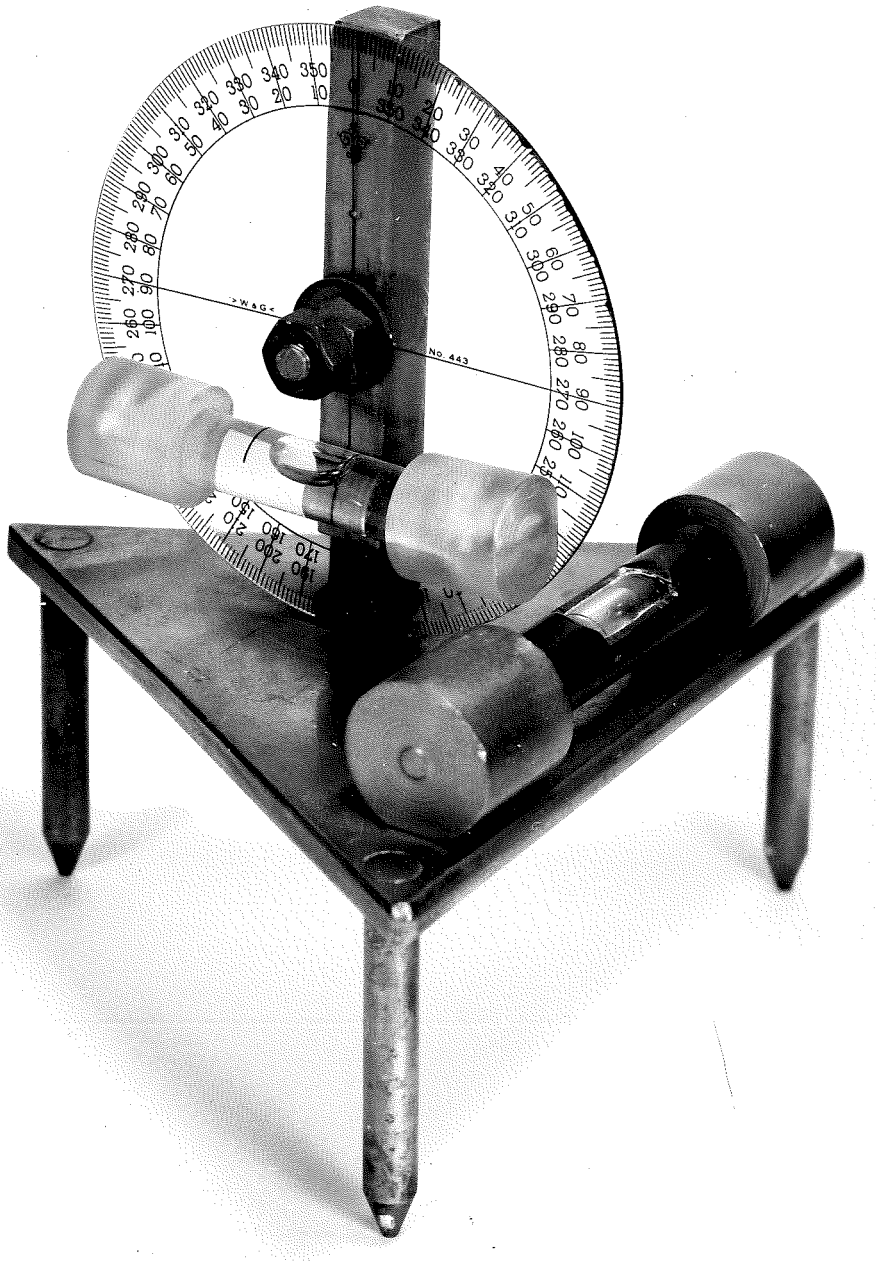

Plate.5.

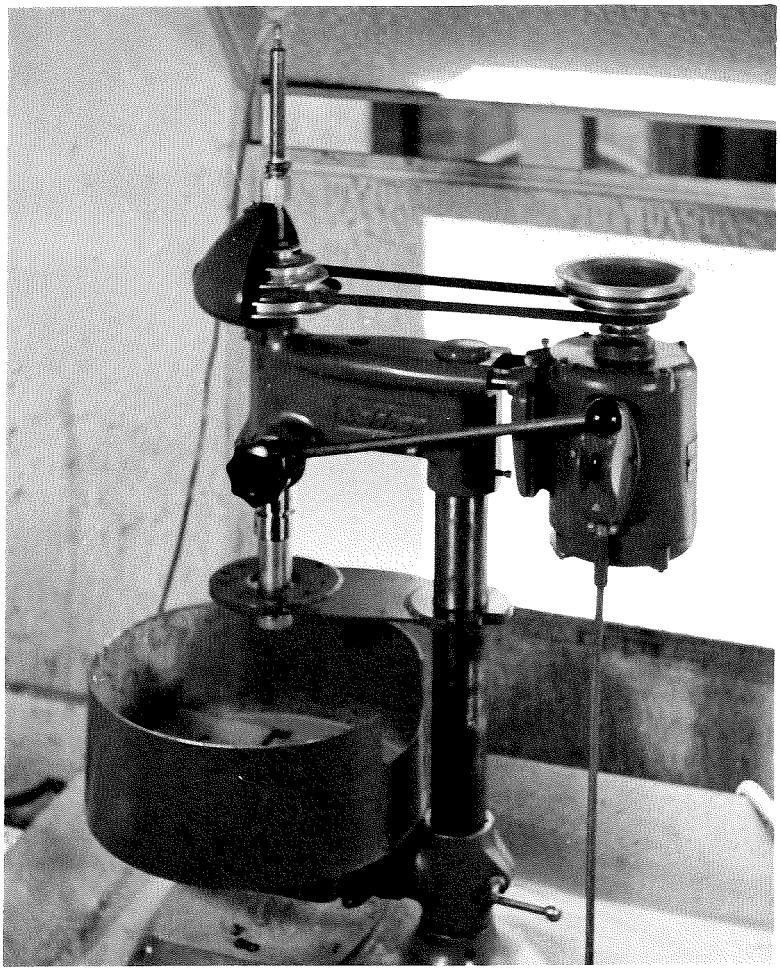

Plate. 6.

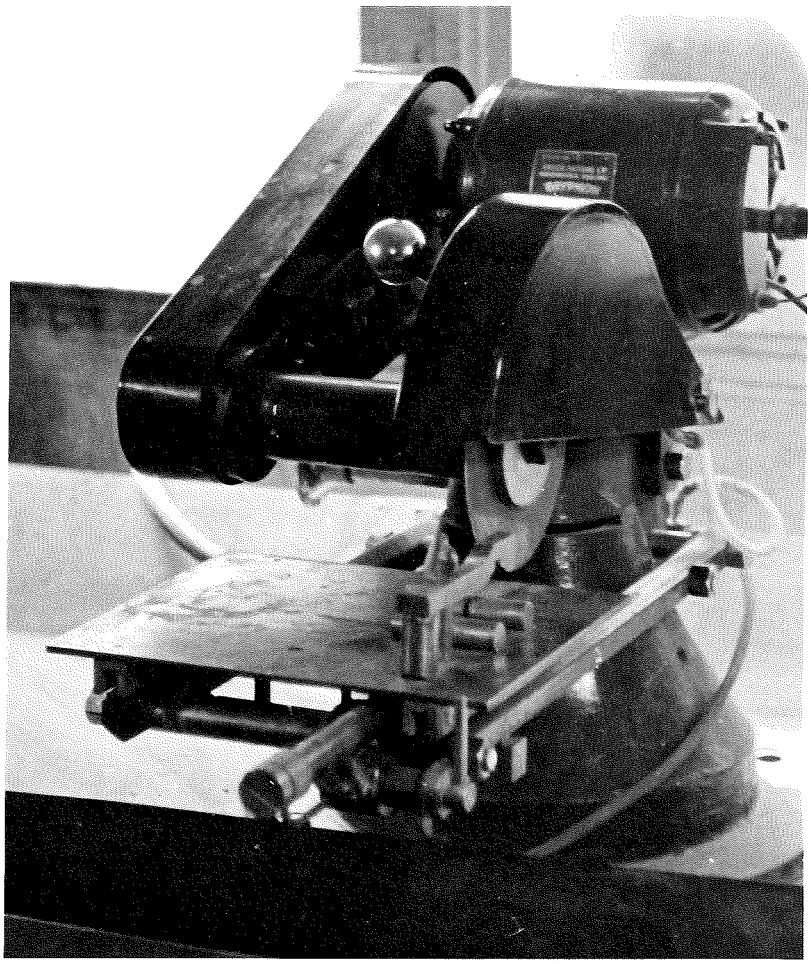

Plate.7.

Directions of magnetization obtained during measurement were therefore directions relative to the abovementioned plane regarded as horizontal, and the direction of strike of this plane. These directions were converted to directions of magnetization relative to the true horizontal plane and the magnetic north direction.

2.1.6 Measurement of the direction of magnetization of rock discs.

Consider the specimen to be placed directly below the magnet system.

The horizontal component of the equivalent dipole, $M_h \cdot v$ will produce a horizontal field at the lower magnet in the direction θ given by

$$H = v \cdot M_h \cdot \text{Cos.} (\theta - D) / Z^3$$

$\theta = 0^o$ in the specimen disc

is the direction of the strike of the plane referred to in 2.1.5.

v = the volume of the disc

M_h = the horizontal component of magnetic intensity / unit volume.

Z = distance of equivalent dipole from the lower magnet. (See Appendix 1)

Plotting the deflection of the magnetometer against azimuth θ, the angle between the plane of the magnets and the direction $\theta = 0^o$ in the disc, a curve is obtained, the phase of which gives D, the declination of the direction of the horizontal component from the direction $\theta = 0^o$ and the amplitude of which allows the value of M_h, the horizontal

component of magnetization per unit volume to be calculated.

$$\text{i.e.} \quad M_h = \frac{S.d.\ Z^3}{v}$$

S = sensitivity in oersted / cm. scale deflection

d = maximum deflection at scale in cm.

The vertical component of magnetization M_z has no effect. Consider the specimen to be traversed off centre a distance x from the axis of rotation, and so the axis of the magnet system.

The field due to the horizontal component of magnetization is given by

$$H = \frac{v\ M_h\ \text{Cos}\ (\theta - D)}{r^3}$$

$$\frac{v\ M_h\ \text{Cos}\ (\theta - D)}{Z^3}$$

as $r^2 = Z^2 + x^2$, and so if x is small compared with Z, then $r \simeq Z$.

The vertical component now has an effect, however, as its field in the 90° azimuth position has a horizontal component which is at right angles to the magnet system. The field due to this component, M_Z is such that

$$H = \frac{v\ M_Z\ x\ \text{Cos}\ \theta}{Z^4}$$

$$r \simeq Z$$

On rotation of the specimen therefore not only is there the sinusoidal deflection produced by the horizontal com-

ponent, but also there is the deflection due to this vertical component. The resultant deflection is due to the sum of these two effects.

If the specimen is inverted and θ is measured in the opposite sense, the effect of the vertical component is reversed, and in this case the resultant deflection is due to the effect of the horizontal component minus the effect of the vertical component.

By adding or subtracting the above resultant deflections in the upright or inverted cases it is possible to separate the effects of the horizontal and vertical dipole components.

In practice the direction of magnetization with respect to a reference line drawn on top of the disc is determined by completing the form shown in figure 5. "a" is the algebraic mean of $\frac{1}{2}$ ($d_1 + d_5$) etc., (deflections in the 0° azimuth position), "b" the algebraic mean of $\frac{1}{2}$ ($d_2 + d_6$) etc. (deflections in the 90° position). The following table indicates whether the declination is N.E., S.W. etc. according to the sign of a and b.

b	a	Quadrant
+	+	N.E.
+	-	N.W.
-	-	S.W.
-	+	S.E.

This is the case for the bottom maguet pointing in the south direction. a and b are in fact proportional to

Height . . . . Traverse . . . . Sensitivity . . . . . Date . . . . . .
Rock type . . . . . Locality . . . . . Spec. No. . . . .

Upright

West		East			
0	d_1 =	0	d_5 =	$d_1 + d_5$ = ☐	$d_1 - d_5$ =
90	d_2 =	90	d_6 =	$d_2 + d_6$ =	
180	d_3 =	180	d_7 =	$-[d_3 + d_7]$ = ☐	$-[d_3 - d_7]$ =
270	d_4 =	270	d_8 =	$-[d_4 + d_8]$ =	
180	s_3 =	180	s_7 =		
0	s_1 =	0	s_5 =		

Inverted

East		West			
360	d_9 =	360	d_{13} =	$d_9 + d_{13}$ = ☐	$d_9 - d_{13}$ =
270	d_{10} =	270	d_{14} =	$d_{10} + d_{14}$ =	
180	d_{11} =	180	d_{15} =	$-[d_{11} + d_{15}]$ = ☐	$-[d_{11} - d_{15}]$ =
90	d_{15} =	90	d_{16} =	$-[d_{12} + d_{16}]$ =	
180	s_{11} =	180	s_{15} =		
0	s_9 =	0	s_{13} =		

$s_3 - d_3$ =
$s_1 - d_1$ =
$s_7 - d_7$ =
$s_5 - d_5$ =
$s_{11} - d_{11}$ =
$s_9 - d_9$ =
$s_{15} - d_{15}$ =
$s_{13} - d_{13}$ =

$\frac{\quad}{8}$

Susceptibility

$= \frac{kz}{3x \cdot \cdot 56 \text{vol.}}$

$=$ _____

$a = \frac{\square}{8}$

$b = \frac{\quad}{8}$

tan =

=

Declination _____

$d_h = \sqrt{a^2 + b^2}$

$= \sqrt{\quad}$

$p_h = k$

_____

$d = \frac{\quad}{8}$

$p = \frac{kz}{3x}$

$= k.$

= _____

$\tan \phi = \frac{p_z}{p_h}$

ϕ =

$p = k\sqrt{d_h^2 + d_u^2 [z/3x]^2}$

_____

Figure.5.

the horizontal dipole components at the 0° and 90° azimuths. Therefore the total horizontal dipole is proportional to

$$A = (a^2 + b^2)^{\frac{1}{2}}$$

B is half the mean of quantities such as (d1 - d5) etc., these being displacements due to M_Z in the off centre positions (0° azimuths).

The above procedure averages out non-uniformities of magnetization in any specimen.

2.1.7 Calculation of total moment of magnetization

A field of 8×10^{-7} oersted at the lower magnet produces 1 mm. scale deflection.

The horizontal field at the lower magnet due to the horizontal components of the equivalent dipole M_h at distance Z,

$$= M_h / Z^3 \qquad \text{(1)}$$

The horizontal field at the bottom magnet due to the vertical component of the dipole M_Z, at distance Z,

$$= M_Z \; 3x / Z^4 \qquad \text{(2)}$$

The specimen is traversed a distance x off centre

The deflection due to (1) = d_h cms.

The deflection due to (2) = d_Z cms.

The field at the bottom magnet due to M_h is therefore

$$d_h \cdot 8 \cdot 10^{-6} \quad \text{oersted}$$

i.e. $M_h = d_h (Z^3\ 8.10^{-6})$

$= K\ d_h$

Where $K = 8.10^{-6}\ Z^3$

Similarly, $M_Z = d_z\ (Z/3x)\ K$

The total moment

$$= \sqrt{M_h^2 + M_Z^2}$$

$$= k\sqrt{d_h^2 + d_z^2\ (Z/3x)^2}$$

$$= k\sqrt{(a^2 + b^2) + d_z^2\ (Z/3x)^2}$$

$$= k\sqrt{A^2 + B^2\ (\frac{Z}{3x})^2}$$

and $\tan \phi$ (where ϕ = inclination)

$$= \frac{M_Z}{M_h}$$

$$= \frac{d_Z}{d_h} \cdot \frac{Z}{3x} = \frac{b}{a} \cdot \frac{Z}{3x}$$

Actually, to consider the effect of the field of the specimen on the lower magnet only is to simplify the situation It must be remembered that the specimen dipole has an effect on both the upper and lower magnets, and if it is raised to the measuring position from some distance away, its field has an effect in both of these positions.

In Appendix 1 a correction is given which takes into account these effects and which can be applied to the values of inclination derived by the method outlined above.

2.1.8 Measurement of susceptibility

The magnetization induced by weak magnetic fields of the order of the earth's field can readily be measured by this magnetometer. The inducing field is the vertical component of the earth's field.

Suppose the difference in readings for the vertical field on and off is ds cms. This will be the deflection due to a vertical dipole M'_Z at a distance x off axis.

$$\text{Field} = \frac{3x\, M'_Z}{Z^4}$$

where M'_Z is the induced moment

$$= d_s \quad (8.10^{-6}) \text{ oersted}$$

$$M'_Z = K \; ds \; Z/3x$$

If I = induced moment /unit volume, then

$$I = M'_Z / \text{volume}$$

$$= k'H$$

k' = volume susceptibility

H = inducing field

$$\text{Thus} \quad k' = \frac{M'_Z}{\text{Volume } (.56)}$$

The value of the vertical component of the earth's field is .56 oersted at Adelaide.

2.1.9 Concluding Remarks

The techniques described in this section and in Appendix 1 are those which the author used to measure directions of magnetization of specimens examined in the investigations reported in the following pages.

2.2 THE THERMAL DEMAGNETIZATION APPARATUS

2.2.1 Introduction

The presence in rocks of specific magnetic minerals can be inferred from thermomagnetic curves by comparison with standard curves for known minerals.

The furnace was constructed by the writer so that thermal demagnetization curves for typical rock specimens from the Older Volcanics could be obtained. It was constructed in such a way that the thermal demagnetization was carried out in zero field.

Stacey (1959) has reported on an instrument which he used to carry out heating tests. The measuring apparatus in this case was a rock generator. As Stacey mentioned in his paper however, he encountered "noise" trouble from the specimen holder even though this was constructed from the reputedly non-magnetic alloy Nimonic.

The effect of this noise was to reduce the sensitivity of the instrument, so that the writer felt that as he was dealing only with a fairly magnetic suite of rocks, the Older Volcanics, it might prove less troublesome to

construct a furnace beneath a moderately sensitive astatic magnetometer, both furnace and magnetometer being set centrally in a Helmholtz coil system, which provided a field free space. Plate 8 shows the general layout of the thermal demagnetization apparatus.

2.2.2 A description of the thermal demagnetization apparatus.

Figure 6 is a diagram of the thermal demagnetization apparatus. As is evident from this diagram, the apparatus consists of two main parts:-

a. the magnetometer
b. the furnace.

a. The magnetometer.

This magnetometer was constructed by the author and is of the conventional astatic type, as has been described previously in 2.1

The Helmholtz Coil

Only two sets of parallel coil systems were used to annul the earth's field in this case, so that the coils used to cancel the horizontal field were set with their axis in the north-south meridian. The radii of these two Helmholtz coil systems were 52 and 56 cm. respectively. The currents required to annul the earth's field were 125 and 390 M.A.

Astaticizing the magnet system

Again, magnets of Alcomax IV were cut and ground to approximately the same shape and weight and were magnetized

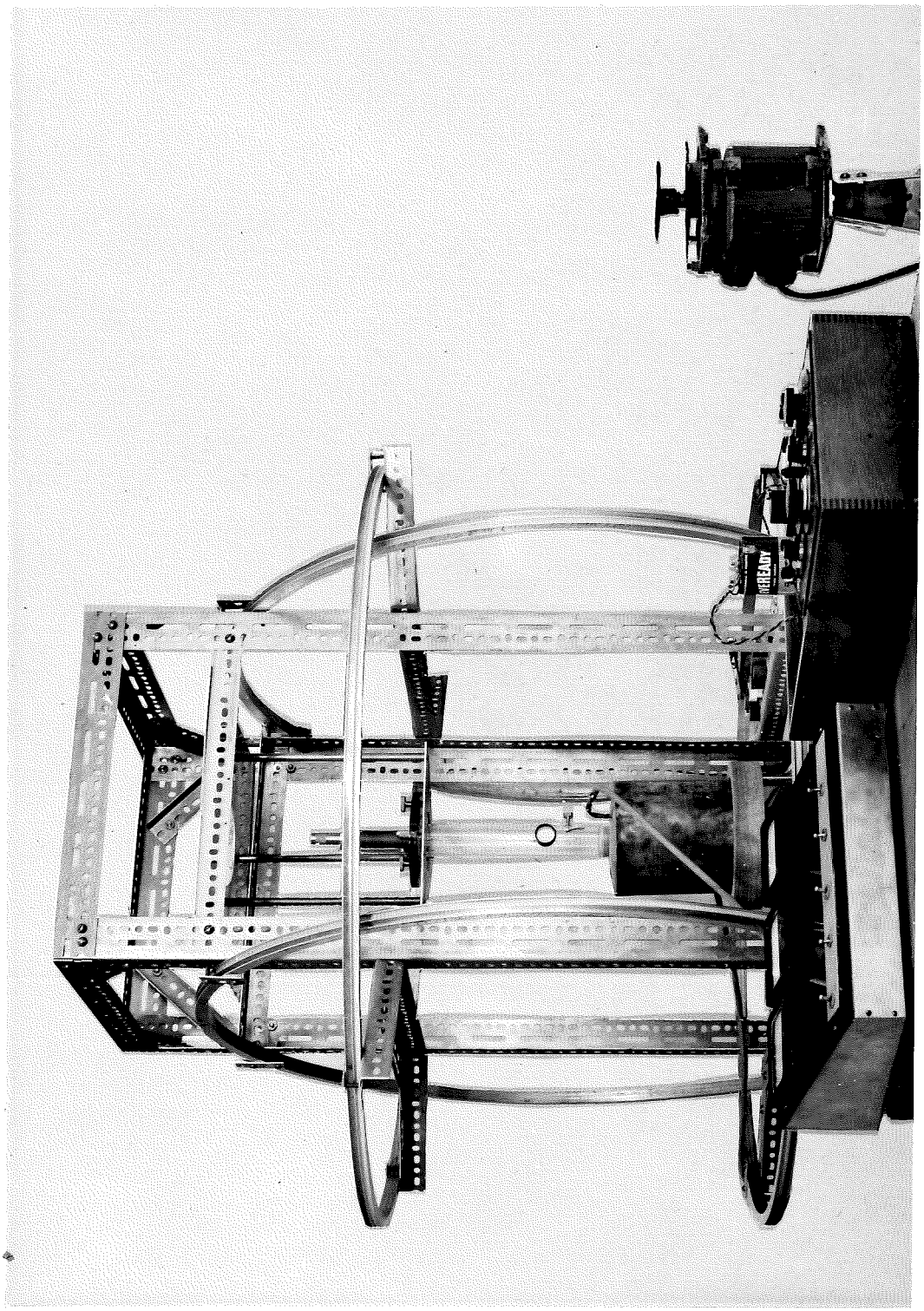

Plate.8.

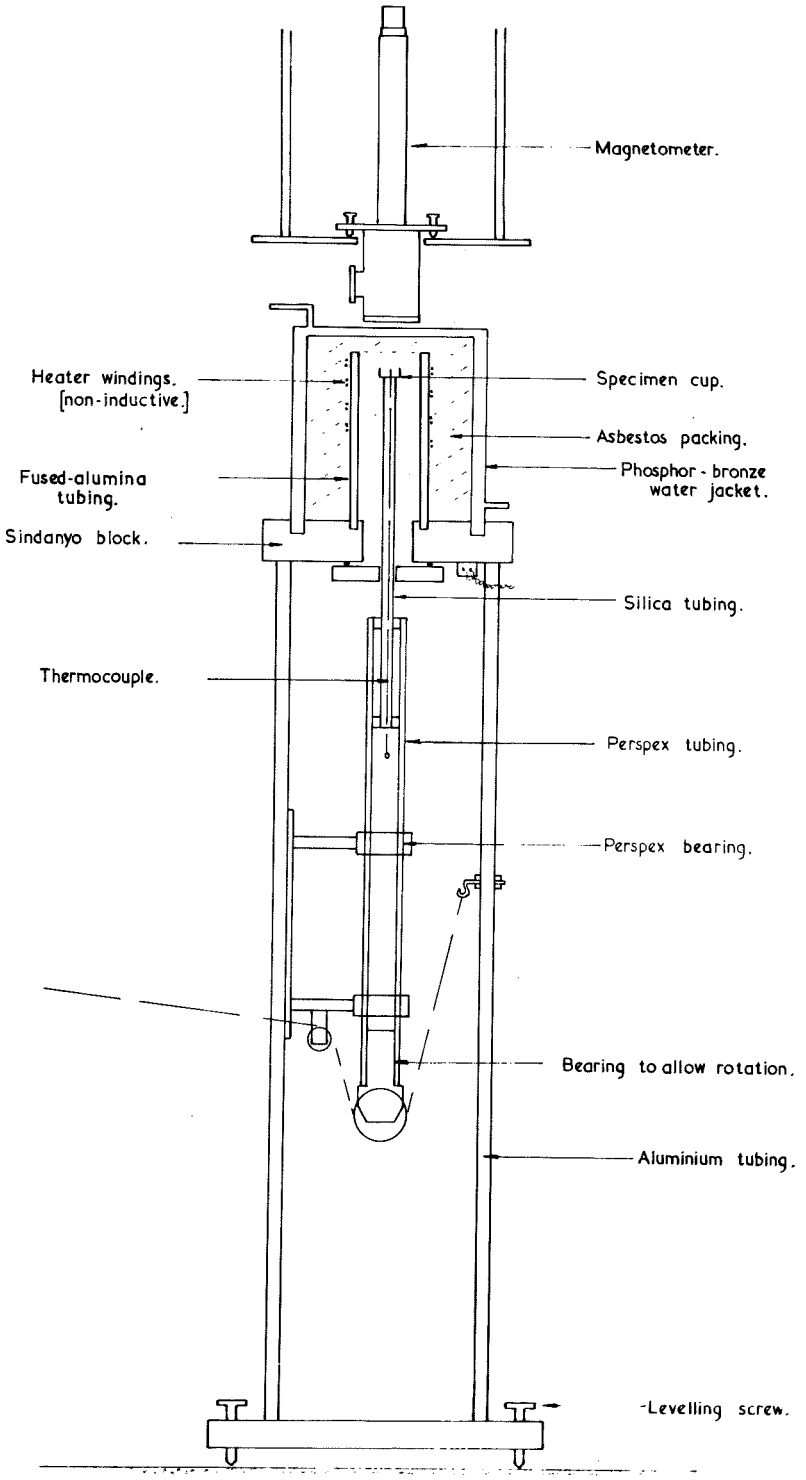
Magnetometer.
Heater windings. [non-inductive.]
Specimen cup.
Asbestos packing.
Fused-alumina tubing.
Phosphor - bronze water jacket.
Sindanyo block.
Silica tubing.
Thermocouple.
Perspex tubing.
Perspex bearing.
Bearing to allow rotation.
Aluminium tubing.
Levelling screw.

Figure .6.

to saturation. Their moments were made equal by the method described in 2.1.4.2 The suspension used for the magnet system was phosphor bronze strip.

Sensitivity

The sensitivity of the magnetometer was determined by the method described in 2.1.4.5, and was found to be 5.8×10^{-6} oersted /cm. scale deflection.

Because the apparatus was such that the specimen was placed with its centre very nearly to Z = 4 cm. from the lower magnet of the system, each cm. deflection of the scale was equivalent to a specimen of moment determined by the equation,

$$\text{Sensitivity} \times \text{deflection} = {}^{p}/_{Z^3}$$

$$\text{thus,} \quad 5.8 \times 10^{-6} \times 64 = p$$

$$p = 3.6 \times 10^{-4} \text{ c.g.s. units}$$

b. The Furnace

The components of the furnace are shown in Figure 6.

The Water Jacket

The water jacket was made out of phosphor-bronze sheet. The inlet and outlet tubes for the circulating water were placed so that the jacket was completely filled with water, and there was no air gap at the top.

Insulation

Asbestos fibre packing was used as the insulating material between the heating element and the water jacket.

The furnace base

The base on which the furnace sits is turned out of

2" asbestos cement slab.

Heating Element

The heating element is wound on a fused alumina tube in which a spiral groove has been cut. The heating element must produce no demagnetizing effects and therefore it is non-inductively wound.

The best method found for doing this was to cover the heating wire (22 gauge nichrome wire) with asbestos-sleeving, double the wire, and twist the two pieces together. The twisted wire could then be wound on to the alumina tube. The asbestos sleeving provides good electrical insulation at the temperatures attained. The current for the heating element is varied by means of a rheostat.

In order to check that no a.c. field was produced by this heating element, one similarly wound was made using copper wire, and a pick up coil was placed inside it. It was found that with 5 amps flowing through the copper wire there was still no pick up discernable above the background pick up in the room.

The specimen is placed in the specimen holder and is raised into the furnace by means of a pulley system. The specimen can also be rotated in azimuth so that it can be rotated in one direction until there is maximum deflection of the magnet system to the left of zero, and then rotated through 180° in azimuth to give the maximum deflection of the magnet system to the right of zero. The sum of these two readings

is recorded for the particular temperature in question, and is due to a moment of twice the horizontal component of the equivalent dipole of the specimen. The specimen was located directly below the magnet system.

2.2.2.3 Measurement of temperature

The temperature of the specimen is measured by means of a platinum-platinum, rhodium (Pt-Pt, 13% Rh) thermocouple. The graph of e.m.f. against temperature for such a thermocouple is shown in figure 7 . It was necessary to use this type of thermocouple even though the e.m.f. obtained is not high, for the reason that it is non-magnetic. A hole was bored in each of the specimens examined so that the thermocouple end could be placed inside the specimen. The e.m.f. produced by the thermocouple was measured with a potentiometer.

In order to find whether the heating of the specimen was uniform, a series of tests was carried out. In these tests another thermocouple was attached with its junction touching the side of the specimen, and during heating, the temperature of the outside and the inside of the specimen were measured. A heating procedure was obtained from these tests which provided fairly uniform heating of the specimens. The inside and outside temperature of the specimen for this heating procedure is shown in table 1 Figure 8 is a graph of these values,

2.2.2.4 Standard thermal demagnetization curves

Thermal demagnetization of specimens of pure nickel,

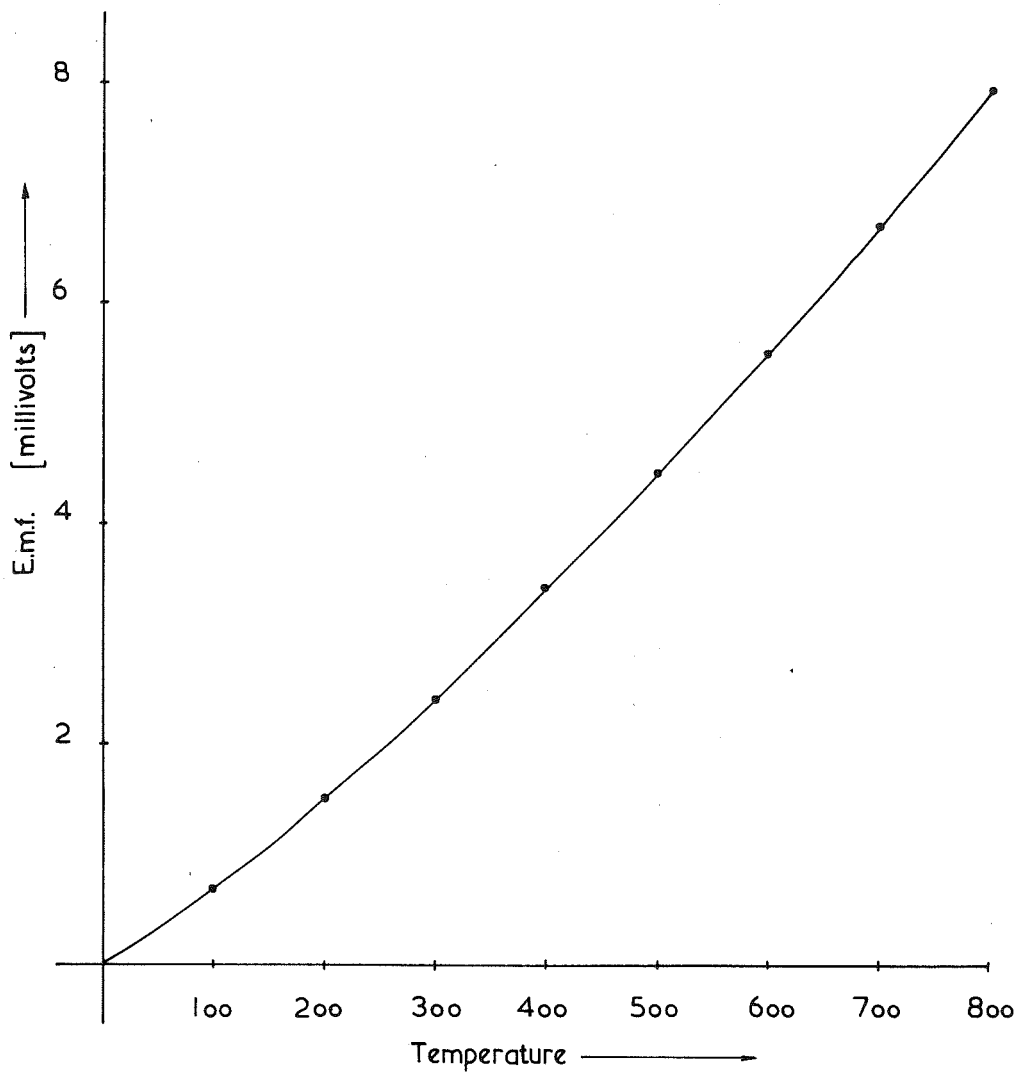
8
6
4
2
E.m.f. [millivolts]
100
200
300
400
500
600
700
800
Temperature

Figure.7.

Figure 8.

hematite and magnetite was carried out in the furnace after it was completed. The hematite, nickel and magnetite were powdered and mixed with plaster of paris and made into cylindrical specimens the size of those normally used (a right cylinder of diameter and height 22mm) Figures 9,10,11 show the thermal demagnetization curves for these materials. The Curie point of nickel is 368°C, magnetite is 578°C, and hematite is approximately 680°C. These results indicate that temperatures are being measured correctly.

TABLE I

Cold temperature junction = 15°C.

CURRENT IN AMPS	INSIDE OF SPECIMEN				OUTSIDE OF SPECIMEN			
	E.M.F. using (Pt - Pt 13% Rh)			Temp. °C	E.M.F. using Chromel-alumel			Temp. °C
			+	+	++	++		+
3 Amps	.06	.10	.16	25	.06	.30	5	20
	.07		.17	30	.11	.55	10	25
	.09		.19	35	.15	.75	17	32
4 Amps	.10		.20	35	.19	.95	22	37
	.13		.32	40	.27	1.35	30	45
	.20		.30	55	.36	1.80	45	60
	.28		.38	65	.45	2.25	52	67
	.31		.41	70	.51	2.55	60	75
	.39		.49	82	.60	3.00	72	87
5 Amps	.46		.56	90	.67	3.35	80	95
	.52		.62	100	.75	3.75	90	105
	.67		.77	120	.91	4.55	105	120
	.76		.86	135	1.01	5.05	120	135

(CONTINUED)

TABLE I (contd.)

CURRENT IN AMPS	INSIDE OF SPECIMEN			OUTSIDE OF SPECIMEN			
	E.M.F. using (Pt - Pt 13%Rh)		Temp. °C	E.M.F. using Chromel-alumel			Temp. °C
		+	+	++	++		+
6 Amps	.88	.98	150	1.14	5.70	135	150
	.98	1.08	165	1.24	6.20	150	165
	1.20	1.30	190	1.44	7.20	175	190
	1.33	1.43	200	1.56	7.80	190	205
	1.47	1.57	215	1.67	8.35	202	217
7 Amps	1.60	1.70	230	1.80	9.00	220	235
	1.69	1.79	240	1.89	9.45	230	245
	1.83	1.93	255	2.01	10.50	245	260
	1.98	2.08	267	2.10	10.50	257	272
	2.08	2.18	277	2.18	10.90	267	282
	2.15	2.25	285	2.25	11.25	275	290
	2.30	2.40	300	2.37	11.85	290	305
	2.46	2.56	315	252	12.60	305	320
8 Amps	2.71	281	340	273	13.65	332	347
	2.95	3.05	365	2.93	14.65	357	372
	3.24	3.34	395	3.14	15.70	385	400
	3.44	3.54	415	3.28	16.40	400	415
	3.59	3.69	428	3.39	16.95	415	430
	4.17	4.27	482	3.82	10.10	465	480
9 Amps	4.45	4.55	510	4.05	20.20	495	510
	4.65	475	525	4.19	20.95	510	525
	4.75	4.85	537	4.26	21.30	520	535
	4.86	4.96	545	4.33	21.65	530	545
10 Amps	5.05	5.15	560	4.53	22.65	545	560
	5.22	5.32	580	4.65	23.25	560	575
	5.30	5.40	585	4.71	23.55	565	580

+ Temperature corrected for cold temperature junction of 15°C.

++ E.M.F.S. were measured on x 5 scale of potentiometer.

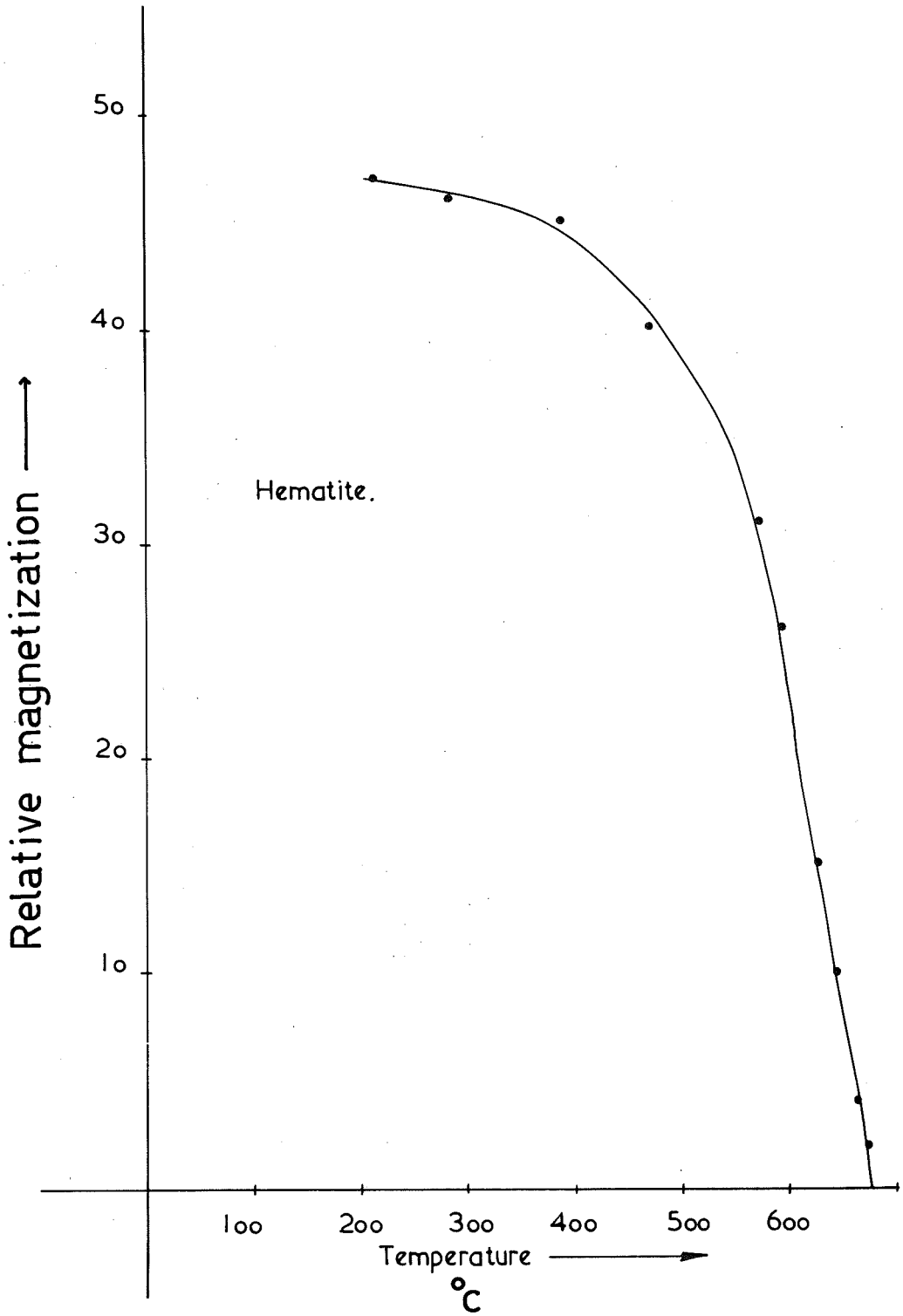
Relative magnetization
5o
4o
3o
2o
1o
Hematite.
1oo
2oo
3oo
4oo
5oo
6oo
Temperature
°C

Figure.9.

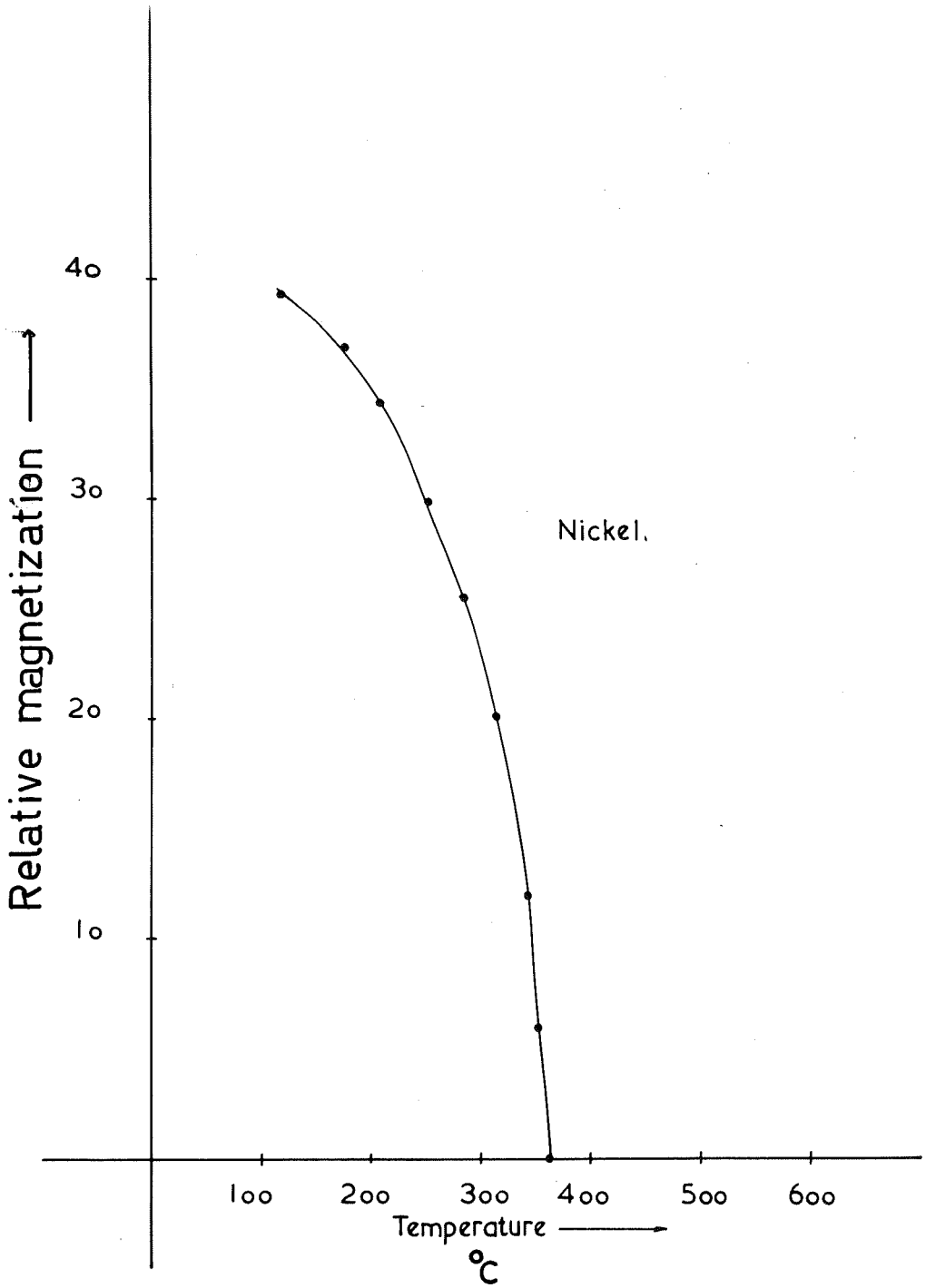
Relative magnetization
40
30
20
10
Nickel.
100
200
300
400
500
600
Temperature
°C

Figure.10.

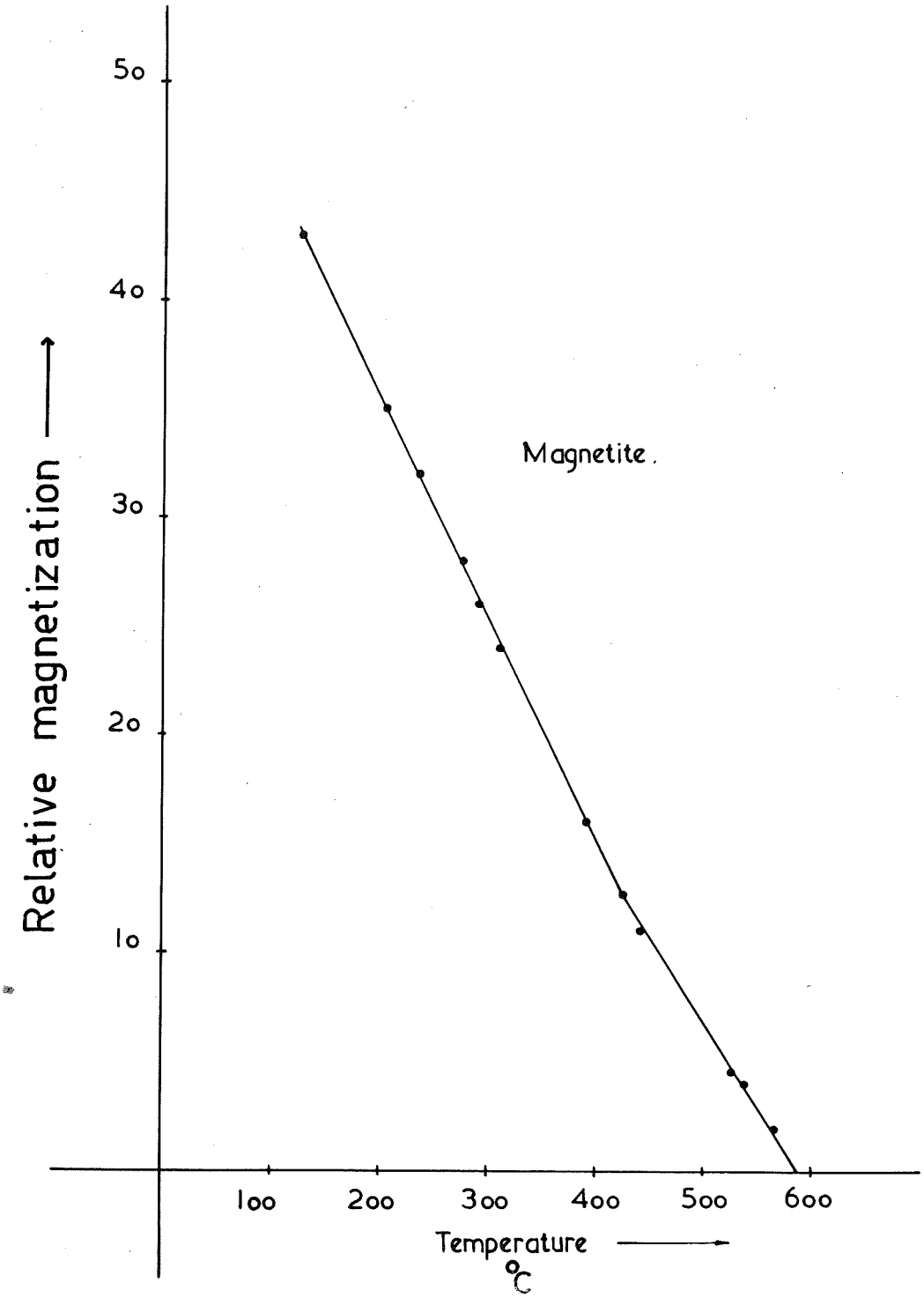
Relative magnetization
5o
4o
3o
2o
1o
Magnetite.
1oo
2oo
3oo
4oo
5oo
6oo
Temperature
°C

Figure.11.

2.3 THE A.C. MAGNETIC FIELD DEMAGNETIZATION APPARATUS

2.3.1 Introduction

Lavas, on cooling through their Curie point, acquire a primary thermoremanent magnetization (T.R.M.) in the direction of the earth's field. If magnetic particles with relaxation times less than the geological age of the rock are present, a secondary component, an isothermal remanent magnetization (I.R.M.) is acquired different in direction from the primary one if the direction of the geomagnetic field has changed since the T.R.M. was acquired. By subjecting rock specimens to gradually decreasing alternating magnetic fields, it is possible to remove unwanted, unstable components of magnetization which may have been acquired since the formation of the rocks. As will be mentioned in 5.6, there is instability present in the Older Volcanics. The presence of these temporary components of magnetization lead the writer to construct the a.c. demagnetization apparatus described here, to study the effect of a.c. demagnetization of the basalts in the hope that a more accurate determination of the ancient pole position could be obtained. Also the relationship between a.c. magnetic field demagnetization and thermal demagnetization was investigated.

The apparatus was constructed by the writer after a visit to Canberra early in 1961, when he used the a.c. magnetic field demagnetization apparatus there to study the effect

of a.c. cleaning on rocks taken from the quarry at Drouin-South. The results of this investigation are described later in 7.

The a.c. magnetic field demagnetization apparatus is shown in Plate 9.

2.3.2 A description of the a.c. magnetic field demagnetization apparatus

2.3.2.1 The demagnetizing coil

The coil was wound on a wooden former. This former was split into 4 segments and this allowed it to collapse when the ends of the former were removed after the winding was completed.

There are 95 turns of 18 S.W.G. enamelled copper wire on each of the 22 layers, making approximately 2,090 turns in all. The coil was constantly shellaced and therefore was well bonded when it dried out.

The dimensions of the coil are -

Length = 12.8 cm.

Internal diameter = 14.1 cm.

External diameter = 19.7 cm.

Two methods were used to measure the inductance of this coil.

(a) The coil was measured as part of an L and C resonant circuit.

Maximum current flowed through the coil when the capacity in series was 18.5 μF

Thus as $\omega^2 = \frac{1}{L.C}$

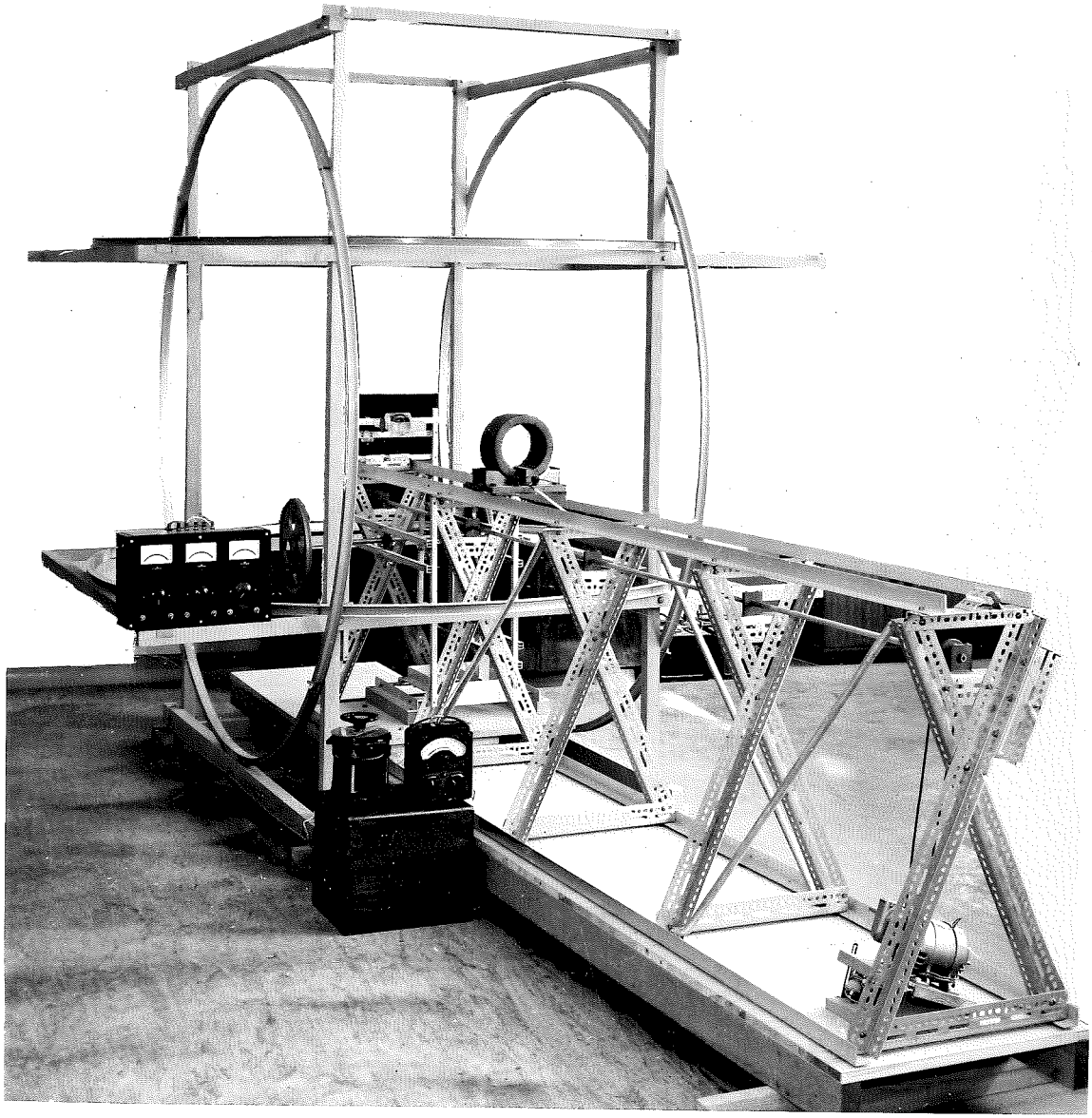

Plate 9.

Where $\omega = 2\pi f$, where f is the frequency of the applied a.c. voltage and equals 50 for mains voltage

$$L = \frac{1}{\omega^2 C}$$

$$= \frac{1}{4\pi^2 \cdot 50^2 \cdot 18.5}$$

$$= \underline{.55 \text{ henries}}$$

(b) The inductance of the coil was measured by means of a Maxwell-Inductance, Capacity Bridge.

The bridge circuit is shown in figure 12.

$C = 1 \mu F$

$R = 182$ ohms

$P = 3{,}000$ ohms

At balance, $L = P R C$

$$= \frac{1}{10^6} \times 3{,}000 \times 182$$

$$= \underline{.55 \text{ henries}}$$

The voltage drop across the condenser C when I = 5 amps passes through the coil is,

$$\frac{I}{C\omega}$$

$$= \frac{20}{10^6} \cdot \frac{I}{2\pi \cdot 50} \cdot 5$$

$$= 800 \text{ volts}$$

Thus the condenser must be able to withstand $800\sqrt{2}$ peak a.c. volts.

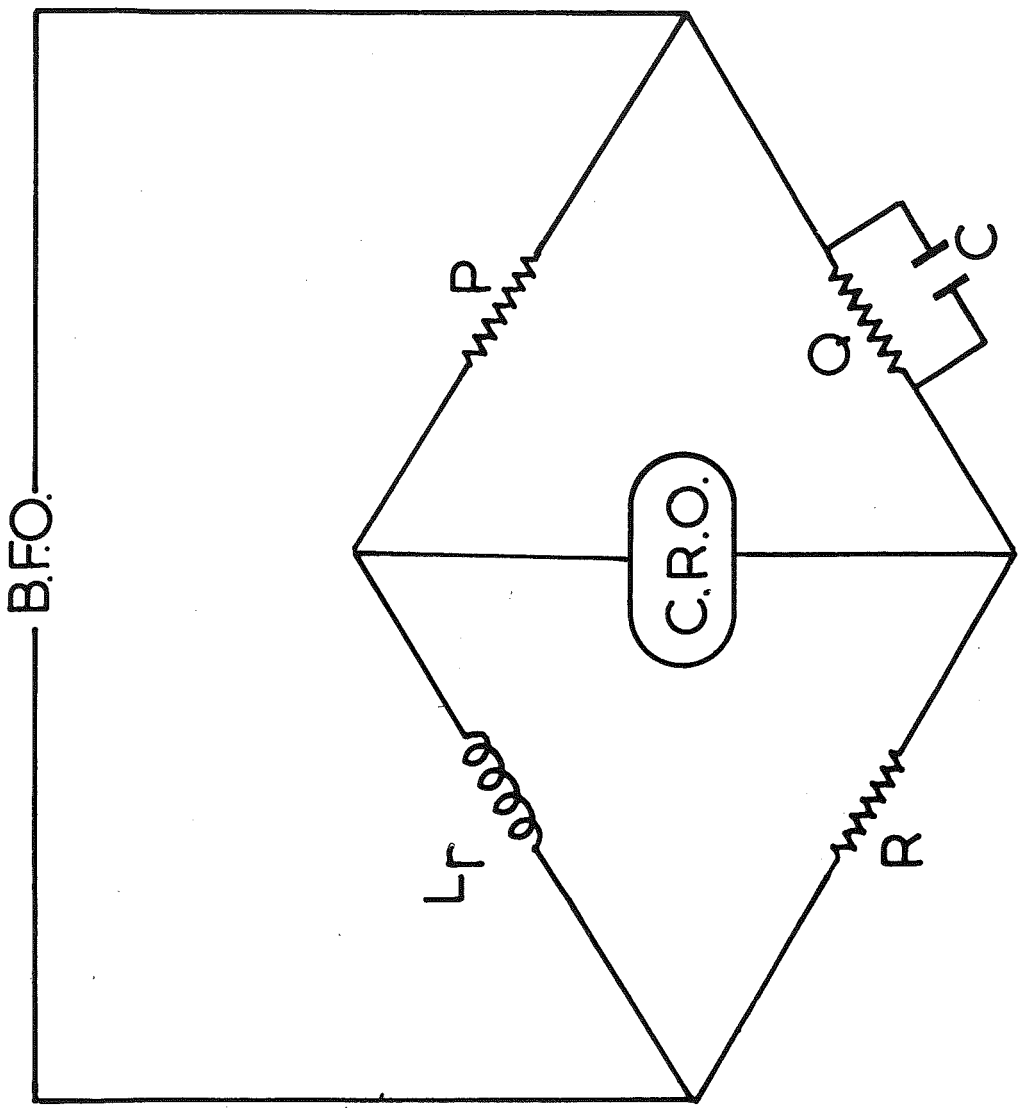

Figure.12.

The alternating field produced by the coil was measured using a search coil containing 420 turns. The mean diameter of this coil was 2.6 cm.

The e.m.f. induced in the search coil by alternating magnetic flux ϕ is given by

$$E = \frac{d\phi}{dt}$$

$$= B.A.N. \text{ where } B = \text{field density}$$

$$= B.420\pi\,(1.3)^2.10^{-4}$$

A = Area of cross section

N = No. of turns

Now $\phi = \phi \text{ max } \sin \omega t$

where $= 2\pi f$ and f is the frequency of the alternating magnetic flux

$$\frac{d\phi}{dt} = \frac{d(\phi \text{ max } \sin \omega t)}{dt}$$

Thus $E = \omega BAN \cos \omega t$

and $E \text{ max} = \omega BAN$

Now $\omega = 2\pi f$

Thus $E \text{ max} = 2\pi f \; B \; 420\pi(1.3)^2 \; 10^{-4}$

$$= 2\pi . \; 50. \; B. \; 420\pi(1.3)^2 \; 10^{-4}$$

$$B = \frac{E}{2\pi.50.420.\pi(1.3)^2 \; 10^{-4}}$$

The peak induced voltage measured from the pick up coil was 2.4 volts when the a.c. current through the coil was 2 amps.

$$\text{Thus } B = \frac{2.4}{2\pi^2.50.420\;(1.3)^2\;10^{-4}}$$

$$= 172 \text{ gauss/amp}$$

The coil is tuned to 50 cycles with the series capacitance of 18.5 μ F. No series resonant circuit tuned to 100 cycles/sec. is connected in parallel as has been described by Irving et al (1961) for their apparatus for the following reasons. The impedance Z of a circuit containing resistance R, inductance L and capacitance C in series is given by

$$Z = \sqrt{R^2 + (L\omega - \frac{1}{C\omega})^2}$$

Where f is the frequency of the applied voltage and $\omega = 2\pi f$.

Then for f = 50, because the circuit containing the demagnetizing coil is tuned to this frequency, the impedance becomes equal to R.

For a voltage of 100 cycles/sec. however, the impedance of the coil, condenser circuit is given by

$$Z = \sqrt{R^2 + \left(100\pi - \frac{10^6}{18.5 \cdot 2\pi 100}\right)^2}$$

$$= \sqrt{R^2 + 228^2}$$

But R $\simeq$ 15 ohms, so that the impedance to 100 cycles/second is equal to 230 ohms.

Thus the natural rejection of the coil-condenser circuit is some 15 times greater to a 100 cycle/second signal than to a 50 cycle/second signal.

This means that if the amount of 100 cycle/second signal in the mains is of the order of 2%, then it is reduced to nearly .1% due to the natural rejection of the coil.

The demagnetizing coil is mounted on a small trolley and can be run along two parallel sets of tracks from a distance of 12 feet away to the specimen which is mounted in the spinning mechanism described in 2.3.2.3. Plate 10 shows the demagnetizing coil.

2.3.2.2 The Helmholtz Coil System

To ensure that the specimen does not acquire an anhysteretic magnetization while it is being demagnetized, all demagnetization is carried out in zero field. Two sets of Helmholtz coils are used to annul the earth's field.

The diameter of these coils are 214.6 and 225.6 cm. respectively. Each coil is wound with 102 turns of 18 S.W.G. single cotton covered wire. The axis of one set of coils is aligned north-south, and its field annuls the horizontal component of the earth's field.

The horizontal component of the earth's field is .20 oersted.

The field due to a Helmholtz pair is given by

$$\frac{2\pi nI}{10.1000} \cdot 1.407$$

Where n = No. of turns on each coil

I = Current in milliamps

r = radius of coils

Thus as the field = .20 oersted.

I = 262 M.A.

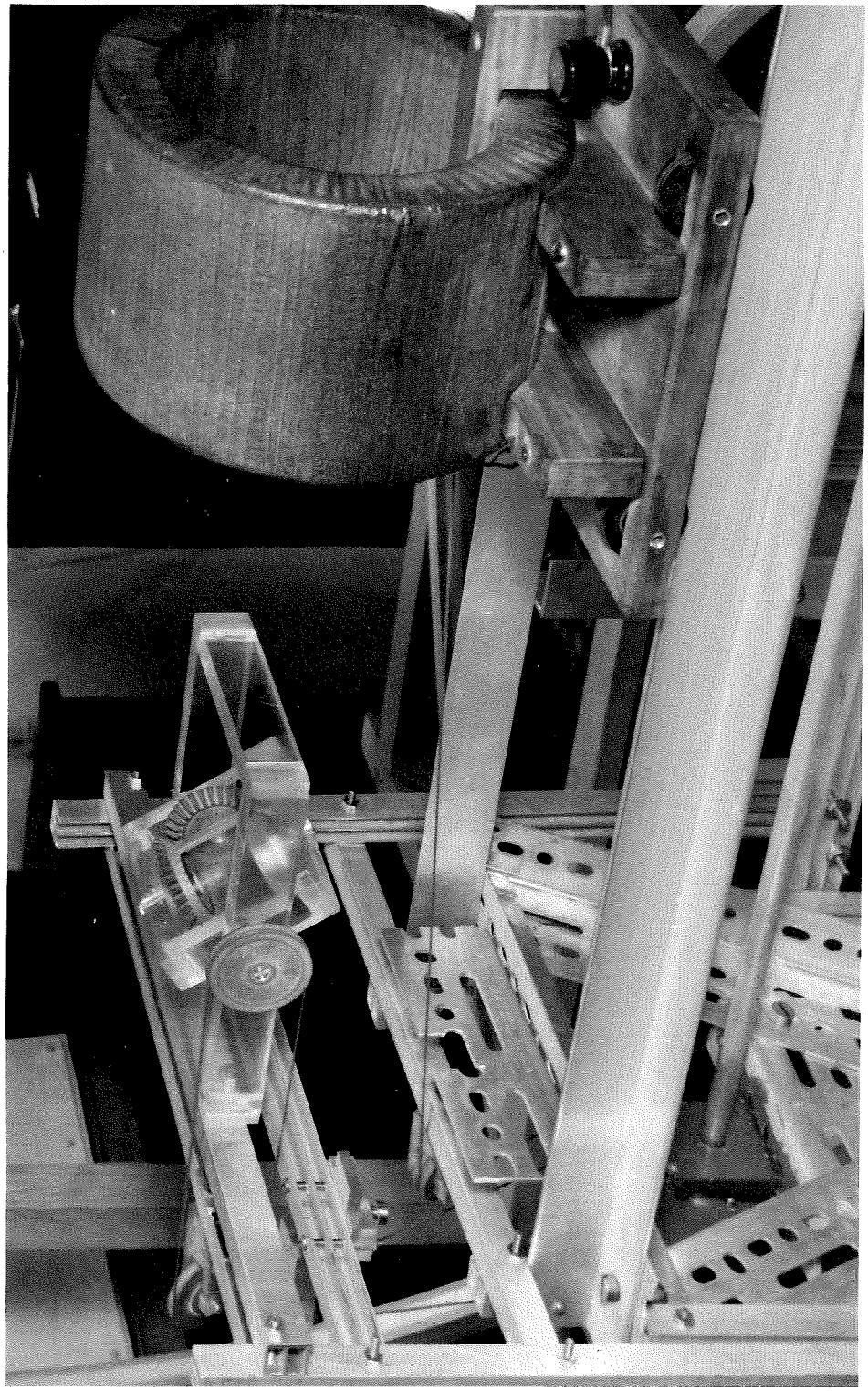

Plate.10.

The vertical component of the earth's field is .56 oersted. Thus the current needed to cancel this field is 706 M.A. The currents through the coils are adjusted by means of the control panel shown in plate 9.

2.3.2.3 The Spinner

The spinning mechanism which ensures that a specimen is demagnetized uniformly in all directions is shown in figure 13. The inner and outer frame works and the specimen holder are constructed of perspex. All bearings are made of P.T.F.E., and shafting of aluminium. The bevel gears are constructed of resin bonded fabric. One geer has 32 teeth and the other 30 teeth so that the specimen rotates about two mutually perpendicular axes at speeds in the ratio 15 : 16.

The inner framework of the spinner is rotated at 140 r.p.m., a speed which has been checked by a stroboscope. This does not resonate with any simple fraction of the mains frequency.

The electric motor used to drive the spinner is situated at the end of the 12' aluminium framework on which the demagnetizing coil runs.

The drive to the spinner is transmitted along $\frac{1}{2}$" aluminium tubing. A close up photograph of the spinning mechanism is shown in plate 10.

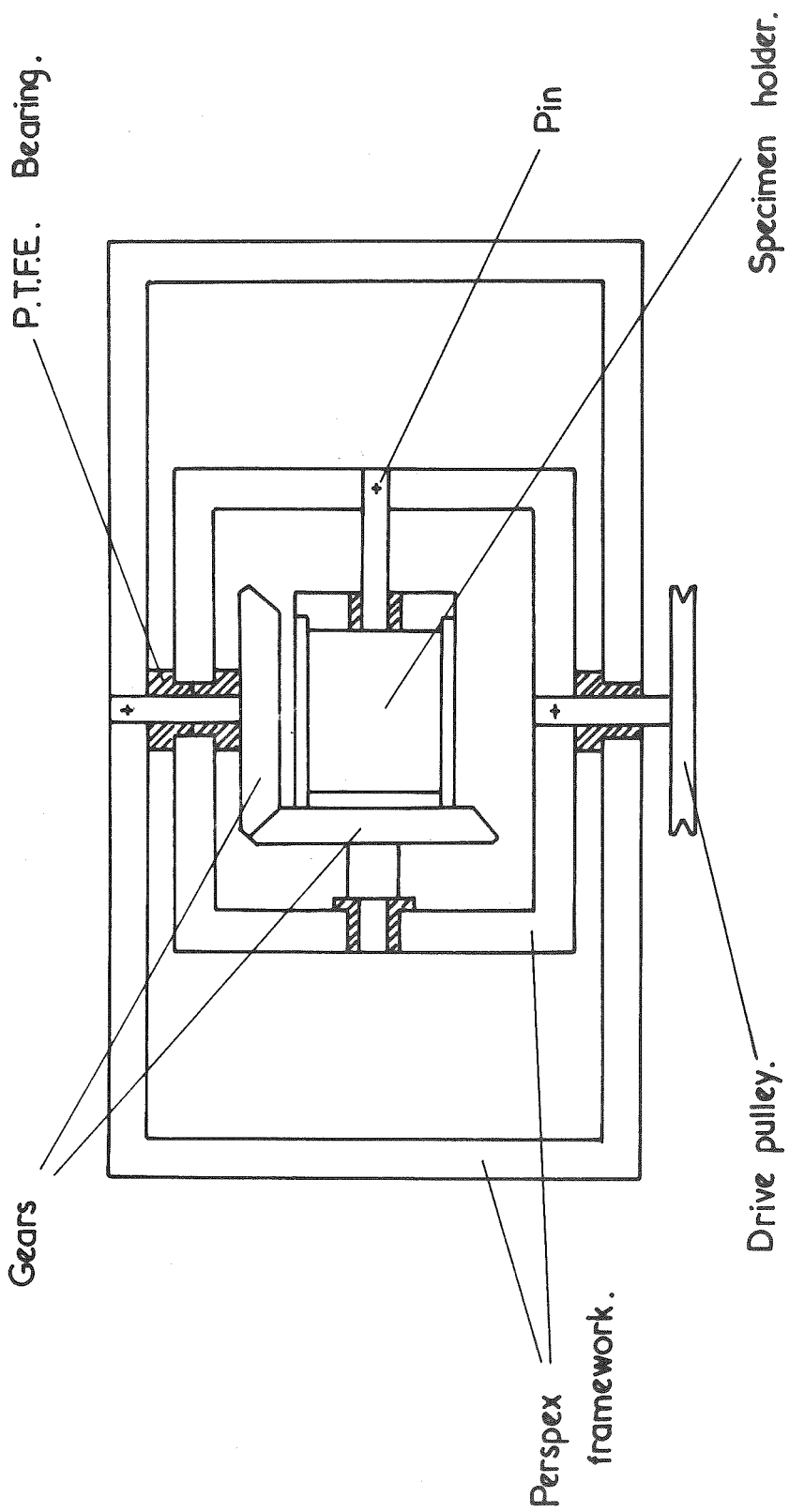
P.T.F.E. Bearing.
Pin
Specimen holder.
Gears
Perspex framework.
Drive pulley.

Figure 13.

3. ESTIMATION OF THE ANCIENT POLE POSITION

3.1 Calculation of the mean direction of magnetization of a rock formation

If measurements of the direction of magnetization are made on a number of specimens taken from a rock formation, the directions will not be parallel. The reasons for this and the method of obtaining the best value of the mean direction are discussed below.

Taking x, y and z axes respectively northwards, eastwards and downwards, the direction of magnetization of the r^{th} specimen is specified by its dip I_r which is the angle between the direction of magnetization and the x, y plane (measured positive downwards), and its declination D_r which is the angle between the x axis and the projection of the direction of magnetization on the xy plane (measured clockwise).

The xy plane for sedimentary rocks is the bedding plane so that the directions are referred to the horizontal at the time of deposition and in this way correction is made for the effect of folding. This assumption that the deposits were originally horizontal will lead to errors in individual observations, but will not affect the mean of a large number of determinations.

The direction cosines l_r, m_r, n_r of the direction of the magnetization of the r^{th} specimen are given by

$$lr = \text{Cos } D_r \text{ Cos } I_r$$

$$mr = \text{Sin } D_r \text{ Cos } I_r$$

$$nr = \text{Sin } I_r$$

An estimate of the mean direction of magnetization (specified by I and D) of a rock formation is obtained by taking an average of the vector direction observed at B sites, W samples being taken at each site.

For the optimum use of a given number of samples it is desirable that they should be spaced evenly through the thickness and areal extent of the rock formation so that W = 1. In practice because of the rarety of suitable rock types or poor exposures, several samples are obtained at each of a limited number of sites. The details of this sampling procedure have been given by Watson and Irving (1957). Usually the W sample directions at each site are averaged to give the site mean direction, and the formation mean direction is obtained by averaging the B site means. The method of averaging the site mean vectors is now given. Fisher (1953) has suggested that the site mean directions will, when regarded as points on a unit sphere, be distributed over the sphere with the probability density.

$$\frac{\kappa}{4\pi \text{ Sinh } \kappa} e^{\kappa \text{ Cos } \psi}$$

where ψ is the angle between the true mean direction of the formation and that of the site.

The parameter κ determines the dispersion of the points. This distribution was suggested by Fisher (1953) and has been shown to fit palaeomagnetic data by Watson and Irving. Fisher showed that the best estimate (l, m, n) of the true direction is the mean of the direction cosines (l_r, m_r, n_r,) that is:

$$l = \sum_{r=1}^{B} \text{Cos } D_r \text{ Cos } I_r / R$$

$$m = \sum_{r=1}^{B} \text{Sin } D_r \text{ Cos } I_r / R$$

$$n = \sum_{r=1}^{B} \text{Sin } I_r / R$$

Where

$$R = \left(\sum_{r=1}^{B} l_r^2 + \sum_{r=1}^{B} m_r^2 + \sum_{r=1}^{B} n_r^2 \right)^{\frac{1}{2}}$$

Fisher also showed that the best estimate k of of κ is given by,

$$k = \frac{N - 1}{N - R}$$

Where reversals occur amongst a group of site mean directions these are averaged without respect to sign, that is Cos ψ in the equation is replaced by | Cos ψ|

The mean dip and declination of a rock formation is given by

$$\text{Tan } I = n / (l^2 + m^2)^{\frac{1}{2}}$$

$$\text{Tan } D = m / n$$

An indication of the accuracy of the estimate (l, m, n) is now required. This may be specified by the semi-vertical angle of the cone about (l, m, n) such that the probability

of the true mean direction lying outside it is P. If c is the cosine of this angle, Fisher showed that,

$$c = 1 - \frac{B - R}{R} \left(P^{-1/B-R} - 1 \right)$$

The method described above is the simplest way of combining palaeomagnetic observations. An alternative method of analysis has recently been suggested by Watson and Irving (1957) whereby the data are more fully utilized. In this discussion it is assumed that W_i samples are taken from the i^{th} of B sites, the sites being spaced uniformly through the thickness and areal extent of the formation; and further that the observations within the i^{th} site obey Fisher's distribution with precision ω and the mean site direction varies from site to site with precision β about the overall mean direction. The formation mean direction may be estimated by the direction of the vector resultant of all the ($N = \Sigma W_i$) observations or as the direction of the vector resultant of B site mean directions.

For igneous rock formations in which ω is constant and whose magnetization is uniform, estimates $\hat{\omega}$ and $\hat{\beta}$ of ω and β may be found by using the analysis of dispersion given by Watson (1956). The observations must first be reduced to give the lengths of the vector resultants at each of the sites $R_1, R_2 \ldots\ldots R_B$, say, and the length of the resultant of all the $N = \Sigma W_i$ observations, R say. These numbers may then be used to complete the analysis of dispersion table.

Source	Degrees of Freedom	Sum of Squares	Mean Square	Expectations of mean squares
Between sites	$2\,(B-1)$	$\Sigma R_i - R$	$\dfrac{\Sigma R_i - R}{2\,(B-1)}$	$\frac{1}{2}\left(\dfrac{1}{\omega} + \dfrac{\overline{W}}{\beta}\right)$
Within sites	$2\{\Sigma\,(W_i - 1)\}$	$\Sigma\,(W_i - R_i)$	$\dfrac{\Sigma\,(W_i - R_i)}{2\Sigma\,(W_i - D)}$	$\frac{1}{2}\ \dfrac{1}{\omega}$
TOTAL	$2\,(N-1)$	$N - R$		

$$\overline{W} = \frac{1}{B-1}\left(N - \frac{\Sigma W_i^2}{N}\right)$$

and is the weighted average of the W_i; if all $W_i = W$, $\overline{W} = W$. The significance of the between-site variation may be judged by an F test. If the result is significant, estimates $\overset{\Lambda}{\omega}$ and $\overset{\Lambda}{\beta}$ may be found by equating the mean squares to their expectations and solving the resulting equations; otherwise between site variation may be ignored, i.e. $\beta \approx \infty$

If the direction of the resultant of all the N observations is used as an estimator of the direction of magnetization of the rock formation, it will be distributed approximately in Fisher's distribution with a precision k given by

$$k = \frac{1}{(\overset{\Lambda}{\omega}\ N)^{-1} + (\overset{\Lambda}{\beta}\ B)^{-1}}$$

The semi-angle α of the cone of confidence for probability

P may be then found from the equation

$$1 - \text{Cos}\ \psi_o = \frac{-\log_e (\text{probability}\ \ \psi > \psi_o\ \ )}{\kappa}$$

a formula which gives with good accuracy the probability that any direction in the distribution described by (1) will make an angle of ψ_o or more with the true mean direction.

Actually the result of an F-test for the original results for the Older Volcanics (Appendix 3) would indicate that estimates of ω and β may be found by equating the mean squares to their expectations. After cleaning, F better approaches unity, when unstable components of magnetization have been removed. (Appendix 4)

3.2 Calculation of pole position.

The statistical treatment of results from collection sites scattered throughout the thickness of a rock formation ensures that it is always the mean dipole field direction which is determined.

The axis of the mean dipole field in which the magnetization was acquired may now be calculated.

The declination D gives the direction of the former pole, and the dip I is related to the former geomagnetic latitude p by the equation of a line of force of a dipole field, namely:

$$\text{Cot}\ p = \tfrac{1}{2} \text{Tan}\ I.$$

The colatitude and longitude θ_1 and ϕ_1 of the former pole

and antipole in present day geographical coordinates may be obtained by solution of the appropriate spherical triangles from the formulae

$$\text{Cos } \theta_1 = \text{Cos } \theta \text{ Cos p} + \text{Sin } \theta \text{ Sin p Cos D}$$

and

$$\text{Sin } (\phi_1 - \phi) = \frac{\text{Sin p Sin D}}{\text{Sin } \theta_1}$$

where θ and ϕ are the geographical colatitude and longitude of the sampling area.

The direction of magnetisation has an error α in both dip and declination so the error δp in p is given by the equation

$$\delta p = \tfrac{1}{2} \alpha (1 + 3 \text{ Cos}^2 p)$$

and the error δm in the direction at right angles to the colatitude is

$$\delta m = \frac{\alpha \text{ Sin p}}{\text{Cos I}}$$

Thus, δm and δp are the semi vertical angles of the oval area around the average pole position within which the true pole lies at a probability of 1 - P. The errors in direction α, and in pole position δm and δp will always be specified at P = .05.

The occurrence of reversals of course introduces an ambiguity in the sign of the pole.

4. PALAEOMAGNETISM OF PRECAMBRIAN ROCKS FROM SOUTH AUSTRALIA

4.1 Introduction

As has already been mentioned in 1, the writer carried out, in August 1958, a preliminary palaeomagnetic survey of some Precambrian rocks in S.A. These were the chocolate slates and sandstones of the Hallet Cove area, a 2,000' thickness near the top of the Marionoan Series of the Adelaide System.

The Marinoan Series is characterized by red-bed conditions which followed the widespread Sturtian glaciation. In the Adelaide area the red bed conditions commence almost exactly at the base of the series.

While more particular attention was paid to the red beds, several samples were also collected from the Tapley Hill laminated slates which are part of the Sturtian Series which lie just below the Marinoan Series and which probably represent the metamorphosed varves associated with the Sturtian Glaciation.

Specimens from these rocks were prepared in Adelaide, 4-5 discs were cut from each of the samples but because of the very weakly magnetic nature of these rocks, it was not possible to carry out any measurements of their magnetic properties at Adelaide. The writer spent several weeks in Canberra at the Department of Geophysics, A.N.U., where use of the sedimentary magnetometer was made available.

4.2 Description of the Apparatus at Canberra

4.2.1 Introduction

The magnetometer at Canberra is basically similar to the one at Adelaide which has already been described in 2.1. It is however much more sensitive and the vertical degaussing system is a Fanselau coil system rather than Helmholtz. The measuring procedure is also somewhat different. The apparatus in this respect is rather more similar to that described in a paper entitled "The measurement of permanent magnetization of rocks," by Collinson et al, which appeared in the Philosophical Transactions of the Royal Society of London (1957).

4.2.2 Measurement of direction of magnetization with Canberra Apparatus

Suppose that the axes of cylindrical co-ordinates (Z, r, θ) are fixed in the disc such that the direction OZ was the upward direction of the vertical, and $\theta = 0$ the present geographical north at the time of the formation of the rock.

Assuming the disc to be uniformly magnetized, the horizontal component of magnetic intensity M_H produces a horizontal field on the axis in the direction θ given by

$$h = M_H \cos(\theta - D)/Zo^3$$

Where v is the volume of the disc and $Zo^2 = a^2 + Z^2$, where a is the radius of the disc. The vertical compoment M_Z of the intensity is equivalent to a spherical

magnetic shell, bounded by the periphery of the disc, of strength $M_z t$, where t is the thickness of the disc. Thus at a distance Z along its axis, the potential is

$$vM_z (Z_o - Z)/aZ_o$$

and as the field is solenoidal

$$\frac{dh}{dr} = \frac{1}{2} \frac{dh_z}{dz}$$

$$= \frac{3v \quad Mz.Z}{Z_o^4 \quad Z_o}$$

Where hz is the vertical component of the field.
An on-centre curve is obtained by plotting the deflection of the magnetometer when the axis of the disc and magnet system coincide, against the azimuth θ , which is the angle between the plane of the magnets and the plane $\theta = 0$ in the disc. The phase of the curve gives D. From the amplitude do of the curve, M_H can be determined

$$M_H = \frac{S \, d_o \, Z_o^3}{v}$$

Similar curves are obtained when the axis of the disc and of rotation is displaced a small distance dr to either side of the axis of the magnet system. The vertical displacement d of this curve from the previous one gives, M_z,

$$M_z = S \, Z_o^5 \, d/_3 \, v \, Z \, dr$$

On inverting the rock disc in the "on centre" position and measuring θ in the opposite sense, the same curve should be obtained. It is commonly found, however, that the

"upright" and "inverted" curves though sinusoidal have different amplitude and phases, and that the vertical displacements of the curves when the disc is moved from the west and east positions in its upright and inverted positions are unequal. This must arise from non-uniformities in the intensity of magnetization.

4.3 Collection and measurement of samples

Directions of magnetization of the discs measured relative to the horizontal, and then corrected for the dip of the bedding are given in Appendix 6.

Site directions from these measurements are plotted in figures 14, 15, 16. The directions corrected for bedding are in figures 17, 18, 19.

It is seen from both of these sets of results that there is no straight-forward interpretation to be placed on these results. The possibility that the area was too complicated structurally seemed to be the likely explanation for the disappointing results obtained, and for this reason the investigation was not persevered with. Other influencing factors were of course the fact that the rocks are only very weakly magnetic and the apparatus available at Adelaide was nowhere near sensitive enough for accurate measurements to be carried out on the rocks, so that as explained in 1, it seemed at the time that the sensible thing to do was to carry out investigations on rocks whose properties could be measured with the magnetometer at Adelaide.

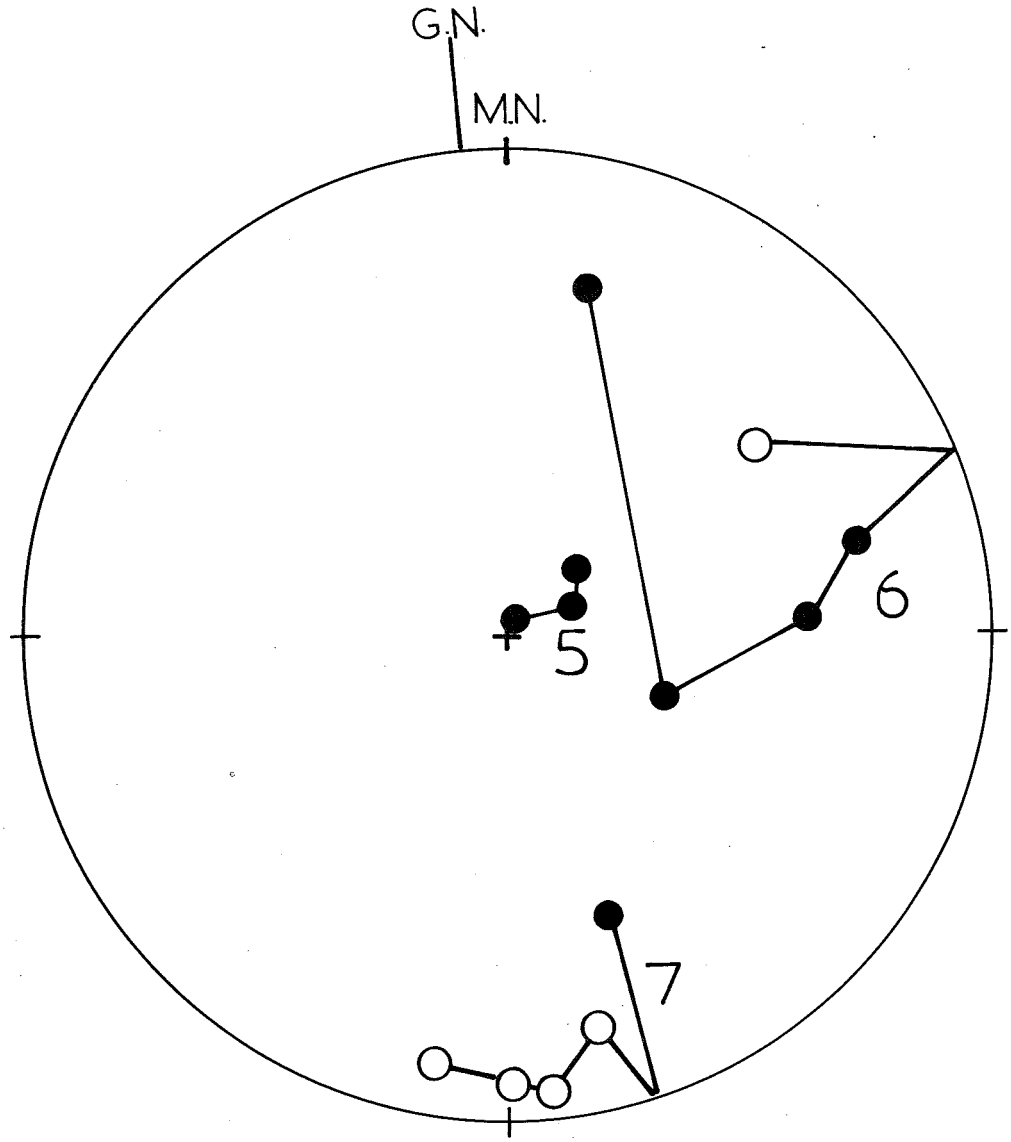

5,6,7 rel. to horizontal plane.

Figure.14.

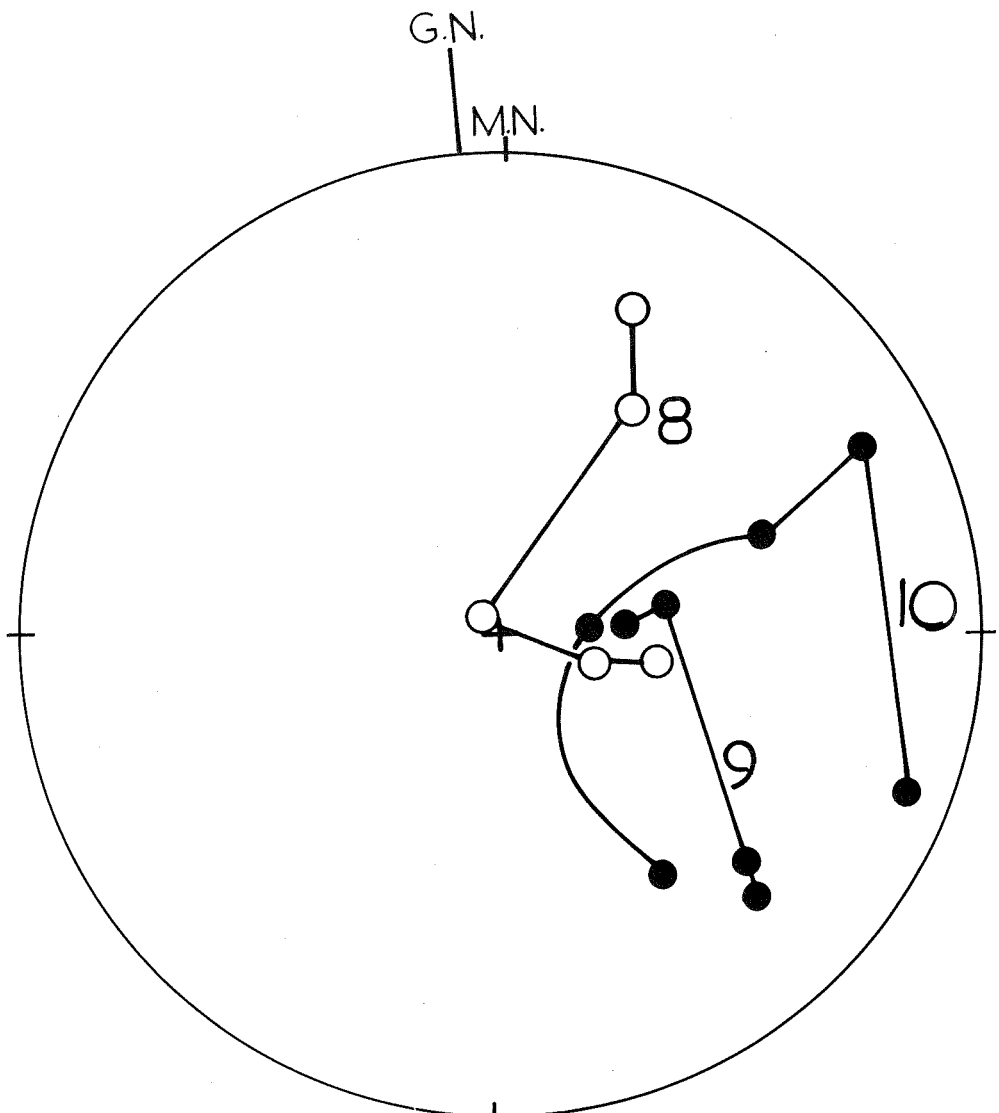

8,9,10 rel.to horizontal plane.

Figure.15.

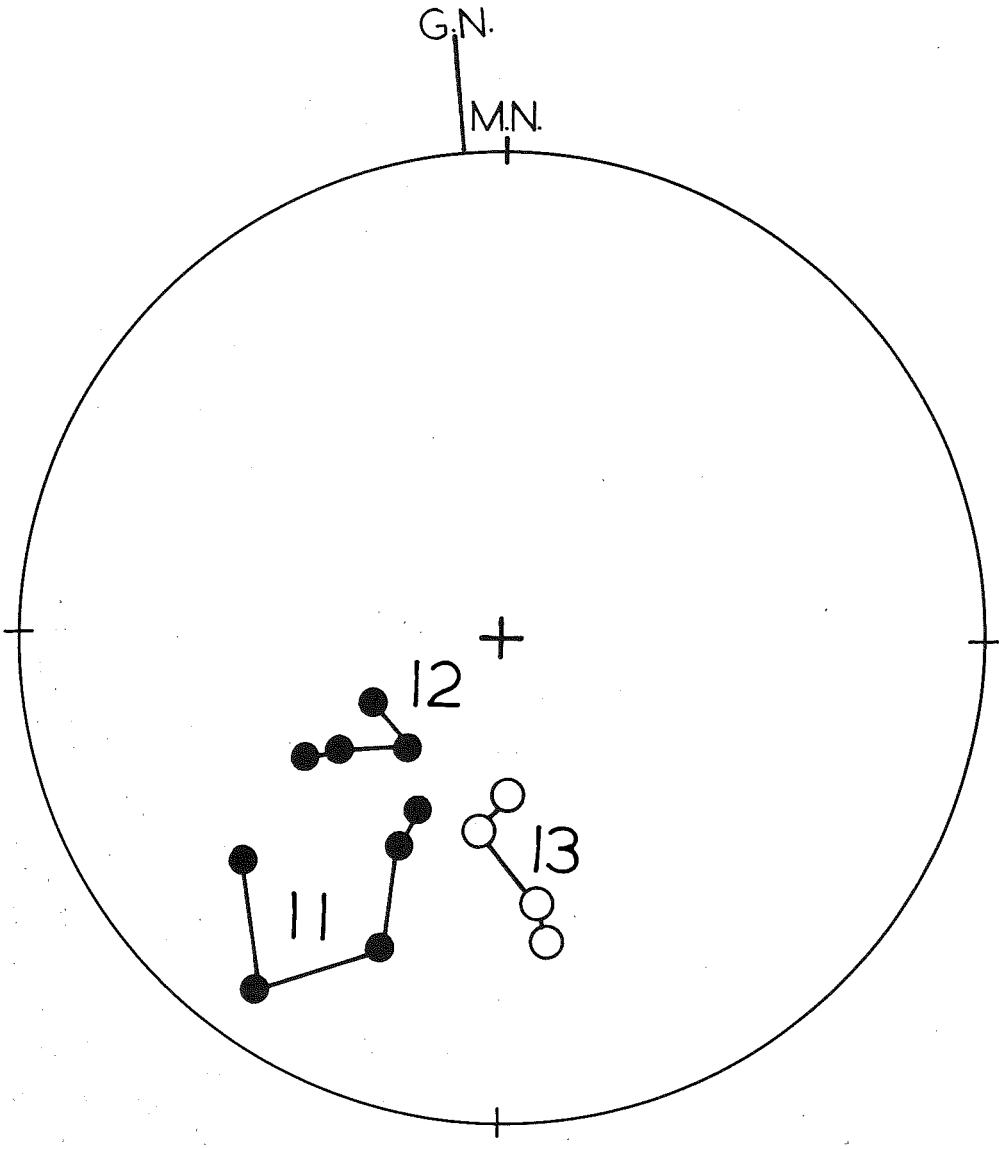

11,12,13 rel. to horizontal plane.

Figure.16.

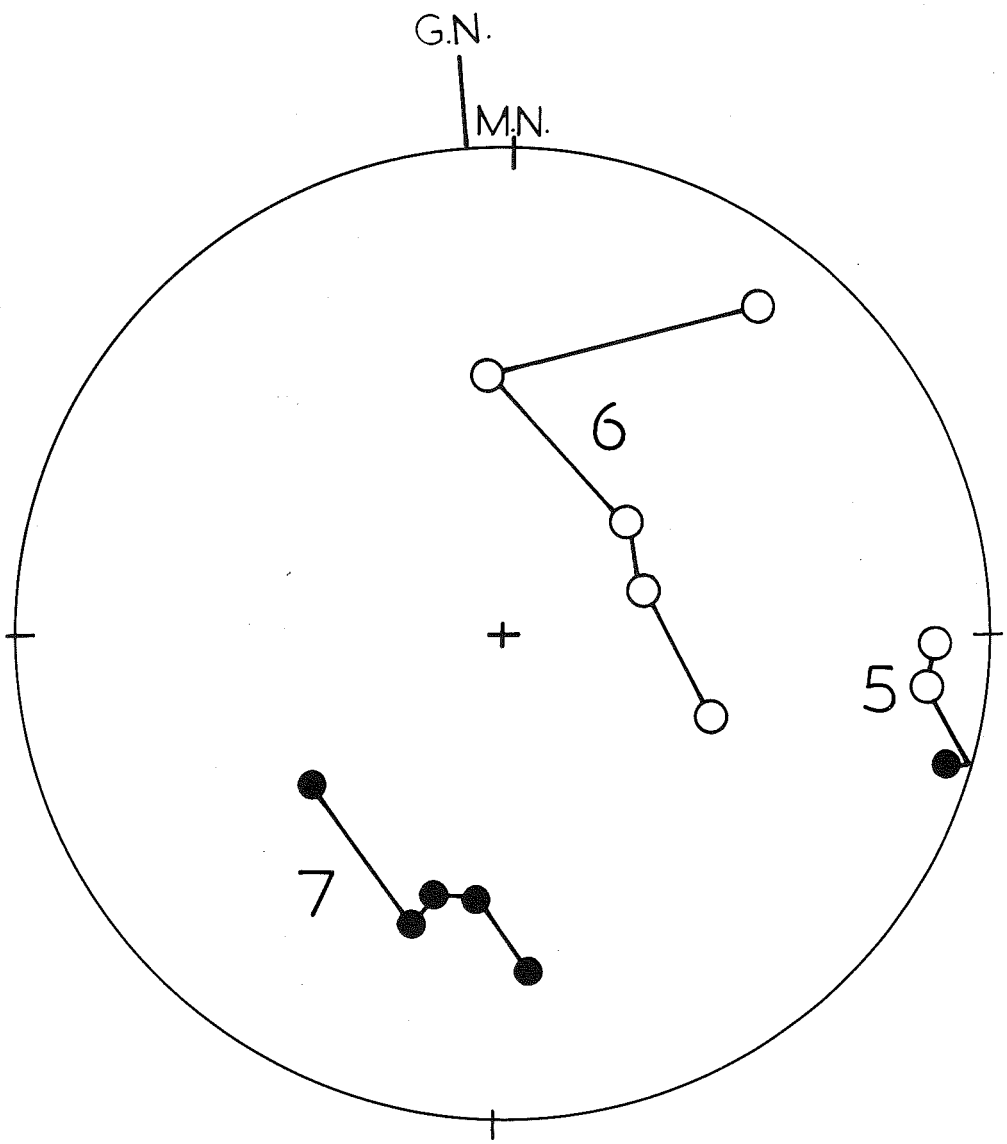

5,6,7 rel. to bedding plane.

Figure. 17

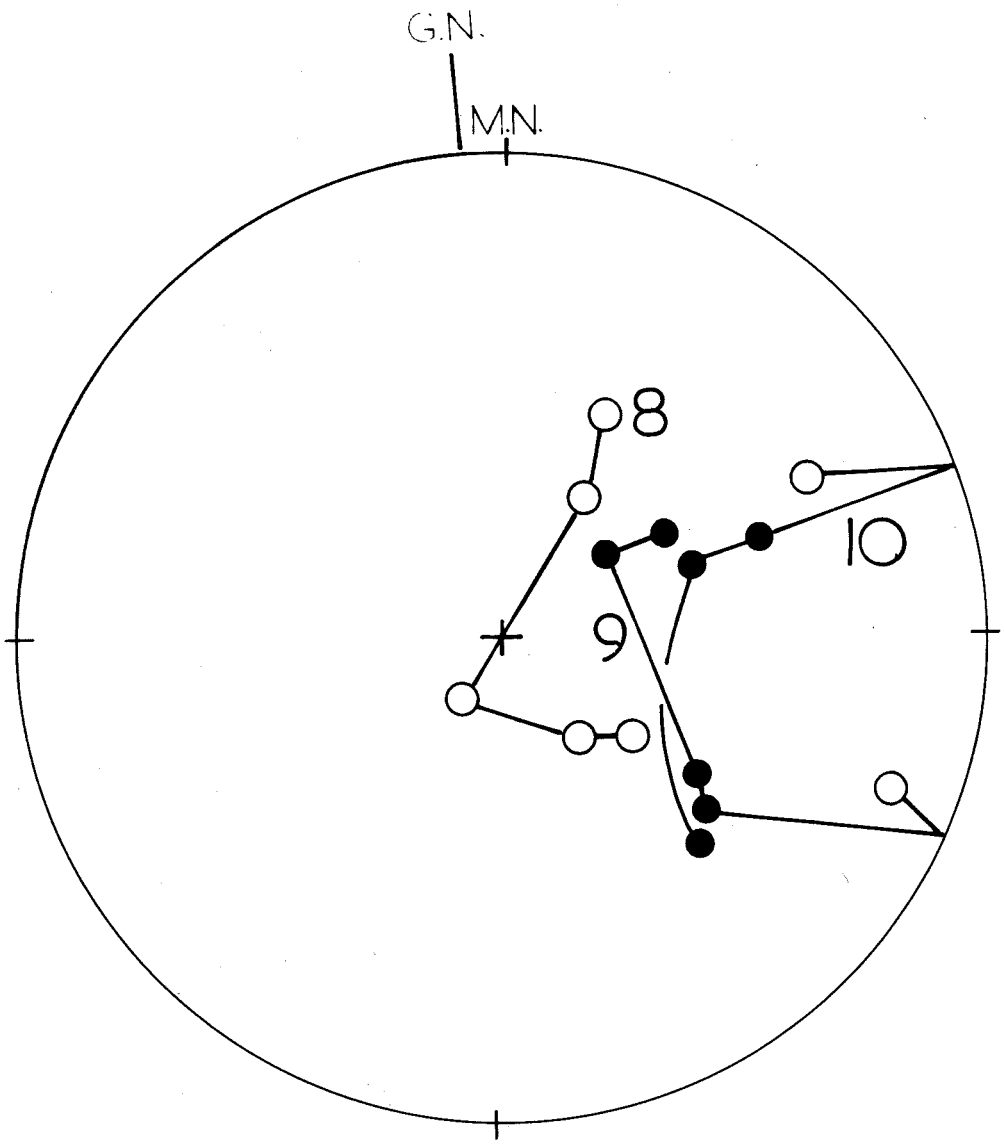

8,9,10 rel. to bedding plane.

Figure.18.

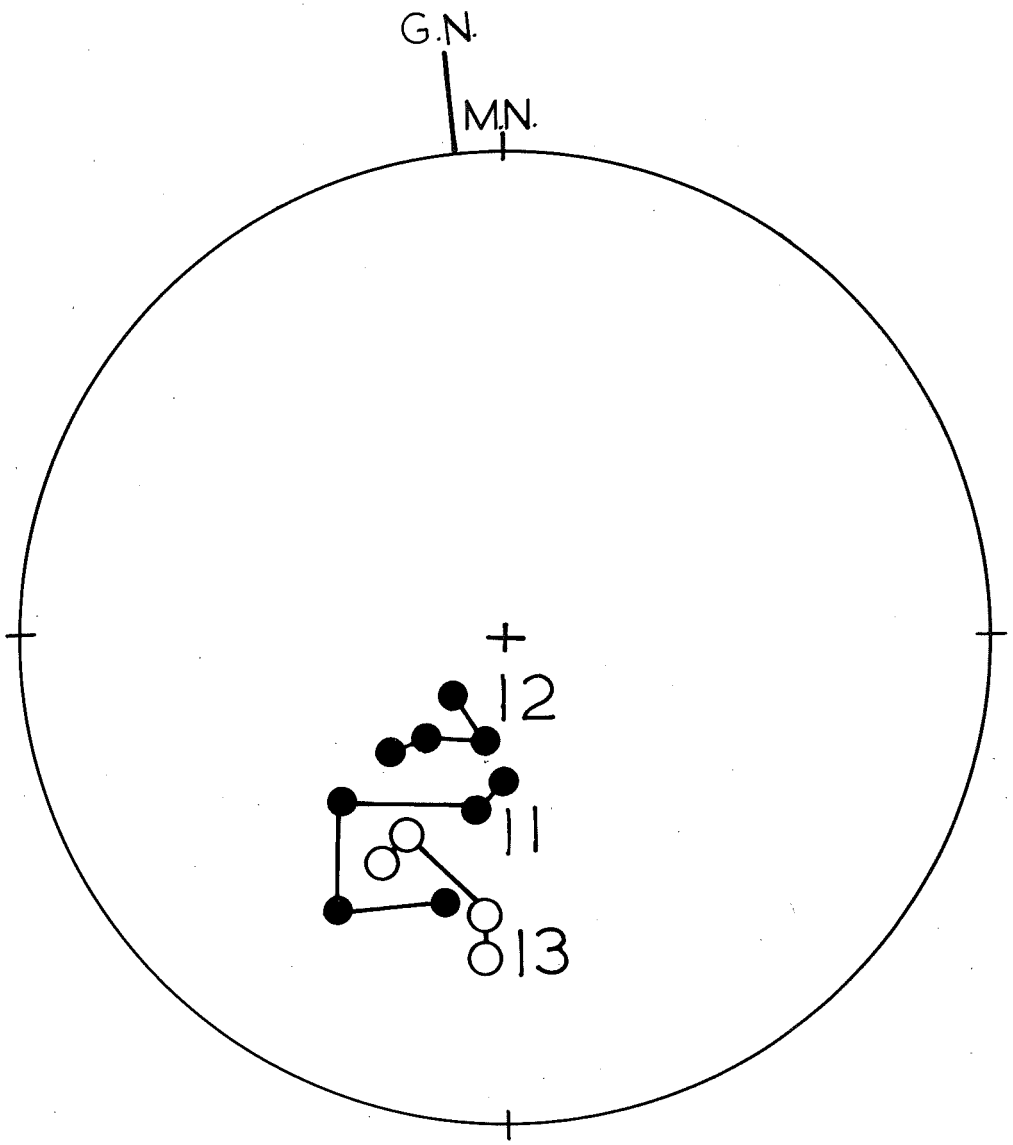

11,12,13 rel. to bedding plane.

Figure.19

Recently, however, Irving et al (1961) have shown how the viscous magnetization which is often imposed on rocks by the earth's magnetic field in geologically recent times causing the directions of magnetization measured in specimens from the same site to be strung out between the stable direction of magnetization and the present earth's field, may be removed by partial thermal demagnetization so that the initial planar distribution condenses around the direction of stable magnetization. The demagnetization is carried out in a non-magnetic oven following by cooling in zero field. It is possible that such a viscous magnetization is possessed by these rocks, and it could be removed by such experimental procedure. However, at the time when the writer first obtained these results such techniques were not available to him. The reversed directions could represent the remains of the originally stable direction of magnetization. This would agree with previous finding made on the Precambrian rocks in Australia reported on by Irving and Green (1958) which do have reversed directions of magnetization. See Table 2.

TABLE 2

Formation	Age	Mean direction of magnetization		
		D	I	α
Buldiva Quartzite	Top of upper Proterozoic	243	+38	12

(contd.)

TABLE 2 (contd.)

Formation	Age	Mean Direction of Magnetization		
		D	I	α
Nullagine Lavas	Upper Proterozoic	143	+64	8
Edith River Volcanics	Lower part of upper proterozoic	90	+48	18

5. THE PALAEOMAGNETISM OF THE OLDER VOLCANIC BASALTS OF VICTORIA

5.1 Introduction

It was thought that the re-investigation of the Older Volcanics would be useful, even though they had already been reported on by Irving and Green (1957), for the reason that this previous investigation had indicated that the inclination of the mean direction of magnetization of these rocks was only 13° greater than the earth's geocentric axial dipole field. In other words, these rocks record in Australia the first departure of the pole from its present position, and thus it was considered important to investigate more fully this important discovery.
The writer therefore resampled these volcanics at most of the sites which were reported on by Irving and Green, as well as collecting samples from several sites not previously sampled.

5.2 The geology of the Older Volcanics

The general division of the Tertiary lavas of Victoria into an Older Volcanic series (Miocene or earlier) and a Newer Volcanic series (Pliocene to Recent) was introduced by the early Geological Survey of Victoria. The division was based on the relationships of the lavas in the Port Phillip district to fossiliferous marine beds, and was then extended "by conjecture or analogy" to lavas in other parts of Victoria. The evidence for correlation was often doubtful and there

was little to indicate "whether the Older Basalts (Older Volcanic Series) were contemporaneous or part of a series of eruptions extending over a long period."

The Older Volcanic series includes both lava flows and dyke intrusions. These consist of practically identical rock types in somewhat different proportions and the distribution is somewhat different.

The rocks constituting the lava flows are Crinanites, titanaugite, dolerites, and basalts, several varieties of Olivene basalt and minor amounts of limbergites and nepheline and possibly acid alkaline rocks. Their age relations are well established in the Port Phillip district where they occur beneath fossiliferous marine beds of lower Miocene age. In South Gippsland the basalts pre-date the tertiary faulting and lie beneath the main seams of brown coal. This has been proved by diamond drilling at Warragul, Yarragon, Morewell, Boolara and Welshpool.

Stirling and Herman have shown that the deposition of the brown coals occurred intermittently over a considerably longer period than was required for the extrusion of the basalts, so that there are pre-basaltic, inter-basaltic and post-basaltic brown coals.

Similarly at Leongatha, seams of lignite 6" and 9" thick were found between basalt flows. The pre-basaltic and inter-basaltic brown coal seams are generally very thin, and never attain the great thickness of the post-basaltic brown coals.

The most extensive development of brown coal beneath the basalts in South Gippsland is at Elizabeth Creek, in Allambie East, where there is a seam 40 feet thick, while in the neighbourhood are seams 12 to 20 feet thick. The brown coals of the Latrobe Valley are generally regarded as of Oligocene or Miocene age. Similar brown coals at Parwan, Altona, Tyabb, Tanjil and in East Gippsland underlie fossiliferous Oligiocene or Miocene beds, while at Hedley near Gelliondale, brown coal is found beneath beds containing Pliocene fossils. On these grounds the basalts of South Gippsland should be Miocene or older. Sussmilch has claimed, however, that they "cannot be older than Lower Pliocene", but in the same paper he arrives at the conclusions that the uppermost beds of the Yallournian (i.e. brown-coal series) are possibly as young as lower Pliocene, which would still make the basalts at least as old as Miocene.
At Dargo, Darlimurla, Narracan, Berwick, Pascoe Vale, Flemington, Beenal, Grices Creek, Mahaikah, and Bacchus Marsh, the Older Volcanics are found associated with Tertiary leaf beds. These leaves have been referred to the Miocene, but are not generally accepted as affording a precise indication of age. Nevertheless, the similarity of the leaf remains does suggest a broad contemporaneity for the lavas associated with them. At Berwick the leaf beds overlie a bed of brown coal from 2 to 3 feet thick.

The other line of evidence as to the age of the Older Volcanic rocks, especially in East Gippsland, are the physiographic, which is described by Hills, and the petrological. Correlation on the petrological grounds tends to be regarded with suspicion, because rocks which originate by similar processes of differentiation must necessarily be generally similar in appearance and composition, even though formed at widely separated geological periods.

It often happens, however, that a group of consanguineous rocks will possess minor peculiar characteristics which readily distinguish it from another generally similar suite. This is fortunately the case in Victoria, where both the Older Volcanics and the Newer Volcanics suites contain types with distinctive features and of widespread occurrence, viz. crinanites and titanaugite -basalts in the Older Volcanics and iddingsite-basalts in the Newer Volcanics as well as other less marked differences.

Moreover, it has been found that the classification of such rocks as Newer Volcanic or Older Volcanic by their petrological characters agrees closely with determinations of their age by physiographic or stratigraphic methods.

5.3 Field Work

Fifty-three samples of Older Volcanic basalt were collected from twenty-one localities.

In Table 3 is a list of these localities.

TABLE 3.

Site No.	Locality	Specimen Number
1	Bayview Quarry	1, 2
2	Quarry at Drouin South	3, 4, 5
3	Jindivick Quarry	6, 7, 8
4	Tarago Quarry	9, 10
5	Jacobs Creek Quarry	11, 12, 13
6	State Electricity Commission Quarry, North of Yallourn	14, 15, 16
7	Paradise Creek Quarry	17, 18
8	Hillside Quarry	19, 20, 21
9	True Blue Quarry	22, 23
10	Quarry on Berries Creek Road	24, 25, 26
11	Quarry at Leongatha	27, 28, 29
12	Evans Quarry	30, 31, 32
13	Nobbies	33, 34, 35
14	Nobbies	36, 37
15	Nobbies	38, 39, 40
16	Nobbies	41, 42, 43
17	Kitty Millers Beach	44, 45
18	Pyramid Rock	46
19	Jennings Quarry	47, 48, 51
20	Beach near Jennings Quarry	49, 50
21	Cape Schlank	52, 53

Samples have been taken from as many sites as possible spread over the outcrop, with two or three samples taken at each to minimize experimental error. In this way, inhomogeneities due to the secular change of the geomagnetic

field and geological tilting are averaged out, and a wider regional picture is obtained than would otherwise be the case if the same number of samples were distributed among fewer sites.

What appeared to be fresh hand samples were collected in the above localities, which were mostly quarries. These hand samples were oriented by means of the small three legged levelling device described in 3.5, prior to their extraction from the rock face. Cylinders were machined from them with non-magnetic tools, orientation being preserved in the process. The diameter of the cylinders so prepared were 35 mm. and each was sliced into approximately five thin specimen discs which were then used for measurement.

5.4 Direction of magnetization on initial measurement.

The results of the initial measurement of the direction of magnetization of the discs prepared are given in Appendix 3. Mean site directions are given.

Figure 20 shows the direction of magnetization of the various sites, and using the method described by Watson and Irving, the measurement of these discs give the mean direction of magnetization shown in Table 4.

TABLE 4.

PRESENT INVESTIGATION			IRVING AND GREEN		
D (T.N.)	I	α	D (T.N.)	I	α
18½	-71	9	17	-73	7

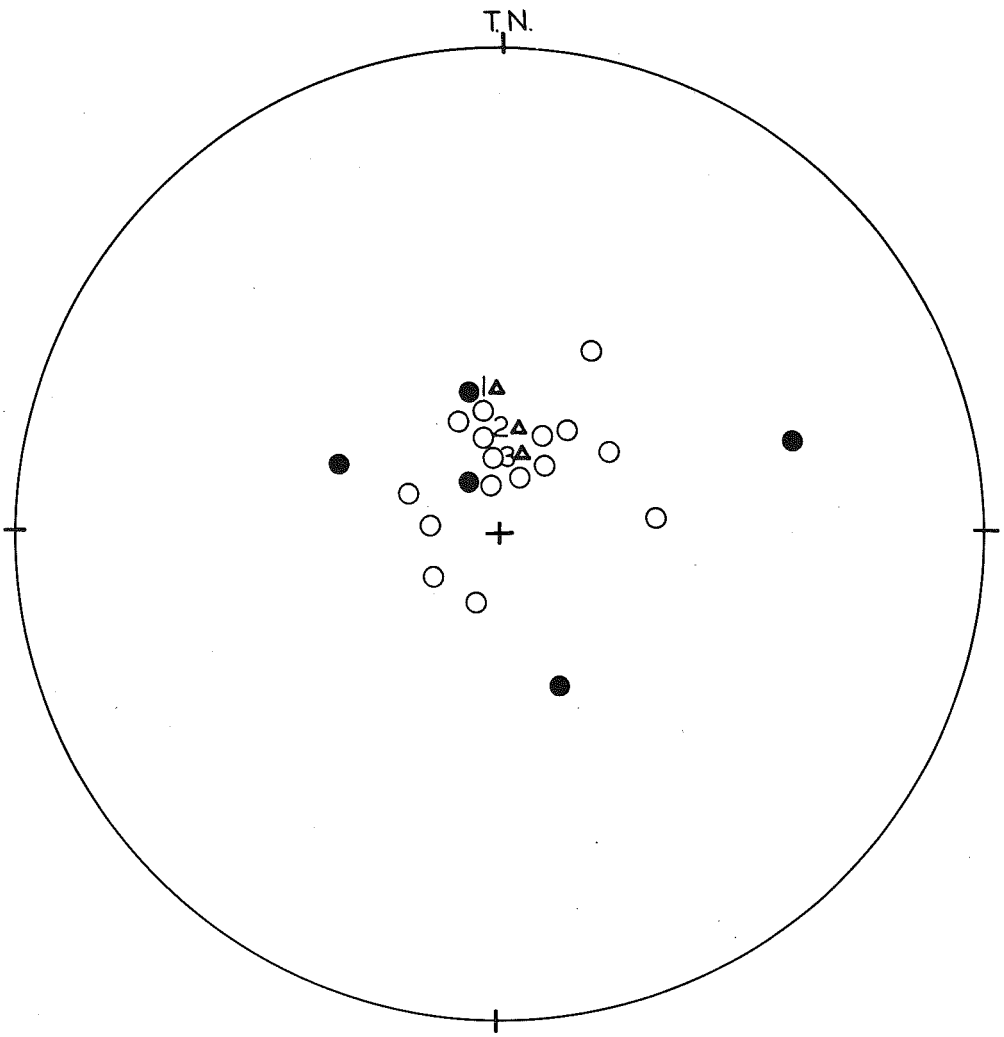

1△ Dipole field
2△ Present field
3△ Mean site direction

Figure. 2o.

These results seem to be in agreement with those of Irving and Green, in that the mean direction of magnetization is greater than expected if the rocks were magnetized in the direction of the present geocentric axial dipole field.

5.5 The result of remeasurement of the directions of magnetization.

In order to check the stability of the magnetization of these basalts, some 9 months after the original measurement the direction of magnetization of the rocks was remeasured. The two sets of results obtained for the initial measurement and the remeasurement are recorded in Appendix 3. The directions given are directions relative to the disc only.

From a comparison of the directions of magnetization obtained it became evident that there were differences between these two sets of results which could not be explained by the experimental errors involved in the measurements. In comparing the directions of magnetization on a stereographic projection, it became evident that while the individual directions of magnetization in some specimens may vary by values greater than would be expected from the experimental errors involved, the actual scatter of the directions of magnetization of the discs taken as a whole

did not vary noticably between the two sets of values obtained for each measurement.

For example, specimen No.1 gives a rather close grouping in the original measurement, while specimen No.36 gives a rather scattered groupihg. After re-measurement, the values of the direction of magnetization obtained for specimen No.1 give very nearly the same values of direction so that the grouping of the points is again very close. Specimen No.36 gives a rather scattered grouping of points on initial measurement, but while the individual directions of the discs vary by larger values than the experimental errors involved on re-measurement, the scatter of the directions of magnetization of the discs after this re-measurement is about the same as it was for the original measurement.

Figures 21,22,23,24,25 show initial and re-measured values of magnetization for specimens No.25,19,38,2,36. These observations naturally arouse interest in the question of why the scatter of the directions of magnetization of some discs as measured initially is greater for some rocks than it is for others.

5.6 Stability of magnetization

Following the investigation of 5.5 it becomes apparent that there is an instability present in these basalts and the writer therefore directed his attention to it. It was thought that an answer to the question proposed in 5.5

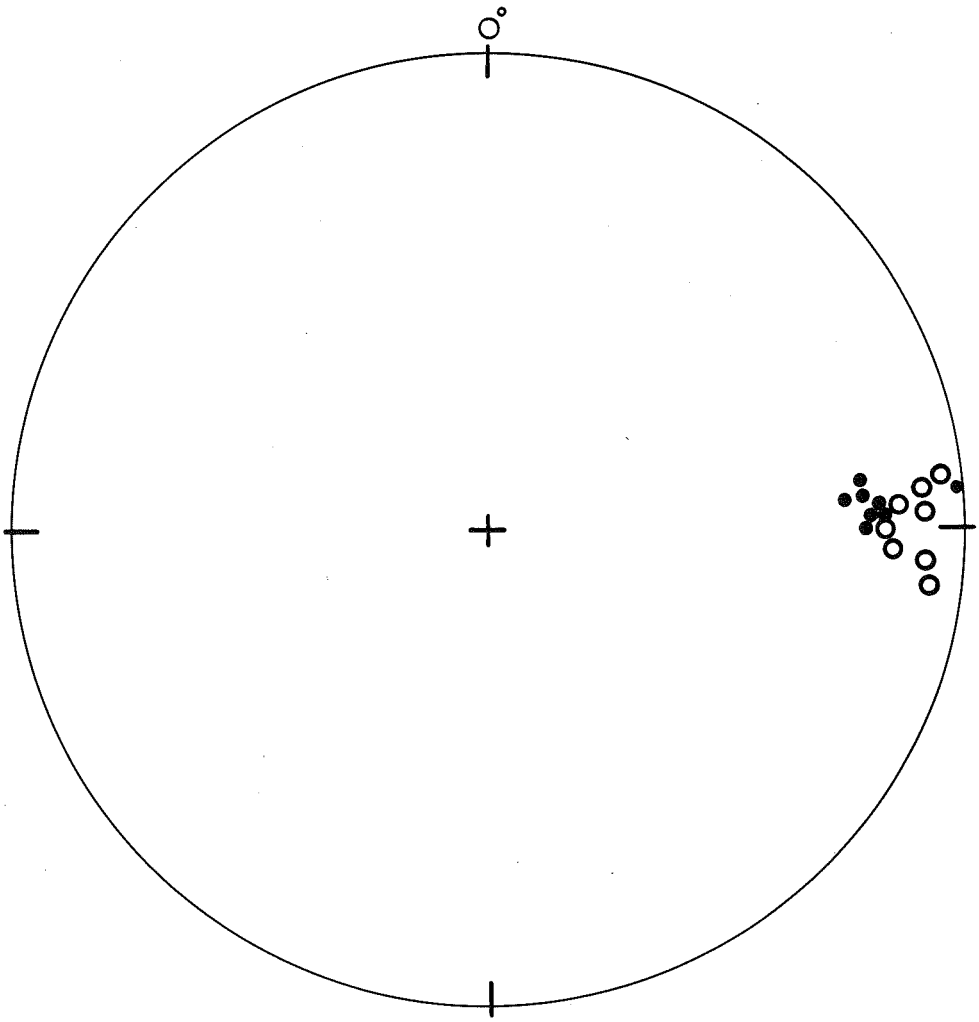

● Original directions.

O Remeasurement.

Specimen 25

Figure.21.

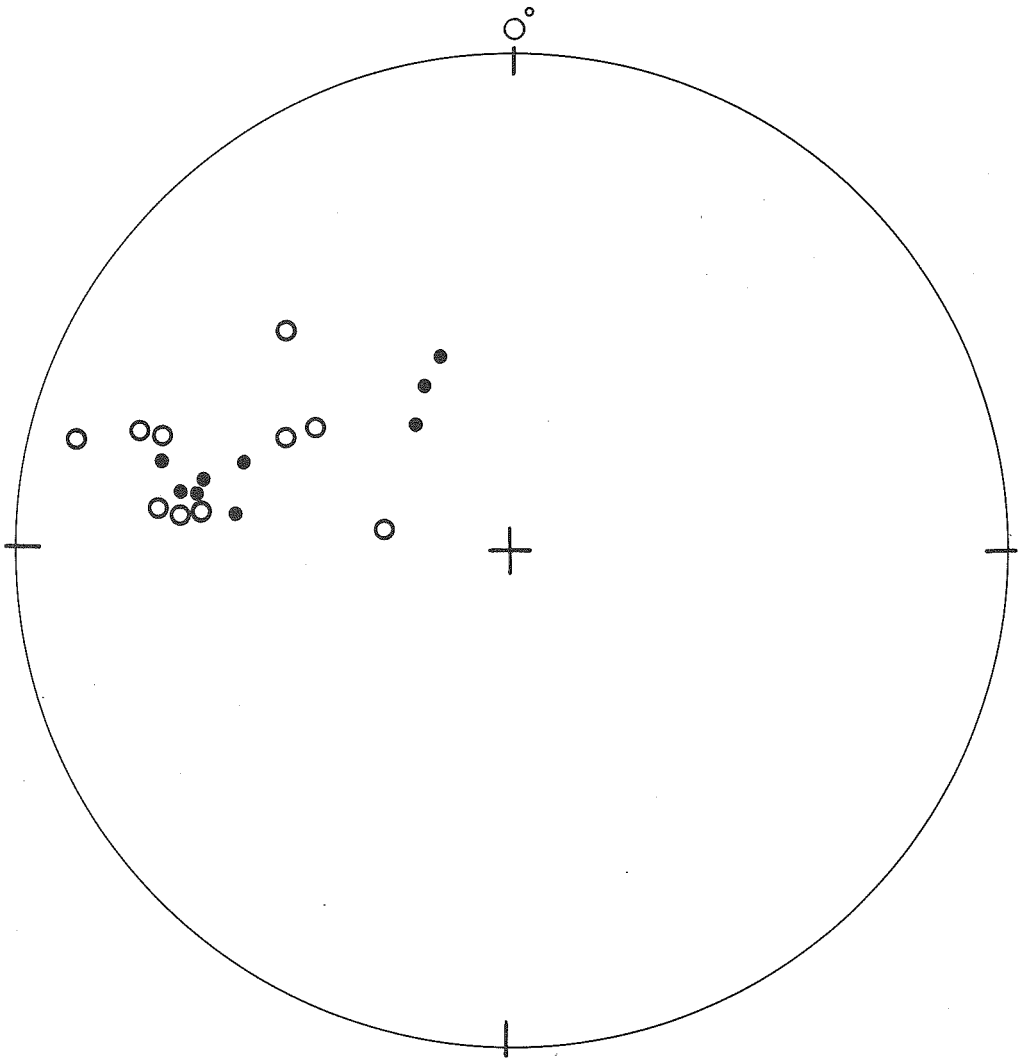

● Original directions
○ Remeasurement

Specimen 19

Figure.22.

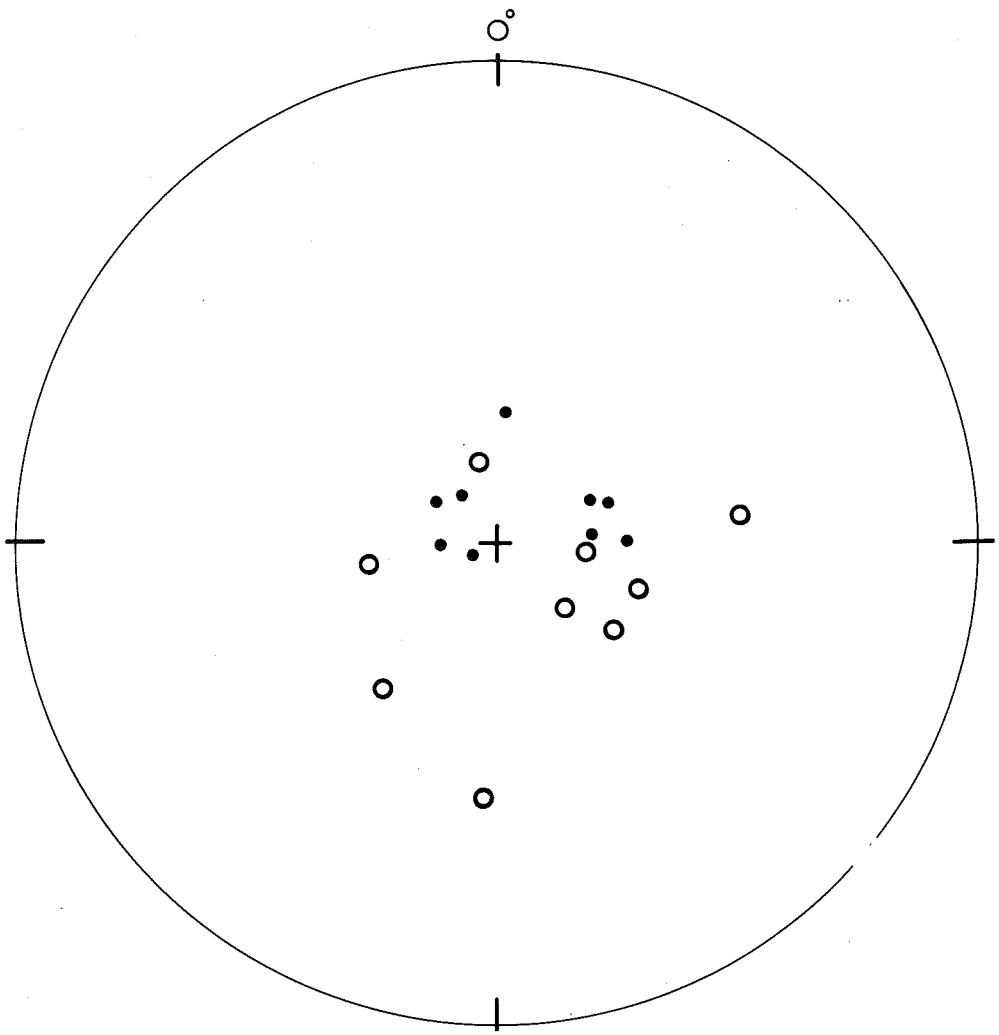

● Original directions.

○ Remeasurement.

Specimen 38

Figure.23.

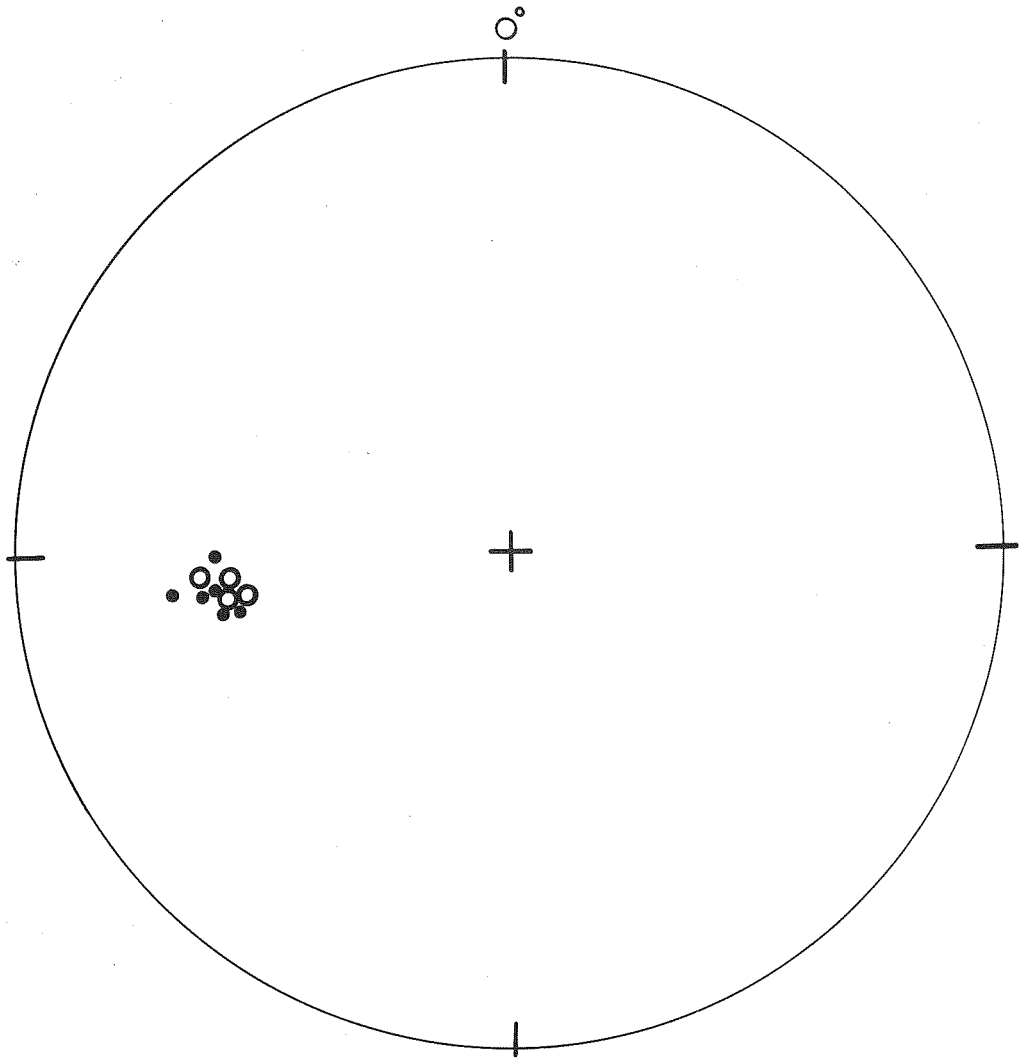

Specimen 2

Figure.24.

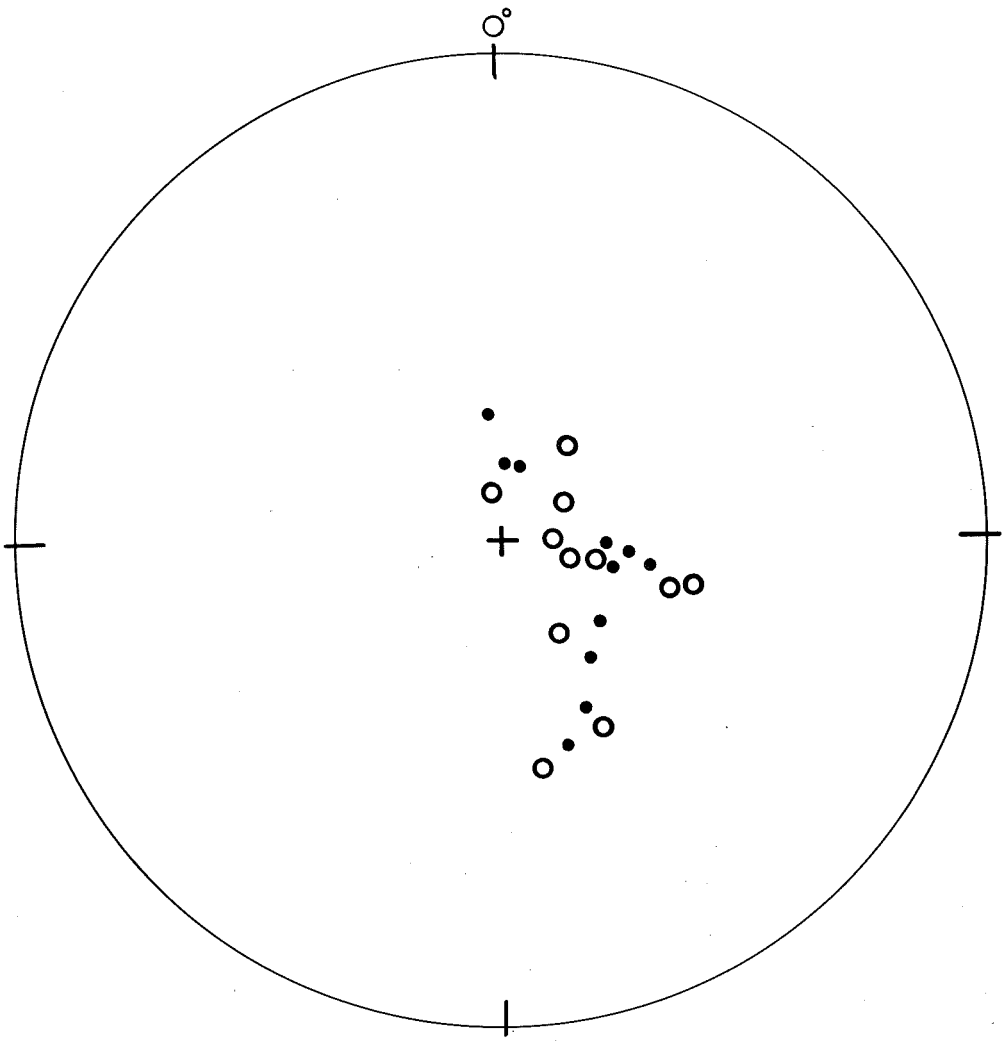

Specimen 36

Figure.25.

might be found if more was known about the magnetic minerals present in the basalts, and so the investigation of 6. was commenced.

5.7 A.c. magnetic field cleaning of the Older Volcanics.

5.7.1 Introduction

It has been shown above in 5.5 that instability of magnetization is present in some of the samples removed from these Older Volcanic basalts, so all the specimens were cleaned in an a.c. magnetic field to see what effect this cleaning would have on the mean direction of magnetization.

The apparatus used has been described in 2.

Two rock discs from each of the samples collected were used in the cleaning experiments. All the discs from any one site were cleaned progressively in fields of 43, 86, 129 and 173 oersted in order to obtain the distribution with minimum dispersion.

5.7.2 The results of a.c. cleaning on the mean direction of magnetization

The direction of magnetization after cleaning in these various fields are given in Appendix 4 and it is seen that within site dispersion was improved by the cleaning in some cases only.

The mean direction of magnetization after cleaning is given in Table 5.

TABLE 5.

DIRECTION OF MAGNETIZATION AFTER A.C. CLEANING			RESULT OF IRVING AND GREEN		
D (T.N.)	I	α	D (T.N.)	I	α
6	-77	9	17	-73	7

Mean site directions after cleaning are shown in figure 26.

5.7.3 Pole position

The pole position using this mean value of magnetization obtained after the cleaning experiments is

63 South
140 East

In figure 27 this pole position is plotted together with the pole for:

(1) The Newer Volcanics of Victoria
(2) The Older Volcanics of Victoria obtained by Irving and Green.
(2) The Older Volcanics of Victoria obtained by this present investigation
(3) Tasmanian dolerite sills
(4) Kuttung volcanics
(5) Kuttung Sediments

This value of the pole position compares very closely with that obtained for the Tertiary Volcanics in N.S.W., which were examined by Irving et al (1961). The value of the pole position obtained for these rocks is

63 South
137 East

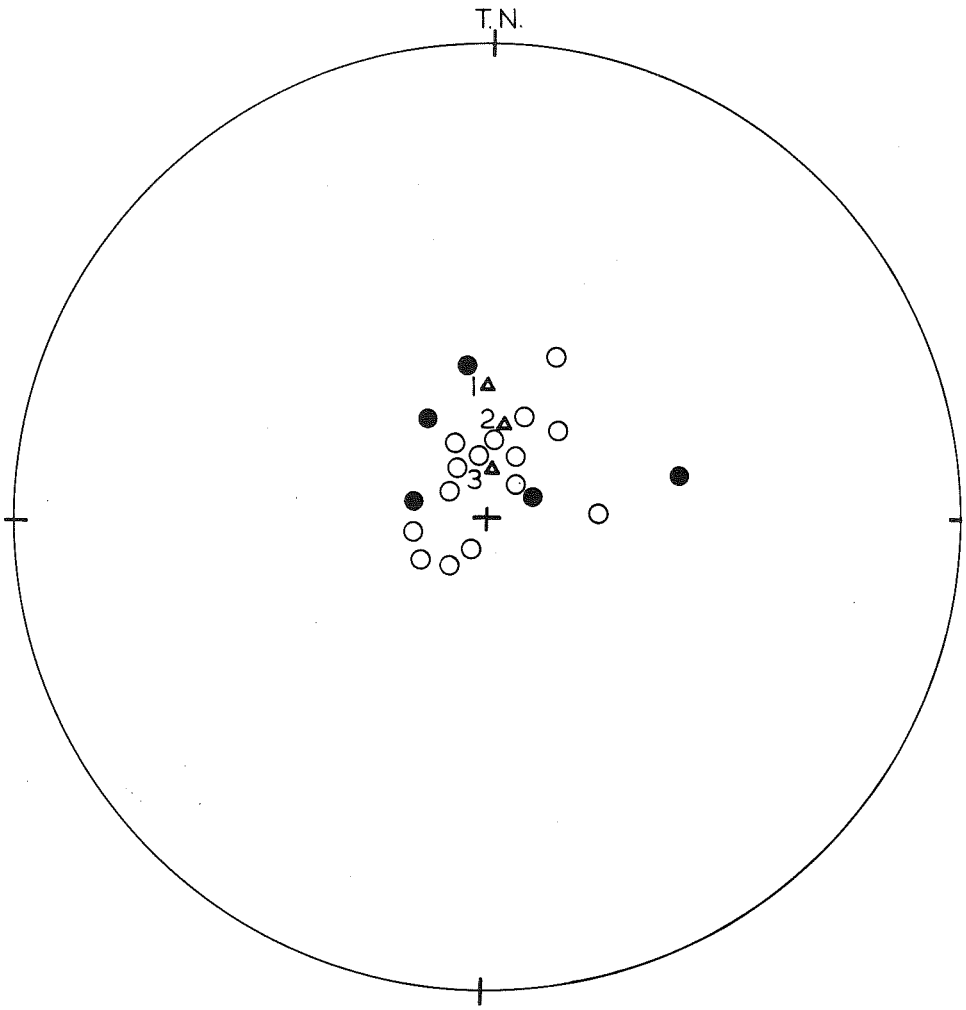

1△ Dipole field
2△ Present field
3△ Mean of site directions

Figure.26.

Figure 27.

The effect of the a.c. cleaning is therefore to remove unstable components of magnetization and the result is a mean direction of magnetization of greater inclination.

6. THE ORIGIN OF THE MAGNETIZATION OF THE OLDER VOLCANICS

6.1 Introduction

In order to understand more about the origin of the magnetism of these volcanic rocks, the writer carried out thermal demagnetization experiments on specimens taken from the samples collected. It was thought that this investigation would provide information as to the nature of the magnetic mineral responsible for the magnetic properties associated with the rocks. The thermal demagnetization apparatus was constructed late in 1959.

6.2 Thermal demagnetization experiments on rock specimens.

6.2.1 Introduction

Heating of rock specimens was carried out in an inert atmosphere of nitrogen. The method of introducing the nitrogen into the furnace is shown in figure 28. A manometer was used to indicate the presence of a small positive pressure inside the furnace. The standard specimen used in heating was a cylindrical one of height and diameter 22 mm.

In the introduction to theories of thermo-remanent magnetization (TRM) in single-domain and multi-domain grains, such as have been advanced by Neel (1955) and Stacey (1958), reference is made to the fact that Nagata (1953) found that while the ferromagnetic character of grains appears at their Curie temperatures, and spontaneous

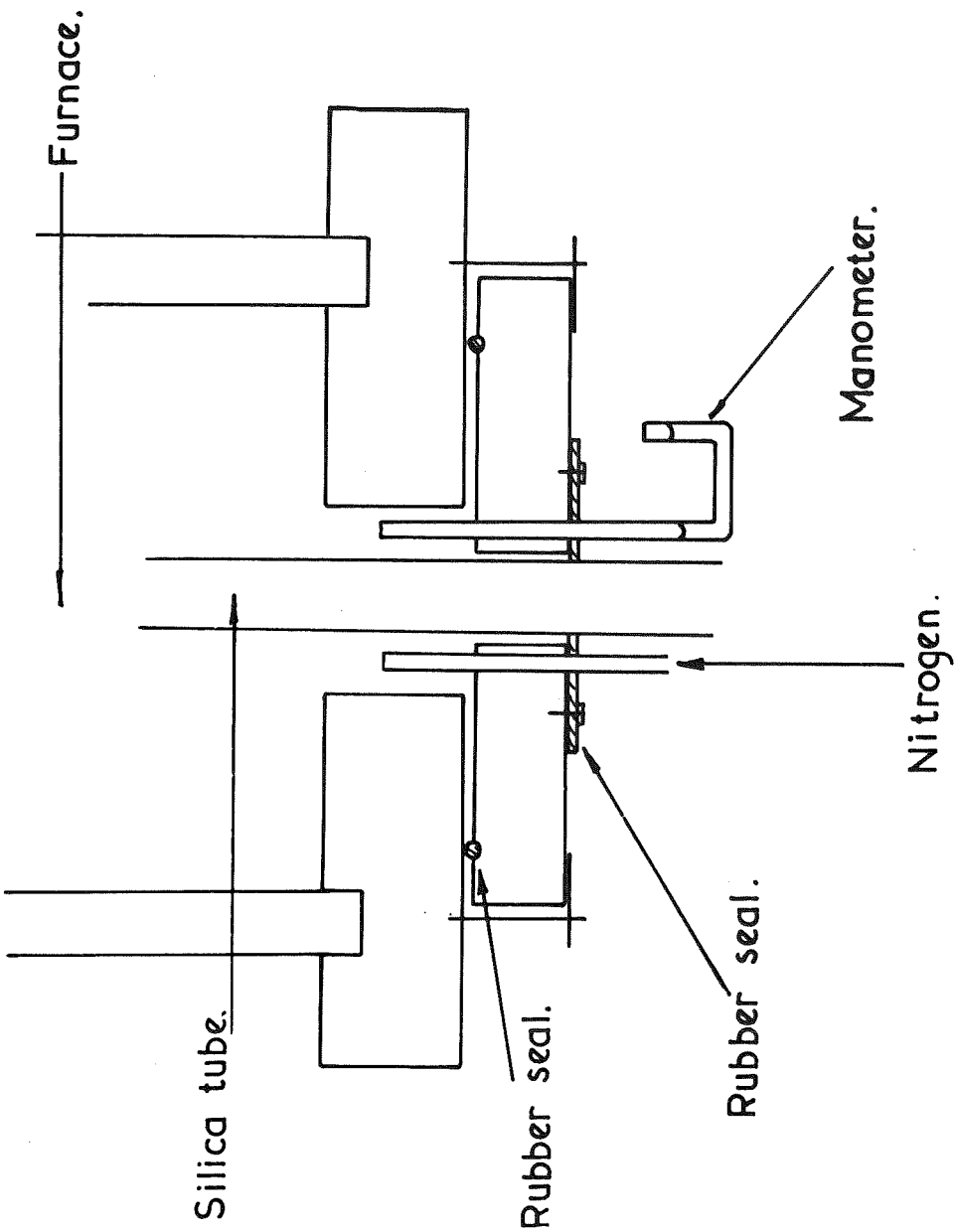
Furnace.
Manometer.
Nitrogen.
Rubber seal.
Rubber seal.
Silica tube.

Figure.28.

magnetization also occurred at these temperatures, it was evident from saturation magnetization measurements that the ability to retain induced moments is not reached until temperatures several tens of degrees lower still are reached.

Neel's theory shows that thermal agitation is responsible for preventing remanence above these lower temperatures which have been termed "blocking temperatures". The moment in a grain at its blocking temperature is "frozen in" by further cooling, and becomes thermo-remanent magnetization. Neel's theory is for single domain grains and he acknowledges that naturally occurring magnetic grains are much larger, and cannot be correctly considered as single domains.

Considering larger multi-domain grains, Neel obtained the expression

$$M(o) = 2 H + H_c^{\frac{1}{2}}/N$$

where H_c is the coercive force at room temperature and N is the demagnetizing factor. In this case TRM is proportional to $H_T^{\frac{1}{2}}$. However it is found experimentally that TRM is proportional to H rather than $H^{\frac{1}{2}}$ in very weak fields of the order of 1 oersted.

Stacey (1958) has presented a theory for thermo-remanence in multi-domain grains in which by proposing that at the blocking temperature crystalline anisotropy and

magnetostriction coefficients equal zero, and only magnetostatic effects control the magnetization, he shows that the magnetic moment at room temperature is given by

$$M(o) = \frac{H_T}{N} \frac{M_S(o)}{M_S(T)} \frac{1}{1 + N k_o}$$

where k_o is the susceptibility at room temperature and M_S is the spontaneous magnetization.

6.2.2 <u>The results of continuous thermal demagnetization in zero field</u>.

Typical curves obtained for heating specimens in zero field are shown in Appendix 5.

It is evident on examination of these curves that different thermal demagnetization properties are possessed by different rocks.

Among the specimens whose thermal demagnetization properties are given in Appendix 5 there are those which -

(1) were originally normally magnetized.

Nos. 6, 7, 31, 33, 36, 38, 41.

(2) were originally reversely magnetized.

Nos. 3, 19, 20, 21, 25, 26.

(3) gave close grouping of the directions of magnetization of the discs removed from one sample, and on remeasurement gave almost similar results to those obtained 9 months before, and so a similarly close grouping.

Nos. 3, 26, 21.

Table 6 summarizes in part the results given in Appendix 5.

TABLE 6

SITE	SPECIMEN	POLARITY	TEMPERATURE AT WHICH ZERO MAGNETIZATION IS ATTAINED
2	3	Reversed	505°C
3	6	Normal	440
	7	Normal	410
8	19	Reversed	450
	20	Reversed	405
	21	Reversed	430
10	25	Reversed	455
	26	Reversed	430
12	31	Normal	295
13	33	Normal	300
14	36	Normal	580
15	38	Normal	580
16	41	Normal	580

(4) gave rather scattered grouping of directions of magnetization of specimen discs removed from one sample, and on remeasurement gave results which differed from those of the initial measurement by values greater than would be expected on the grounds of experimental error in measurements.

Nos. 19, 36, 38

6.2.3 A discussion of the results of continuous thermal demagnetization in zero field

The writer in carrying out the thermal demagnetization experiments on specimens of Older Volcanic basalt, heated the specimens in a field free space, and by means of a magnetometer above the furnace, recorded the continuous variation of magnetization with temperature.

This being the case it is not entirely correct to refer to the point of final demagnetization of the specimens examined in later sections as the Curie temperature, but this is done in the light of the experiments described on pages 105, 106.

An examination of the thermal demagnetization curves obtained from many of the specimens, such as figures 89, 90, 91, 92, 96 for specimens 7, 7a, 19, 19a and 26 show the behaviour previously reported by Nagata, in that the rate of acquiring TRM is greatest at a temperature which is some degrees lower than the temperature at which final demagnetization takes place, and does in fact suggest to

the writer that the final point of demagnetization is the Curie temperature.

Also in figures 124, 125, 126 are shown the thermal demagnetization curves for specimens 33, 25 and 21 carried out in a vertical field of twice the value of the earth's vertical component of field. This was done by reversing the vertical field compensating coils of the Helmholtz system. The field in which the continuous thermal demagnetization was carried out was therefore a field of 1.12 oersted.

This experiment was done to see if it were possible to detect an induced magnetization which might exist through reason of the inducing field being present between a blocking temperature of the rock and the Curie temperature of the magnetic mineral it contains. Thermal demagnetization became complete at the same temperature in both cases of the heating in zero field and in the field of 1.12 oersted. Any magnetization induced by such a field at temperatures near the Curie temperature might be too small to detect, however, and this experiment need not be sufficient proof that the point at which thermal demagnetization becomes complete is the Curie temperature rather than a blocking temperature. In this experiment the specimen holder was moved to an off central position

to ensure that any vertical induced moment would produce a field at the magnet system.

Results which show that the temperature at which final demagnetization of the specimen takes place is very likely the actual Curie temperature, are given in figures 127, 128. These curves show the final portion of the thermal demagnetization curves of specimens which have been given an isothermal remanent magnetization (I.R.M.) in a field of 3,000 oersted. As can be seen from the thermal demagnetization curves, the point at which final demagnetization would occur is the same as that obtained by the thermal demagnetization of the N.R.M. which has been described above. The small discrepancy at the end of these curves is probably due to small amounts of high Curie point material in the rocks.

The results obtained from the four different types of specimen mentioned in 6.2.2 will now be discussed.

(1) Specimens numbered 6, 7, 31, 33, 38, 41, were all normally magnetized. The temperature at which final demagnetization occurs is variable between 300°C and 580°C, and there are single component and two component types present.

(2) Specimens numbered 3, 19, 20, 21, 25, 26, were reversely magnetized. Again the temperature at which final demagnetization occurred is variable, this time being between the limits 400°C and 500°C. There are no

multi-component types present, but generally comparing the demagnetization curves with those of the single component types among the normally magnetized specimens, it is seen that there is no noticable difference in behaviour of either the normally and reversely magnetized specimens to thermal demagnetization.

(3) & (4) The amount of scatter in the directions of magnetization of the discs removed from a sample, observed in 5.5, is seen to depend on the type of thermal demagnetization curve obtained. Those with the higher Curie points and slower initial loss of magnetization such as 21, 25 (see figures 94, 95) have smaller scatter in the directions of magnetization than do those which lose their initial magnetization fairly rapidly, and so have low Curie point components in them of the order of 100°C. For example Nos. 19, 36, 38 are of this type (see figures 91, 100, 101).

5.2.4 Discontinuous thermal demagnetization in zero field

Another method which is sometimes used in thermal demagnetization is to take the specimen to be examined, and to heat it in the earth's field to a particular temperature T1 and then allow it to cool in zero field. The magnetic moment is measured after the specimen has completely cooled. The specimen is then heated to temperature T2, T2 > T1 and again allowed to cool in zero field. The magnetic moment of the specimen is again measured. Since a rock

specimen cooled in non-magnetic space shows no remanent magnetization in the ideal case, the abovementioned cooling from T to 0°C in non-magnetic space cannot cause a change in T.R.M., the changes observed being chiefly due to heat. The above procedure of heating and cooling is continued until the specimen becomes demagnetized. However, in practice this procedure never produces complete demagnetization of the rock specimen and a minimum intensity of magnetization always remains. This minimum intensity of magnetization has also been observed by Irving et al (1961). Ideally, this method should give the Curie point of the magnetic mineral in the specimen, but because of this minimum intensity of magnetization that remains, the writer feels that the significant point which is obtained is the extrapolated intersection of the thermal demagnetization curve, usually the steepest portion, with the temperature axis, as is shown in figure 36. This temperature the writer considers is closer to the blocking temperature than to the Curie temperature.

The demagnetization curve for pure magnetite corrected for the minimum intensity is given in figure 104. Figures 105,106, 107, 108 also corrected for the minimum intensity are the thermal demagnetization curves for specimens 6, 41, 33, 36. In figures 30, 31, 32, 33, 34, 35 are the changes in the direction of natural remanent magnetization for specimens

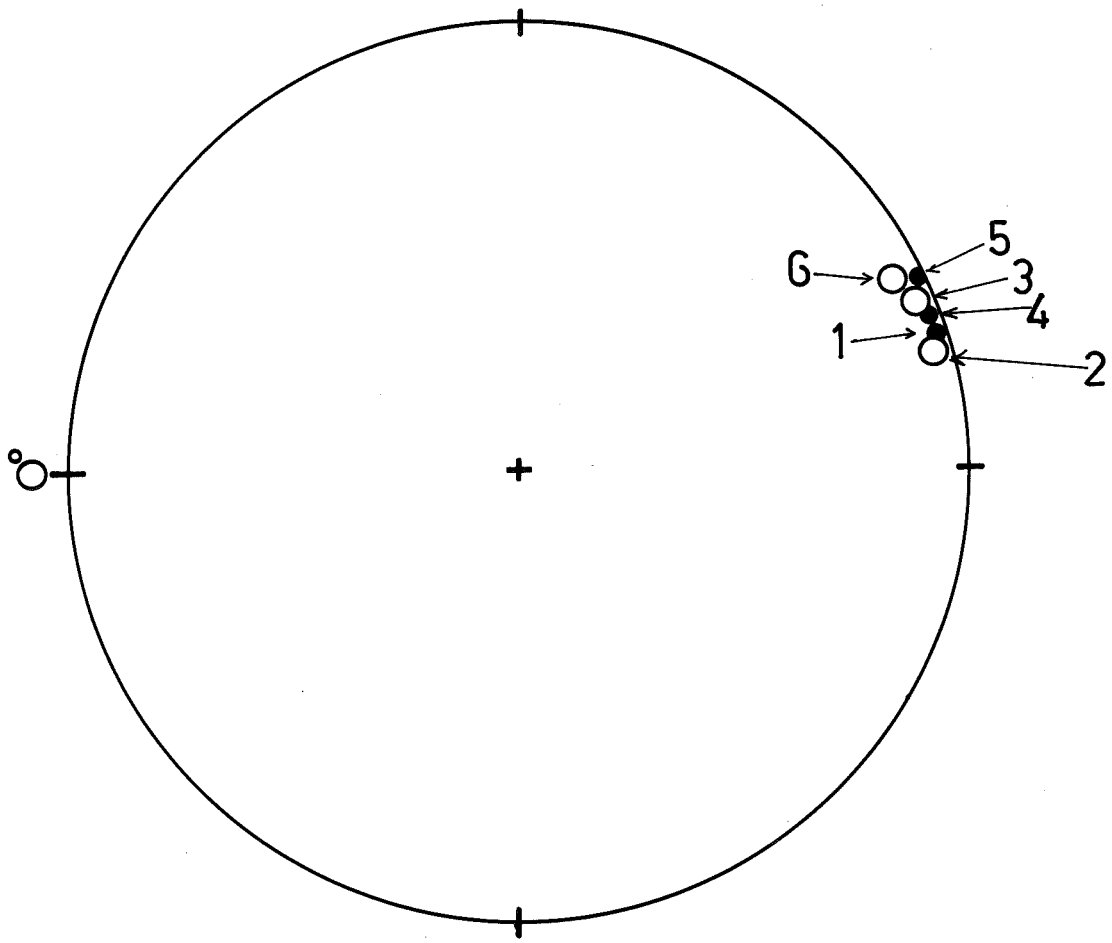

Magnetite

1	15°C
2	185
3	380
4	505
5	540
6	575

Figure.29

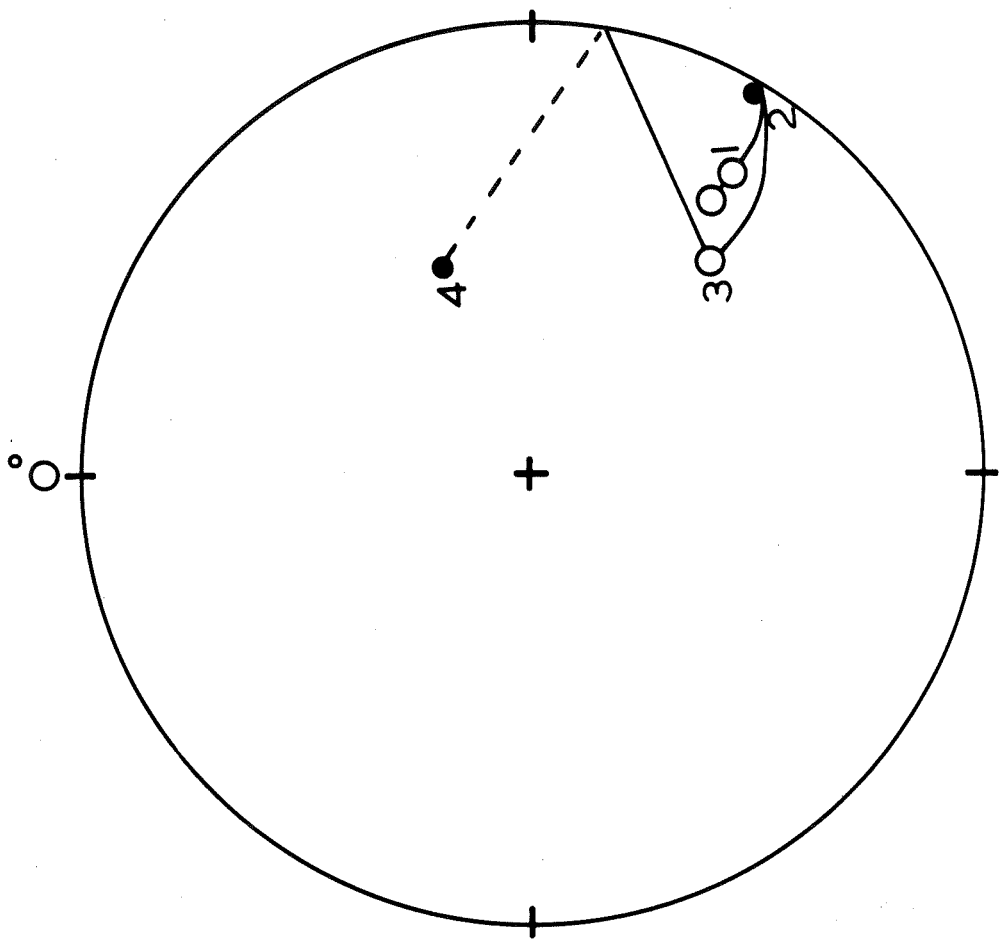

Specimen 6

1	110°C
2	240
3	330
4	455

Figure.3o.

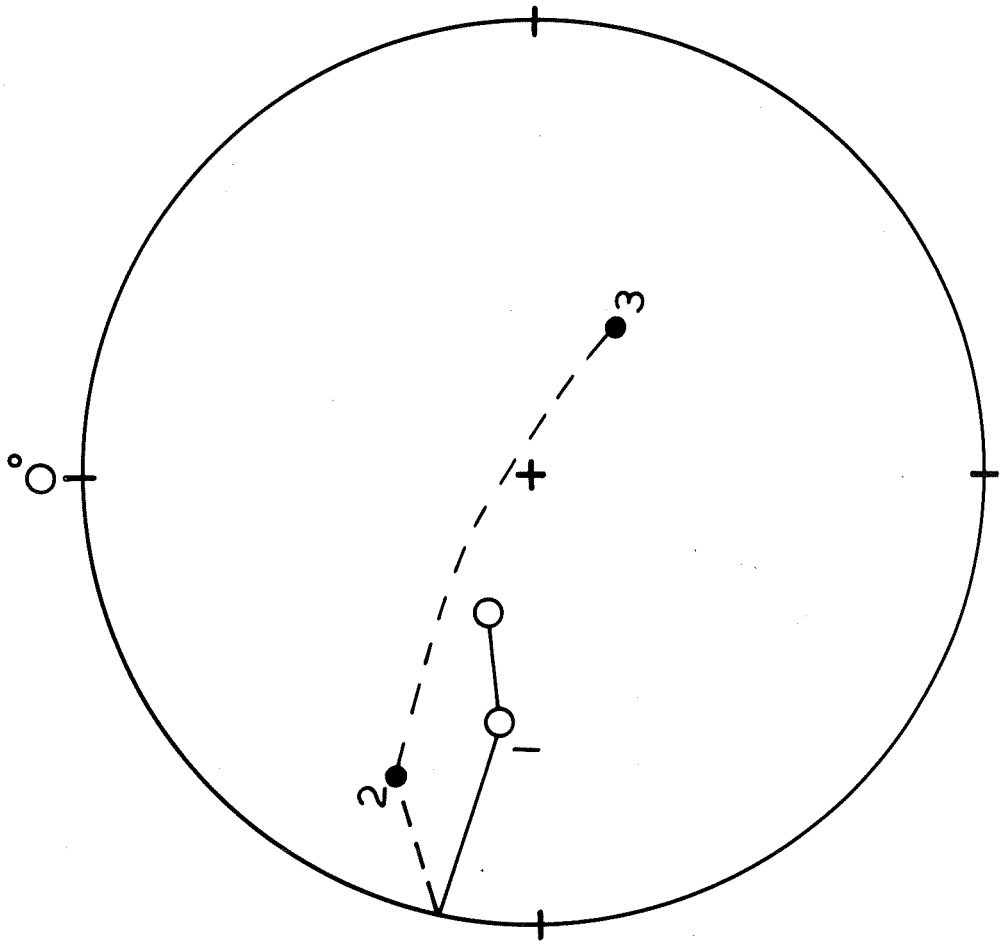

Specimen 33

1	100°C
2	180
3	330

Figure.31.

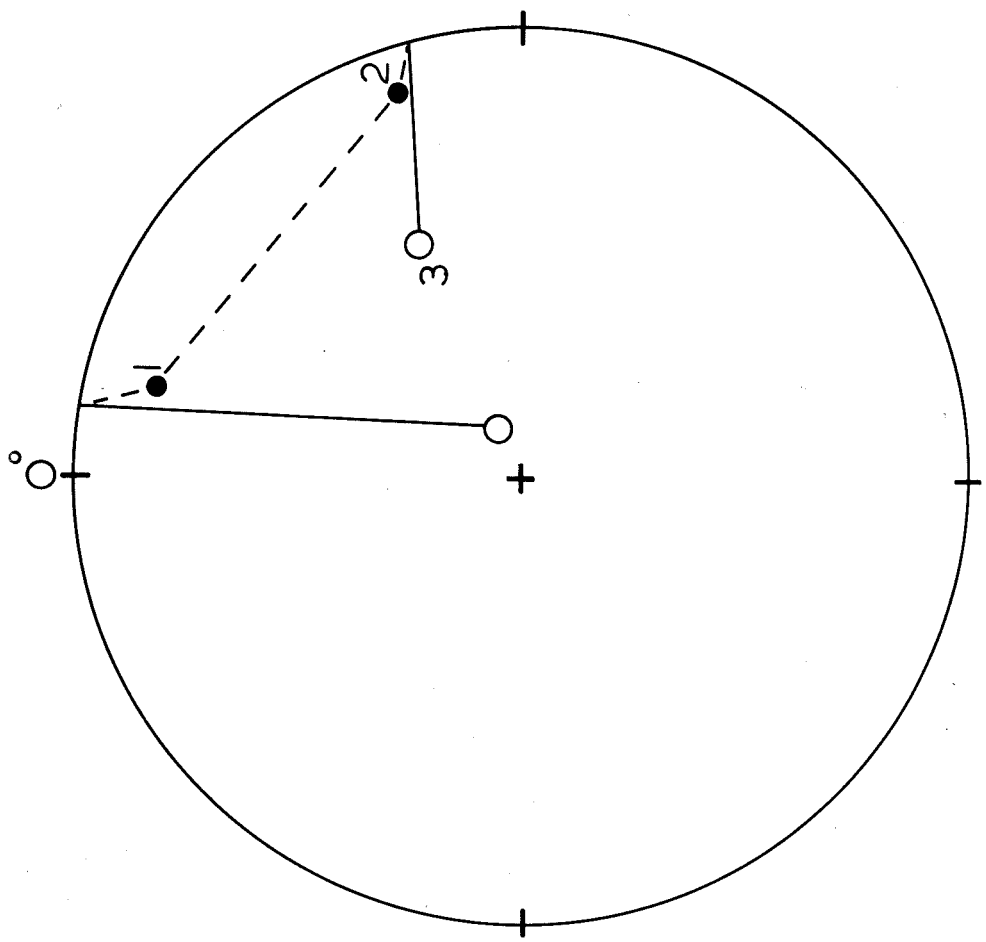

Specimen 36

1	135°C
2	290
3	390

Figure.32.

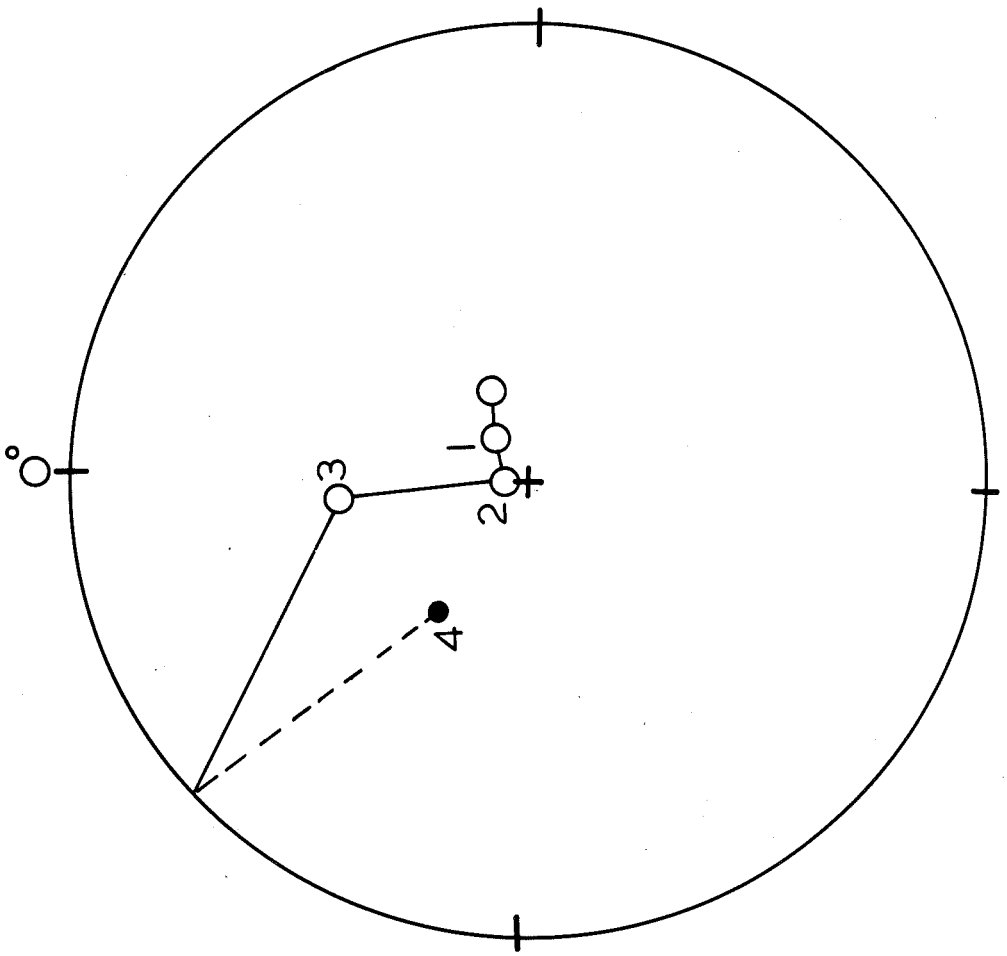

Specimen 41

1	130°C
2	280
3	420
4	515

Figure.33.

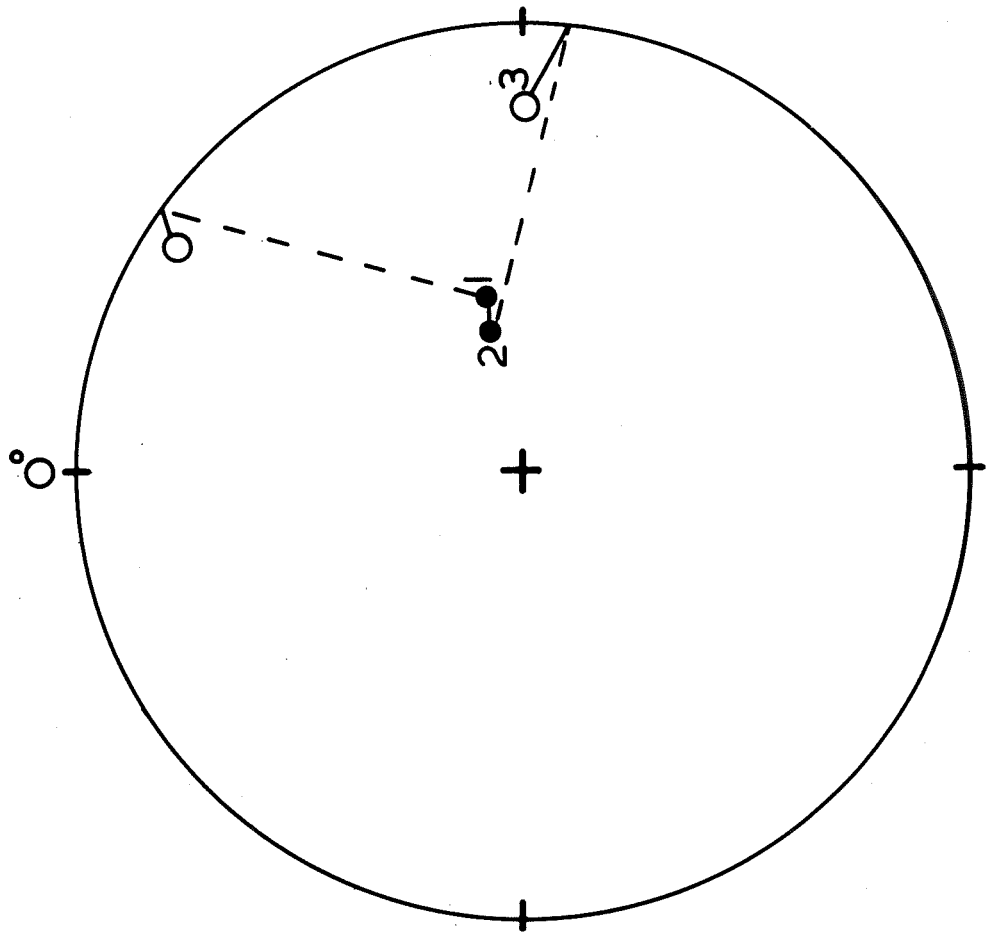

Specimen 2/58

1	50°C
2	170
3	260

Figure.34.

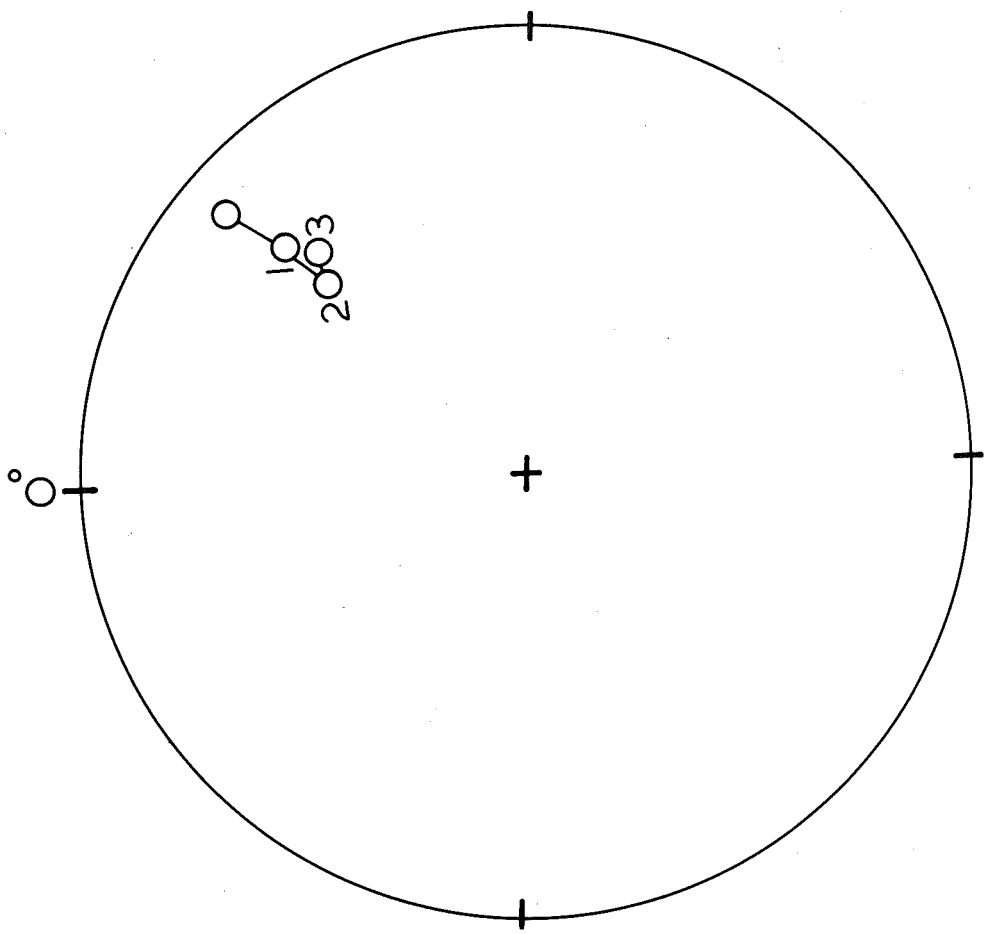

Specimen 2/45

1 50°C

2 170

3 260

Figure.35.

6, 33, 36, 41, 2/58 and 2/45 on heating to the different temperatures involved following by cooling in zero field. The specimens with the more stable thermal demagnetization properties retain their original direction of magnetization to higher temperatures than do those specimens which have low Curie points. Specimens 2/45, 41 and 6 possess more stable thermal demagnetization properties than do the other three specimens 2/58, 33 and 36.

It is interesting to compare these results with those discussed later in section 6.1.6 where changes in direction of magnetization after a.c. magnetic field demagnetization are observed for the basalt specimens.

The magnetite in the artificial specimen was very fine grained, of the order of 10 μ and this could account in part or wholly for the fact that the direction of magnetization remains constant during the thermal demagnetization experiments, because of the increased coercive force of material with small grain size (Gottschalk 1953). However, specimens 2/58 and 2/45, both from the same flow have very similar grain size spectra (See figures 56, 54).

6.2.5 A discussion of the results of discontinuous thermal demagnetization.

The thermal demagnetization curves obtained by this method in the opinion of the writer contain slightly less information than those obtained by heating in zero field continuously. The reason for this is that as mentioned in 6.2.2 continuous thermal demagnetization in

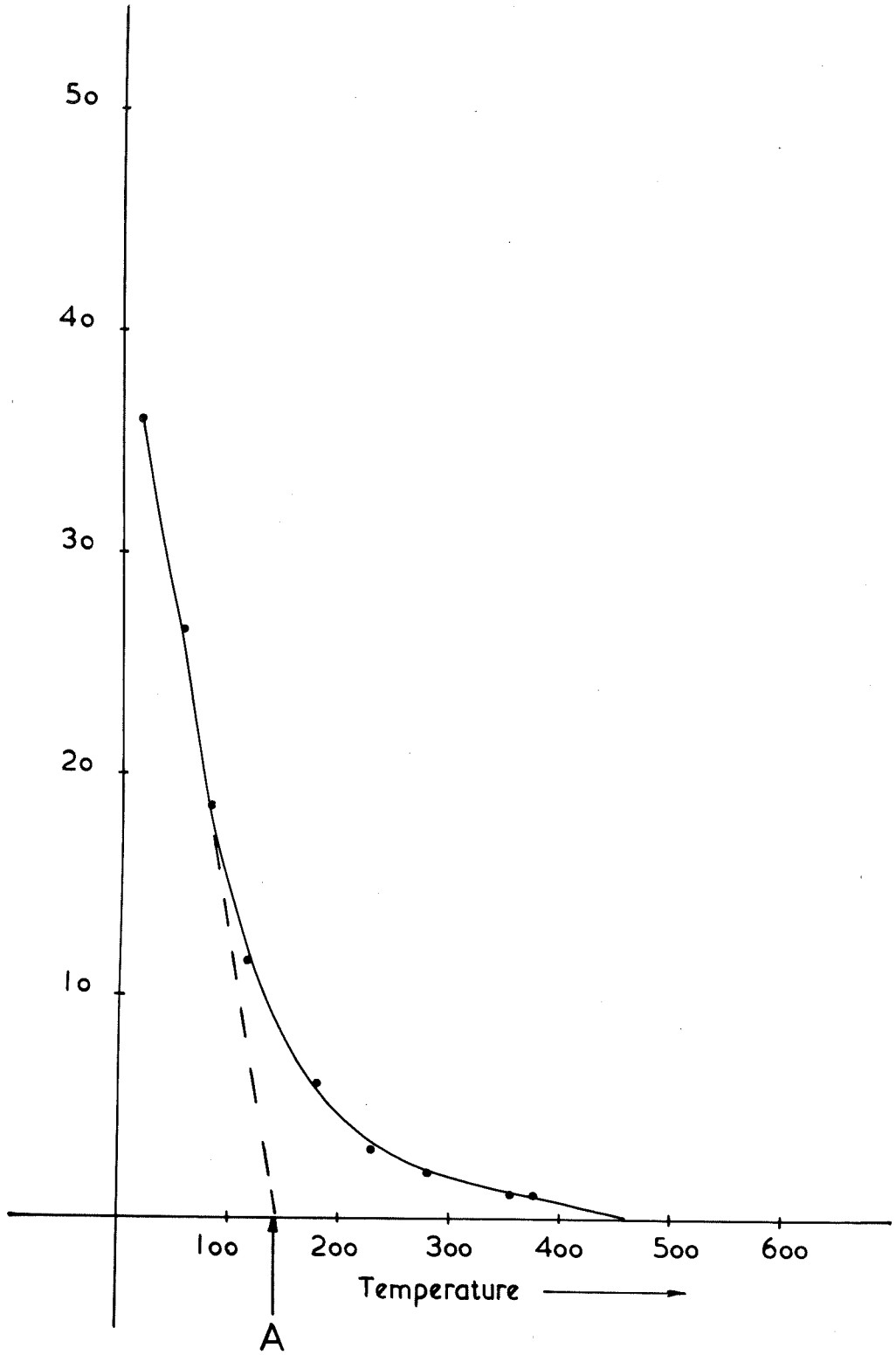

Figure.36.

zero field does give the Curie temperature as the point at which the thermal demagnetization becomes complete. It also gives the blocking temperature as originally described by Nagata. Heating and cooling in zero field gives less information because of the minimum intensity of magnetization remaining after heating is large enough to mask the smaller end effects which can be observed when the heating is carried out continuously in zero field.

Table 7 lists results obtained by the two methods of heating. The location of the point A which is mentioned in this table is given in figure 36.

It is evident from this comparison of the results obtained by the two methods that a certain amount of information is lost by the method of discontinuous heating in this case, although the method would certainly indicate that the magnetic minerals possess a range of temperatures over which "complete" thermal demagnetization takes place.

TABLE 7

DISCONTINUOUS THERMAL DEMAGNETIZATION		CONTINUOUS THERMAL DEMAGNETIZATION	
SPECIMEN NO.	The temperature at which thermal demagnetization becomes complete.	Temperature at which thermal demagnetization becomes complete	Temperature of Point A
41	420	575	425
6	275	440	250
33	110	300	125
36	150	575	125

6.2.6 Discussion of results of thermal demagnetization experiments and of Titanomagnetites.

It is evident from the thermal demagnetization curves obtained, that the Curie point of the specimens varies considerably in the range 295°C to 580°C, and also that there are some rock types present which give results which strongly suggest that there are two component types present in the rocks producing the magnetization (no.36,38). These results together with those of 6.3 indicate that the magnetic mineral present in these basalts is a titanomagnetite rather than a pure magnetite.

Natural magnetites have been found usually to consist, not only of Fe_2O_3 and FeO, but also of a fair amount of TiO_2, according to chemical analysis.

Such magnetite containing an excessive amount of TiO_2 is generally called titanomagnetite. According to Chevallier and Pierre (1932), the titanomagnetite has chemical composition $FeO\ (Fe, Ti)_2O_3$, its crystal structure belonging to the spinel type. As indicated by the results of Pouillards studies, the so-called titanomagnetites are solid solutions between Fe_3O_4 and $Ti\ Fe_2O_4$, both having the inverse spinel structure, and their composition can generally be given by:-

$$Fe^{+++}_{2-2x}\ ,\ Ti^{++++}_{x}\ ,\ Fe^{++}_{1+x}\ O_4 \quad --$$

$$0 \leqslant x \leqslant 1$$

Here the lattice constant of $TiFe_2O_4$ which is not ferromagnetic is a = 8.534 Å so that the lattice constant of a solid solution between Fe_3O_4 and $TiFe_2O_4$ changes from 8.413 Å to 8.534 Å. Accordingly the Curie point also changes continuously from 578°C to 0°K. (Poullard (1950)).

	Fe_3O_4	Sample made of x Fe_2O_3 + y TiO_2				Sample made of Fe_2O_3 + TiO_2		$TiFe_2O_4$
$TiFe_2O_4$% mol.	0	8	10	18	25	42	42	100
Lattice constant	8.413Å	8.420	8.428	8.430	8.440	8.460	8.460	8.534
Curie point	575	524	485	475	468	230	215	-

In another investigation carried out by Akimoto (1957), the ferromagnetic minerals were separated from a large number of typical igneous rocks in Japan. The ferromagnetic properties of these rocks could be attributed to the ferromagnetism of the titanomagnetites having a spinel type structure. Expressing the chemical composition of these titanomagnetites on a diagram of the FeO - Fe_2O_3 - TiO_2 ternary system, it is found that they are distributed around the straight line connecting $TiFe_2O_4$ and Fe_3O_4. The data in this investigation show the calculated content of ulvospinel ($TiFe_2O_4$) in the

titanomagnetite ranges from 0% to about 70%, resulting in the changes in the lattice parameter, intensity of saturation magnetization and Curie point in the ranges from 8.38Å to 8.49Å, and from 93 e.m.u. /gm. to 14 e.m.u./gm. and from 580°C to 120°C respectively.

In a later paper, Akimoto, Katsura and Yoshida (1957) describe how a series of solid solutions x $TiFe_2O_4$ - (1 - x) Fe_3O_4 was synthesized over a whole range of the composition They measured changes of the Curie point, saturation moment and lattice parameter with the composition.

Generalized titanomagnetites having some vacant site in their structure were also prepared by oxidizing the $TiFe_2O_4$ - Fe_3O_4 solid solution series. The region within which the spinel structure can be in existence as a single phase was settled in a FeO - Fe_2O_3 - TiO_2 system. An equal lattice parameter line, equal Curie point line, and equal saturation moment line for the generalized titanomagnetite were drawn in the FeO - Fe_2O_3 - TiO_2 system. It could be concluded from the experimental results that the spinel phase can be in existence as a single phase in fairly broad region between $TiFe_2O_4$ - Fe_3O_4 join and the $TiFeO_3$ - Fe_2O_3 join.

In a still later paper Akimoto and Katsura (1958) applied the information concerning the synthetic titanomagnetites to an interpretation of the chemical, crystallographic and magnetic properties of the natural titanomagnetites contained in volcanic rocks.

In this paper Akimoto and Katsura made reference to a paper by Vincent, Wright, Chevallier and Matheu (1957) who had studied heating experiments on some natural titaniferous magnetites having unmixing lamellae of magnetite and ilmenite, and the mineralogical changes occurring during heating experiments were followed microscopically and by determining the change in unit cell dimensions of the various phases, and also by quantitative measurements of their magnetic properties. Vincent et al concluded that at high temperatures fairly extensive solid solution probably exists over much of the magnetite-ulvospinel-ilmenite compositional field, and that homogeneous titano-magnetite (called by Akimoto et al (1957) a generalized titano-magnetite) of widely varying composition and magnetic properties may persist without unmixing in some rapidly cooled lavas. These considerations are quite accepted in general for the titanomagnetites in Japanese volcanic rocks, but it is also established that the titanomagnetites in Japanese volcanic rocks enters into the magnetite-ilmenite-hematite compositional field beyond the magnetite-ilmenite join. Vincent et al pointed out the fairly poor correlation between chemical crystallographic and magnetic data in the previous study of Akimoto (1957) and suggested that some of these specimens concerned might have unmixed to various extents, and in different ways according to composition. Because of this criticism Akimoto and Katsura selected specimens from the previous study of Akimoto (1957), plus some more for their

present study, and special care was paid to the identification of the unmixing ilmenite-hematite series minerals in specimens, and no sample with exsolution lamellae of ilmenite and/or hematite in them was used.

From the results obtained using these specimens it is clear that the chemical composition of naturally occurring titanomagnetites does not always accord with $TiFe_2O_4$ - Fe_3O_4 solid solution line, but in most cases deviates from this join towards the $TiFeO_3$ - Fe_2O_3 join side. The chemical composition of about 80% of samples are distributed between these two principal lines, Fe_3O_4 - $TiFe_2O_4$, and Fe_3O_4 - $TiFeO_3$, but again, some eight samples, especially six, deviate greatly from these two principal lines and enter into the Fe_3O_4 - Fe_2O_3 - $TiFeO_3$ compositional field. Akimoto and Katsura call these six titanomagnetites very abnormal titanomagnetites, those between the lines Fe_3O_4 - $TiFe_2O_4$, Fe_3O_4 - $TiFeO_3$ the intermediate titanomagnetites, and the titanomagnetites on the line, or near the line Fe_3O_4 - $TiFe_2O_4$ join, the normal titanomagnetites.

It was reported by Nagata, Akimoto and Uyeda (1953) that an ensemble of ferromagnetic minerals separated from the original volcanic rocks generally consists of a large number of grains of different chemical composition, having different Curie temperatures, with the result that the magnetic properties of a rock specimen represent those of the average composition of the ensemble.

In their study Akimoto and Katsura (1958) also separated a certain amount of the titanomagnetite grains from a rock specimen and further classified it with respect to Curie temperature by magnetic separation at various temperatures. The groups of minerals fractionized every 20°C range were used as specimens for the detailed study of chemical composition and lattice parameter.

Here too it was found that the titanomagnetite in an olivene basalt, a dacite, and a rhyolite, consisted of several kinds of grains of different chemical composition having different separation temperatures.

It was also interesting to observe that the chemical compcsition of the thermo-magnetically separated specimens changed continuously along the reduction-oxidation line of the $FeO - Fe_2O_3 - TiO_2$ ternary system.

These authors, Akimoto and Katsura, suggest that it may be a most important problem of volcanic petrology that titanomagnetites in some volcanic rocks consist of a large number of grains with different chemical composition, which are easily separated as the individual homogeneous phases without any unmixing lamallae. This fact suggests that the formation of the titanomagnetites is quite complicated even in volcanic rocks which were considered to be the most simple form of igneous rocks. The titanomagnetite in volcanic rocks which was presumed to be quenched from a high temperature state at the time of their outflow over the earth's surface may be affected not

only by the physical and chemical conditions of the magma, but also by its total history during solidification. A simple equilibrium state in chemical reaction cannot be assumed.

Further reference to specimens containing titanomagnetite grains of differing composition is made in 7.1.7.

6.3 X-ray diffraction analysis of the magnetic minerals

6.3.1 Introduction

The magnetic mineral found in the basalts being investigated was removed from certain samples, as is described in the following section, and X-ray diffraction analyses were carried out on it.

6.3.2 Procedure

Small amounts of the magnetic mineral were separated from the basalts by crushing and using a small hand magnet to separate the magnetic fraction. The sample was first placed between two brass plates and broken, and the fragments which were small enough were placed in a specially prepared brass mortar and crushed still further. Final crushing was done in a corundum mortar and pestle. Any introduction of iron was therefore eliminated.

The final powder was passed through a 180 mesh sieve and the metallic fraction was removed by passing a small hand magnet, with shiny paper over its pole pieces, above it.

6.3.3 Results

An x-ray diffraction photograph of this material indicated the presence of a cubic mineral with a cell spacing just greater than that for magnetite. The accurate cell spacing for this material was 8.442 Å.

An x-ray spectrograph test on some of the magnetic fraction from another sample was also carried out in the following manner. Equal amounts of unseparated crushed rock and separated fraction were used in an x-ray spectrograph determination of the amount of titanium present in each case. The test showed that there was at least 10 times more titanium present in the separated fraction than in the unseparated crushed rock. The test was not an exact one and was carried out in this fashion because some of the pyroxene and other minerals present were attached to the magnetic grains, and so the magnetically separated fraction of the sample was not pure. However, the conclusion must be that in it was concentrated most of the titanium found in the rock.

Table 8 is a chemical analysis of an Older Volcanic basalt, Edwards (1939).

TABLE 8.

SiO_2	46.04
Al_2O_3	15.08
Fe_2O_3	5.08
FeO	6.95
MgO	7.02
CaO	7.75
Na_2O	3.76
K_2O	2.41
H_2O+	1.20
H_2O-	.57
CO_2	Nil
TiO_2	2.78
P_2O_5	1.44
MnO	.28
Li_2O	
Cl	trace
S	trace
BaO	
	100.36

Up to 3% titanium has been recorded in these rocks. It would appear then that the magnetic mineral rather than being a pure magnetite is actually a titanomagnetite.

6.4. Conclusions.

These thermal demagnetization experiments carried out in zero magnetic field indicate that the magnetic mineral present in these Older Volcanic basalts is a titanomagnetite. Some specimens have a dominant single phase with a very low Curie point; in others the composition is near to that of magnetite, and various intermediate multiphase systems of oxide also occur.

The results do not indicate any difference in the thermomagnetic behaviour between the rocks of normal and reversed polarity.

These conclusions are similar to those drawn by Parry (1960) in his investigation of the thermo-remanent properties of basalts from the Newer Volcanics. The experiments he carried out were done with a translation balance, and values of saturation magnetization were obtained at various temperatures.

7. A.C. DEMAGNETIZATION EXPERIMENTS

7.1 The investigation of the mixed polarity of magnetization at Drouin-South quarry

7.1.1 Introduction

In the paper of Irving and Green (1957) on the palaeomagnetism of the Older and Newer Volcanics, it was reported that there were localities where mixed polarities occurred in these basalts. It was suggested that the occurrence of sites of mixed polarities is a matter of some interest. Contiguous samples with opposed polarities have been noticed previously in these basalts by Rayner (private communication to Irving and Green). The three explanations given for this behaviour were:

(1) At each of these sites several lava flows, although not distinguishable, may in fact be represented, so that the specimen can have cooled through the Curie point at different times between which the magnetic field reversed.

(2) Self reversal process such as those described by Neel (1955) may have operated.

(3) Errors in orientation may have occurred despite the great care taken to avoid them.

The writer considered that if these were true occurrences of mixed polarities then a more detailed examination of one of these sites would naturally be of some interest. For this reason, very detailed sampling in one of these sites, Drouin-South, was carried out, and the directions of magnetization of the samples collected were examined.

7.1.2 Field Work

The quarrying at Drouin-South is taking place on two levels at the present time. Samples were collected on the two quarry faces, and also around the base of each quarry face. The localities of the samples are given in Table 9.

TABLE 9

Sample No.	Locality
2/36	Base of lower quarry
2/35	5 feet above 2/36
2/37	1 foot above 2/35
2/38	3 feet above 2/37
2/39	3 feet above 2/38
2/40	4 feet above 2/39
2/41	8 feet above 2/40
2/42	2 feet above 2/41
2/43	Base of upper quarry
2/44	7 feet above 2/43
2/45	6 feet above 2/44

(contd.)

Sample No.	Locality
2/52 2/53 2/54 2/55 2/56	Collected around the base of the lower quarry face from left to right.
2/59 2/58 2/57	Collected around the base of the upper quarry face from left to right.

Rock cylinders were prepared from these samples in the usual way, and the directions of magnetization of these cylinders were measured.

7.1.3 Results of the measurement of the directions of magnetization

The directions of magnetization of all specimens removed from these samples are given in Table 10.

TABLE 10

Specimen	D (M.N.)	I
2/36	315	-76
36a	240	-66
36c	285	-74
35	334	-24
35a	346	-31
35c	345	-46
37	267	-33
37a	270	-36
37c	285	-36
38	197	-27

(contd.)

Specimen	D (M.M.)	I
38a	179	-52
38c	187	-41
39	157	-68
39a	179	-60
39c	180	-75
40	292	-38
40a	292	-42
40c	303	-51
41	249	-13
41a	252	0
41c	265	-8
42	166	-85
42a	166	-85
42c	310	-84
44	233	+30
44a	244	+14
45	334	+72
45a	338	+66
52	49	-54
52a	34	-55
53	77	-63
54	106	-38
54a	116	-43
55	182	-59
55a	195	-72
56	148	-83
56a	161	-88
58	191	-74
58a	214	-52
59	21	-34
59a	15	-11

The directions of magnetization are plotted in figure 37. The specimens plotted are 2/36, 2/35, 2/37 etc. It is easily seen from this figure that the mixed polarities reported by Irving and Green do occur, but the normally and reversely magnetized rocks are not magnetized in directions 180° apart, for the directions of magnetization are random.

7.1.4 The geology of the quarry at Drouin-South

The quarry at Drouin-South has been described by Mahoney (1931). The olivene-nephelinite from near Drouin comes from the quarry worked for road metal by the Shire of Drouin and Warragul in Allotment 91, parish of Drouin West, about 2 miles south of Drouin township. Volcanic rocks in this district extend to about 25 miles north and south and 12 miles east and west; they generally decompose to deep soils and outcrops are rare. On the geological map of Victoria they are marked Older Volcanics (that is middle and lower Tertiary), but apart from physiographic considerations and analogy with similar areas in other parts of Gippsland, there is no evidence of their exact age. Owing to the paucity of outcrops in this area, the nature of the underlying rock can only be judged from the soil. Samples from quarries near Crossover and near the southern boundary of the parish of Warragul are Olivene Basalts. The quarry where the olivene-nephelinite is worked is situated on the western slope of a small hill which rises

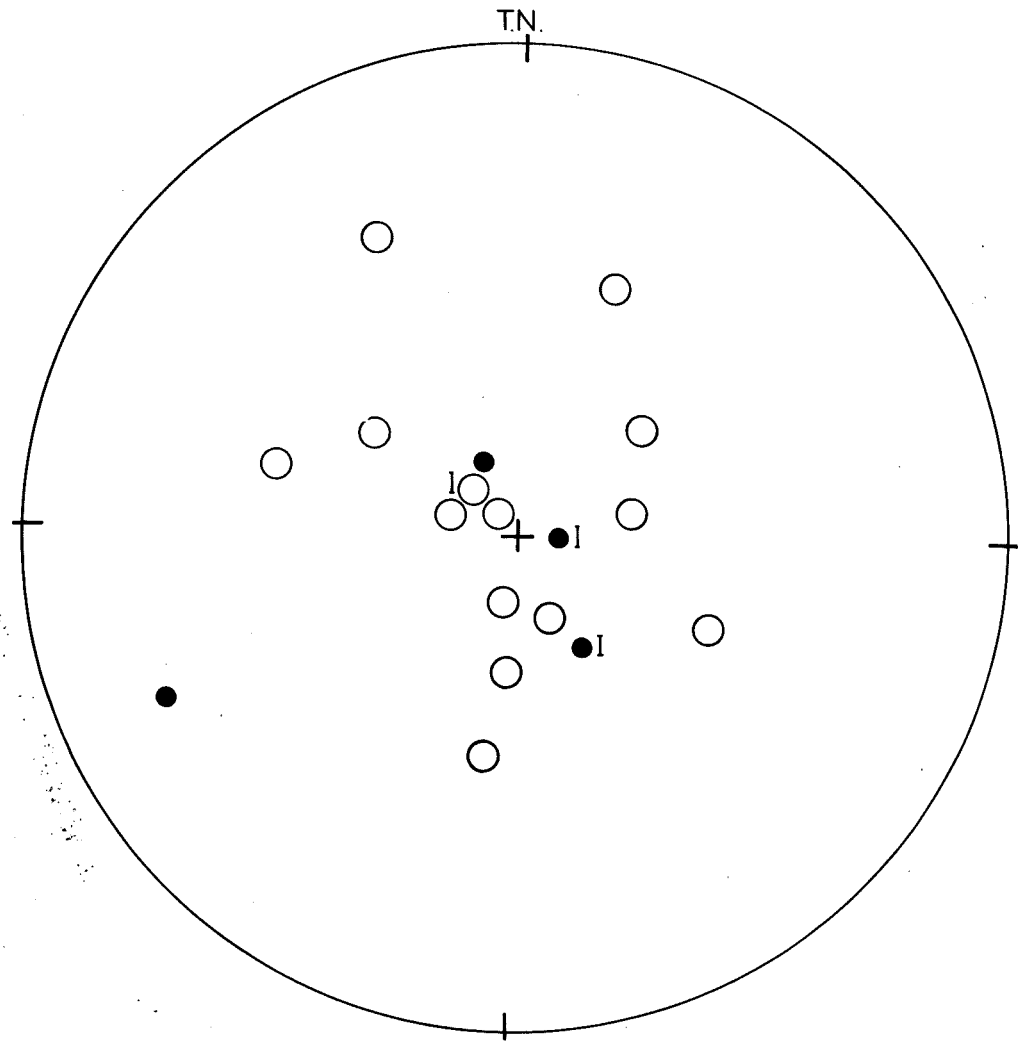

Drouin South - directions before cleaning

Figure.37.

to about 700 ft. above sea level. Some years ago, several bores were put down to test the area of solid rock, and according to reports, it is a volcanic plug. The surrounding soil is typically volcanic, but contains fragments of indurated slate and sandstone which are probably ejected blocks.

The face of the quarry as it was, exposed about 40 feet of solid rock with no signs of successive flows. In some parts a rough columnar structure is developed. The rock is dense and free from vesicules, but contains occasional patches of solid white zeolites which were probably the final minerals to consolidate from the magma.

Under the microscope it is holocrystalline and panidiomorphic. It consists of nepheline, augite, olivene, iron ore and apatite; felspar is absent; Nepheline forms about one third of the rock; it is limpid and colourless and the crystals are from .05 to .25 m.m. across. Augite, the next most abundant mineral forms greenish prisms about .08 m.m. long in felted aggregates between the nepheline crystals. Olivene is fairly abundant in crystals about 1 m.m. to 1.5 m.m. long; it is generally fresh but is partly altered to serpentine. Abundant cubes of iron ore probably titaniferous magnetite are scattered through the rock.

7.1.5 A.c. magnetic field cleaning of the rocks from Drouin-South

7.1.5.1. Introduction

Following the investigation of the direction of magnetization

of the samples taken from the quarry at Drouin-South, the writer carried out a.c. cleaning experiments in order to see if there were unstable components of magnetization present in these rocks.

The writer thought that these rocks might possess a mixed polarity of magnetizations as reported by Green and Irving but the presence of temporary unstable components of magnetization superimposed on the stable directions of magnetization had caused the directions to become scattered. Cleaning might remove these temporary unstable components. The cleaning was done at Canberra where a.c. demagnetization apparatus was made available to the writer. This apparatus has been described by Irving et al (1961).

7.1.5.2 Cleaning experiments

The first thing that was done was to clean the specimens from the samples numbered 2/36, 2/35, 2/37 ... etc. in a.c. magnetic fields of 150 and 225 oersted. Figures 38, 39 are plots on an equal angle stereographic projection of the directions of magnetization after cleaning in these two fields.

It can be seen from these figures that the minimum scatter of directions after cleaning occurs from 150 oersted when most of these specimens become reversely magnetized.

The value of the precision K (Fisher (1953)) for the two distributions obtained after cleaning in fields of 150 and 225 oersted are given in Table 11.

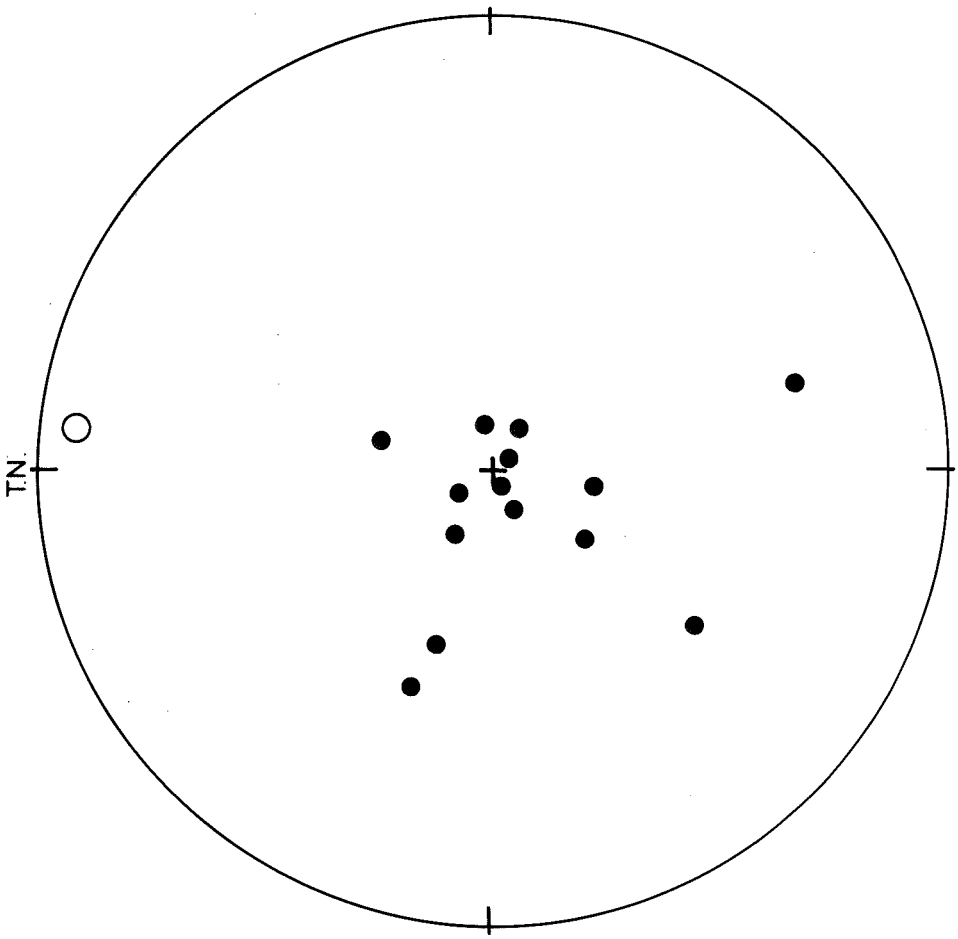

Drouin South directions after cleaning in 150 oersted.

Figure.38.

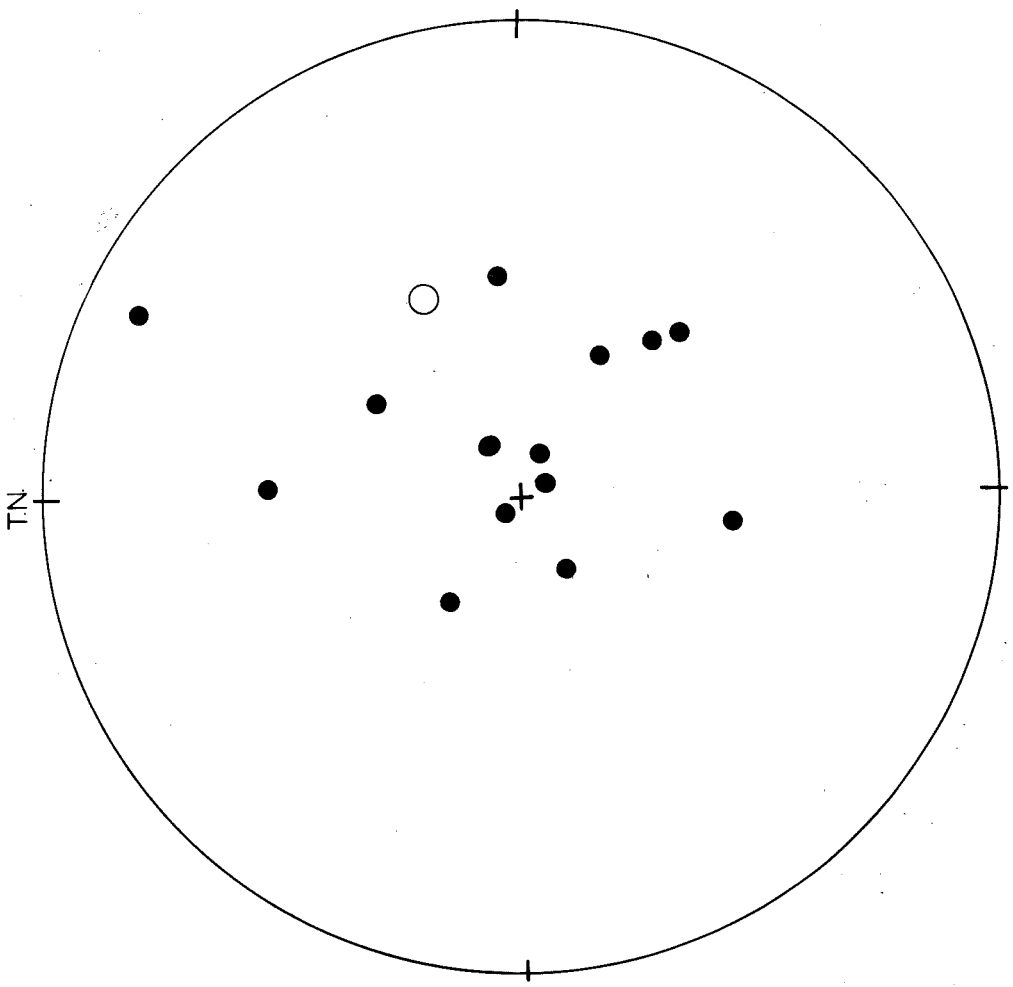

Drouin South - directions after cleaning in 225 oersted.

Figure.39

TABLE 11

A.c. Cleaning field	K	Mean direction of magnetization	
		D (M.N.)	I
150	4.4	256	+80
225	3.2	75	+71

As is seen from the figures and also from the value of K for both of these distributions, the scatter of the points is still great. More will be said about this scatter in 9. Two of the specimens 2/45, a typically reversed one, and 2/59 a typically normally magnetized one, were washed progressively in fields of 45,90, 150, 300, 450, 600, 750 oersted.

The a.c. demagnetization curves for these two specimens are shown in figure 40.

The values of the moment of magnetization for the fields mentioned are given in Table 12.

TABLE 12

A.c. Field (oersted)	2/45 Moment c.g.s. Units	2/59 Moment c.g.s. Units
Initial	3.18×10^{-3}	2.34×10^{-3}
45	3.22×10^{-3}	5.68×10^{-4}
90	2.81×10^{-3}	4.10×10^{-4}
150	2.52×10^{-3}	2.68×10^{-4}
300	1.29×10^{-3}	1.26×10^{-4}
450	7.55×10^{-4}	1.97×10^{-4}
600	3.37×10^{-4}	1.97×10^{-4}
750	4.44×10^{-4}	1.16×10^{-4}

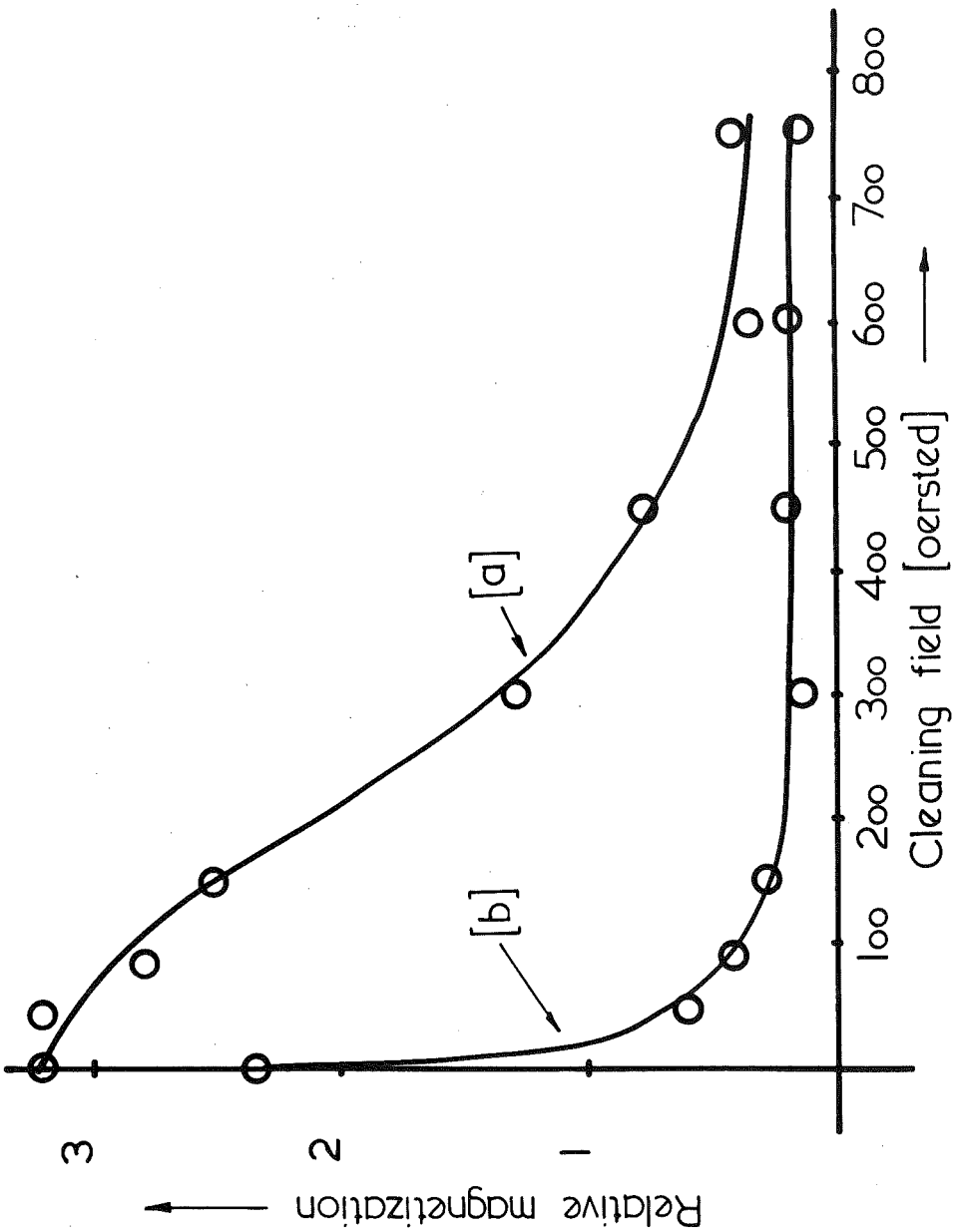

a - Specimen 2/45

b - Specimen 2/59

Figure.4o.

It is seen from the a.c. demagnetization curves that the reversely magnetized specimen is less easily demagnetized than is the normally magnetized specimen which reaches a value of minimum intensity of magnetization for a.c. cleaning at about 200 oersted.

Also, by subjecting these specimens to high d.c. fields it is possible to magnetize them to a considerable intensity of isothermal remanent intensity (I.R.M.), which, however, does not reach saturation in 3,000 gauss for specimen 2/45. The opposing field required to remove this I.R.M. is called the coercivity of remanence and is about 500 oersted for 2/45 and 200 oersted for 2/59. Figures 41,42 show the results of such experiments for these two specimens 2/45, 2/59.

7.1.6 Thermal demagnetization of specimens from Drouin-South quarry

Thermal demagnetization curves for specimens from Drouin-South which were used in the a.c. cleaning experiments were obtained. The curves are shown in Appendix 5 See also figure 44.

In Table 13 are given the values of the Curie points obtained for these specimens.

TABLE 13

Specimen	Curie point °C
2/52a	300
54a	260
55a	220
56a	330
35a	230

(contd.)

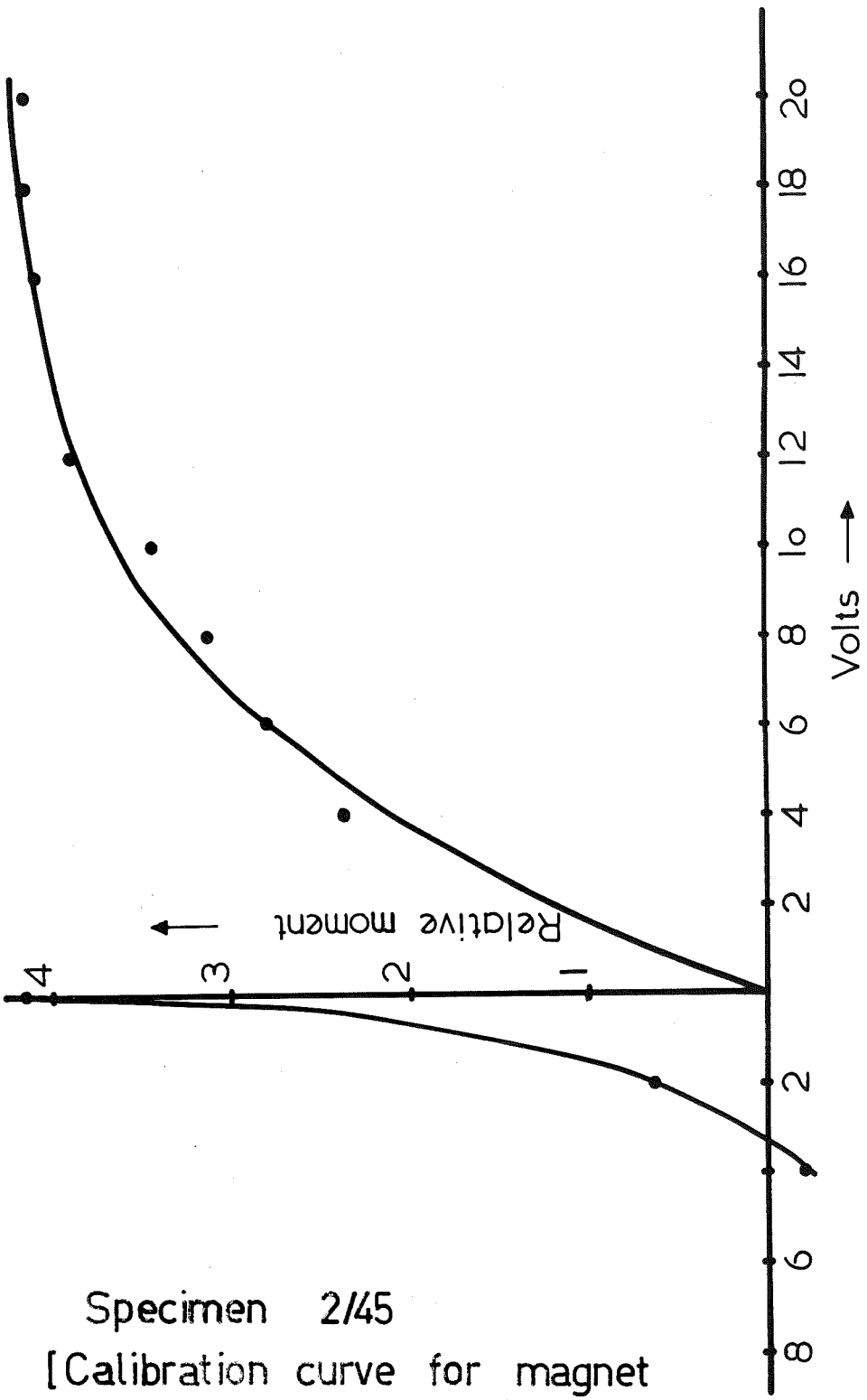

Specimen 2/45

[Calibration curve for magnet is shown in figure 43]

Figure 41.

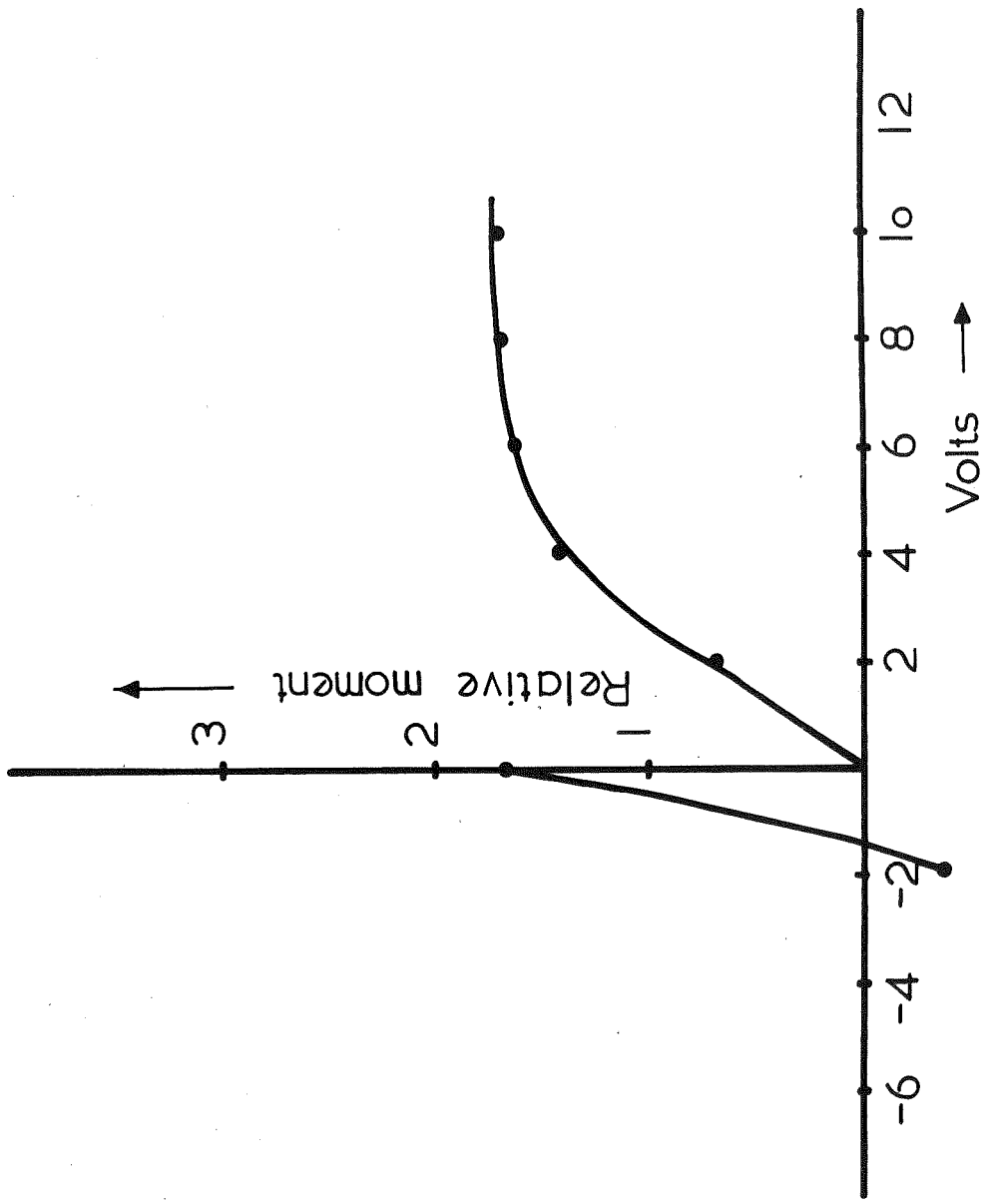

Specimen 2/59

Figure 42.

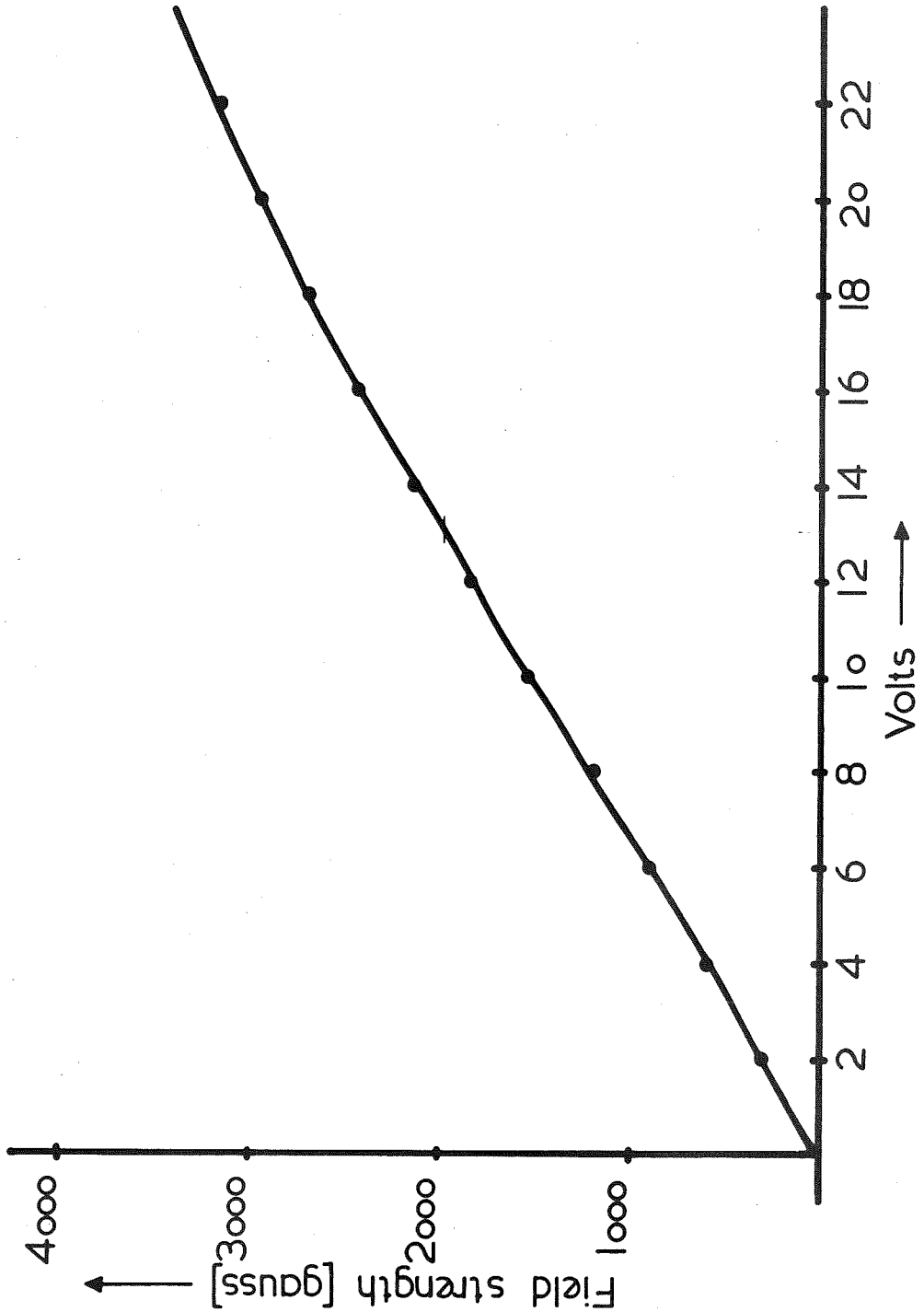

Calibration curve for magnet

Figure 43.

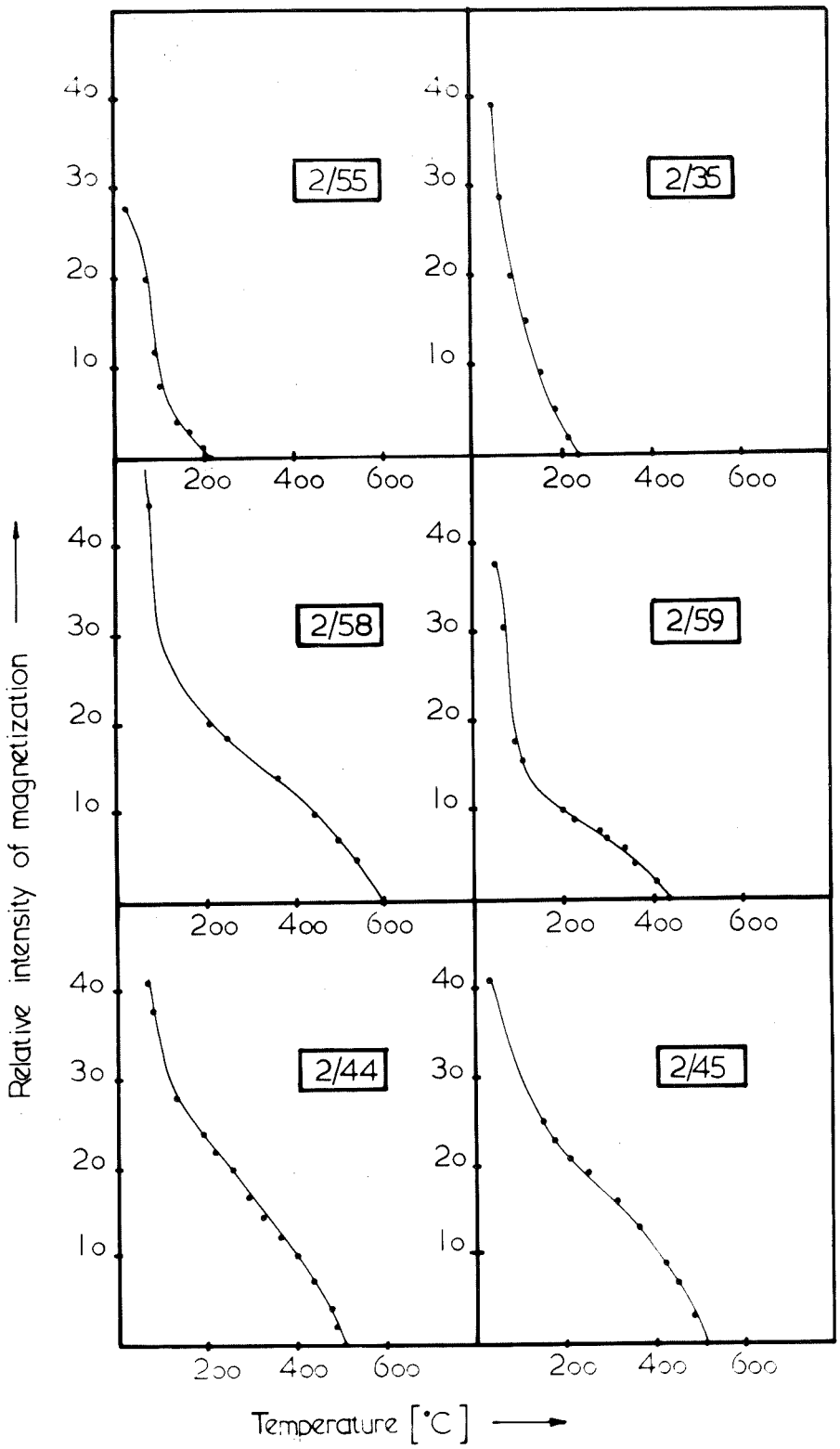
2/55
2/35
2/58
2/59
2/44
2/45
40
30
20
10
200
400
600
Relative intensity of magnetization
Temperature [°C]

Figure 44.

Specimen	Curie Point °C
37a	310
40a	260
41a	430
58a	200, 580
59a	175, 435
44a	225, 500
45a	400, 510

The changes in the directions of magnetization after washing specimens in fields of 45, 90 and 150 oersted are given in Table 14 together with the Curie temperature obtained. This was carried out using the apparatus built at Adelaide.

TABLE 14

Specimen	Curie Point	CLEANING FIELD (Oersted)							
		0		45		90		150	
		D(MN)	I	D(MN)	I	D(MN)	I	D(MN)	I
2/41b	430	265	-8	217	+75	143	+80	60	+44
44b	225,500	233	+30	204	+76	222	+84	76	+80
52b	300	34	-55	50	-56	85	-20	292	+18
54b	260	106	-38	0	-62	27	-11	355	+54
55b	220	195	-72	207	-55	44	+56	283	+55
56b	330	148	-83	92	-75	68	-38	68	+26
58b	300,580	191	-74	181	+66	122	+80	123	+80
59b	175,435	21	-34	18	+33	25	+69	47	+74
45b	400,510	338	+66	6	+72	314	+80	324	+80

There is thus a definite correlation between the Curie temperature of the main magnetic components and the stability of these rocks, if we assume that the stability of the specimen is in some way dependent on the angle between the magneti-

zation of the specimen and the originally stable reversed direction. That is, specimens 2/44, 2/45 (See figure 44) contain a large amount of high Curie point titanomagnetite, and are the only two specimens which still retain their original direction of magnetization. The other rocks including 2/58, 2/59 which contain mainly a low Curie point titanomagnetite have acquired large unstable components of magnetization which can, however, be removed by a.c. cleaning as has already been described.

In order to indicate further the relationship between stability of magnetization to a.c. demagnetization and Curie temperature, or composition of the titanomagnetites in these basalts, the writer took specimens of different thermal demagnetization characteristics and subjected them to a.c. demagnetization. The results of these experiments are shown in figures 45,46,47. In figure 45 are shown the thermal demagnetization curves for specimens 2/45, 2/59 2/41, taken from Drouin-South together with those for specimens 33, 36, 41 also collected from the Older Volcanic basalts of Victoria. In figure 46 are given the a.c. demagnetization curves for specimens from these rocks, while in figure 47 are curves which show $\frac{\Delta M}{\Delta H}$ for ΔH equal to intervals of 50 oersted.

It is seen from these last figures that the stability of the magnetization to a.c. demagnetization seems to depend

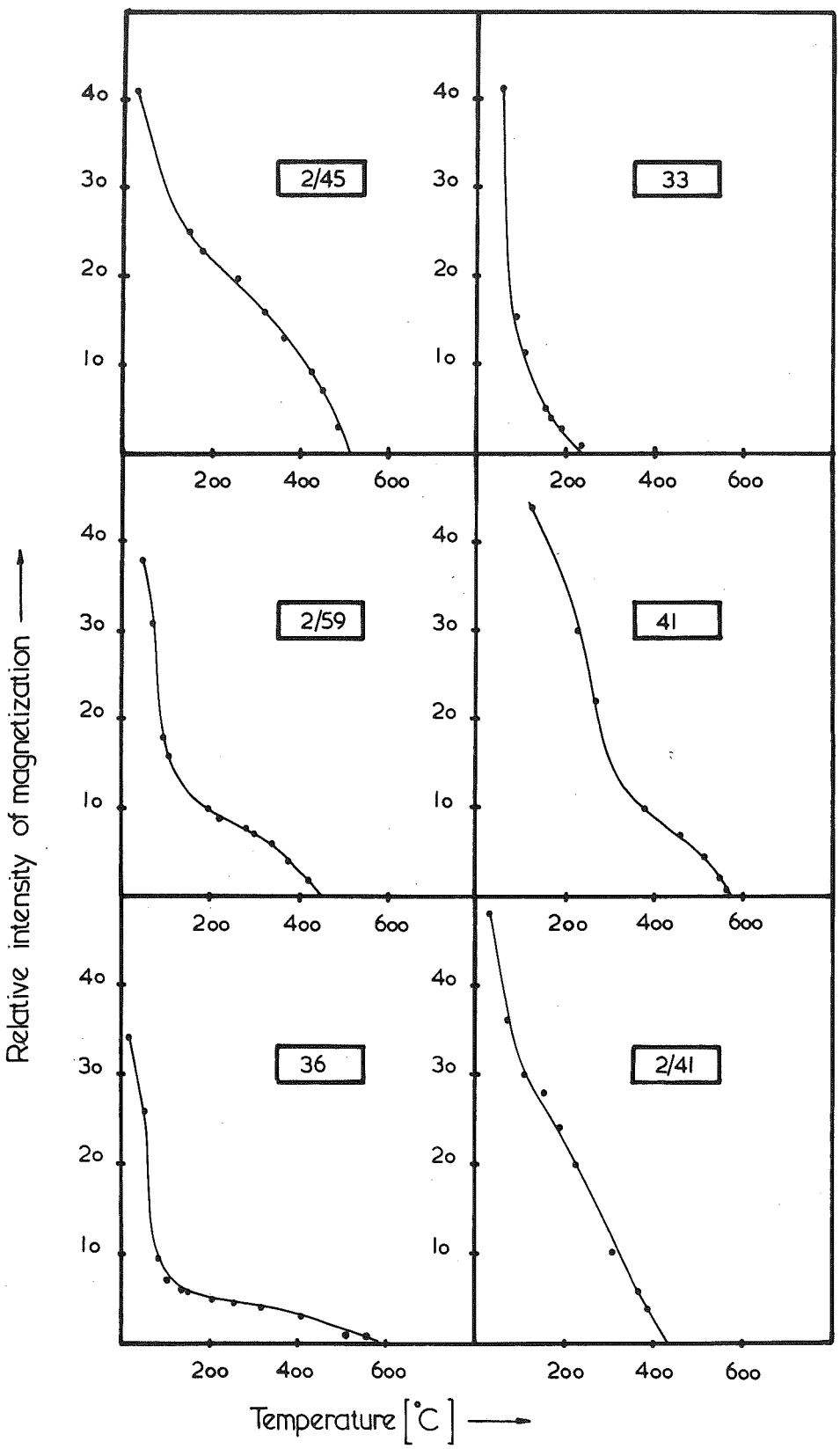
2/45
33
2/59
41
36
2/41
4o
3o
2o
1o
200
400
600
Relative intensity of magnetization
Temperature [°C]

Figure 45

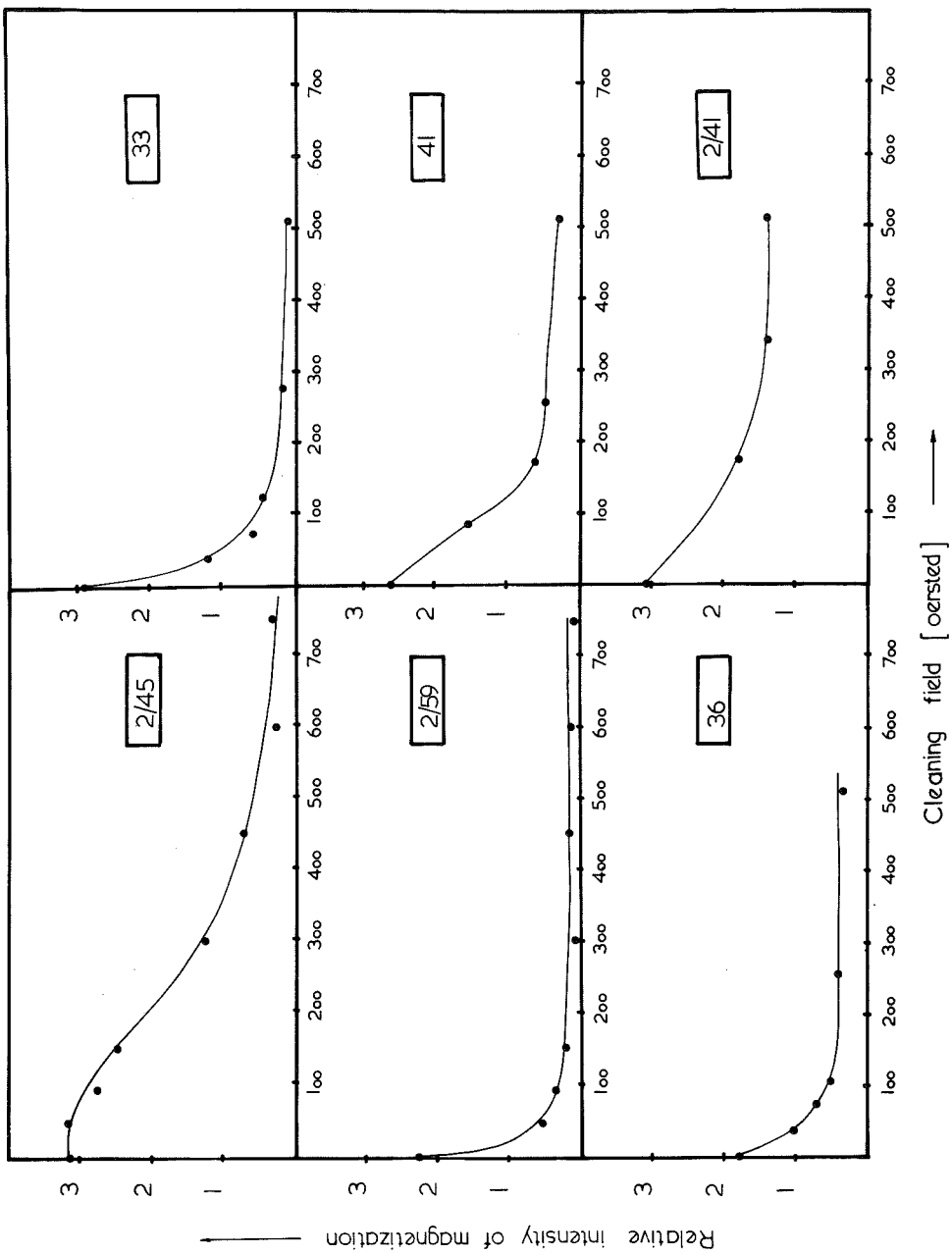
33
41
2/41
2/45
2/59
36
Relative intensity of magnetization
Cleaning field [oersted]
1
2
3
100
200
300
400
500
600
700

Figure 46.

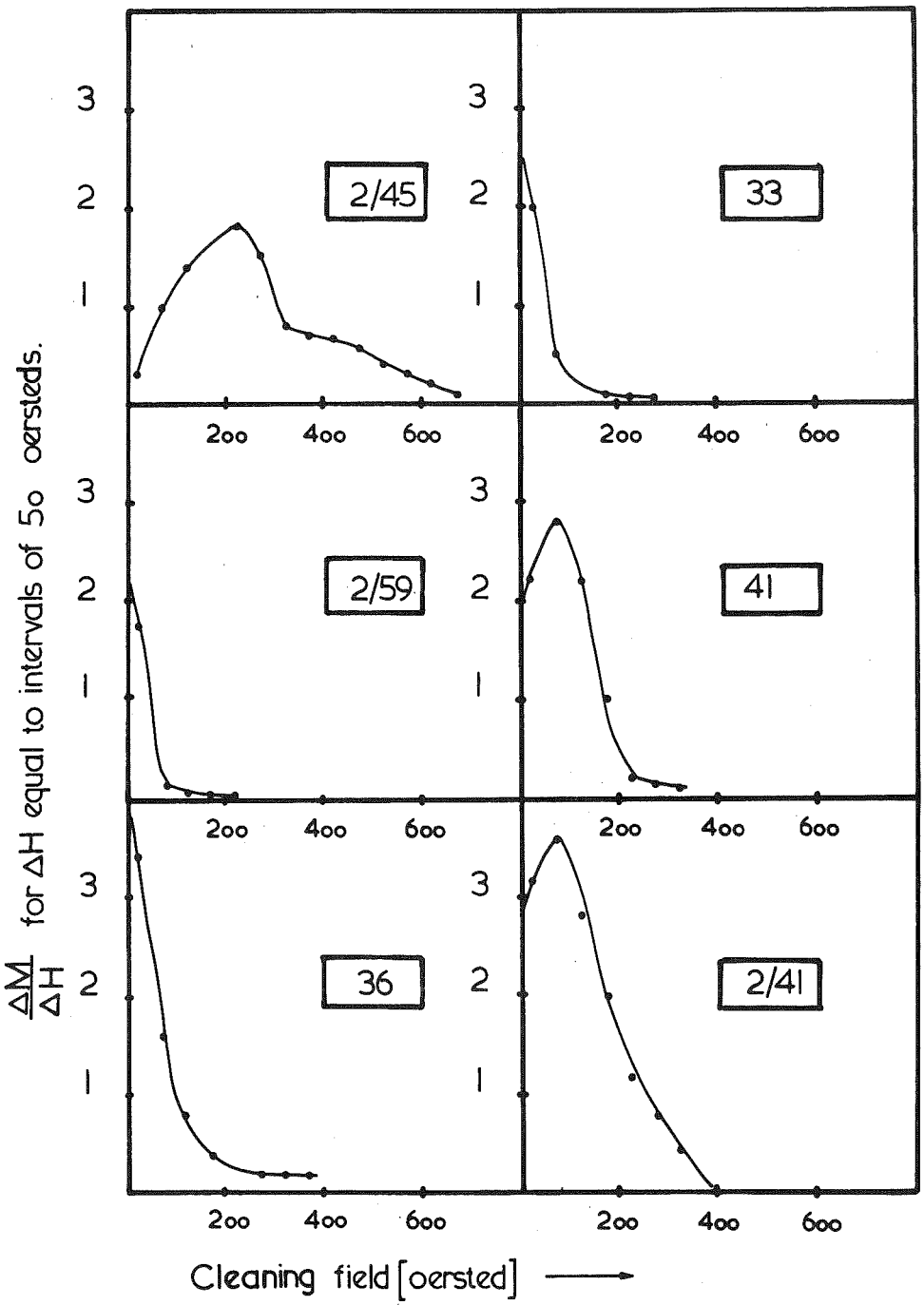
2/45
33
2/59
41
36
2/41
3
2
1
200
400
600
ΔM/ΔH for ΔH equal to intervals of 50 oersteds.
Cleaning field [oersted] ⟶

Figure 47

in part at least on the Curie temperature of the main titanomagnetite which the basalt contains, as the rate of change of magnetization is greatest at higher a.c. fields for those specimens which contain mainly the higher Curie point titanomagnetites.

Grain size undoubtedly has some effect, but it must be remembered that specimens 2/45 and 2/59 are similar rocks (see the grain size analyses in figures 54, 56) and so represent two extremes of the dependence of stability on composition.

The other specimens 2/41, 33, 36 and 41 were chosen as having intermediate compositions in an effort to show that intermediate points do exist in the relationship between stability of magnetization and Curie temperature.

The changes in the direction of magnetization for specimens from the samples just referred to, namely 2/59, 2/45, 33, 36 and 41, are shown in figures 48, 49, 50, 51, 52. For specimens 33, 36 and 41, the change in direction of magnetization for two discs are shown. It is seen that in higher a.c. fields, specimen 2/45 almost retains its original direction of magnetization, while in specimens 33, 36 and 41, where the variation of direction of two specimen discs is observed, the two directions of magnetization after remaining nearly parallel in the smaller a.c. fields, gradually disperse in higher demagnetizing fields when the intensity of magnetization reaches a minimum condition (M min).

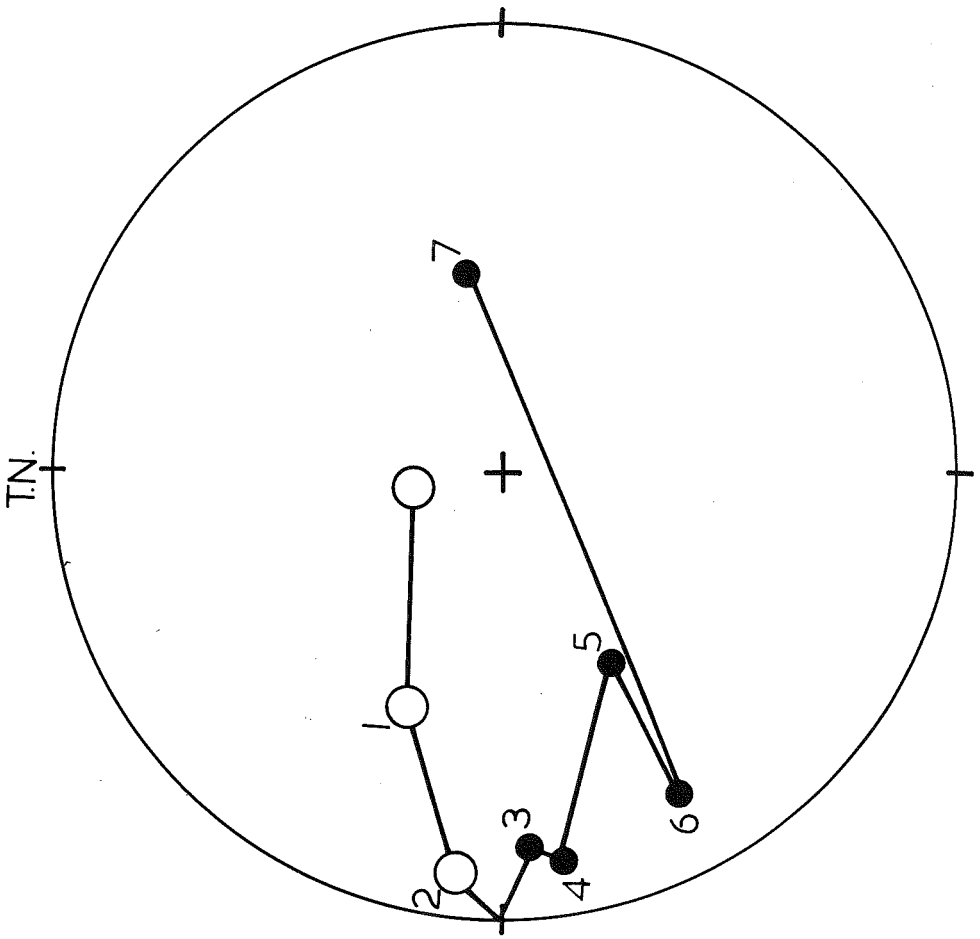

Specimen 2/59

1	-	45 oersted
2	-	90
3	-	150
4	-	300
5	-	450
6	-	600
7	-	750

Figure 48.

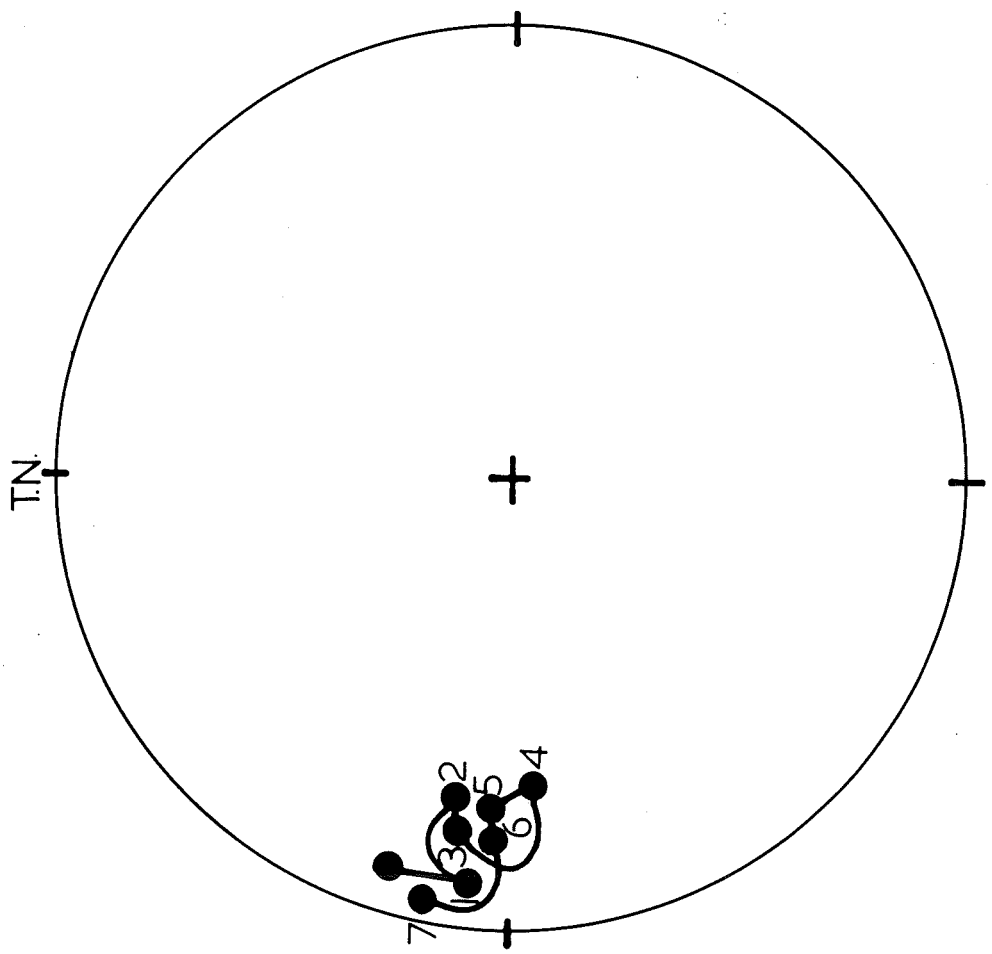

Specimen 2/45

1 - 45 oersted.
2 - 90
3 - 150
4 - 300
5 - 450
6 - 600
7 - 750

Figure 49.

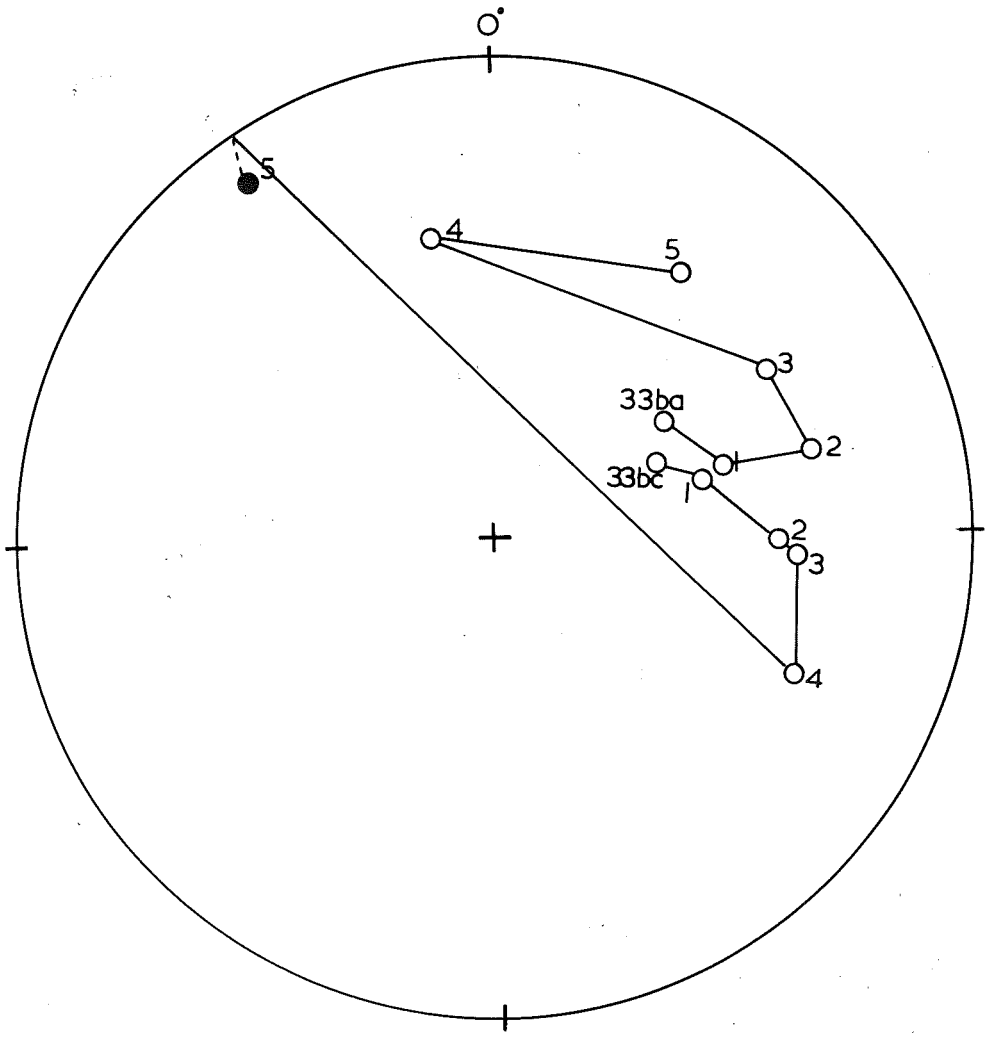

Specimen 33

1 - 34 oersted
2 - 68
3 - 119
4 - 225
5 - 510

Figure.5o.

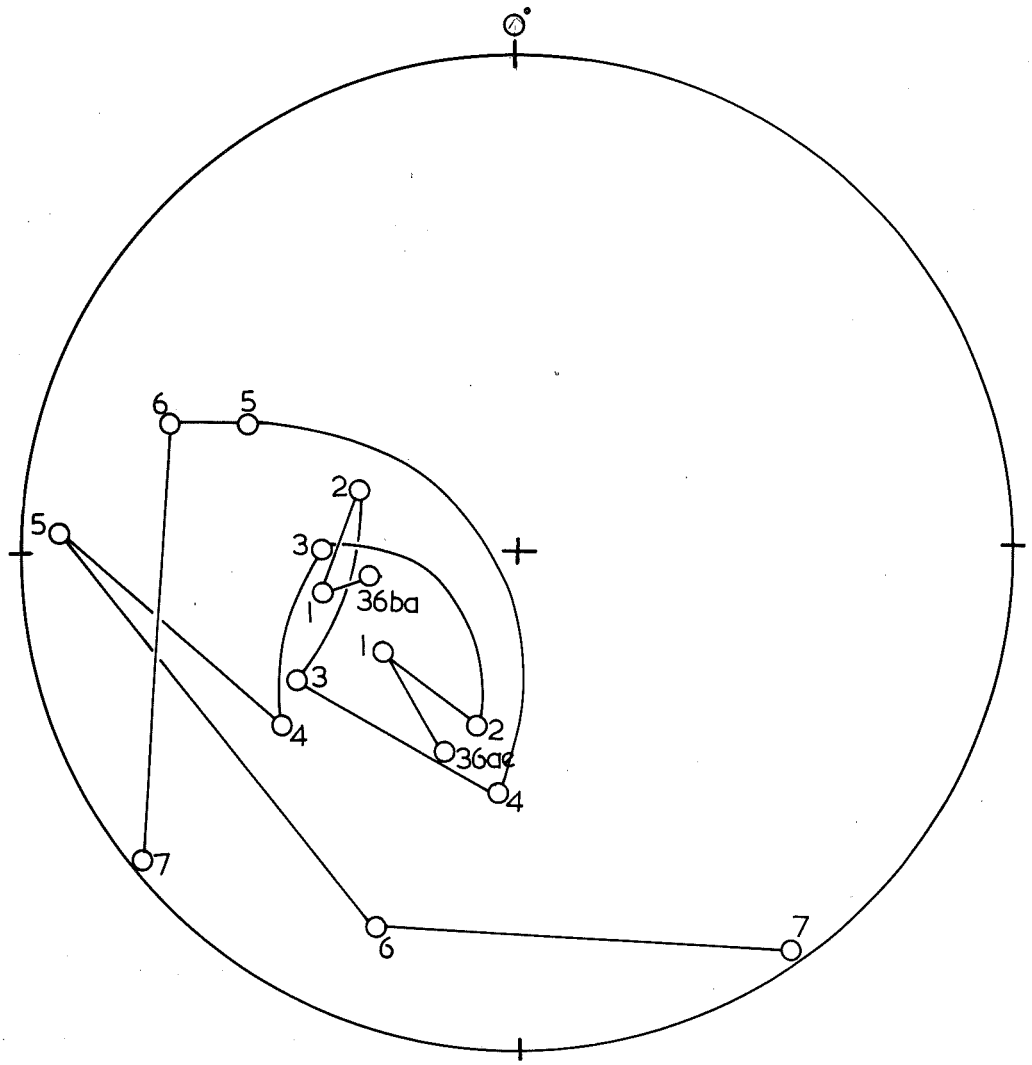

Specimen 36

1	-	34oersted	4	-	170
2	-	68	5	-	340
3	-	119	6	-	510
			7	-	680

Figure.51.

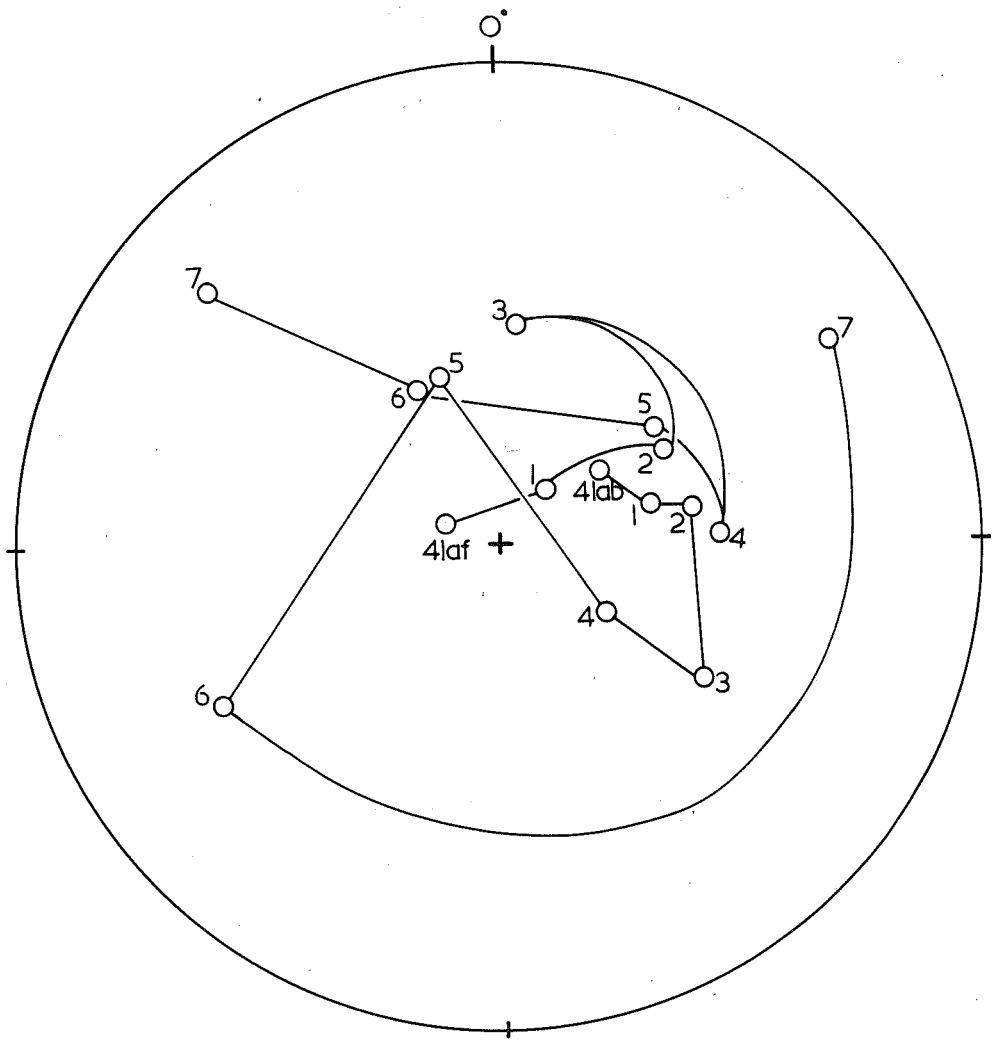

Specimen 41

1	-	43oersted	4	-	170
2	-	86	5	-	225
3	-	129	6	-	510
		7 - 710			

Figure.52.

7.1.7 The petrology and grain size analysis of specimens from Drouin-South quarry.

After the thermal demagnetization experiments on the rocks from Drouin-South were carried out and showed that the stability of magnetization depends on the composition of the titanomagnetite they contain, thin sections of some of the specimens were made to study grain size variations in the iron minerals.

Thin sections of specimens numbered 2/52, 2/41, 2/56, 2/55, 2/54, 2/45, 2/59, 2/58, 2/44 were cut and examined. The specimens could be divided into two groups on petrological grounds.

(1) Lower quarry group

The numbers of these specimens are 2/52, 2/41, 2/56, 2/55, 2/54. All of these slides are very similar and are quite distinctive in that they contain nepheline. The main minerals present in these slides are:-

(i) Augite
(ii) Nepheline
(iii) Olivene rimmed with iddingsite
(iv) Magnetite (titaniferous)

As has already been outlined in 7.1.4 these rocks are part of a plug of olivene-nephelinite rock.

(2) The Upper quarry group

The numbers of these specimens are 2/58, 2/59, 2/44 and 2/45.

These slides are also very similar to each other in appearance and are quite different from the lower quarry group. They are much finer grained in appearance. The main minerals present are:-

(i) Augite
(ii) Olivene, mostly gone to iddingsite
(iii) Felspar, probably plagioclase.
(iv) Magnetite.

The felspar of the upper quarry group is completely different in appearance from the nepheline contained in the lower quarry group, and it is biaxial (positive) in any case. Albite twinning can also be seen in places throughout the thin sections.

The writer thus feels that it is reasonably certain that these two sets of slides represent two different groups of rocks, if only because of the absence of the rather distinctive mineral nepheline in one group. Figures 53-61 show the results of grain size analysis on the magnetite in these slides. The magnetic mineral of specimens 2/44, 2/45, 2/59, 2/58 has obviously got a very much small grain size than that of the specimens 2/56, 2/55, 2/41, 2/54, 2/52. This is a further indication that these rocks belong to two different groups.

The upper group may represent a basalt flow which is either being intruded by the lower quarry group or has come into very close contact with it.

Stability differences on the grounds of variations in grain size alone of the titanomagnetite in these rocks is not

feasible as specimens 2/58, 2/59 are quite unstable types, while specimens 2/44 and 2/45 are stable.

Polished sections of specimens 2/44, 2/45, 2/56, 2/52 were also made and were examined by the writer. One of the objects of this investigation was to examine the iron minerals in these basalts in more detail to see if they exhibited the effects of weathering. Also, in the case of specimens 2/44 and 2/45 some attention was to be paid to exsolution phenomena, as these were samples which gave thermal demagnetization curves, indicating that multiphase magnetic systems were present in the rocks.

An examination of these specimens showed, however, that as has been described in 7.2.6, grains of different composition exist in these particular basalt specimens, and are the cause of the rocks having thermal demagnetization curves which indicate the presence of a multiphase magnetic system, not exsolution phenomena as was thought by the writer would be the case.

These observations, in view of the previous discussion of the findings of Akimoto and Katsura (1958) in 7.2.6, suggest to the writer that at Drouin-South we have at the top of the quarry a basalt flow which was intruded at a later date by a large olivene-nephelinite plug. The basalt has been re-heated by the plug and the stable direction of magnetization it has acquired represents the direction of

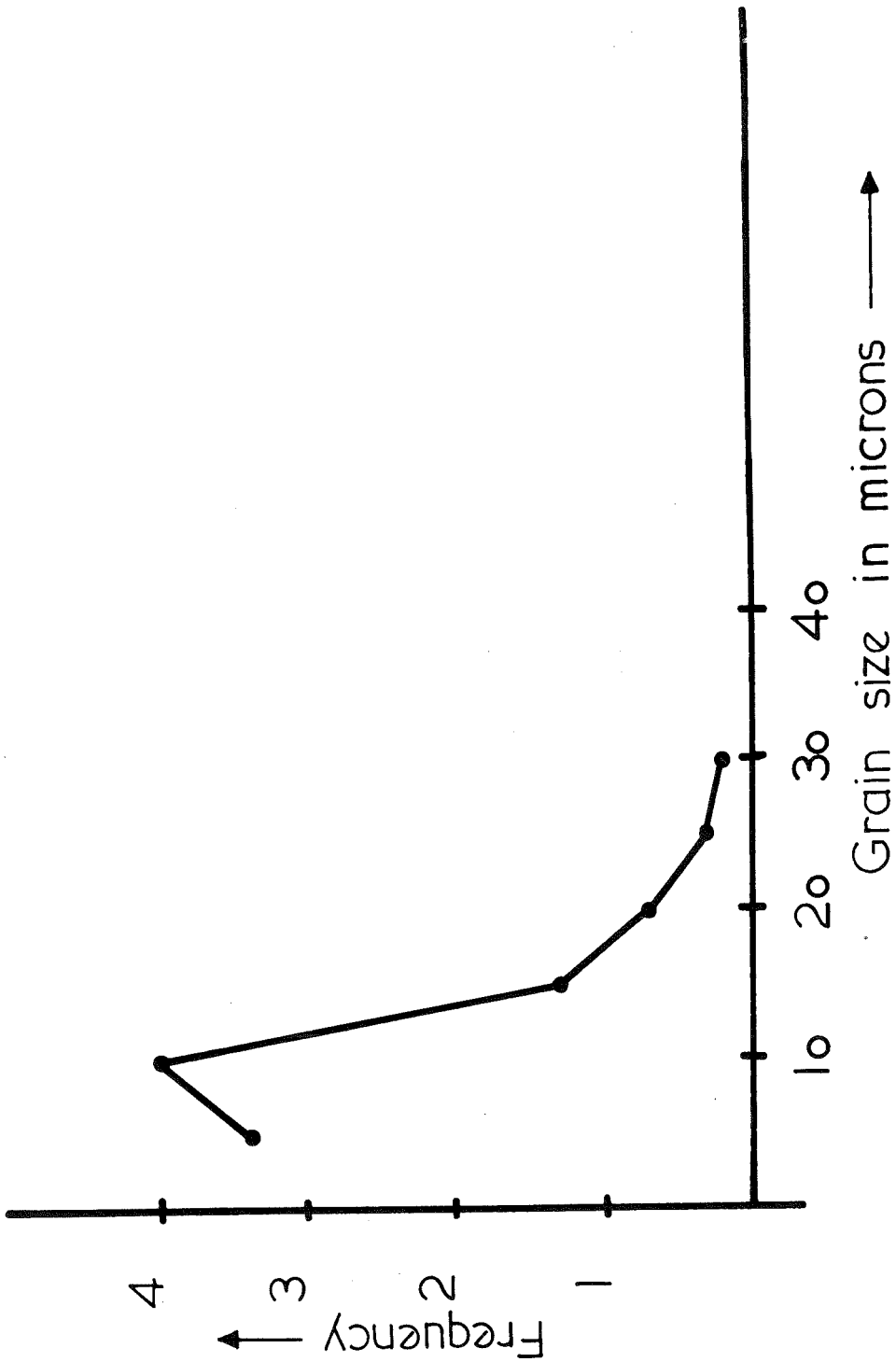

Specimen 2/44

Figure.53

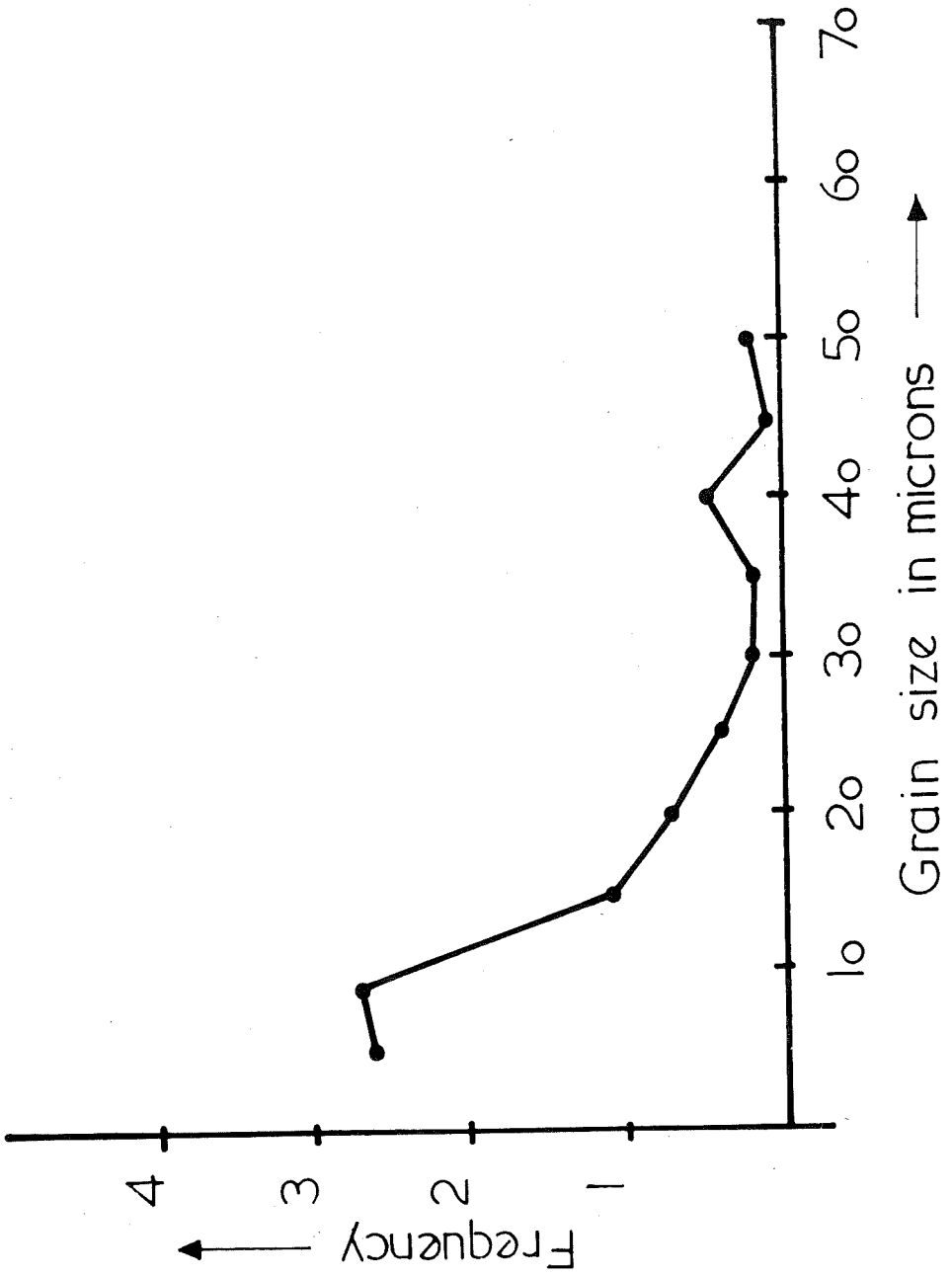

Specimen 2/45

Figure 54

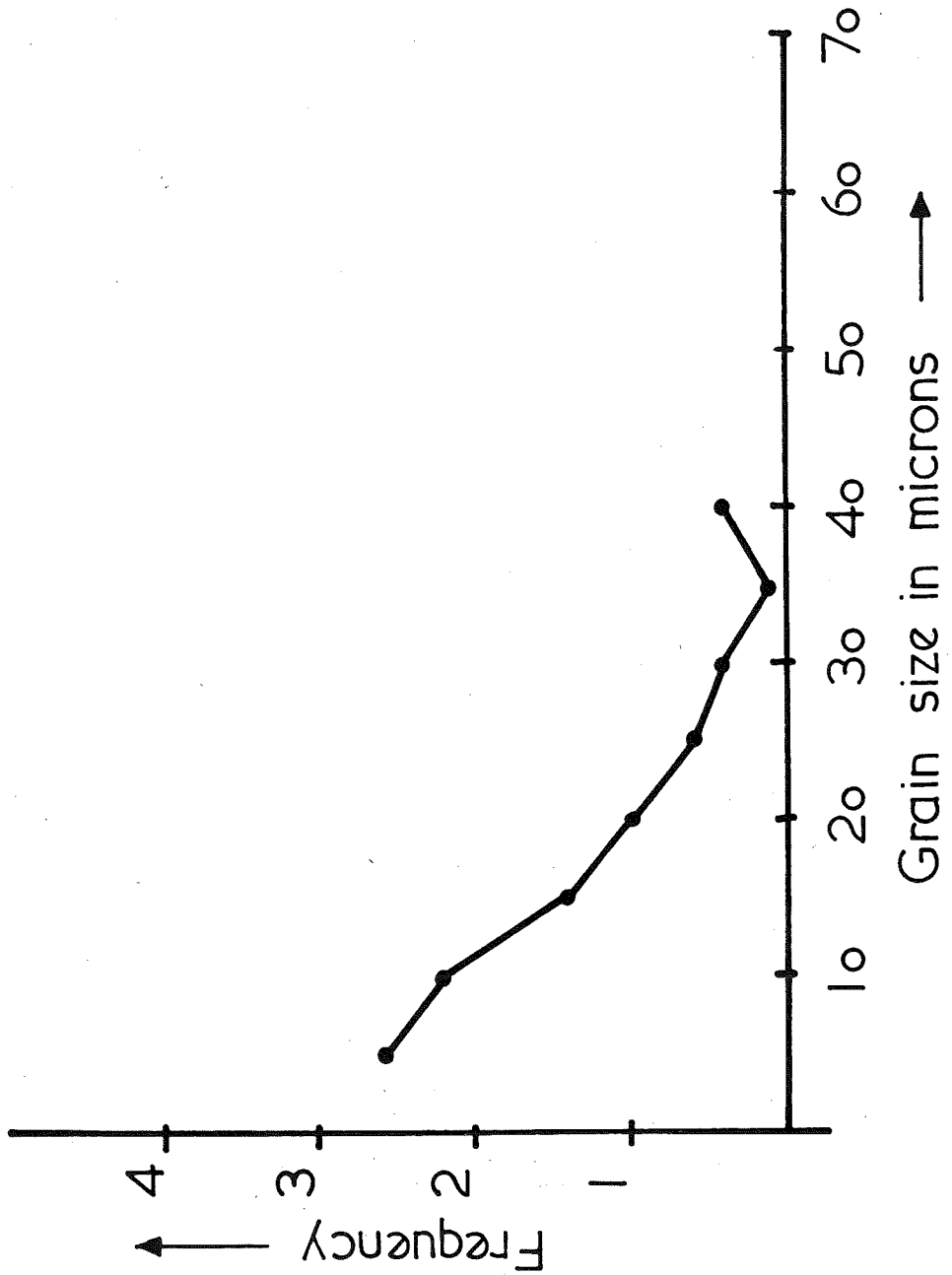

Specimen 2/59

Figure 55.

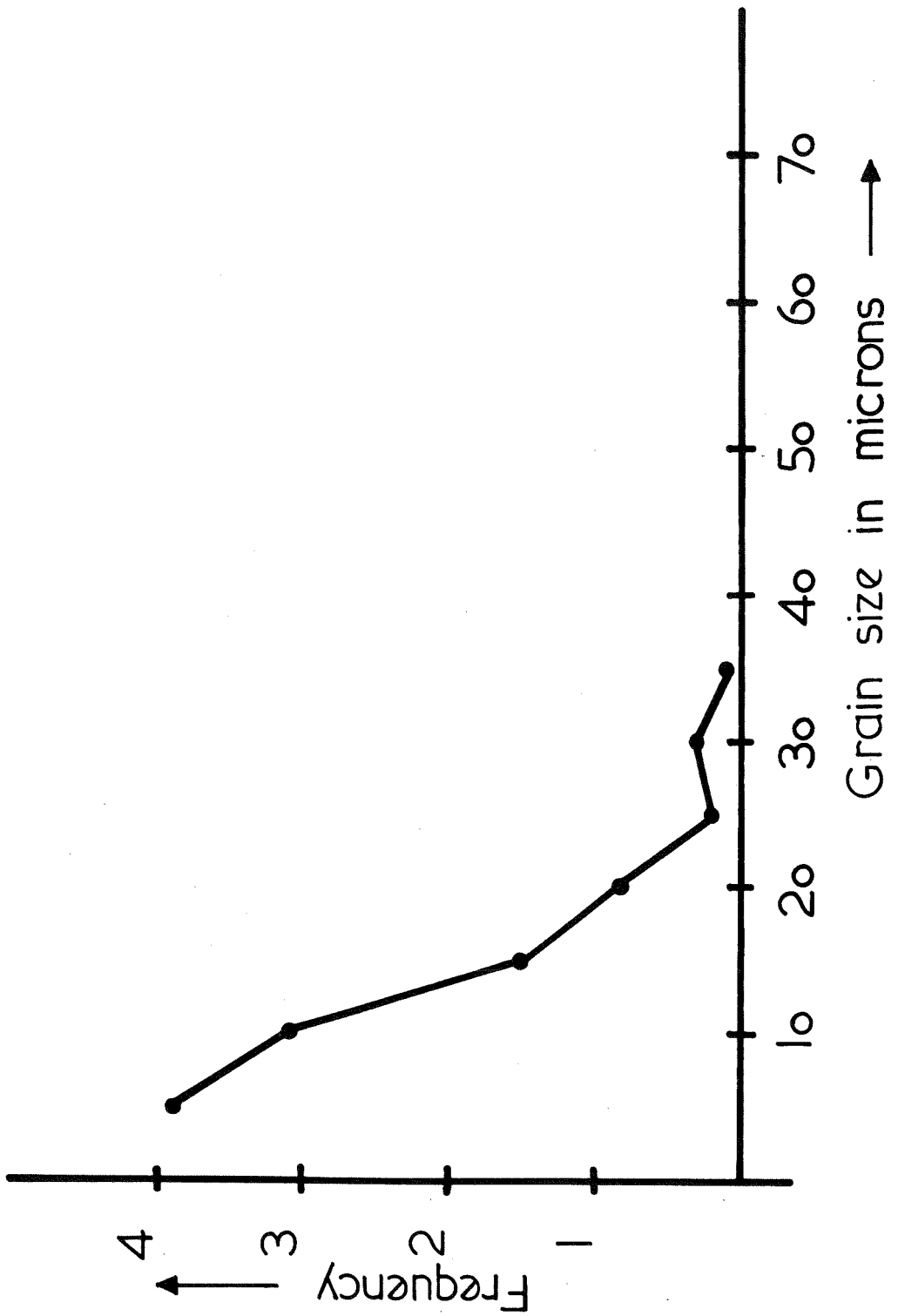

Specimen 2/58

Figure.56.

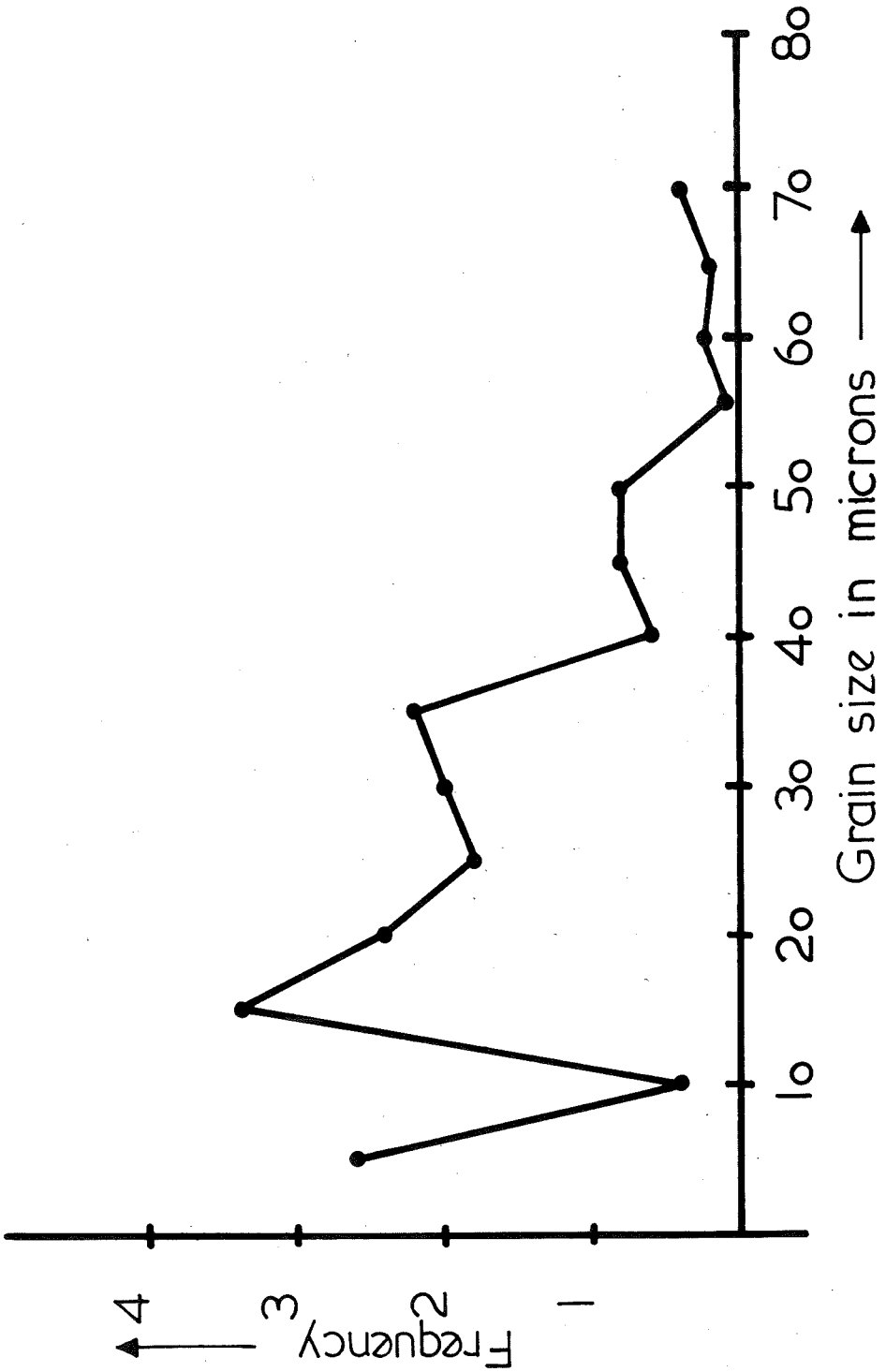

Specimen 2/56

Figure 57

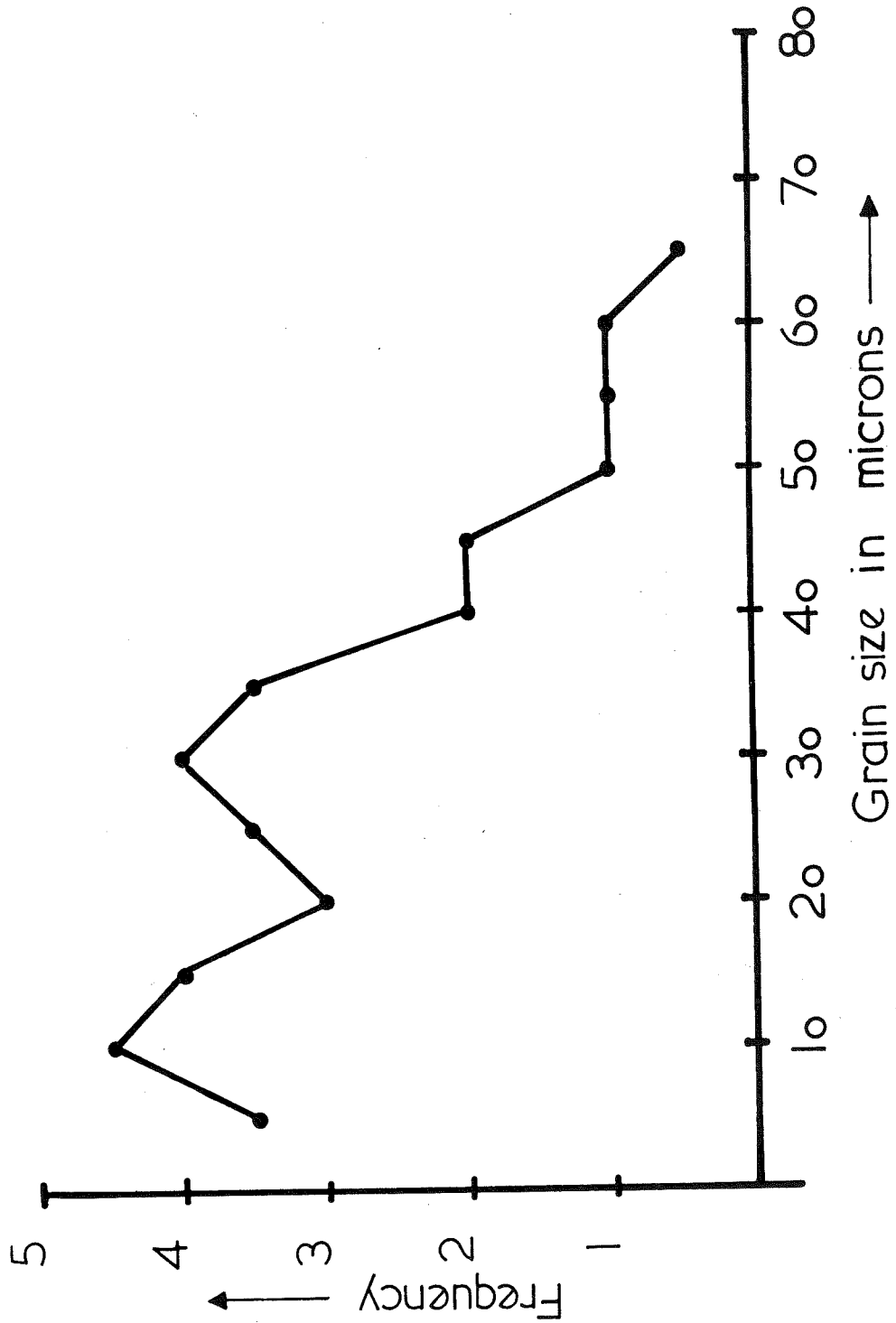

Specimen 2/55

Figure.58.

Specimen 2/41
Frequency
1
2
3
4
5
1o
2o
3o
4o
5o
6o
7o
8o
Grain size in microns

Figure 59.

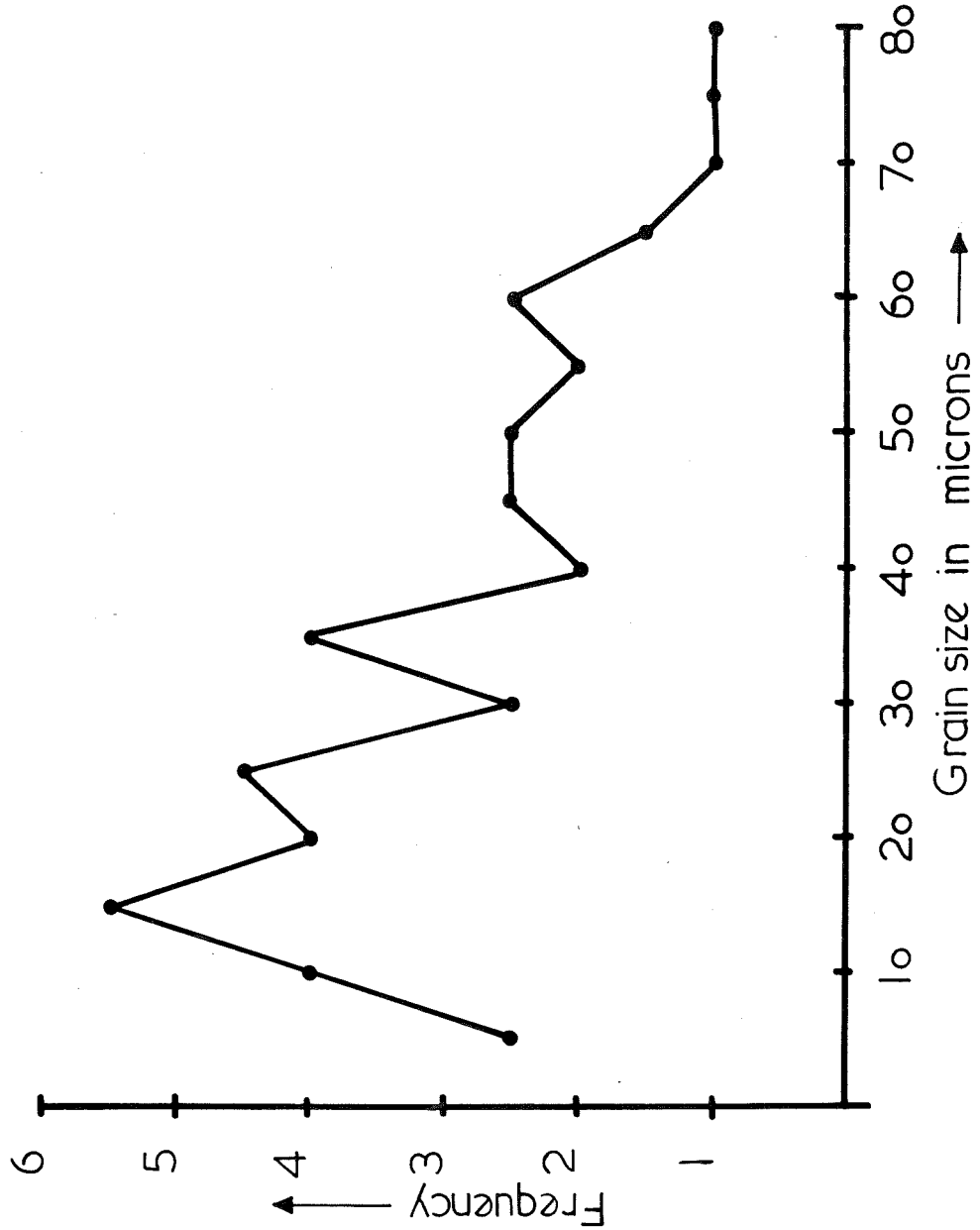

Specimen 2/54

Figure.60.

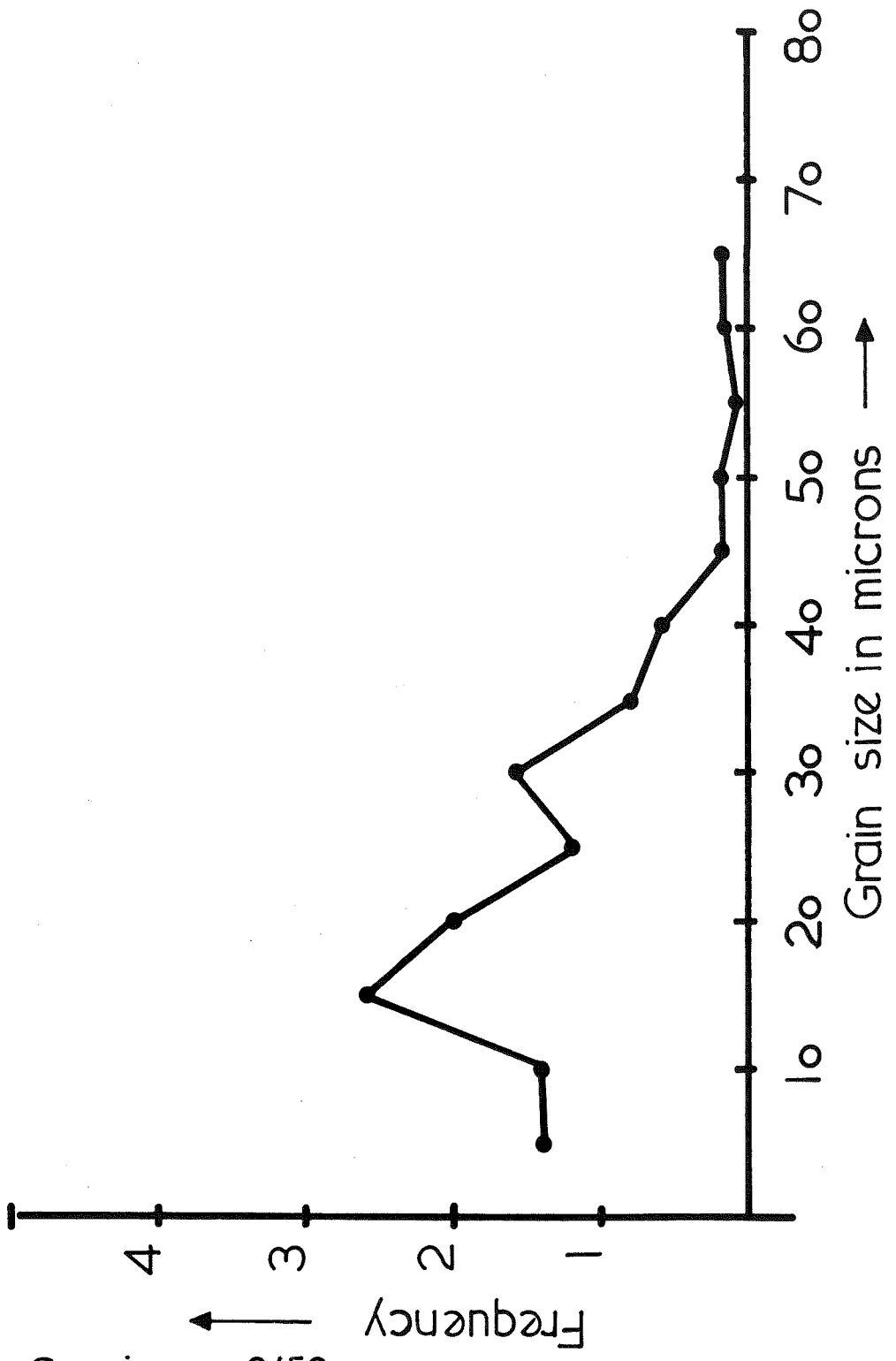
Grain size in microns
10
20
30
40
50
60
70
80
Frequency
1
2
3
4
Specimen 2/52

Figure.61.

magnetization of the earth's field not at the time of its extrusion, but at the time of intrusion of the olivene-nephelinite plug. The writer suggests that the intrusion of the plug has caused post-formational reheating of the basalt flow and so has brought about oxidation of the magnetic mineral in the basalts which was originally a low Curie point titanomagnetite, to a titanomagnetite rather near the composition of pure magnetite.

These higher Curie point titanomagnetites which the writer considers have been formed by this reheating and oxidation, possess a more stable T.R.M. than the original low Curie point types. Further experiments are described in 9.

7.1.8 A discussion of the reversals of magnetization observed in the Older Volcanic basalts.

These basalts are among the many examples which exhibit reversed magnetization. Neel (1951) has proposed four methods of rocks acquiring a reversed T.R.M. in a normal magnetic field.

(1) The rock may contain a mineral having the specific property of developing a thermo-remanent magnetization reversed to the field in which it cools, such as the Li-Fe-Cr spinel synthesized by Gorter and Schulkes (1953).

Specimens from the Older Volcanics which exhibited reversed magnetization became normally magnetized when heated in N_2 above their Curie temperature, and cooled in the earth's field.

(2) The rock may have originally contained a ferrimagnetic mineral which subsequently suffered chemical change, the effect of which was to decrease or destroy the partial magnetization in the direction of the earth's field, leaving the partial magnetization reversed to the earth's field. The magnetic mineral in these basalts is a titanomagnetite which is ferrimagnetic, but from the study of thin and polished sections it does not seem to have undergone any chemical change other than oxidation, in the case of some of the specimens from Drouin-South.

(3) The rock may contain aggregates of two finely divided ferrimagnetics of different Curie points which were in existence when the rock cooled through the higher Curie point (A).

The ferrimagnetic of higher Curie point (A) would be magnetized parallel to the external field; that of lower Curie point (B) would then be magnetized in a field which would be the resultant of the external field and the demagnetization field of (A), which according to the hypothesis may be in a direction opposed to the external field.

Two such constituents did not seem to be present in the rocks. Neel (1955) also proposes reversed T.R.M. may occur due to multi-phase magnetic systems, but the thermal demagnetization experiments on specimens from Drouin-South show that both single and two component

titanomagnetites are present in this locality and both possess a reversed magnetization.

(4) The rock may have originally contained similar aggregates to those just mentioned, but may have suffered chemical alterations involving the destruction (complete or partial) of A subsequent to the magnetization of B. This hypothesis could apply even if the thermo-remanent magnetization of B never outweighed that of A before alteration.

Considering all these possibilities it would seem that there are the two explanations for the reversed T.R.M.

(1) The Tertiary magnetic field was reversed during periods and this accounts for the reversed natural magnetization.

(2) The rocks are self-reversed while the Tertiary magnetic field was then normal as it is today. The self-reversing properties of all the rocks have subsequently disappeared. This second explanation does not seem entirely feasible when one considers the fresh, unaltered appearance of many of these rocks when examined in thin and polished section.

8. AN INVESTIGATION OF THE SCATTER OF DIRECTIONS OF MAGNETIZATION IN A SINGLE LAVA FLOW.

8.1 Introduction

It has been observed by E. Irving (private communication) that the scatter of the directions of magnetization in a single lava flow is larger than would be accounted for by the experimental errors involved.

To study the variation of the directions of magnetization within single lava flows, quarries at Merri Creek and Abberfeldie, both in the Newer Volcanics, were sampled.

8.2 Fieldwork

Seventeen oriented samples were collected over a vertical interval of about 130 ft. at Merri Creek. At Abberfeldie a smaller thickness was sampled.

The localities of the specimens are given in Table 15.

Both of these quarries were reversely magnetized sites.

TABLE 15

MERRI CREEK QUARRY

Specimen No.	Locality
2/34	Base
33	13 feet above 34
32	5½ feet above 33
31	8 feet above 32
30	15 feet above 31
18	In line with 30
19	10 feet above 18
20	5 feet above 19
21	9 feet above 20
22	6 feet above 21
23	8 feet above 22
24	8 feet above 23
25	13 feet above 24

(contd.)

TABLE 15 Merri Creek Quarry (contd.)

Specimen No.	Locality
26	6 feet above 25
27	6 feet above 26
28	8 feet above 27
29	6½ feet above 28

ABERFELDIE QUARRY

Specimen No.	Locality
2/9	At base
8	4 feet above 9
10	4 feet above 8
11	4½ feet above 10
12	4½ feet above 11
13	4½ feet above 12
14	5 feet above 13
15	5 feet above 14
16	3 feet above 15
17	3 feet above 16

8.3 Results

The directions of magnetization of the specimens from Merri Creek are given in Table 16

TABLE 16 (Merri Creek)

Specimen No.	Moment c.g.s/c.c.	D (M.N.)	I
2/34	1.36×10^{-3}	155	55
33	1.12	124	53
32	1.65	127	64
31	2.16	127	66

(contd.)

TABLE 16 (Morri Creek) contd.

Specimen No.	Moment c.g.s/c.c.	D (M.N.)	I
30	1.29	162	61
18	1.21	167	53
19	1.43	169	53
20	1.87	183	56
21	1.78	168	57
22	2.93	174	56
23	2.14	170	60
24	2.03	155	54
25	.60	177	50
26	.46	173	48
27	.94	184	57
28	1.57	153	58
29	1.32	155	65

These directions are plotted in figure 62 . The mean direction of magnetization of these directions is

$$D\ M.N. = 161^{\circ}$$
$$I = 58^{\circ}$$

The Fisher precision K is given by

$$K = \frac{N - 1}{N - R}$$

$$= \frac{17 - 1}{17 - 16.7} = 53$$

The direction of magnetization of the specimens from Abberfeldie quarry are given in Table 17.

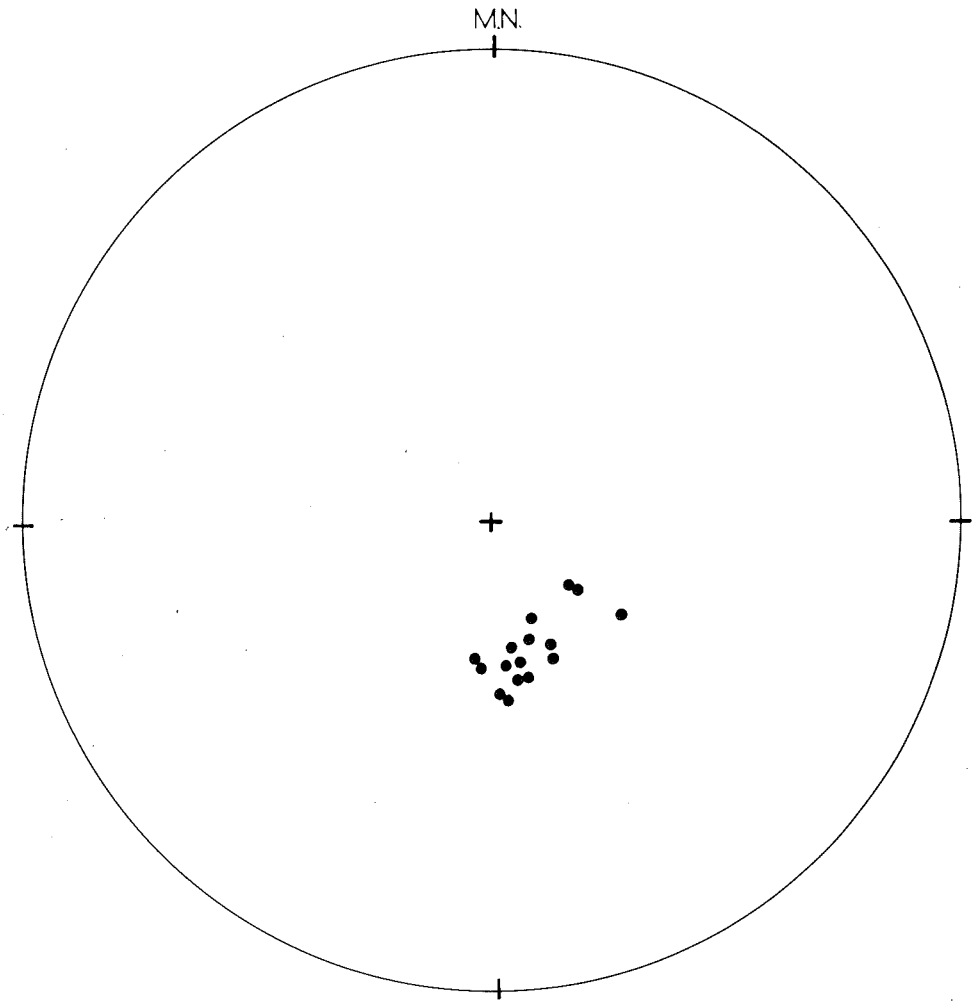

Merri Creek Quarry

Figure.62.

TABLE 17 (Abberfeldie Quarry)

Specimen No.	D (M.N.)	I
2/8	128	53
9	138	29
10	147	58
11	149	45
12	139	40
13	127	42
14	145	45
15	160	31
16	167	42
17	170	39

The mean direction of magnetization of these directions is

$$D\ (M.N.) = 147^{\circ}$$

$$I = 44^{\circ}$$

$$K = \frac{N - 1}{N - R}$$

$$= \frac{10 - 1}{10 - 9.74} = 34.6$$

The dispersion of the directions of magnetization of the specimens from Abberfeldie quarry is thus greater than those from Merri Creek quarry, but the difference is not large.

8.4 The effect of a.c. cleaning on the dispersion.

The specimens from Abberfeldie quarry were cleaned in fields of 86 and 173 oersted. The directions of magnetization after the cleaning are given in Table 18.

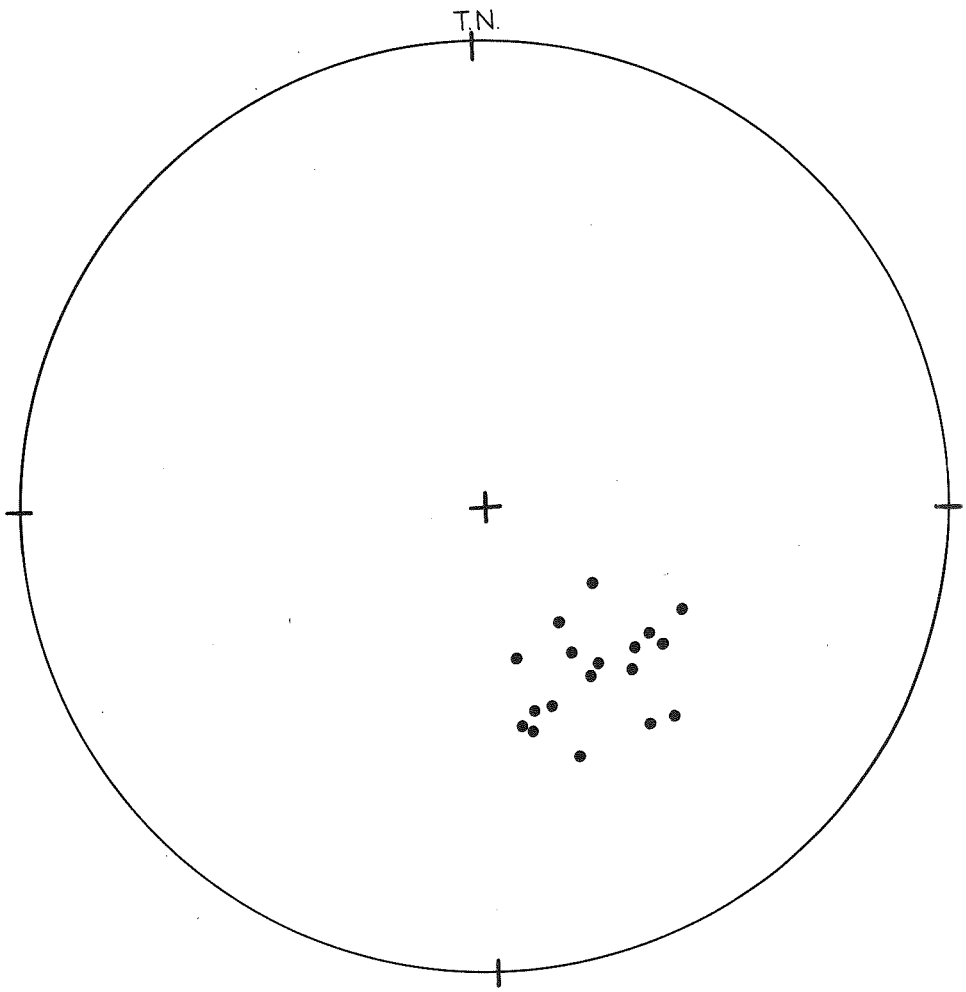

Abberfeldie Quarry - before cleaning.

Figure 63.

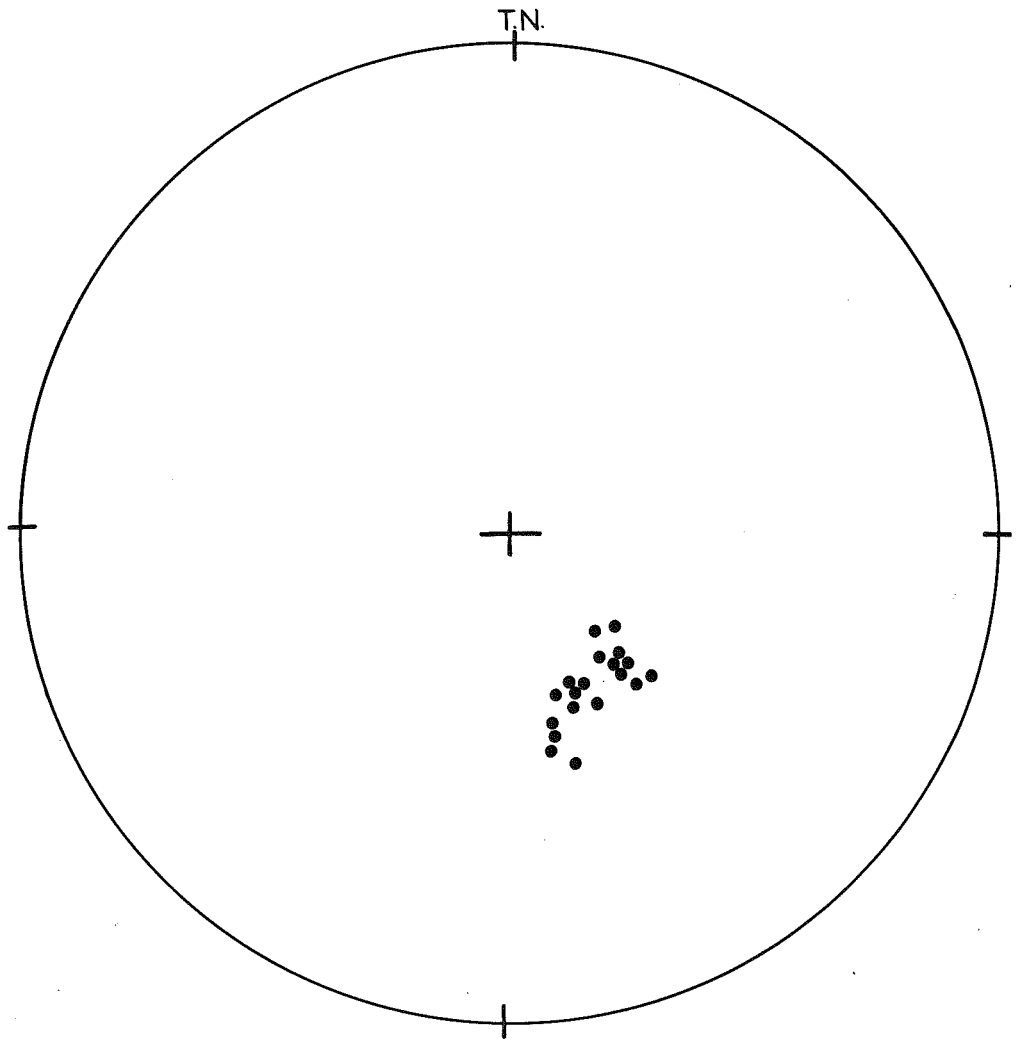

Abberfeldie Quarry - 86oersted

Figure.64.

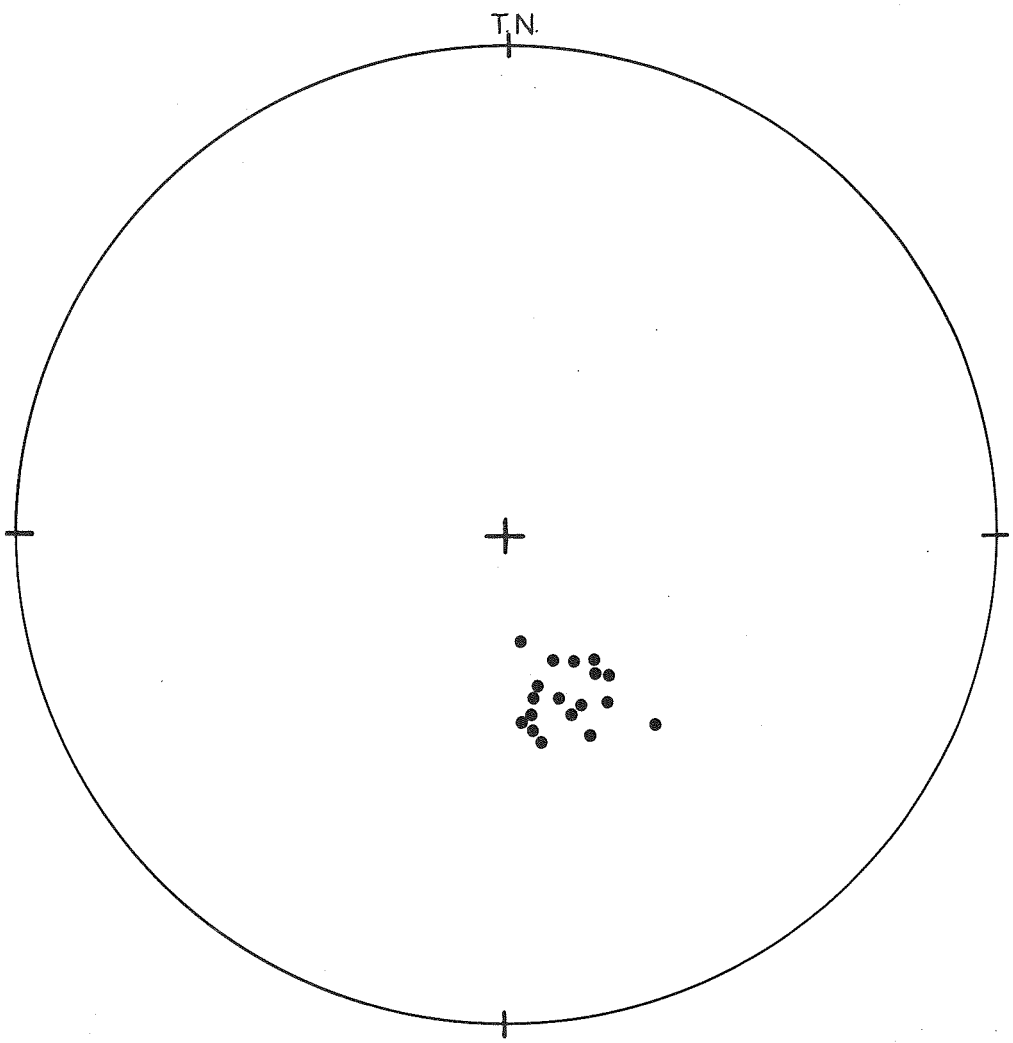

Abberfeldie Quarry - 173 oersted

Figure.65.

TABLE 18

SPECIMEN NO.	A.C. CLEANING FIELD			
	86 oersted		173 oersted	
	D (M.N.)	I	D (M.N.)	I
2/8	137	59	143	53
9	138	51	146	45
10	155	53	148	58
11	152	48	155	59
12	156	52	168	49
13	134	45	147	57
14	142	54	142	54
15	163	38	170	48
16	166	46	166	48
17	167	43	168	44

The value of K after cleaning in these fields is set out in Table 19.

TABLE 19

A.c. cleaning field (oersted)	K
86	450
173	82

Thus the a.c. cleaning has improved the scatter of the directions of magnetization considerably.

It would appear then that the scatter of the directions of magnetization of specimens taken from a single basalt flow is in part due to the fact that the rocks acquire small temporary components of magnetization.

8.5 Thermal demagnetization of specimens from Merri Creek quarry

Three specimens, one from near the top, another near the middle and a third from near the base of the quarry face at Merri Creek were thermally demagnetized.
The Curie points are given in Table 20.

TABLE 20

Specimen	Curie Point ^{o}C
2/34	400
2/21	325
2/29	350

Figures 121, 122, 123 are the thermal demagnetization curves for these specimens.

The magnetic mineral here is most likely a titano-magnetite and from the results obtained is one which is slightly more stable thermally than most of the specimens from Drouin-South (see Figures 109 to 120).

It is also seen that while there is a variation of Curie point over the thickness of the lava flow here, this variation is small compared with the situation at Drouin-South quarry and may be in part the explanation for the uniform magnetization of the flow.

9. FURTHER EXPERIMENTS ON STABILITY OF MAGNETIZATION IN NATURAL AND SYNTHETIC ROCK SPECIMENS.

9.1 Introduction

There has been increasing literature in recent years on the stability of magnetization in rocks, and perhaps the most up to date investigation of this type was carried out on igneous rocks by Irving et al (1961). They have given a satisfactory method for treating igneous rocks to remove unstable components of magnetization, and this is the method used in 5.7 and 7.1.5. They also discuss how rocks retain the stable N.R.M. and suggest that the stable magnetization is retained in high stability regions within the ferromagnetic grains, and that the explanation for the hard and soft magnetic components which are found not only in basalts, but also in other igneous rocks, is to be sought in exsolved phases of differing grain size in ferromagnetic grains.

The magnetic minerals in most basalts are titanomagnetites as is the case with the specimens collected from Drouin-South. A relation between stability and Curie temperature of the titanomagnetites has been indicated by the a.c. and thermal demagnetization experiments described in 6, and such a relation explains in part the findings of previous investigations of Irving et al.

The procedure outlined by Irving et al to remove unstable components of magnetization involves cleaning the rock

specimens in gradually increasing peak a.c. fields and choosing the distribution of directions of magnetization which has the least scatter. They also report that after treatment in high alternating fields, the intensity of magnetization of a specimen does not diminish regularly with increasing alternating field, but levels off to an almost constant average value when directions of magnetization become nearly random. This value is called the minimum intensity (M min) of magnetization.

These authors suggest that the cause for this M min is that the spontaneous magnetization of domains is lost only at temperatures above the Curie point, that the effect of alternating magnetic fields is one of rearrangement of domains, and because of statistical fluctuation the resultant moment of a specimen is never likely to be zero. The results of experiments that the writer has carried out seem to suggest that the reason why different cleaning fields produce minimum scatter of direction in different sites is in large part due to the fact that the magnetic minerals present in one site may have Curie temperatures hundreds of degrees different from those present in another site, and so possess a different degree of instability.

One of the reasons for the poor grouping of directions of magnetization after cleaning the specimens from a particular site is due to the fact that the specimens may have a large range of Curie temperatures, as they do at Drouin-South,

and so the stability varies widely within this one site. While a specimen which has ferromagnetic grains composed mainly of magnetite probably does not acquire large temporary components of magnetization, quite large cleaning fields can be used to remove any temporary components of magnetization before the T.R.M. is affected too much by the cleaning.

On the other hand, those specimens which are composed mainly of a titanomagnetite with a low Curie temperature are very likely to acquire large unstable components of magnetization, but only small washing fields can be used to demagnetize such specimens, for the magnetic moment reaches a minimum intensity of magnetization after cleaning in fairly small fields, and the directions of magnetization begin to become scattered - almost random. This type of behaviour is shown in 9.2.2.

9.2 Further Experiments on stability of magnetization.

9.2.1 An experiment showing the effect of minimum intensity of magnetization and the variation of directions of magnetization after a.c. magnetic field cleaning in basalts containing both high and low Curie point titanomagnetites.

Irving et al have suggested that the accuracy of the procedure of removal of unwanted secondary magnetizations by alternating magnetic fields will be limited by the presence of the minimum intensity in those cases where

the magnitude of the soft component is large, since the minimum intensity of this may exceed the magnitude of the hard component.

To show what effect this minimum intensity of magnetization of a soft component can have in those cases where there are high Curie temperature and low Curie temperature components present, the writer has taken three specimens, the thermal demagnetization curves of which are given in figures 117, 119, 113. These are specimens 2/55, 2/58 and 2/44. It is seen that two of these are two component types, one containing mostly a low Curie temperature titanomagnetite. The third contains a low Curie point titanomagnetite only. The Curie temperatures of the various components in these specimens are given in Table 21.

TABLE 21

Specimen No.	Curie Temp. ^{o}C
2/55	225
2/58	150, 580
2/44	225, 500

These specimens were demagnetized repeatedly in an a.c. field of 500 oersted and the direction and the moment of magnetization were measured after each demagnetization. The demagnetization was repeated ten times for each specimen in this same field of 500 oersted. In a field of this magnitude, specimen 2/55 and the low Curie

temperature titanomagnetite of 2/58 and 2/44 should have reached the minimum intensity condition, but the high Curie temperature titanomagnetite of 2/58 and 2/44 should not yet have reached this condition, as is indicated by figure 40, the a.c. demagnetization curve for specimen 2/45 which contains a high Curie temperature titanomagnetite having a Curie temperature of 510°C compared with 500°C for specimen 2/44.

The directions of magnetization and the moment of the specimen after each demagnetization is given in Table 22.

TABLE 22

Specimen 2/55			Specimen 2/58			Specimen 2/44		
M(c.g.s)	D(MN)	I	M(c.g.s)	D(MN)	I	M(c.g.s)	D(MN)	I
1.50×10^{-2}	217	4	1.25×10^{-2}	161	-30	1.79×10^{-2}	187	44
1.79×10^{-2}	194	-30	1.28×10^{-2}	133	-61	1.55×10^{-2}	357	34
1.90×10^{-2}	248	5	1.74×10^{-2}	274	54	1.28×10^{-2}	42	-2
1.91×10^{-2}	285	0	1.42×10^{-2}	354	24	1.59×10^{-2}	41	46
1.48×10^{-2}	152	-56	1.18×10^{-2}	350	4	$.89 \times 10^{-2}$	309	-58
1.72×10^{-2}	321	-2	2.04×10^{-2}	305	46	1.86×10^{-2}	36	61
1.48×10^{-2}	85	-8	$.85 \times 10^{-2}$	337	-67	1.17×10^{-2}	317	-51
1.50×10^{-2}	326	-1	1.15×10^{-2}	168	-5	1.21×10^{-2}	161	6
1.30×10^{-2}	239	45	1.95×10^{-2}	274	59	1.69×10^{-2}	126	67
1.48×10^{-2}	86	3	1.26×10^{-2}	204	36	1.59×10^{-2}	173	4

In figure 66 the angle of inclination and the magnetic moment of each specimen is plotted against the number of

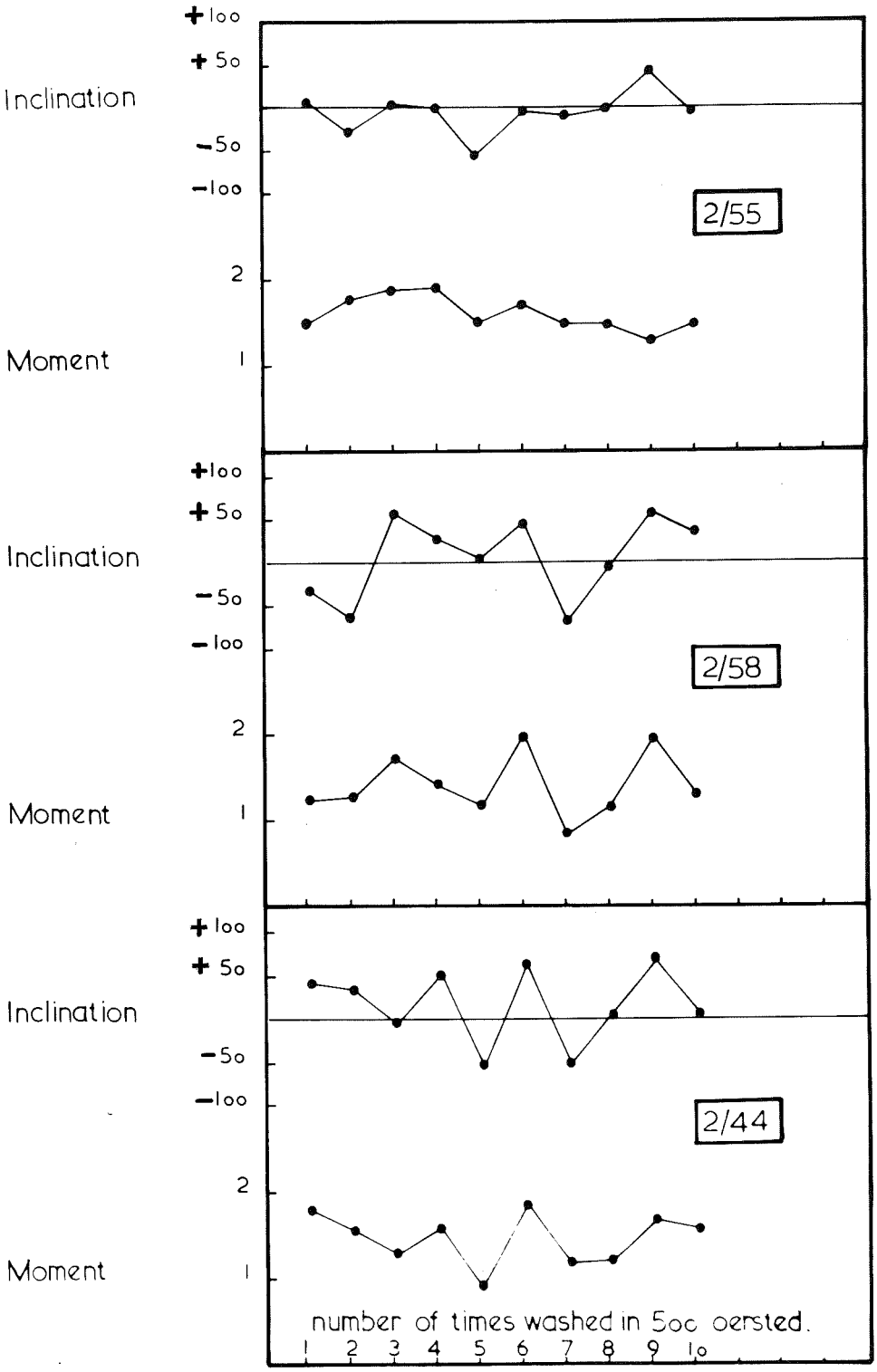
+ loo
+ 5o
Inclination
−5o
−loo
2/55
2
Moment
1
+loo
+ 5o
Inclination
−5o
−loo
2/58
2
Moment
1
+ loo
+ 5o
Inclination
−5o
−loo
2/44
2
Moment
1
number of times washed in 5oc oersted.
1 2 3 4 5 6 7 8 9 lo

Figure .66.

times the specimen has been demagnetized. It is quite readily seen that in the case of the specimens which have both high Curie temperature and low Curie temperature components of magnetization, the magnetic moment varies as the direction of magnetization. When the direction of magnetization is reversed, the stable direction for the site determined in 6.1.5. the magnetic moment is greatest. These results of course suggest that there is a reversed stable direction in the specimen which is not affected much by the repeated cleaning, together with a direction which varies with cleaning.

In other words, there is a hard magnetization, the direction of which does not change greatly on cleaning, together with a soft magnetization, the direction of which does vary considerably with cleaning, because it has reached the minimum intensity condition in demagnetization and the direction of magnetization takes near random position after repeated cleaning in the same high field.

9.2.2 <u>An experiment on the stability of T.R.M. in low and high Curie point titanomagnetites</u>.

In figures 67,68 are shown the effect of cleaning two specimens, one which contains a very low Curie temperature titanomagnetite (2/55) and the other which contains a high Curie temperature titanomagnetite (2/44) under the following circumstances. Both of the specimens have been given a

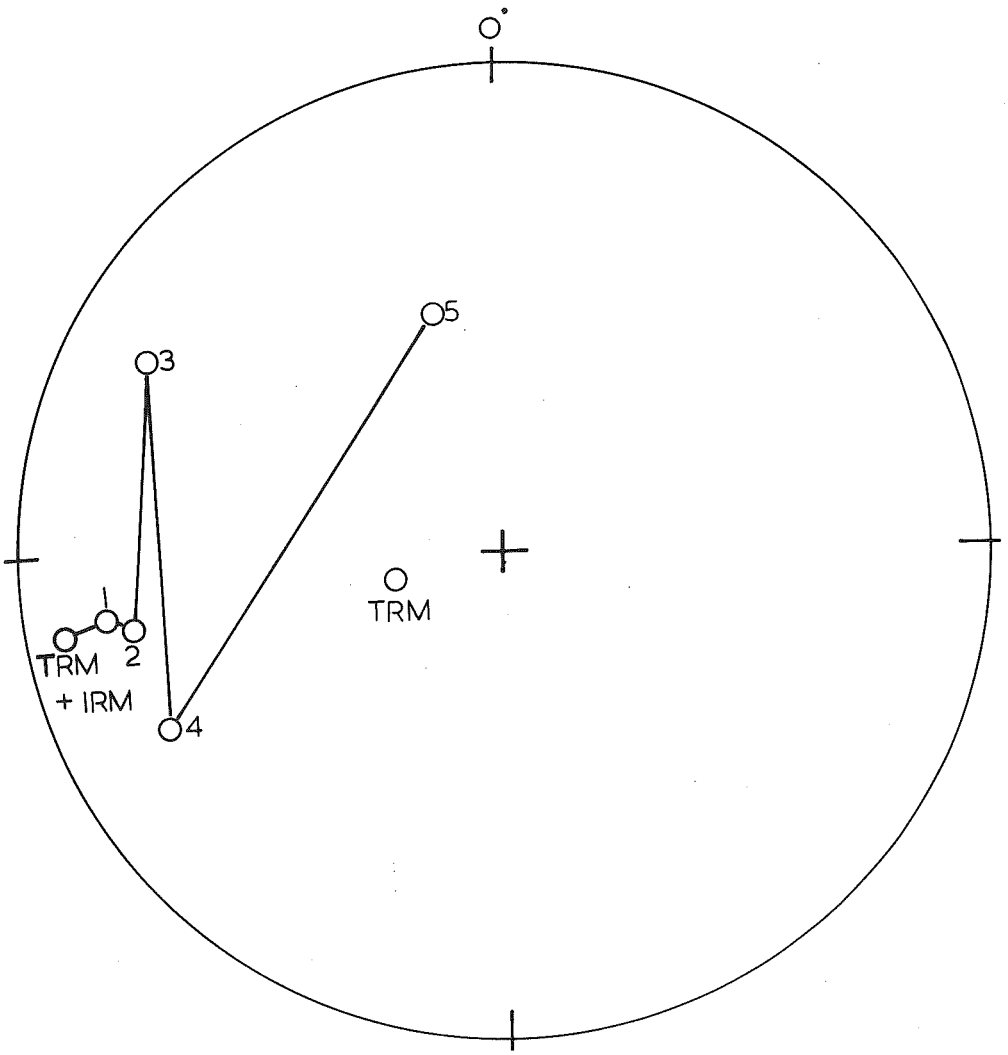

Specimen 2/55

1	–	45 oersted
2		90
3		170
4		260
5		340

Figure 67.

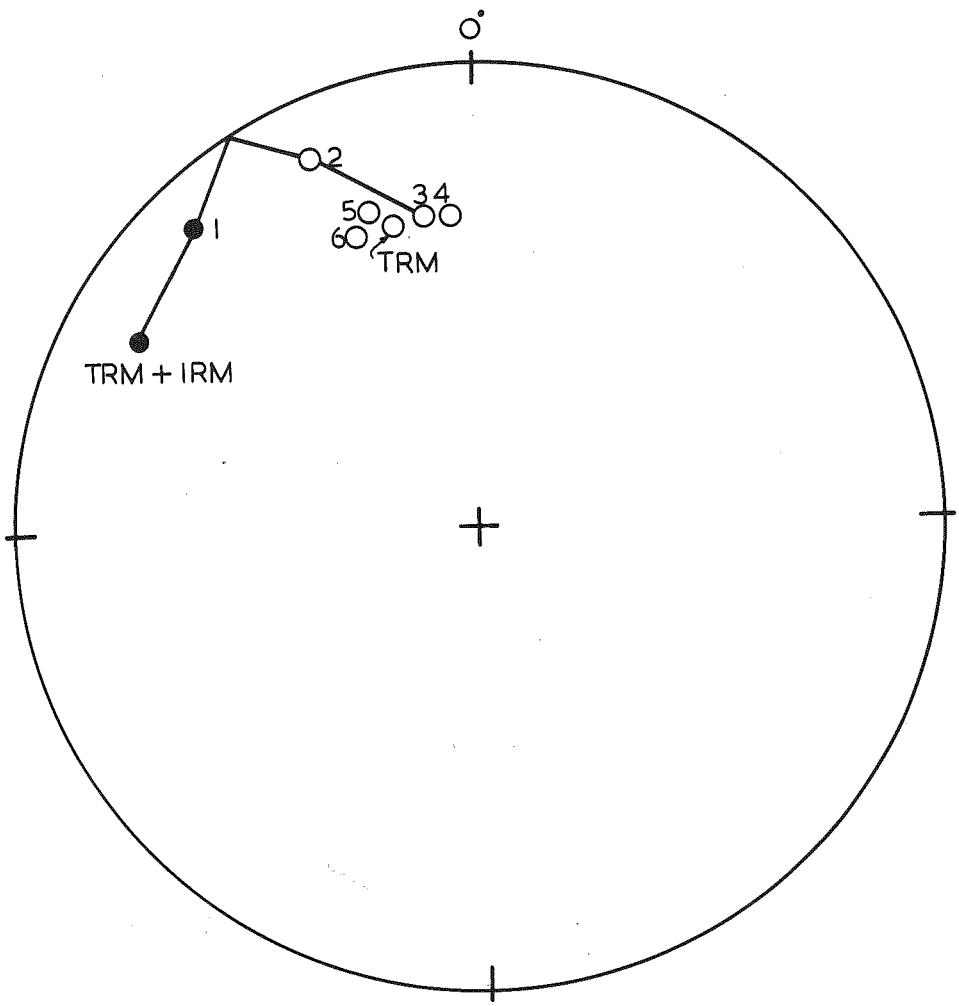

Specimen 2/44

1 – 45 oersted.
2 90
3 170
4 260
5 340

Figure 68.

T.R.M. by heating them above their Curie temperatures to 250°C and 500°C respectively, and allowing them to cool in the earth's field. They were then given an I.R.M. of about 100 oersted and were cleaned in fields of 45, 90, 170, 260 and 340 oersted.

It is seen that in the case of the specimen which contains the high Curie temperature titanomagnetite, the I.R.M. is removed by the cleaning, and the direction of magnetization of the specimen returns to the direction of the original T.R.M. In the case of the rock containing the low Curie temperature titanomagnetite, however, after initial cleaning the direction of magnetization begins to return to the direction of magnetization of the T.R.M. given to the specimen but before the I.R.M. is completely removed, the T.R.M. of the specimen itself begins to be affected by the increased cleaning field and the direction of magnetization after cleaning in these higher fields becomes almost random.

9.2.3 <u>The effect of sustained heating in air on the stability of magnetization in basalt specimens</u>.

In figures 69, 72 are shown the effect of demagnetizing specimens 33 bc, 33 ba after they have been held at 400°C for one hour in an atmosphere of air, and were allowed to cool slowly in the earth's field. These curves are compared with the a.c. demagnetization curves obtained for the two specimens before they were heated in the manner just described.

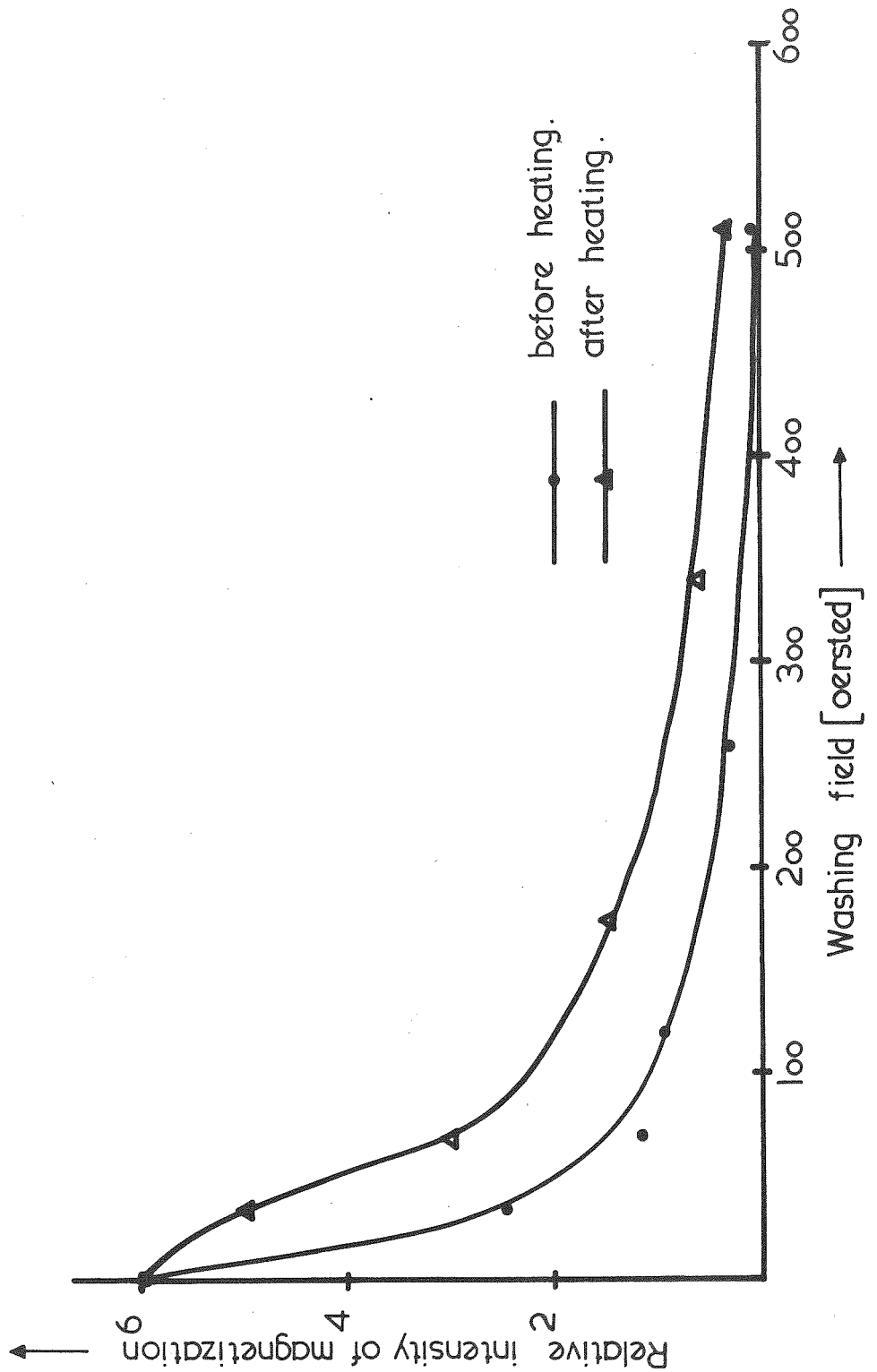

Specimen 33bc

Figure.69.

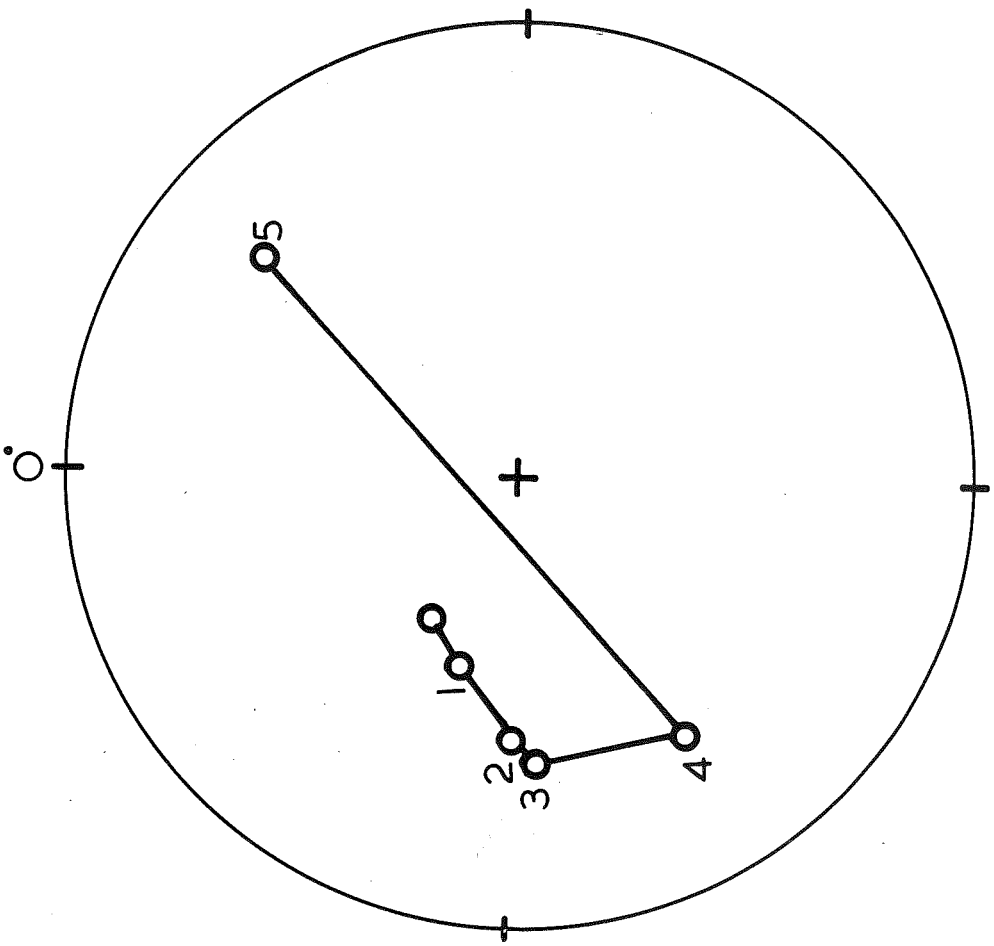

Specimen 33bc - before heating

1	–	34 oersted.
2		68
3		119
4		255
5		510

Figure.7o.

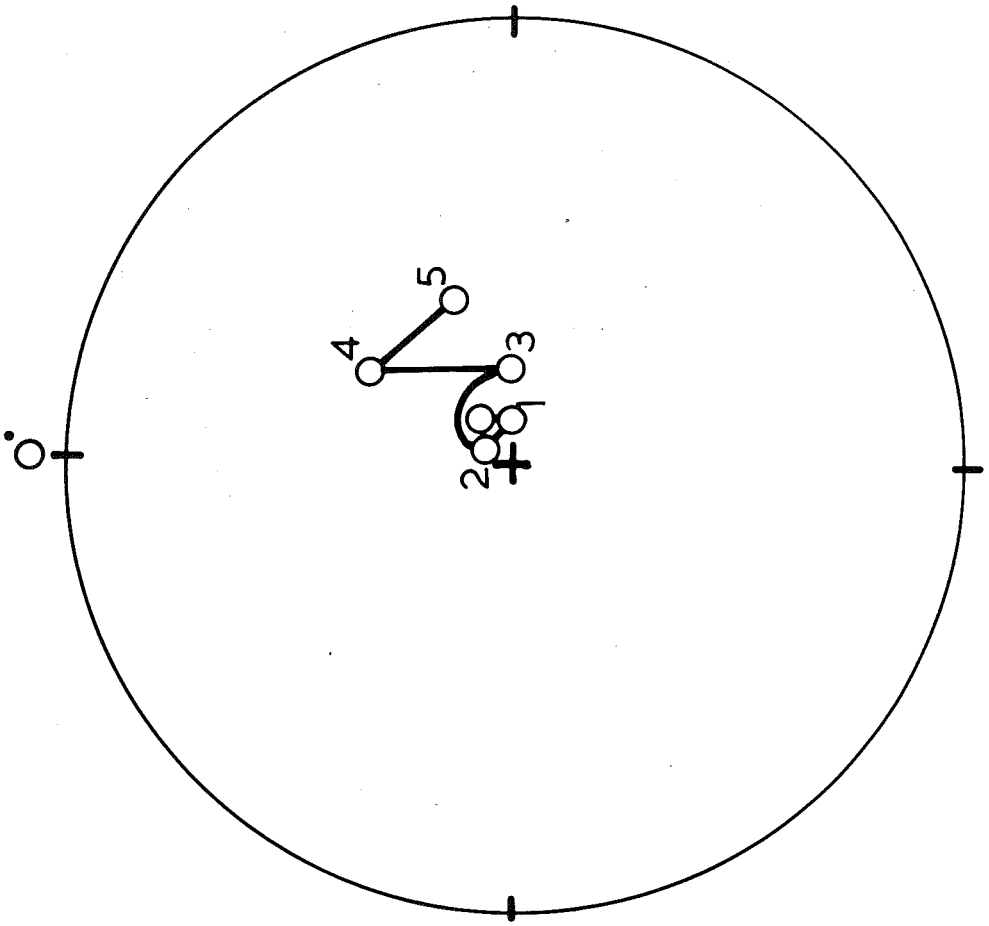

Specimen 33bc - after heating

1	-	34oersted
2		68
3		119
4		225
5		510

Figure.71.

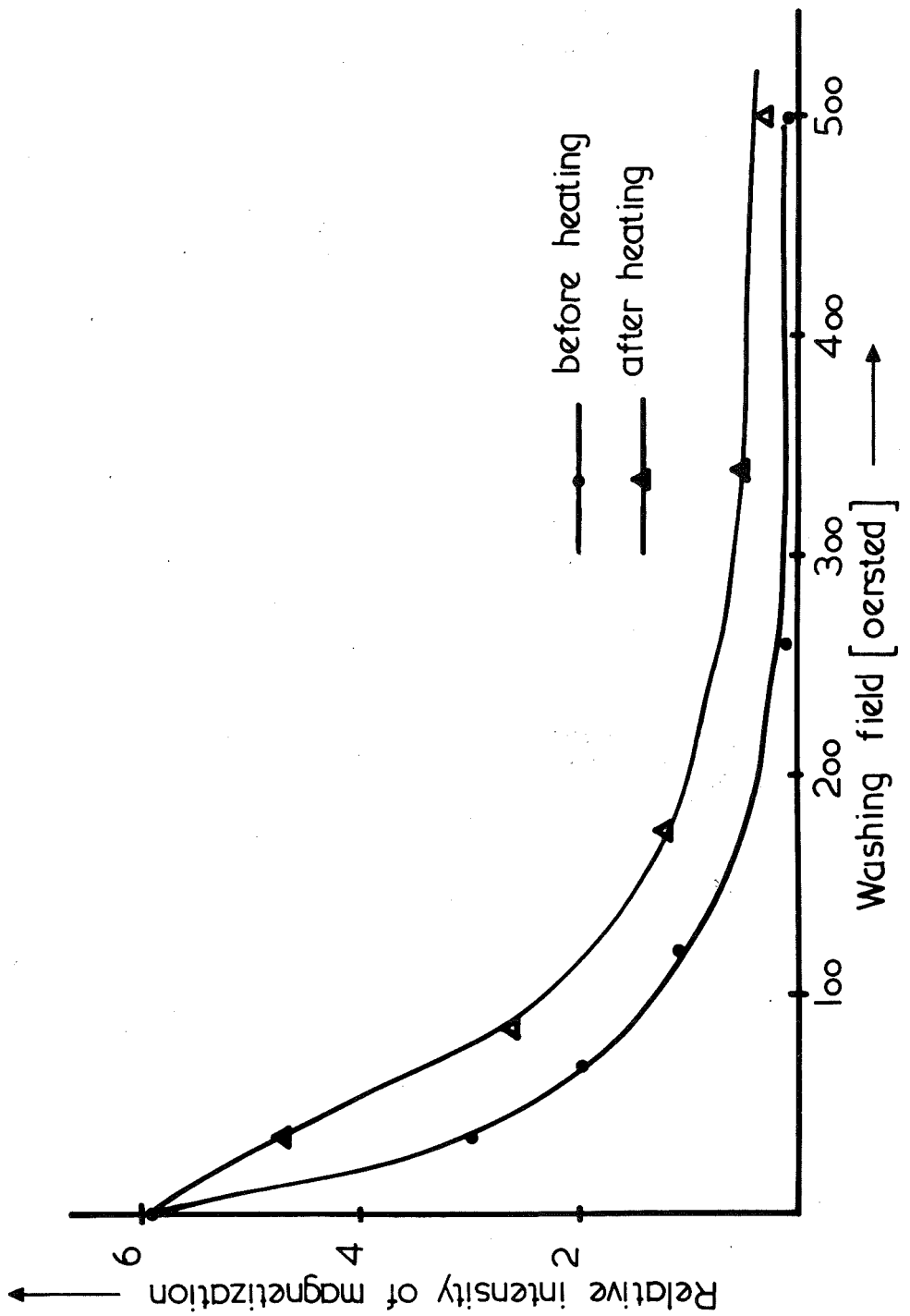

Specimen 33 ba

Figure 72.

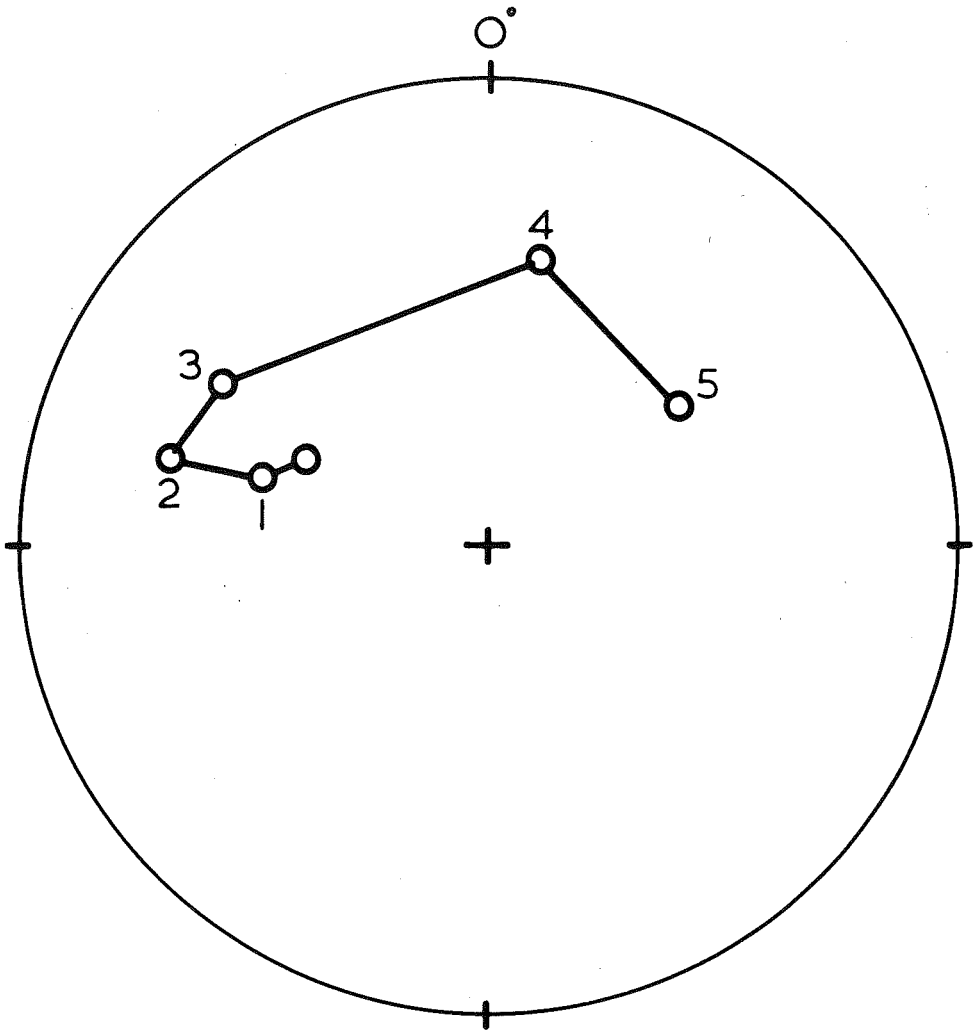

Specimen 33ba – before heating

1	–	34 oersted
2		68
3		119
4		255
5		510

Figure.73.

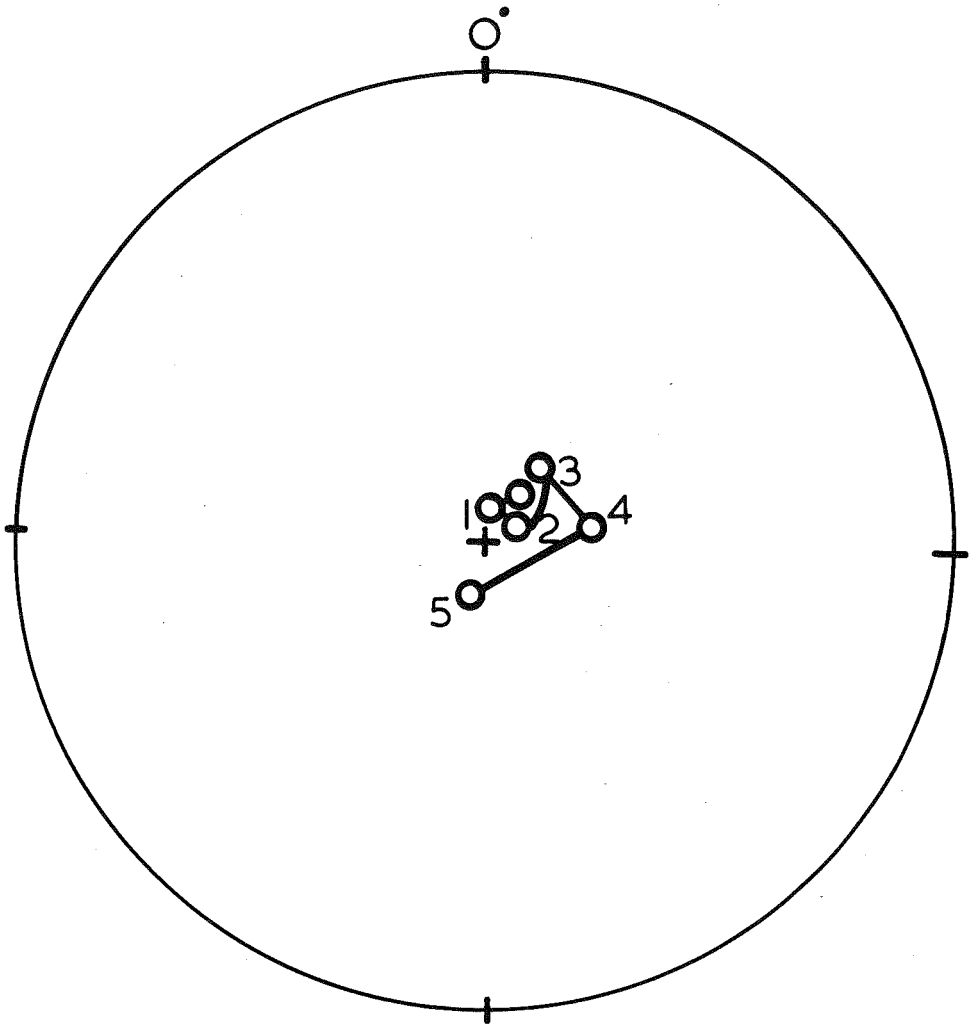

Specimen 33 ba - after heating

1	–	34 oersted
2		85
3		170
4		255
5		510

Figure 74.

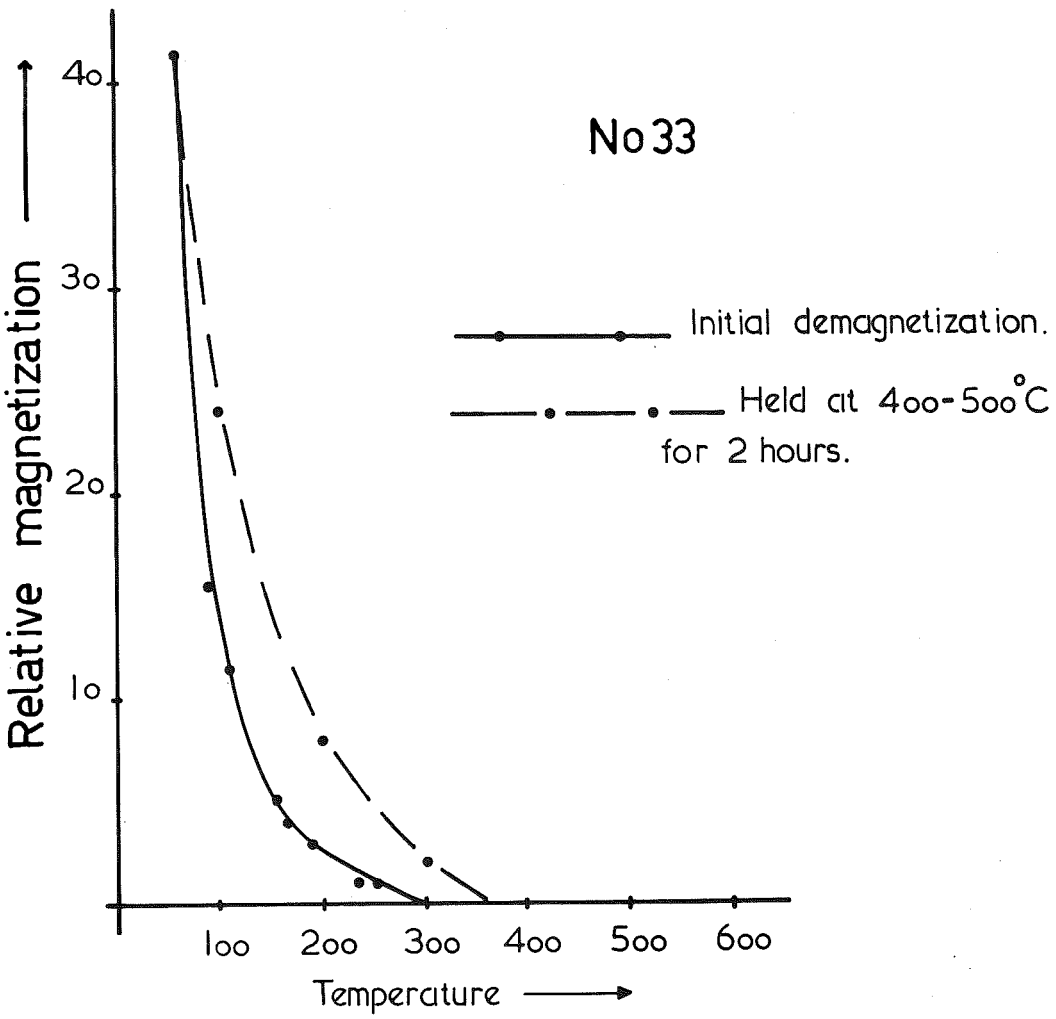
No 33
Initial demagnetization.
Held at 400-500°C
for 2 hours.
Relative magnetization
40
30
20
10
100
200
300
400
500
600
Temperature

Figure 75.

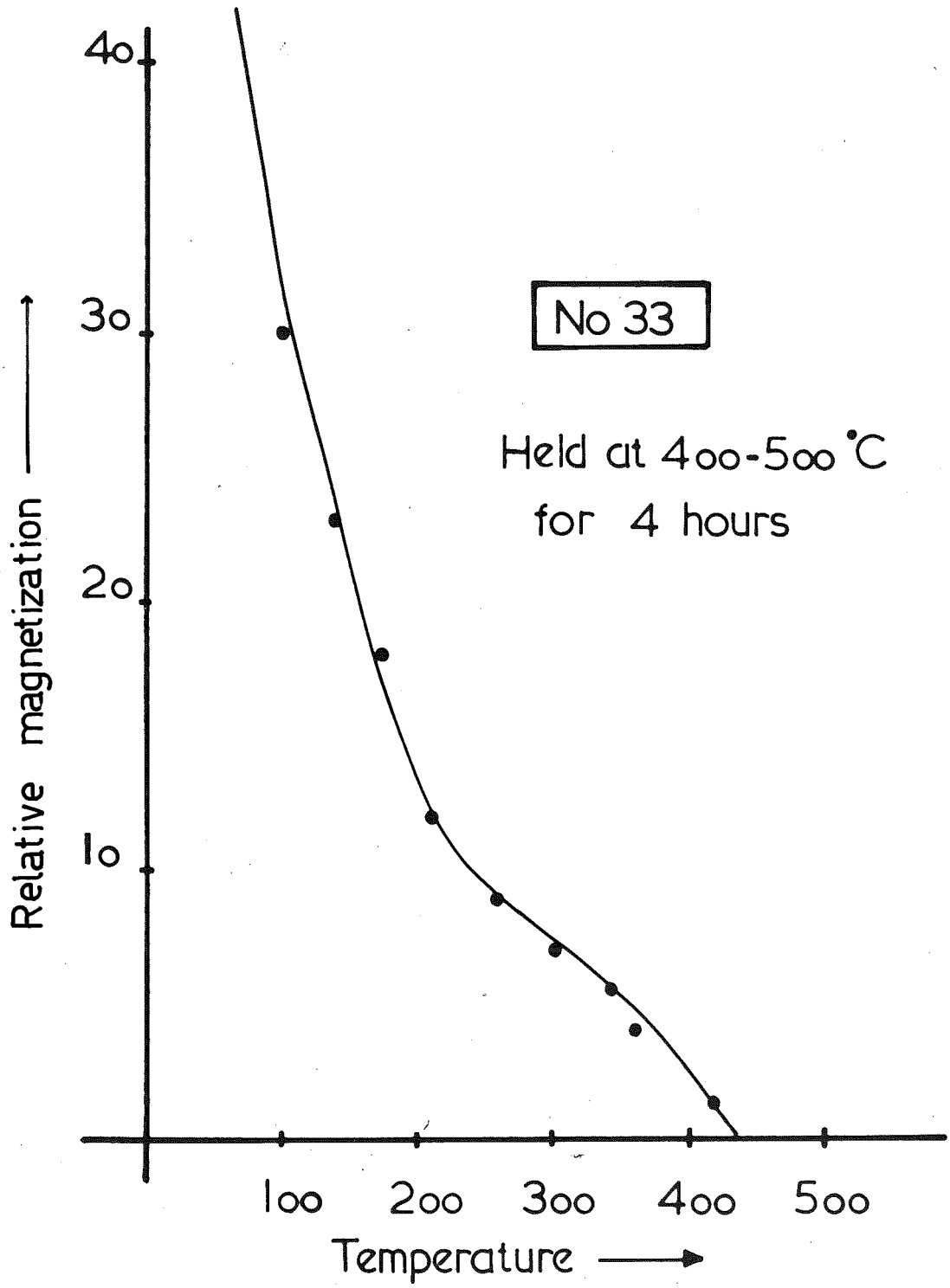
No 33
Held at 400-500 °C
for 4 hours
Relative magnetization
4o
3o
2o
1o
100
200
300
400
500
Temperature

Figure.76.

Figures 70, 71, 73, 74 show the change in direction of magnetization at the particular washing fields used in obtaining the a.c. demagnetization curves shown in figures 69, 70. After the sustained heating the direction of the T.R.M. is not affected much by the a.c. cleaning.

In figures 75, 76 are the thermal demagnetization curves obtained after specimen 33 has been held at elevated temperatures for periods of 2 hours and 4 hours respectively. Figure 75 shows the thermal demagnetization curve after specimen 33 had been held at 400-500°C for 2 hours. Figure 76 shows the thermal demagnetization curve for the same specimen after it had been held at 400-500°C for an additional 2 hours.

It appears that the effect of this sustained heating in air is to cause the formation of a higher Curie point material due to oxidation.

An X-ray powder photograph of the magnetic fraction separated from 33 after the sustained heating, showed that this was still a titanomagnetite in that it had a slightly expanded cell size compared with magnetite ($\simeq 8.42\text{Å}$). No hematite lines could be detected so that the increased stability was not due to the formation of an impure hematite. Similar changes in thermal demagnetization properties on heating in air have been reported by Parry (1960).

The object of this experiment was to link the formation of a phase of higher Curie temperature with increased

stability of magnetization as has been observed in 7.1.

9.2.4 Experiments on the stability of magnetization of laboratory synthesized titanomagnetites.

It was thought that if it were possible to synthesize titanomagnetite in the laboratory, it might be possible to reproduce the a.c. demagnetization experiments which have been carried out using naturally occurring rocks. Titanomagnetites have been prepared artificially by Pouillard (1950), who studied the variations of cell size with Curie temperature, and the writer hoped by similar methods to produce such materials.

Mixtures of finely powdered magnetite and TiO_2 were mixed intimately by further grinding in an agate mortar, and the mixtures were held at high temperatures by placing them inside a furnace. The apparatus used is shown in figure 77. It consists of the main parts

(1) Furnace

(2) Silica tube and end seal (figure 78)

(3) Backing pump

(4) A means of controlling the argon atmosphere.

Heating was carried out in an atmosphere of argon which was continually flushed through the silica tubing. In order to ensure that the oxygen pressure was originally reduced to a low value, the air inside the silica tube was pumped out by means of a backing pump and reduced to a valve of 10^{-2} m.m. before flushing with argon was commenced.

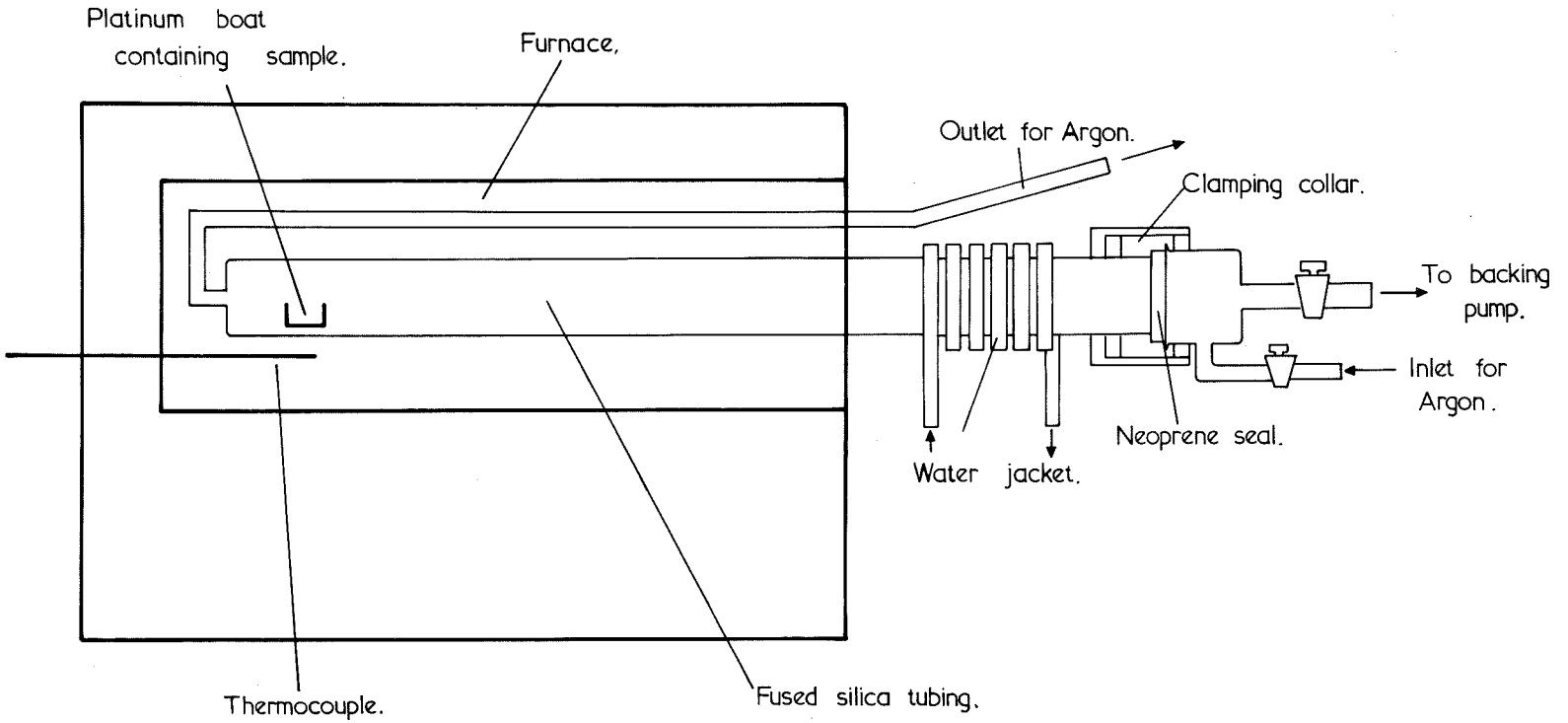
Platinum boat
containing sample.
Furnace,
Outlet for Argon.
Clamping collar.
To backing
pump.
Inlet for
Argon.
Neoprene seal.
Water jacket.
Thermocouple.
Fused silica tubing.

Figure 7.7.

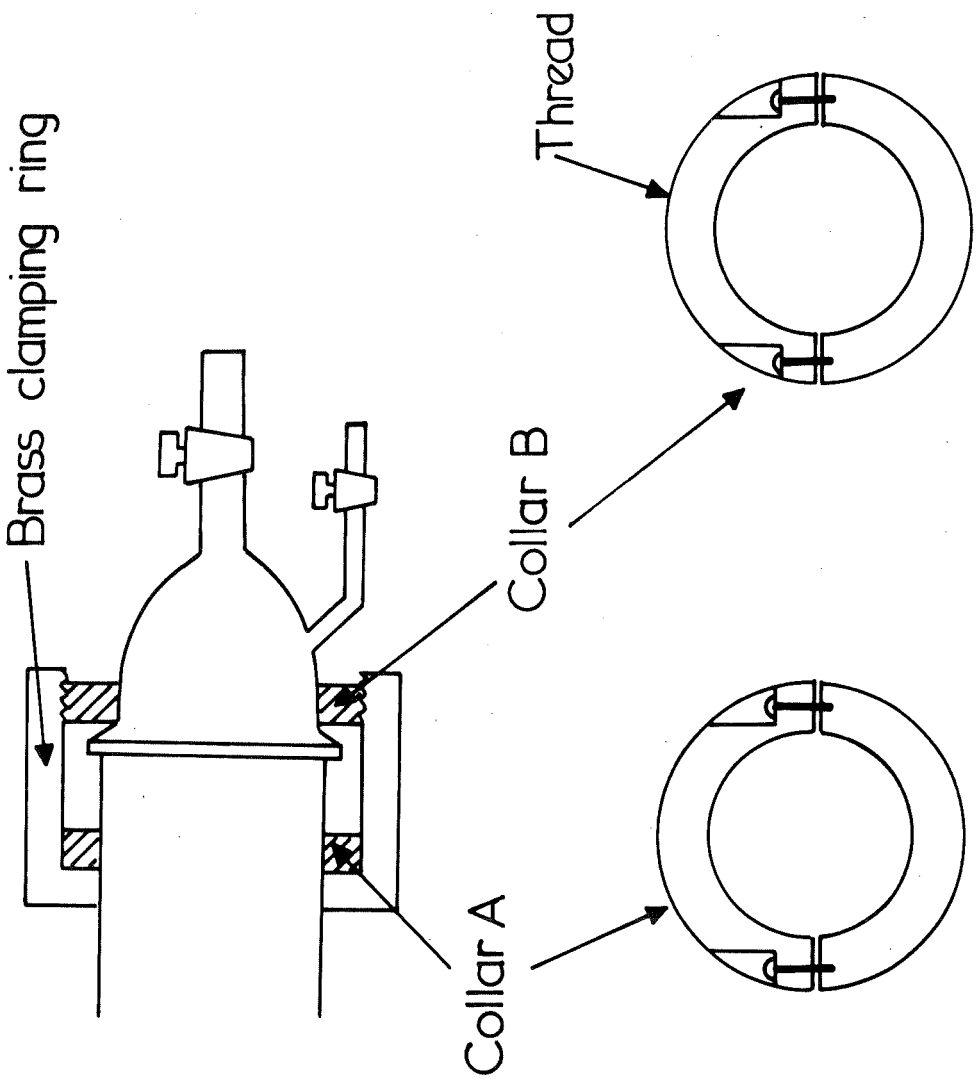

Figure.78.

Temperatures were measured by means of a thermocouple and potentiometer.

The mixtures were held at a temperature of 1,000°C for about an hour and a half and were then allowed to cool.

Cooling was quite fast in that the silica tube was removed from the furnace and allowed to cool in air.

The sample was removed from the plantinum crucible and crushed in an agate mortar.

In order to determine the changes which had taken place, X-ray diffraction photographs using an 11 cm. camera were taken. The results of these investigations showed that the magnetite lattice expanded quite considerably to produce a titanomagnetite of cell dimension $\simeq 8.49\text{Å}$ compared with 8.39Å for pure magnetite which was also photographed.

An accurate determination of the cell dimension was obtained by using standard methods as described in Henry, Lipson and Wooster (1953). Figures 79,80,81 show the "a" spacings found for the different diffraction lines plotted against

$$\tfrac{1}{2}\ \frac{\text{Cos}^2\theta}{\text{Sin}\ \theta}\ +\ \frac{\text{Cos}^2\theta}{\theta}$$

The best fit straight line was then drawn through the points and the value of "a" at

$$\tfrac{1}{2}\ \frac{\text{Cos}^2\theta}{\text{Sin}\ \theta}\ +\ \frac{\text{Cos}^2\theta}{\theta}\ = 0$$ was recorded.

For magnetite $a = 8.39\ \text{Å}$

specimen 654 $a = 8.51\ \text{Å}$

Å
8·50
8·40
8·30
Magnetite
1
2
3
4
5
6
$\frac{1}{2}\left[\frac{\cos^2\theta}{\sin\theta} + \frac{\cos^2\theta}{\theta}\right]$

Figure 79.

Å
8.60
8.50
8.40
Specimen 654
1
2
3
4
5
6
$\frac{1}{2}\left[\frac{\cos^2\theta}{\sin\theta} + \frac{\cos^2\theta}{\theta}\right]$

Figure 80.

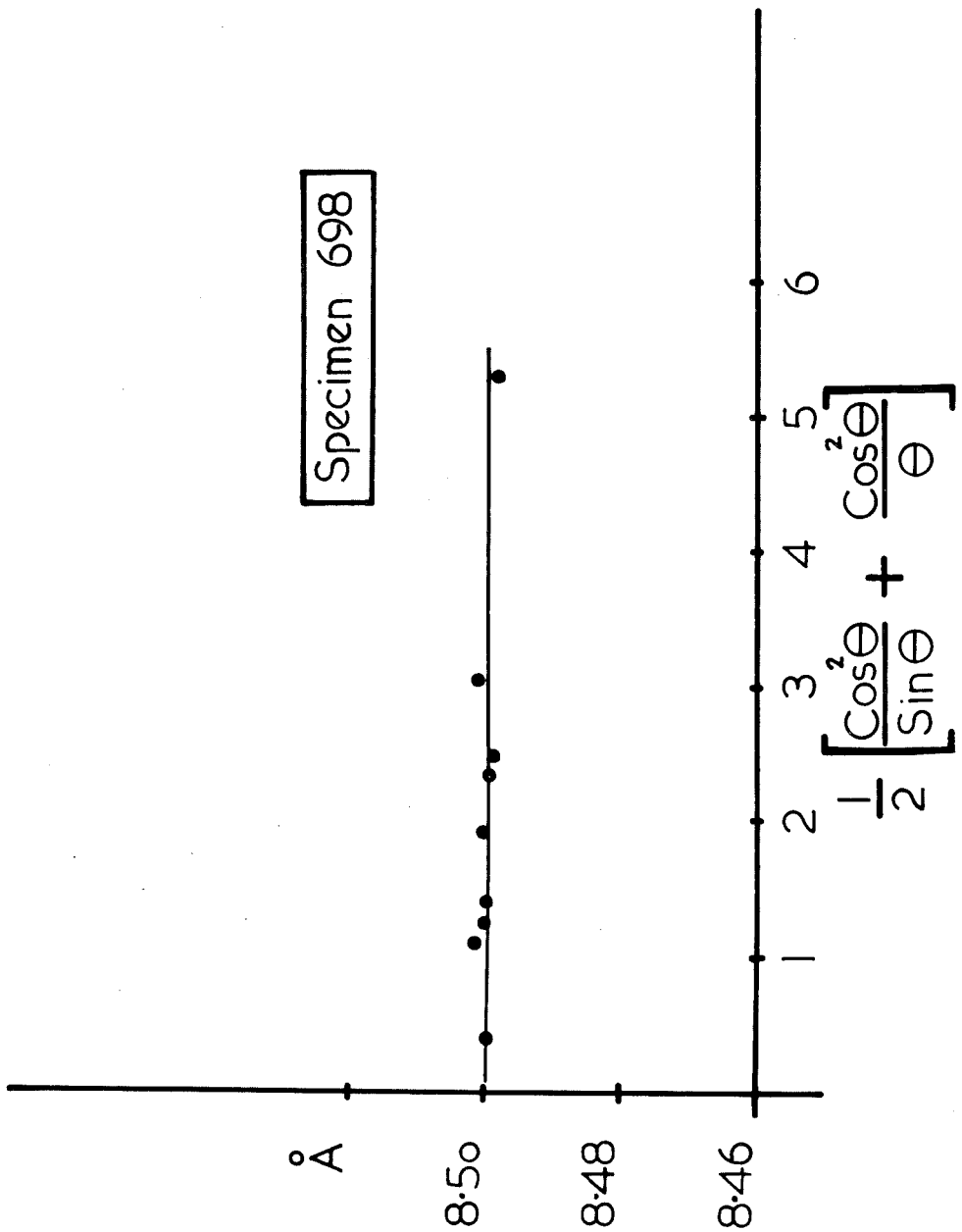
Specimen 698
Å
8·50
8·48
8·46
1
2
3
4
5
6
$\frac{1}{2}\left[\frac{\cos^2\theta}{\sin\theta} + \frac{\cos^2\theta}{\theta}\right]$

Figure 81.

specimen 698 $a = 8.50$ Å

Specimens 654 and 698 on the basis of the findings of Akimoto, Katsura and Yoshida (1957) would have Curie temperatures of approximately 100°C, and should therefore be very unstable types magnetically according to 7.1.6.

Some of the material produced was crushed and mixed in plaster of paris to resemble a rock specimen. The crushed material was passed through a 120 mesh sieve and a grain size analysis of it showed particles between 5-50 μ . The grain size spectrum of 698 is shown in figure 82. Compare this with the spectrum for the naturally occurring rock 2/59 shown in figure 55.

Specimen 654 was crushed and sieved such that an equal amount of material less than 50 μ mesh and between 50-120 μ was mixed in the final sample.

Figure 83 shows the a.c. demagnetization curves for these two artificial specimens prepared from 654 and 698, together with that obtained for an artificial specimen containing magnetite powder. In order to give the specimens a T.R.M. each was heated to 600°C in N_2 and cooled in the earth's field. The three curves are very similar.

The above result might appear puzzling when viewed in comparison with the naturally occurring rocks. The explanation offered is that in the formation of the titanomagnetite, little actual crystal growth was promoted and the fused

Figure 82.

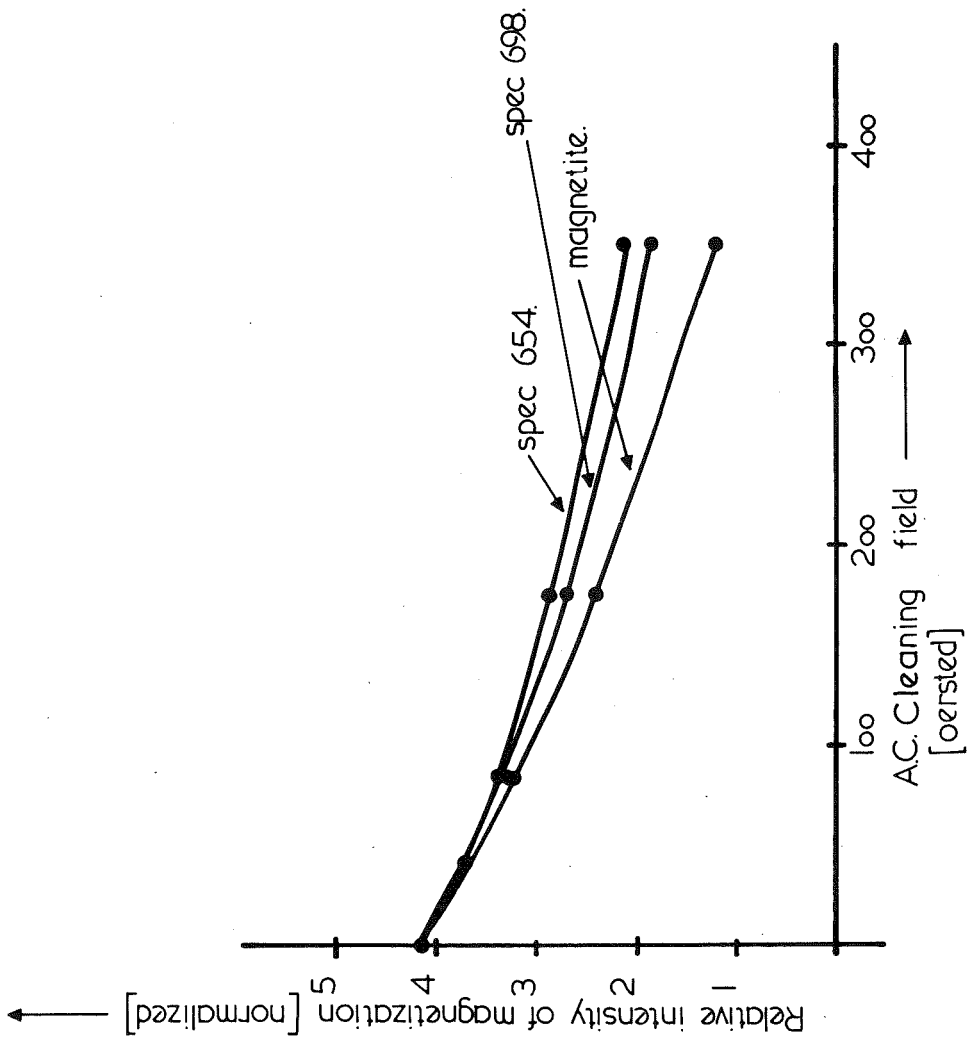
spec 698.
magnetite.
spec 654.
100
200
300
400
A.C. Cleaning field [oersted]
1
2
3
4
5
Relative intensity of magnetization [normalized]

Figure 83.

product was made up of very small crystals of the expanded lattice titanomagnetite of the order of size of the grains of magnetite originally used. Thus even the larger grains $> 50\mu$ are made up of small units.

A fact which indicates that the physical size of the grain in this case is not a controlling factor in stability of magnetization, is that both a.c. demagnetization curves for specimens 654 and 698, which are composed of different sized particles, are very similar.

Polished sections of some of the fused titanomagnetite was made, namely of 654, and it was observed that the specimen had a sintered appearance, being made up of particles of $< 20\mu$.

Since this investigation was carried out, the writer has noted a somewhat similar study which was reported by Uyeda (1958).

Uyeda synthesized titanomagnetite in the range of cell size $8.397 \pm .001\text{Å}$ to $8.485 \pm .002\text{Å}$, that is in the series of solid solution $(1-y)\ Fe_3O_4 .\ yFe_2TiO_4$.

The results of his experiments are shown in part in Table 23.

TABLE 23

y	Lattice constant	T_c °C	Hc oersted	Grain size microns	Hc^+ oersted
.67	8.485 ± .002	120	20	10	20
.50	8.458 ± .002	260	21	10	21
.36	8.437 ± .001	380	26	10	26
.27	8.423 ± .001	430	26	10	26
.18	8.409 ± .001	490	22	100	123
.17	8.406 ± .001	500	8	100	44
.11	8.397 ± .001	550	7	100	39

Figure 8.4

Uyeda points out that the effect of grain size on coercive force is very evident in these results. He indicates that the grain-size was 10μ in mean diameter for the specimens $y \geq .27$. However, the grain size for specimens $y \leq .18$ was found to be as large as 100 μ. This being the case, it is very difficult to reconcile the rapid change of coercive force between the samples where y = .18 and y = .17, for, as is evident from the table, their compositions are very nearly identical, as supposedly is their grain size. Using the relation

$$Hc \propto d^{-\frac{3}{4}} \qquad \text{(Stacey (1958))}$$

where d is the diameter of the grains in microns, the coercive force H_c^+ reduced to the same grain size of 10 μ for specimens where y = .17 and .11 is given in the last column of the table. These results suggest the relationship between coercive force and cell size shown in figure 84, which shows an increase of coercive force towards pure magnetite. The value of H_c^+ for y = .18 is omitted on the graph.

9.3 Conclusions

From the experiments described in 9.2 it seems possible to draw several conclusions about the stability of these basalts. Stability of magnetization is dependant on the Curie temperature of the main magnetic minerals present in the rock.

In section 7 it was shown that specimens 2/44 and 2/45 (see figures 113,114) contain a large amount of high Curie point titanomagnetite, and are the only two specimens in the locality which still retain an original reversed direction of magnetization. The other rocks, including 2/58, 2/59 which contain mostly low Curie point titanomagnetite have acquired large unstable components of magnetization. Figures 40(a) and (b) show quite well the different behaviour to a.c. demagnetization of these two rocks, one containing mostly a high Curie point titanomagnetite. These two specimens 2/45 and 2/59 have similar grain size spectra (see figures 54,55) so the difference in stability of magnetization seems to be due to the composition of the magnetic minerals.

The rocks containing a high Curie point titanomagnetite of the composition near magnetite possess a stable hard magnetization; those which contain a low Curie point titanomagnetite possess an unstable soft magnetization. Other experiments which show that the stability of magnetization is dependent on the Curie temperature, or composition of the main magnetic mineral have been given in Section 9. Of course it is evident from the results of the a.c. demagnetization experiments carried out on the rocks from Drouin-South that some of the originally stable T.R.M. is retained even in the very unstable low Curie point titanomagnetites. The reason why any of the original magnetization is retained is probably due to the fact that there are

many grains of ferromagnetic mineral present in these basalts which are $< 20\mu$ in size. These smaller grains would tend to retain the direction of the original T.R.M. because of the large increase of coercive force with decrease in grain size (Gottschalk (1935)).

The experiment described in 9.2.4 suggests that fineness of grain size is the chief reason for a titanomagnetite retaining any of its originally stable T.R.M. in a basalt.

A recent theory for remanent magnetization in multidomain grains by Everitt (1962) also implies that the abovementioned relationship between Curie temperature and coercive force should hold.

Everitt suggests that the fundamental equation relating blocking temperature and coercive force is of the form.

$$\frac{1}{T_b} \left\{ \frac{\Delta T_b}{T_c} \right\}^n = \frac{a}{H_{co}}$$

Where T_b is the blocking temperature (^oK).

T_c is the Curie temperature (^oC).

$\Delta T_b = (T_c + 273) - T_b$

H_{co} is the coercive force.

n is a constant and equals $1.2 \pm .03$.

a is a constant and equals $(7 \pm) \times 10^{-2}$.

This equation indicates that H_{co} increases with T_c.

Everitt C.W.F., (1962), Thermoremanent magnetization III. Theory of multidomain grains, Phil. Mag., 7, 76, 599.

APPENDIX I

DETERMINATION OF CORRECTION FACTOR TO BE APPLIED TO THE DIRECTIONS OF MAGNETIZATION AS MEASURED IN 2.1

1. Introduction

In 2.1.6 it was assumed that:-

(1) The magnetic field of the specimen does not have an effect on the upper magnet of the magnet system.

(2) It is possible to introduce the specimen to the measuring position from another position which is so far away from the magnet system that the field of the specimen in this latter position has no effect on the magnet system.

(3) Although measurements are made in off-centre positions, the vertical distance of the specimen below the magnet system is equal to the distance of the specimen from the magnet system.

These assumptions are not entirely permissible. For example in case (1) above, the effect on the top magnet is not negligible compared with that on the bottom magnet, when the distances from the measuring position to either magnet become large, and so more nearly equal in magnitude. In case (2) the specimen is actually introduced to the measuring position from a distance of 17.6 cms. below the lower magnet. Deflections produced by the specimen in this position although comparatively small, are nevertheless

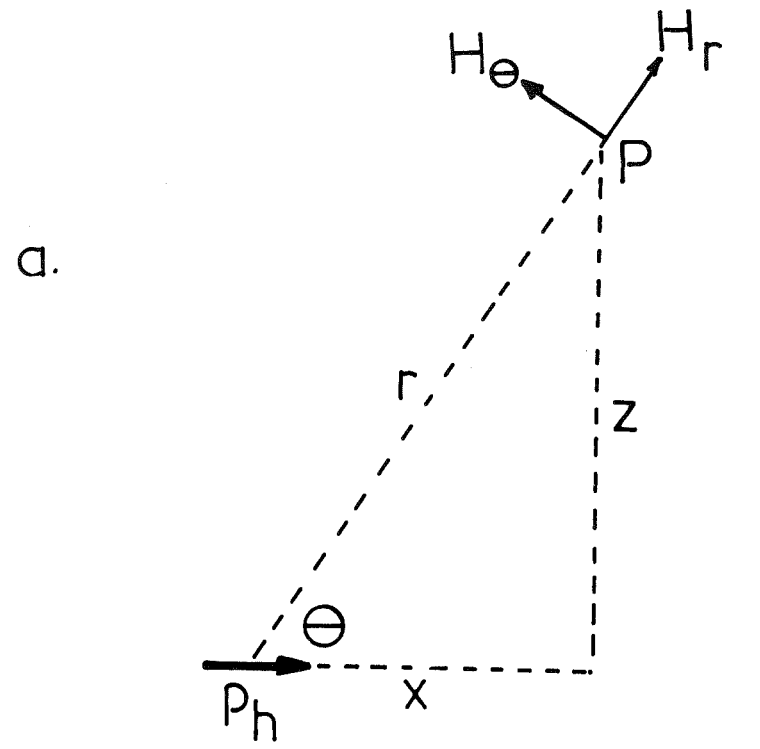

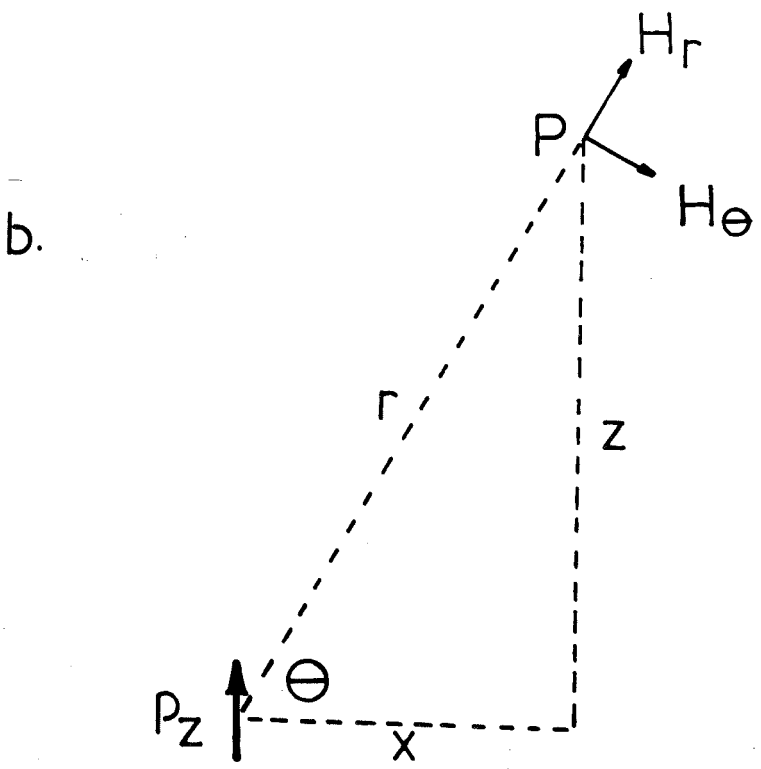

Figure.85.

present.

In case (3), the difference in distance can be appreciable when the distance traversed off-centre is of the same order of magnitude as the distance of the specimen vertically below the lower magnet.

Thus the following correction factor is applied to the measured directions of magnetization to take into account the above departures from the assumed conditions.

2. Evaluation of the correction factor

The magnetic field of the horizontal component of the dipole, pH, has components (figure 85a),

$$Hr = \frac{2pH \quad \text{Cos}\,\theta}{r^3}$$

$$H\theta = \frac{pH \quad \text{Sin}\,\theta}{r^3}$$

Thus the horizontal field at P due to pH is,

$$H\theta \quad \text{Sin}\,\theta \quad - \quad Hr \quad \text{Cos}\,\theta$$

$$= -2pH \quad \frac{\text{Cos}\,\theta \quad \text{Cos}\,\theta}{r^3} + pH \quad \frac{\text{Sin}\,\theta \quad \text{Sin}\,\theta}{r^3}$$

$$= pH/r^3 \quad (-2\text{Cos}^2\theta \quad + \quad \text{Sin}^2\theta \quad)$$

But $z/r = \text{Sin}\,\theta$, where z for a thin disc is given by

$z = z'^2 + a^2$.

z' = distance of centre of disc from lower magnet

a = radius of disc

Thus the horizontal field

$$= {}^{pH}/_{z^3} \quad (\mathrm{Sin}^2\theta \quad - \; 2\,\mathrm{Cos}^2\theta \quad)\;\mathrm{Sin}^3\theta$$

$$= {}^{pH}/_{z^3} \quad (\mathrm{Cos}^2\psi \quad - \; 2\,\mathrm{Sin}^2\psi \quad)\;\mathrm{Cos}^3\psi$$

The magnetic field due to the vertical component of the dipole has components (figure85b),

$$Hr = \frac{2p_z \quad \mathrm{Cos}\,\psi}{r^3}$$

$$H_\theta \quad = \quad \frac{p_z \quad \mathrm{Sin}\,\psi}{r^3}$$

The horizontal field at P due to p_z is,

$$Hr\;\mathrm{Sin}\,\psi \quad + \quad H_\theta \quad \mathrm{Cos}\,\psi$$

$$= \frac{2p_z \quad \mathrm{Cos}\,\psi \quad \mathrm{Sin}\,\psi}{r^3} \quad + \quad \frac{p_z \quad \mathrm{Sin}\,\psi \quad \mathrm{Cos}\,\psi}{r^3}$$

$$= {}^{p_z}/_{r^3} \quad (2\;\mathrm{Cos}\,\psi \quad \mathrm{Sin}\,\psi \quad + \mathrm{Cos}\,\psi \quad \mathrm{Sin}\,\psi \quad)$$

$$= 3\;{}^{p_z}/_{r^3} \quad \mathrm{Cos}\,\psi \quad \mathrm{Sin}\,\psi$$

$$= 3p_z\;{}^{x}/_{z^4} \quad \mathrm{Cos}^5\psi$$

At the upper magnet (10 cms. above) the horizontal field due to the horizontal component of the dipole is,

$${}^{pH}/_{(z\,+\,10)^3} \quad (\mathrm{Cos}^2 \quad \psi' \; - \; 2\,\mathrm{Sin}^2 \quad \psi' \,) \quad \mathrm{Cos}^3 \quad \psi'$$

and the horizontal field at the upper magnet due to the

vertical component of the dipole is,

$$3\, p_z\, x/(z+10)^4 \quad \cos^5 \psi'$$

where $\tan \psi' = x/z+10$

It must be remembered also that the specimen will produce a field at the magnet system of the magnetometer when the specimen is in the lowered position before it is raised to the point z below the bottom magnet.

The horizontal field at the bottom magnet due to the horizontal component of the dipole in this base position is

$$pH/17.6^3 \quad (\cos^2 \psi'' - 2 \sin^2 \psi'') \cos^3 \psi''$$

Where $\tan \psi'' = x/17.6$, since in the lowered position the distance to bottom magnet is 17.6 cms.

The horizontal field at the upper magnet due to the horizontal component of the dipole in this base position is

$$pH/27.6^3 \quad (\cos^2 \psi''' - \sin^3 \psi''') \cos^3 \psi'''$$

where $\tan \psi''' = x/27.6$

The horizontal field at the lower magent due to the vertical component of the dipole with the specimen in the base position is

$$3\, p_z\, x/17.6^4 \quad \cos^5 \psi''$$

The horizontal field at the upper magnet due to the vertical

dipole component with the specimen in the base position is

$$3pz\, x/27.6^4 \quad \cos^5\psi'''$$

Now the resultant deflections due to the horizontal field of the vertical and horizontal dipole components (which are separated by the method of measurement) are actually due to the differences between these various fields.

The measured horizontal field of the horizontal component

= measured deflection x sensitivity

$$= D'_H \times S$$

$$= p_H/z^3 \ (\cos^2\psi - 2\sin^2\psi) \cos^3\psi$$

$$- p_H/(z+10)^3 \ (\cos^2\psi' - 2\sin^2\psi') \cos^3\psi'$$

$$+ p_H/17.6^3 \ (\cos^2\psi'' - 2\sin^2\psi'') \cos^3\psi''$$

$$- p_H/27.6^3 \ (\cos^2\psi''' - 2\sin^2\psi''') \cos^3\psi'''$$

Thus $p_H =$

$$\frac{z^3 (D'_H \times S)}{K_z - K_{(z+10)} z^3/(z+10)^3 + K_{17.6} z^3/17.6^3 - K_{27.6} z^3/27.6^3}$$

Where $K_z = (\cos^2\psi - 2\sin^2\psi) \cos^3\psi$

$K_{(z+10)} = (\cos^2\psi' - 2\sin^2\psi') \cos^3\psi'$

$K_{17.6} = (\cos^2\psi'' - 2\sin\psi'') \cos^3\psi''$

$$K_{27.6} = (\cos^2\psi''' - 2\sin^2\psi''')\cos^3\psi'''$$

Similarly,

$$p_z = \frac{(D'_z \times S)}{3x/z^4\left(k_z - k_{(z+10)}\frac{z^4}{(z+10)^4} + k_{17.6}\frac{z^4}{17.6^4} - k_{27.6}\frac{z^4}{27.6^4}\right)}$$

where

$$k\,z = \cos^5\psi$$
$$k(z+10) = \cos^5\psi'$$
$$k\,17.6 = \cos^5\psi''$$
$$k\,27.6 = \cos^5\psi'''$$

$$\tan\phi = p_z/p_H$$

$$= \frac{D'_z}{D'_H}\frac{z^4}{3xz^3}\,\frac{Kz - K(z+10)\frac{z^3}{(z+10)3} + K17.6\frac{z^3}{17.6^3} - K27.6\frac{z^3}{27.6^3}}{k\,z - k\,(z+10)\frac{z}{(z+10)^4} + k17.6\frac{z}{17.6^4} - k27.6\frac{z}{27.6}}$$

$$= \frac{D'_z}{D'_H}\;{}^{z}/_{3x}\;C$$

If we put $\frac{D'_z}{D'_H}\;{}^{z}/_{zx} = \tan\phi'$

as is the method as indicated in the factor C can be evaluated for various z, and a correction can be applied accordingly.

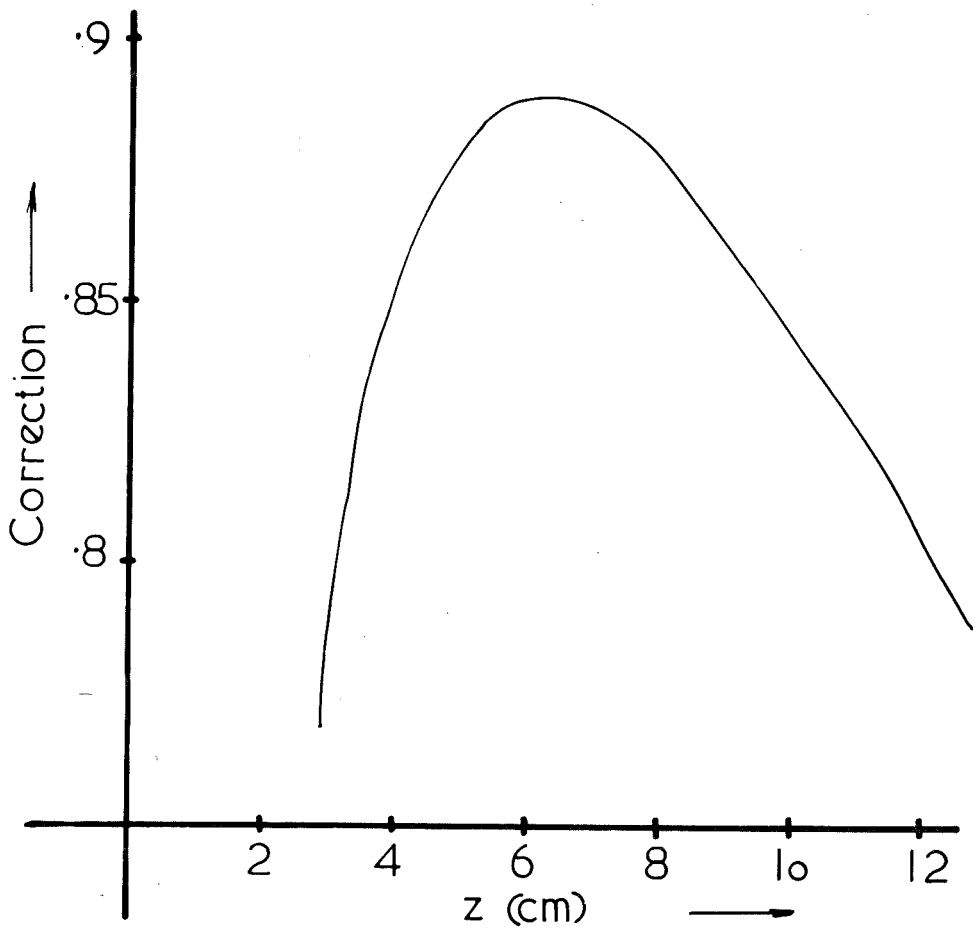

Figure 86

3. Correction factor

This is evaluated for various z, at x = 1.

z (cm)	Correction to tan ϕ
3	.7673
4	.8470
5	.8781
6	.8866
7	.8845
8	.8751
9	.8625
10	.8458
11	.8265
12	.8070
13	.7869

This correction is plotted in figure 86.

4. Experimental verification

A standard specimen simulating a dipole at a known inclination was made using alnico wire set in perspex. The angle of inclination was known to be approximately 30°. The value of inclination was obtained at various z, and was corrected using the correction given above.

The results are given in Table 24

TABLE 24

z	ϕ calculated	ϕ corrected
5	31°46'	28°30'
6	31°16'	28°12'
7	31°51'	28°48'
8	32°16'	28°54'
9	32°24'	28°42'

Also, in order to obtain another check that the results were correct for measurement of directions, a specimen of basalt UB 194/1, provided by Mr. Irving was measured both at Canberra and at Adelaide on the magnetometers. The results of the measurements are given in Table 25.

TABLE 25

	Z	D	I	I'	M x 10^{-4}	M' x 10^{-4}
ADELAIDE						
	8.45	220	-21	-18	18.2	24.6
	9.05	220	-22	-19	19.0	23.1
	10.05	220	-22	-19	16.0	23.0
	11.45	220	-23	-19	13.7	21.8
Average		220		-19		23.1
CANBERRA						
	9.08	221	-17	-17	18.2	21.9
	9.08	222	-20	-20	18.0	22.1
Average		221.5		-18.5		22.0

I' and M' are corrected values. The mean taken is a simple arithmetic mean which is strictly not correct but is quite adequate for the divergences involved. The mean directions differ by about 1^{o} and the moments by less than 5%.

APPENDIX 2.

CONVERSION OF MEASURED DIRECTIONS OF MAGNETIZATION

1. Introduction

As already indicated, the orientation of the rock collected in the field is determined using a small three-legged level. Three points are marked on the surface of the rock which determine a plane (in future referred to as the "dip" plane). The strike and dip of this "dip" plane are measured and recorded.

When the rock is cored to obtain a specimen, the "dip" plane is set in a horizontal position. Thus the directions of magnetization obtained are measurements relative to the normal to this dip plane and its strike.

The problem is then to convert these directions to directions relative to the true horizontal plane and the magnetic north direction.

Both trigonometrical formulae and a quick graphical method which produces quite accurate results are given.

2. Conversion formulae

It can be shown that -

$$\text{Tan } D = \frac{\text{Cos } \phi \text{ Sin } D' \text{ Cos } I' - \text{Sin } \phi \text{ Sin } I'}{\text{Cos } D' \text{ Cos } I'}$$

$$\text{Sin } I = \text{Cos } I' \text{ Sin } D' \text{ Sin } \phi + \text{Sin } I' \text{ Cos } \phi$$

Where,

ϕ = The dip of the "dip" plane which is positive if the plane dips to the right of the direction of strike.

D' = Declination and inclination of magnetization
I' regarding the "dip" plane as horizontal. Declination is measured anticlockwise from the direction of strike of this plane.

D = The required declination and inclination of magneti-
I zation relative to the true horizontal plane and the strike of the "dip" plane. Declination is again anticlockwise from the direction of strike of the "dip" plane which is measured clockwise from magnetic north.

3. Graphical method

A much quicker method, the accuracy of which has been checked using the above formulae, involves the use of the stereographic projection.

The direction of polarization with respect to the "dip" plane as horizontal is plotted on a stereographic net. This point is then rotated through the angle ϕ (the dip of the "dip" plane) which involves moving the point through ϕ along the appropriate small circle. The value of inclination and declination with respect to the horizontal plane can now be read directly from the stereographic projection as the "dip" plane has, in effect, been rotated to take up its real orientation. The mechanics of this method are outlined in Figure 87.

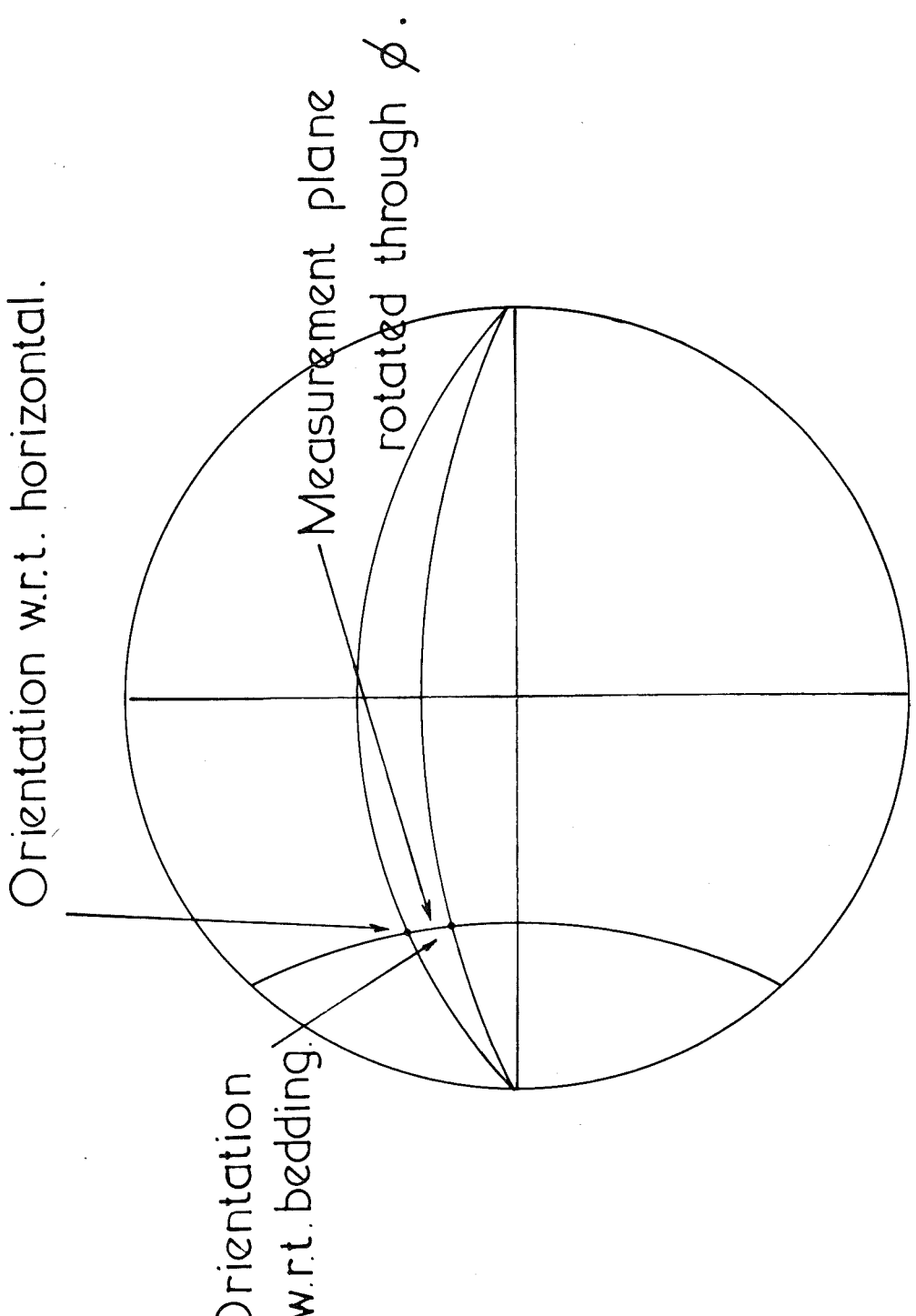
Orientation w.r.t. horizontal.
Measurement plane rotated through ϕ.
Orientation w.r.t. bedding.

Figure 87.

A P P E N D I X 3.

These are directions of magnetization relative to the disc for specimens of basalt collected for the field survey.

In the first list are measurements taken immediately after collection, and in the second list are measurements obtained about 9-12 months later.

Specimen No.		Direction of magnetization relative to disc			
		Declination	Inclination	Declination	Inclination
1	ac	304	-34	304	-32
	ad	306	-34	302	-36
	aa	304	-35	308	-38
	bb	302	-36	303	-38
	ba	304	-37	304	-34
	ac	302	-33	305	-32
	ab	302	-34		
2	ad	96	-22		
	ab	99	-32	100	-33
	ae	94	-28	95	-28
	af	102	-30		
	ac	96	-29	97	-31
	aa	90	-29	96	-29
3	ac	271	-22	277	-21
	bb	273	-25	268	-26
	aa	273	-22	274	-25
	bc	274	-25	276	-27
	ab	270	-28	276	-27
	ba	270	-24	271	-23

Specimen No.		Direction of magnetization relative to disc			
		Declination	Inclination	Declination	Inclination
4	bb	271	-7	270	-13
	ba	271	-14		
	bc	271	-14		
	ab	275	-11		
	ac	241	-13	244	-14
	aa	274	-12	259	-10
5	ba	18	-71	260	-83
	ac	41	-70	310	-73
	aa	1	-62	294	-64
	ab	19	-72	0	-86
	bc	46	-68	292	-72
	bb	32	-67	327	-21
	ad	83	-69		
	bd	65	-62		
6	be	127	-27	123	-26
	ad	120	-28	126	-21
	bb	116	-15	59	-14
	bc	118	-20	118	-21
	ba	118	-18	61	-16
	bd	125	-28	123	-16
	ac	120	-27	124	-15
	ab	120	-21	114	-14
	aa	123	-18	123	-10
	cb	120	-21	112	-15
	ca	127	-25	113	-15
7	bb	105	-48	98	-38
	ba	101	-44	93	-38
	bc	99	-45	104	-35
	ac	117	-54	114	-46
	ad	105	-44	104	-42
	be	110	-49	111	-51

Specimen No.		Direction of magnetization relative to disc			
		Declination	Inclination	Declination	Inclination
7	bd	100	-41	106	-38
	aa	110	-43	102	-39
	ac	100	-40	95	-31
	ab	108	-46		
8	bd	268	-2	267	+1
	be	274	-3	274	-4
	ab	268	-4	269	-1
	aa	267	-2	269	-1
	bc	263	-2	266	-3
	ba	262	+2	260	+2
	bb	261	+1	264	+1
	ad	295	-31	295	-31
	ac	277	-9	277	-8
	ae	314	-56	322	-54
9	bg	139	-67	138	-66
	aa	166	-74	165	-75
	ba	124	-65	129	-62
	ac	149	-64	152	-68
	bd	151	-75	148	-76
	bf	137	-70		
	ad	149	-60	150	-59
	be	145	-68	143	-70
	bb	129	-67		
	bc	146	-73	149	-72
10	ac	-13	-62	-24	-57
	bb	-32	-63	-29	-60
	ba	-30	-64	-32	-62
	be	-40	-57	-39	-54
	bd	-22	-59		
	ad	-39	-62	-36	-66
	aa	-33	-60	-38	-59

Specimen No.		Direction of magnetization relative to disc			
		Declination	Inclination	Declination	Inclination
10	ab	-37	-63	-32	-56
12	aa	96	-3	98	-4
	ab	97	-0	90	-2
	ac	99	-1	98	-4
	ad	96	-2	89	-1
	ae	96	+1	100	-3
13	ad	56	+7	59	+3
	ac	57	+10	61	+9
	ba	60	+8	61	+6
	ab	59	+8	63	+6
	aa	60	+9	65	+6
17	bc	320	-32	337	-35
	aa	318	-31	290	-43
	ae	307	-28	321	-31
	bd	316	-24	304	-25
	be	326	-23	322	-38
	bb	311	-43	295	-41
	ab	309	-39		
	ba	316	-40	340	-46
18	aa	221	-40	247	-52
	be	239	-46	230	-47
	ac	224	-47		
	bb	232	-53	254	-58
	ba	247	-51	263	-44
	bd	230	-49	246	-45
	ab	220	-48	236	-45
19	ab	72	-32	80	-62
	bb	83	-32	72	-16
	ac	37	-56	64	-37
	ba	79	-25	73	-15
	bc	80	-24	84	-22

Specimen No.		Direction of magnetization relative to disc			
		Declination	Inclination	Declination	Inclination
19	ae	21	-46	46	-27
	bd	82	-24	82	-25
	ba	81	-23	84	-22
	aa	76	-19	76	-6
	ad	28	-50	59	-41
20	aa	92	-22	78	-4
	bd	108	-10	96	-9
	ad	105	-12	108	-10
	bb	99	-19	97	-13
	ac	106	-16	100	-15
	ba	88	-15	80	-10
	ab	91	-10	96	-10
	bc	108	-14	97	-12
21	aa	84	-26	80	-19
	bd	100	-23	97	-16
	ac	98	-18	89	-18
	ab	94	-21	87	-18
	be	103	-21	110	-21
	ba	84	-10	83	-9
	bc	93	-26	95	-12
	bb	82	-21	89	-15
22	bb	146	+57	167	+47
	bc	226	+60	219	+52
	ab	165	+47	161	+72
	ad	237	+50	232	+54
	bd	272	+45	154	+59
	ac	240	+33	167	+74
	aa	140	+62	125	+44
	ba	150	+62		

Specimen No.		Direction of magnetization relative to disc			
		Declination	Inclination	Declination	Inclination
24	bb	276	-13	283	-14
	ba	276	-14	282	-12
	ac	277	-14	273	-13
	aa	279	-14	275	-15
	ab	277	-14	282	-13
25	af	-86	-16	-88	-5
	aa	-86	0	-95	-5
	ad	-88	-12	-93	-10
	ab	-87	-11	-83	-3
	ag	-83	-14	-88	-10
	ah	-84	-14	-88	-11
	ac	-88	-11	-86	-5
	ae	-90	-13	-97	-5
26	ac	253	-8	261	-11
	aa	256	-3	256	-2
	ba	263	+1	264	-1
	bc	251	-6	253	-7
	ae	247	-5	253	-10
	bb	261	-1	262	-2
	ad	254	-3	253	-11
	bd	245	-2	254	-7
	ab	258	-3	265	-5
27	aa	37	-66		
	ae	28	-70	29	-70
	ad	39	-68	45	-60
	ac	43	-68	67	-68
	ab	37	-70		
28	ad	260	-70	265	-67
	ac	268	-71	268	-68
	aa	262	-66	260	-69
	ab	256	-69	250	-62

Specimen No.		Direction of magnetization relative to disc			
		Declination	Inclination	Declination	Inclination
28	ba	266	-70		
	bb	266	-70		
29	bb	98	-37	103	-37
	ab	100	-35	102	-37
	ba	99	-34	98	-36
	ad	103	-31	100	-36
	ac	100	-35	95	-36
	bc	102	-37	91	-39
	bd	95	-38	100	-38
	aa	102	-34	96	-28
30	ae	3	-20	6	-22
	ab	5	-21	5	-26
	ac	4	-20	3	-24
	aa	8	-21	9	-26
	ad	8	-23	4	-28
31	ac	22	-31	28	-29
	aa	12	-21	14	-20
	bb	42	-25	44	-27
	ab	16	-24	20	-26
32	ac	120	-56	107	-65
	ba	112	-60	113	-66
	bb	118	-63	113	-72
	ab	117	-57	130	-65
	aa	123	-59	129	-57
	ad	123	-61	126	-64
33	aa	-79	-49	-72	-51
	bc	-72	-49	-86	-47
	bb	-81	-50	-75	-45
	ac	-81	-48	-82	-27
	ab	-70	-51	-73	-28
	ba	-72	-50	-75	-34

Specimen No.		Direction of magnetization relative to disc			
		Declination	Inclination	Declination	Inclination
36	ba	100	-56	114	-47
	be	2	-72	35	-64
	ab	130	-61	101	-67
	ac	143	-56	149	-66
	aa	106	-65	103	-74
	ad	154	-48	170	-39
	bb	96	-61	106	-52
	bf	353	-61	348	-79
	bd	13	-72	57	-74
	bc	92	-66	89	-78
	ae	162	-42	152	-43
37	bb	100	-19	76	-19
	aa	100	-25	77	-29
	ba	99	-18	78	-13
	ac	102	-18	93	-21
	bd	99	-17	91	-21
	be	101	-17	91	-20
	ab	103	-20		
	bc	102	-22	91	-23
38	aa	267	-77	218	-48
	bc	64	-67	108	-57
	ab	262	-84	183	-34
	ac	86	-68	127	-57
	ba	302	-73	260	-60
	bd	70	-63	346	-71
	ad	4	-60	132	-67
	bb	323	-78	94	-69
	ae	88	-60	83	-36

Specimen No.		Direction of magnetization relative to disc			
		Declination	Inclination	Declination	Inclination
39	ac	76	-72	169	-58
	ad	66	-69	81	-63
	ab	61	-79	345	-70
	ba	43	-76	311	-48
	aa	73	-80	281	-64
40	be	196	-42	193	-44
	aa	276	-27	257	-9
	bb	263	-55	299	-52
	bd	197	-40	182	-37
	ba	276	-55	294	-39
	ac	234	-37	228	-39
	ab	273	-48	280	-22
	ad	208	-49	162	-76
	bc	203	-21	219	-47
41	ae	67	-69	68	-62
	ad	307	-74	221	-81
	aa	60	-72	101	-65
	af	62	-68	59	-78
	ag	63	-71	39	-88
	ac	290	-69	319	-78
	ab	288	-68	304	-61
42	bc	69	-14	81	-9
	ba	68	-15	79	-4
	bd	62	-13	65	-21
	be	65	-13	69	-7
	ad	62	-15	76	-7
	aa	74	-12	57	-11
	bb	74	-14	65	-6
	ac	63	-17	54	-13
	ab	62	-19	59	-10

Specimen No.		Direction of magnetization relative to disc			
		Declination	Inclination	Declination	Inclination
43	aa	54	+20	56	+26
	bb	76	+29	30	+29
	ad	80	+3	47	+7
	bc	48	+24	50	+27
	ba	45	+24	39	+31
	bd	53	+24	42	+20
	ac	66	-1	55	+11
	ab	52	+12	59	+14
	ae	79	+6	40	+16
44	ab	121	-44	120	-48
	aa	121	-40	126	-40
	bb	132	-54	158	-54
	ba	132	-53	143	-63
45	bd	97	-35	89	-47
	ba	100	-60	104	-71
	z	124	-32	137	-34
	ab	97	-51	109	-37
	bb	87	-59	146	-74
	y	106	-39	112	-38
	bc	99	-42	123	-47
	aa	95	-51	121	-51
	x	92	-38	85	-43
46	aa	206	+46	201	+52
	ac	215	+48	196	+49
	ad	205	+45	214	+46
	af	211	+46	212	+43
	ab	201	+46	218	+47
	ae	209	+45	200	+46
47	aa	-80	-62	-75	-78
	ba	-80	-60	-78	-45

Specimen No.		Direction of magnetization relative to disc			
		Declination	Inclination	Declination	Inclination
47	ac	-71	-63	-68	-54
	ad	-53	-48	-51	-68
	ab	-78	-60	220	-67
	bd	238	-57	254	-44
	bc	247	-60	259	-55
	be	240	-55	252	-46
	ae	-61	-49	-46	-51
	bb	264	-67	-59	-67
48	ad	92	-84	212	-69
	ab	97	-83	236	-69
	ae	143	-77	215	-74
	aa	87	-82	148	-62
	ac	67	-87	142	-74
	af	149	-68	199	-79
	ag	148	-72	195	-69
49	aa	-80	-87	256	-80
	ad	153	-79	172	-71
	ba	96	-55	82	-43
	ae	162	-53	171	-64
	ab	-2	-83	18	-72
	af	156	-56	137	-50
	ac	18	-83	-57	-67
50	aa	88	-22	79	-22
	bb	101	-22	80	-23
	ab	98	-24	103	-22
	ba	96	-24	96	-23
	ad	107	-24	105	-24
	bc	96	-26	99	-22
	ac	98	-21	92	-25

Specimen No.		Direction of magnetization relative to disc			
		Declination	Inclination	Declination	Inclination
51	aa	87	-22	51	-33
	ba	72	-16		
	be	114	-26	126	-33
	ab	88	-23	74	-53
	bd	67	-40	99	-32
	bb	71	-26	79	-21
	bc	89	-40	96	-57
	ac	136	-68	114	-21
52	af	79	-53	81	-53
	ac	74	-59	76	-64
	ad	79	-50	83	-49
	ab	69	-56	63	-58
	aa	63	-50	65	-50
	ae	80	-48	80	-50
53	ad	-91	-45	-76	-44
	ac	-90	-49	-76	-44
	aa	-94	-56	-91	-68
	ab	-85	-43	-84	-40

The method of calculation of the mean direction of magnetization, according to Watson and Irving, now follows.

Mean site directions for the original measurements are given in the following table.

Site No.	D (M.N.)	I
1	22	-62
2	-38	-77
3	8	-76
4	-17	-61
5	18	-62
6	17	-73
7	16	-44
8	64	26
9	342	62
10	299	51
11	-19	-72
12	72	-55
13	-24	-63
14	-74	-67
15	229	-72
16	40	-59
17	87	-73
18	330	53
19	14	-73
20	188	-74
21	-21	68

Mean direction of magnetization is:

$$D\ (T.N.) = 18\tfrac{1}{2}^{\circ}$$

$$I = -71^{\circ}$$

$$\alpha_{o} = 9^{\circ}$$

$$\bar{W} = \frac{1}{B - 1}\left(N - \frac{\Sigma Wi^{2}}{N} \right)$$

Where $\bar{W}$ is the weighted average of the Wi

$$= \frac{1}{20} \left(362 - \frac{7,252}{362}\right)$$

$$= \frac{1}{20} (362 - 20.03)$$

$$= \frac{341.97}{20} = 17.1$$

i	Ri	Wi	Wi-Ri
1	12.91	13	.09
2	18.48	19	.52
3	25.97	31	5.03
4	17.86	18	.14
5	9.45	10	.55
6	24.07	25	.93
7	14.83	15	.17
8	24.85	26	1.15
9	6.58	8	1.42
10	21.80	22	.20
11	18.78	19	.22
12	11.53	15	3.47
13	5.97	6	.03
14	17.46	19	1.54
15	19.20	23	3.80
16	21.62	25	3.38
17	10.92	13	2.08
18	5.93	6	.07
19	23.26	25	1.74
20	13.31	14	.69
21	9.75	10	.25
	334.53	362	27.45

Site No.	Cos I Cos D	Cos I Sin D	Sin I
1	5.731	2.268	11.352
2	3.233	-2.560	18.013
3	7.283	1.054	24.909
4	8.288	-2.566	15.626
5	5.385	2.262	7.433
6	7.482	2.260	22.765
7	10.217	2.990	10.336
8	9.868	20.056	10.867
9	2.928	-.982	5.808
10	8.709	-10.626	16.937
11	5.353	-1.844	17.903
12	2.049	6.365	9.401
13	2.490	-1.125	9.309
14	1.831	-6.470	16.106
15	-3.966	-4.483	18.241
16	.523	8.783	19.715
17	.175	-2.998	10.492
18	3.053	-1.797	4.759
19	6.553	-1.668	22.236
20	-3.623	-.472	12.799
21	3.439	-1.322	9.022
	86.999	7.159	290.031

$$R^2 = 7570 + 51.3 + 84100$$

$$R = 303.3$$

Site	Wi	Wi^2
1	13	169
2	19	361
3	31	961
4	18	324
5	10	100
6	25	625
7	15	225
8	26	676
9	8	64
10	22	484
11	19	361
12	15	225
13	6	36
14	19	361
15	23	529
16	25	625
17	13	169
18	6	36
19	25	625
20	14	196
21	10	100

Σ Wi = 362 Σ Wi^2 = 7252

Completing the analysis of dispersion table, we obtain:-

Source	Degree of freedom	Sum of Squares	Mean Squares	Expectations of mean Squares
Between Sites	$2(B - 1)$ $= 2.20$ $= 40$	$\Sigma R_i - R$ 334.533 303.3 31.233	$31.233/40$ $= .7807$	$\frac{1}{2}\left(\frac{1}{\omega} + \frac{\overline{W}}{\beta}\right)$
Within Site	$2(\Sigma (W_i - 1))$ 2.342 $= 682$	$\Sigma (W_i - R_i)$ 27.467	$27.467/682$ $= .0403$	$\frac{1}{2\omega}$
TOTAL	$2 (N - 1)$ $= 2(362-1)$ $=722$	$N - R$ $= 362 -$ 303.3 $= 58.7$		$\overline{W} = \frac{1}{B-1} \cdot \left(N - \frac{\Sigma W_i^2}{N}\right)$

$$F = 19.4$$

$$\frac{1}{2\omega} = .04028$$

$$\omega = 12.43$$

$$\text{and } .7807 = \tfrac{1}{2}\left(.08056 + \frac{17.1}{\beta}\right)$$

$$\beta = \frac{17.1}{1.4808} = 11.54$$

$$K = \frac{1}{(12.43.362)^{-1} + (11.54.21)^{-1}}$$

$$= \frac{1}{.000222 + .00414}$$

$$= \frac{1}{.004349}$$

$$= 229.4$$

$$1 - \cos \alpha_o = - \frac{\log .05}{229.4}$$

$$1 - \cos \alpha_o = \frac{2.9958}{229.4}$$

$$= .01306$$

$$\cos \alpha_o = .9869$$

$$\underline{\alpha_o = 9^\circ}$$

APPENDIX 4

Results of a.c. cleaning experiment on Older Basalts are given in the following tables.

Spec. No.	A.C. CLEANING FIELD (OERSTED)										Locality
	0		43		86		129		173		
	D	I	D	I	D	I	D	I	D	I	
1 ac	32	-60			42	-57			42	-58	Site No. 1
bb	24	-61			15	-57			17	-53	
2 aa	21	-62			30	-62			0	-55	
3 bb	111	+79			133	+84			118	+82	Site No. 2
4 aa	77	+77			325	+82			178	+85	
5 bb	4	-9			89	+31			161	-26	
6 ad	-66	-64	-38	-77	-16	-68	-47	-60			Site No. 3
bc	-44	-63	-24	-67	-15	-71	21	-71			
7 bd	-35	-74	-33	-77	-8	-66	-18	-63			
bb	-37	-68	-9	-78	-59	-59	-55	-70			
8 bc	94	-33	89	-35	90	-58	63	-43			
ad	47	-57	46	-53	42	-60	30	-53			
9 ba	334	-70	5	-69	8	-71					Site No. 4
bc	350	-61	-19	-69	356	-58					
10 ad	339	-60	-4	-64	353	-71					
bc	346	-62	-4	-64	351	-63					

Spec. No.	FIELD 0		43		86		129		173		Locality
	D	I	D	I	D	I	D	I	D	I	
11 ba	327	-30	343	-26	327	-50			4	-11	Site No. 5
aa	220	+70	357	-32	3	-59			12	-50	
12 ae	-1	-68	20	-69	4	-68			28	-65	
aa	-4	-72	20	-69	15	-72			0	-59	
13 aa	28	-60	24	-58	22	-86			33	-46	
ab	28	-60	26	-56	31	-54			37	-77	
17 aa	41	-60	296	+2	355	-25					Site No. 7
bc	349	-40	345	-20	260	-9					
18 bd	6	-40	15	-34	-37	-16					
ab	15	-42	10	-35	43	-20					
19 aa	250	+52	244	+53	261	+58	323	-40			Site No. 8
ae	269	+20	273	+42	261	+53	299	-27			
20 ba	259	+28	220	+41	219	+35	4	-1			
ab	241	+28	264	+50	230	+37	351	+3			
21 bc	245	+43	248	+46	200	+6	274	+46			
ba	262	+47	277	+45	208	+40	331	+3			
22 ad	118	+41	216	+46	326	+51					Site No. 9
bc	128	+53	234	+46	195	+38					
23 ad	105	+20	62	+55	277	+69					
bd	79	-7	-3	+73	30	+68					
24 bb	135	+45	148	+63	107	+42					Site No. 10
aa	142	+45	137	+59	54	+49					
25 ag	121	+55	132	+63	111	+59					
af	123	+61	128	+63	104	+59					
26 ad	119	+43	104	+66	71	+53					
bd	130	+48	134	+62	131	+58					

Spec. No.	FIELD 0		43		86		129		173		Locality
	D	I	D	I	D	I	D	I	D	I	
27 aa	348	-68	299	-66	347	-76					Site No. 11
ac	349	-70	326	-74	317	-63					
28 ba	0	-69	2	-70	260	-81					
ab	-6	-68	6	-69	-6	-76					
29 ac	-11	-73	-5	-74	-6	-68					
bc	-11	-73	6	-71	1	-70					
30 ac	94	-21			47	-46			307	-34	Site No. 12
aa	91	-26			250	-82			184	+14	
31 ab	92	-28			50	-80			338	-65	
aa	96	-24			314	-78			332	-56	
32 ac	43	-71			331	-69			352	-38	
aa	319	-72			50	-71			309	+9	
33 ab	-25	-59	156	-80	167	-70					Site No. 13
bb	-34	-63	-46	-72	289	-74					
34 ca	1	-23	-30	-36	-22	-20					
bb	-23	-54	143	-81	84	-70					
35 aa	228	-18	196	-33	203	-39					
ad	185	-58	151	-47	164	-31					
36 aa	227	-58	188	-68	240	+27					Site No. 14
bc	215	-63	222	-78	100	-45					
37 aa	311	-54	-28	-71	295	-71					
bd	316	-62	248	-53	237	-60					
38 ba	210	-81	279	-61	65	-41					Site No. 15
ac	94	-79	47	-78	310	+2					
39 ab	63	-84	163	-68	329	-27					
ba	23	-66	166	-56	135	-45					
40 aa	270	-73	220	-78	250	-84					
bb	244	-49	300	-68	170	-64					

Spec. No.	FIELD										Locality
	0		43		86		129		173		
	D	I	D	I	D	I	D	I	D	I	
41 ab	71	-70	105	-67	112	-60			176	-72	Site No. 16
af	317	-65	32	-78	84	-56			122	-52	
42 ba	61	-78	29	-75	19	-77			31	-46	
bc	53	-69	26	-73	15	-78			16	-74	
43 bd	115	-18	123	-20	70	-39			44	-51	
ad	98	-56	117	-26	63	-47			39	-50	
44 aa	237	-58	242	-38					-12	-19	Site No. 17
ab	264	-62	215	-12					155	+18	
45 bb	274	-71	321	-80					225	-52	
ba	103	-69	198	-30					235	+40	
46 ac	152	+55	160	+57	170	+60					Site No. 18
ae	150	+49	156	+54	160	+50					
47 aa	347	-62	-53	-59	45	-66					Site No. 19
ac	355	-59	-19	-60	6	-32					
48 ab	324	-66	-28	-81	93	-83					
af	303	-56	-23	-62	304	-50					
51 be	206	-68	34	-88	277	-63					
bb	9	-72	-21	-74	1	-72					
49 ab	9	-73	335	-70	187	-79					Site No. 20
ad	183	-67	337	-72	158	-77					
50 ac	205	-83	-35	-75	302	-70					
bb	196	-80	-48	-76	298	-79					
52 ae	328	-53	325	-62	325	-63			305	61	Site No. 21
ad	327	-56	335	-69	323	-65			339	74	
53 aa	328	-70	316	-78	21	-89			122	80	
ad	344	-85	192	-80	14	-86			310	72	

The calculation of the mean direction of magnetization follows. Mean site directions are given in the following table:

SITE	D(M.N.)	I
1	26	-61
2	266	+71
3	9	-72
4	-6	-67
5	6	-62
6		
7	10	-47
8	66	+46
9	50	+79
10	311	+63
11	-15	-72
12	20	-77
13	216	-79
14	243	-75
15	220	-82
16	71	-62
17	246	-75
18	338	+56
19	-30	-72
20	-32	-74
21	-41	-76

The mean direction of magnetization is:

$$D\ (M.N.) = 6^{o}$$
$$I = -77^{o}$$
$$\alpha_{o} = 9^{o}$$

SITE NO.	Cos I Cos D	Cos I Sin D	Sin I
1	1.305	.630	2.624
2	.058	.854	2.499
3	1.714	.277	5.358
4	1.571	-.147	3.665
5	2.748	.295	5.140
6			
7	2.609	.454	2.821
8	-1.649	-3.753	4.316
9	- .409	-.479	3.214
10	-1.780	2.031	5.319
11	1.722	-.450	5.655
12	1.205	.436	5.552
13	-.771	-.551	4.787
14	-.463	-.902	3.649
15	-.655	-.540	5.514
16	.861	2.485	5.008
17	-.396	-.887	3.610
18	-1.048	.425	1.648
19	1.639	-.910	5.554
20	.968	-.594	3.827
21	.689	-.601	3.780
	9.918	-1.927	83.539

$$R^2 = 98.37 + 3.71 + 6978.76$$

$$= 7080.84$$

$$R = 84.15$$

i	Ri	Wi	Wi - Ri
1	2.99	3	.01
2	2.64	3	.36
3	5.63	6	.37
4	3.99	4	.01
5	5.83	6	.17
6			
7	3.94	4	.06
8	5.95	6	.05
9	3.27	4	.73
10	5.97	6	.03
11	5.93	6	.07
12	5.69	6	.31
13	4.89	6	.11
14	3.78	4	.22
15	5.58	6	.42
16	5.66	6	.34
17	3.74	4	.26
18	1.99	2	.01
19	5.87	6	.13
20	3.99	4	.01
21	3.89	4	.11
	91.22	96	4.78

Site	Wi	Wi^2
1	3	9
2	3	9
3	6	36
4	4	16
5	6	36
6		
7	4	16
8	6	36
9	4	16
10	6	36
11	6	36
12	6	36
13	6	36
14	4	16
15	6	36
16	6	36
17	4	16
18	2	4
19	6	36
20	4	16
21	4	16

$\Sigma Wi = 96 \qquad \Sigma Wi^2 = 494$

$$\frac{1}{W} = \frac{1}{B - 1} \left(N - \frac{\Sigma Wi^2}{N} \right)$$

$\bar{W}$ is the weighted mean of the Wi

$$\frac{1}{W} = \frac{1}{20 - 1} (96 - 5.1464)$$

$$= \frac{90.8536}{19} = 4.786$$

Completing the analysis of dispersion table we have:-

Source	Degrees of freedom	Sum of squares	Mean Squares	Expectations of Mean Squares
Between Sites	$2\ (B - 1)$ $= 2\ (20 - 1)$ $= 38$	$\Sigma\ Ri - R$ $= 91.22 - 84.15$	$\frac{7.07}{38}$ $= .1862$	$\frac{1}{2}\left(\frac{1}{W} + \frac{\overline{W}}{\beta}\right)$
Within Sites	$2(\Sigma\ (Wi - 1))$ 2.76 $= 152$	$\Sigma\ (Wi - Ri)$ 4.78	$\frac{4.78}{152}$ $= .0315$	$\frac{1}{2\omega}$
Total	$2\ (96 - 1)$ $= 2.95$ $= 190$	$N - R$ 96 -84.15 11.85	$\overline{W} = \frac{1}{(B-1)}$	$\left(N - \frac{\Sigma\ Wi^2}{N}\right)$

$$F = 5.8$$

$$\frac{1}{2\ \omega} = .0315$$

$$\frac{1}{\omega} = .0630$$

$$\omega = \frac{1}{.0630} = 15.89$$

$$.1862 = \frac{1}{2}\left\{.0630 + \frac{4.786}{\beta}\right\}$$

$$.3094 = .0630 + \frac{4.786}{\beta}$$

$$\beta = \frac{4.786}{.3094}$$

$$\underline{\beta = 15.49}$$

$$K = \frac{1}{(\omega N)^{-1} + (\beta B)^{-1}}$$

$$= \frac{1}{(15.89.96)^{-1} + (15.49.20)^{-1}}$$

$$= \frac{1}{.000653 + .00324}$$

$$= \frac{1}{.00389} = 257$$

$$1 - \cos\alpha_o = -\frac{\log .05}{257}$$

$$1 - \cos\alpha_o = \frac{2.9958}{257}$$

$$1 - \cos\alpha_o = .0117$$

$$\cos\alpha_o = .9883$$

$$\underline{\alpha_o = 9^o}$$

APPENDIX 5

In this Appendix are given the results of the thermal demagnetization experiments carried out on the Older Volcanic Basalts.

1. Results obtained by the method of continuous thermal Demagnetization

The vertical scale on all figures represents the relative intensity of magnetization, or the deflection produced by the magnetometer, at the particular temperature involved. Each unit on the scale represents a moment of magnetization of horizontal component of magnetization equal to 3.6×10^{-4} c.g.s.

SPECIMEN

Powdered Magnetite

Cold temperature junction
= 15°C.

E.M.F. (millivolts)	Temperature °C	Deflection
.7	125	43
1.4	205	35
1.65	235	32
2.05	275	28
2.25	290	26
2.40	310	24
3.20	390	16
3.50	420	13
3.75	440	11
4.45	510	6
4.60	525	4.5
4.75	537	4.0
5.10	565	2.0
5.20		

SPECIMEN

Powdered Hematite

Cold temperature junction
= 15°C

E.M.F. (millivolts)	Temperature °C	Deflection
1.5	215	47
2.15	285	46
3.2	390	45
4.0	470	40
5.2	575	31
5.4	595	26
5.75	630	15
5.9	645	10
6.2	665	4
6.3	675	2
6.4		0

SPECIMEN

Powdered Nickel

Cold temperature junction
= 15°C

E.M.F. (millivolts)	Temperature °C	Deflection
.7	120	39.5
1.15	180	37
1.50	210	34.5
1.90	255	30
2.20	285	25.5
2.50	315	20.1
2.80	345	12.0
2.90	355	6.0
2.95		
3.00	365	0
3.05		

SPECIMEN

No.6b

Cold temperature junction

= 15°C

E.M.F. (millivolts)	Temperature °C	Deflection
.2	50	30
.36	75	21
.70	125	9
	175	5
1.30	200	3
3.05	375	1

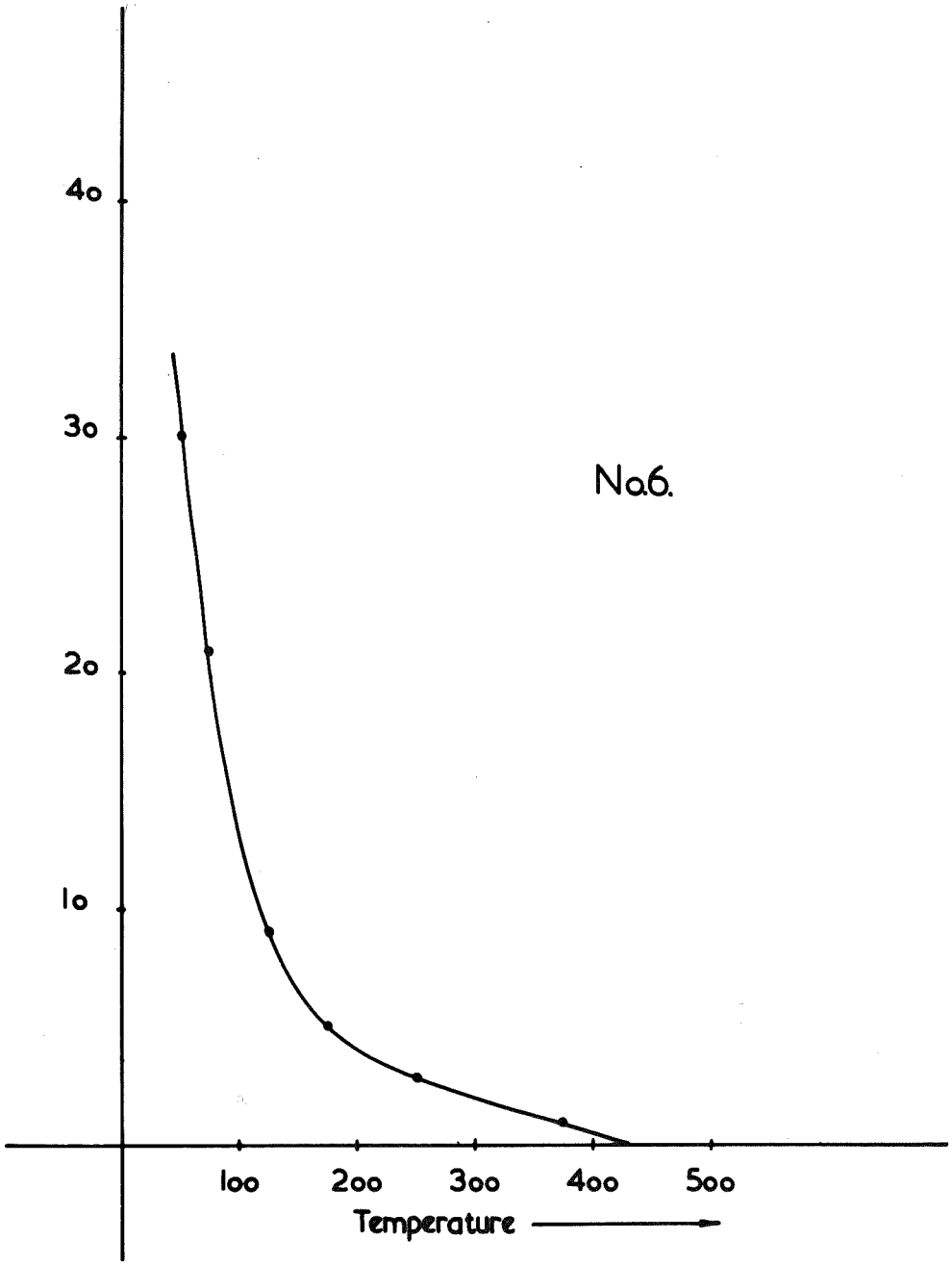

Figure.88.

SPECIMEN

No.7

Cold temperature junction

= 15°C

E.M.F. (Millivolts)	Temperature °C	Deflection
.35	75	25
.50	95	22
.70	125	16
1.15	180	8
1.30	200	6
1.40	210	5
1.85	255	2.5
2.15	275	2
2.30	300	1.5
2.40	310	1.5
2.70	340	1.0
3.00	370	.5

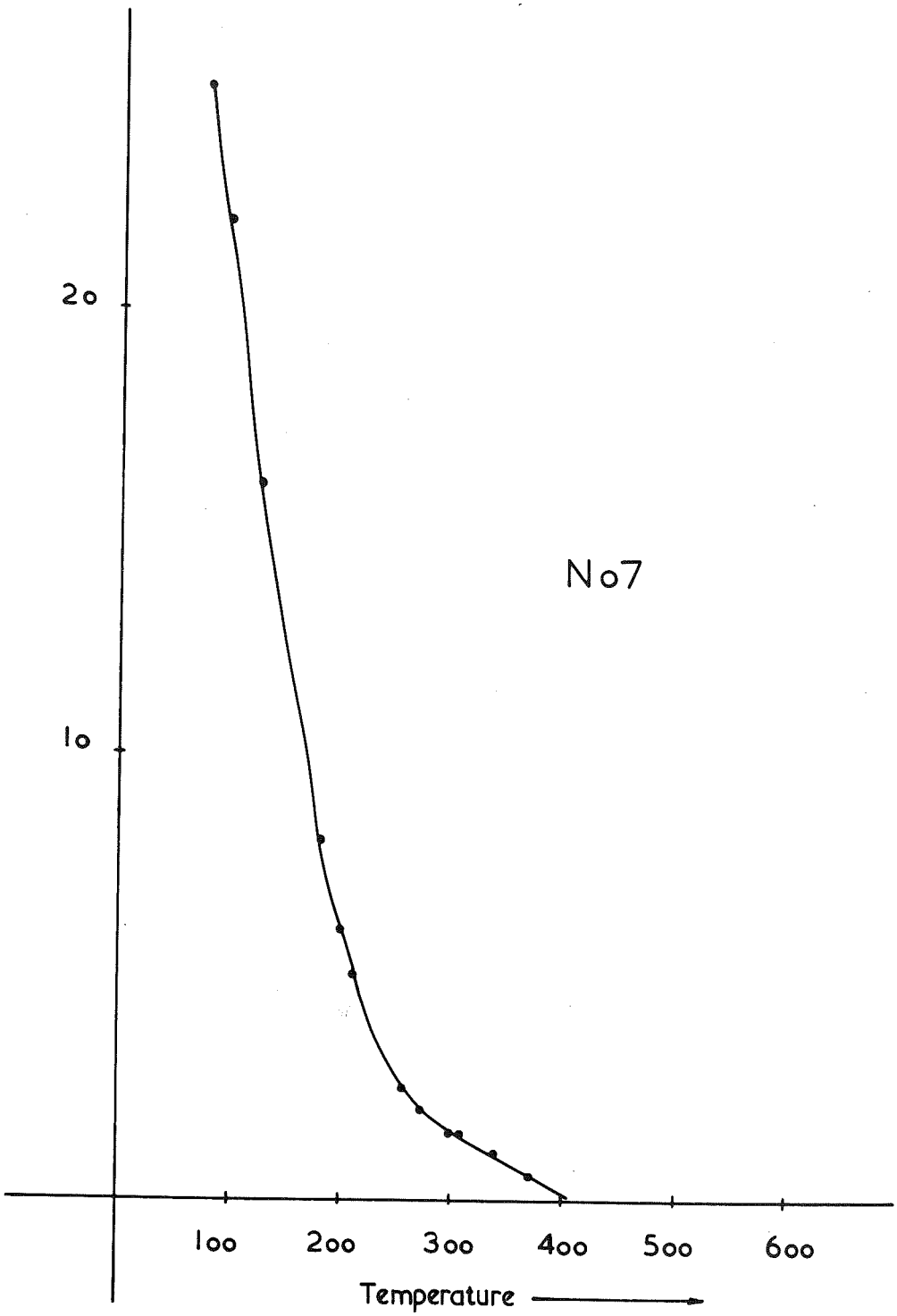

Figure.89.

SPECIMEN

No.7a

Cold temperature junction

= 15°C

E.M.F. (millivolts)	Temperature °C	Deflection
.1	35	48
.2	50	45
.3	70	38
.45	85	33
.6	110	24
.85	150	15
1.4	210	6
1.8	250	3.5
2.0	270	3
2.71	340	1.5
3.0	360	1
3.2	390	.5

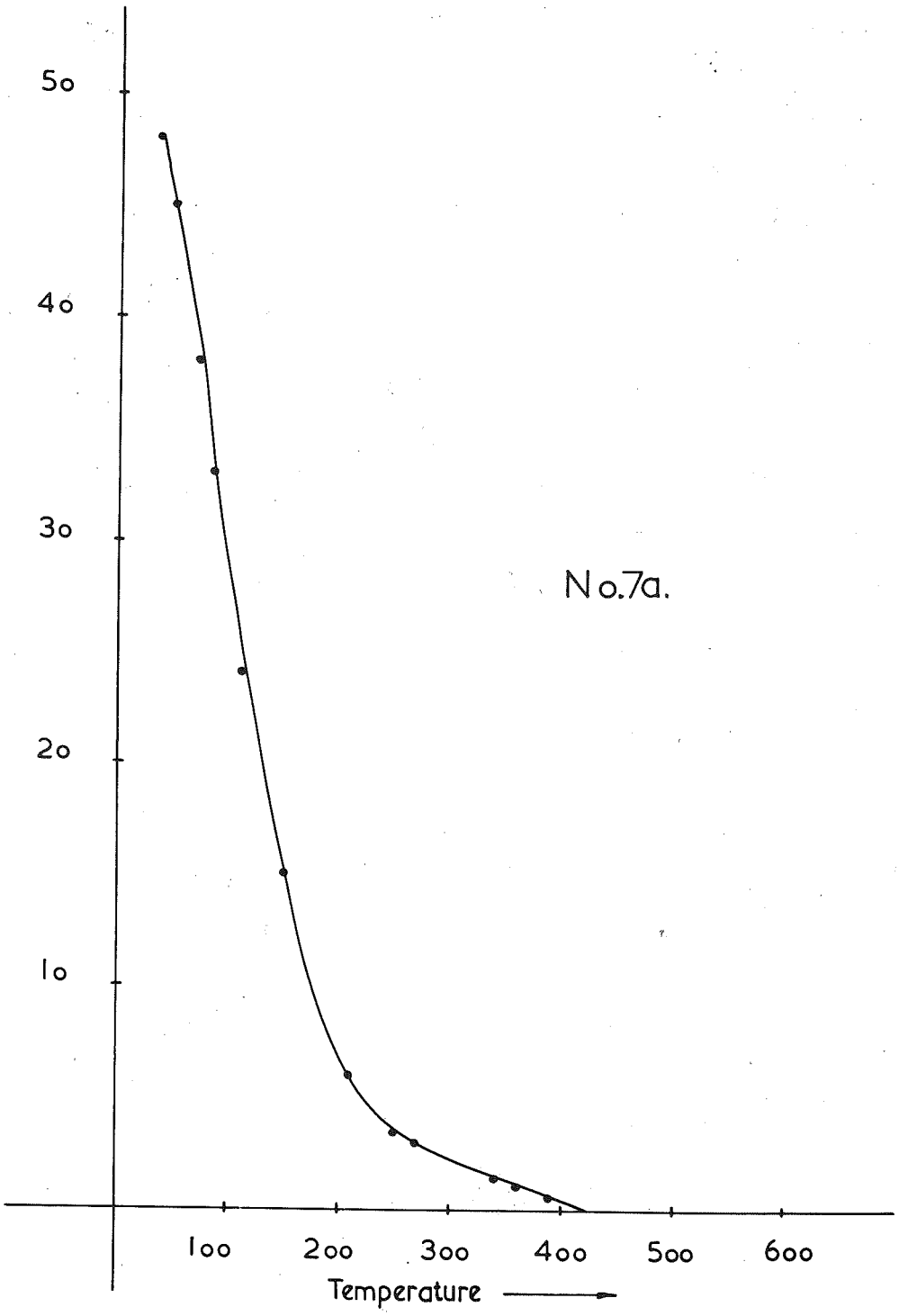

Figure 9o.

SPECIMEN

No.19

Cold temperature junction

= 15°C

E.M.F. (millivolts)	Temperature °C	Deflection
0	15	36
.2	55	26.5
.38	80	18.5
.65	115	11.5
1.12	180	6.0
1.35	200	4.5
1.60	230	3.0
2.10	280	2.0
2.85	355	1.0
3.10	375	1.0

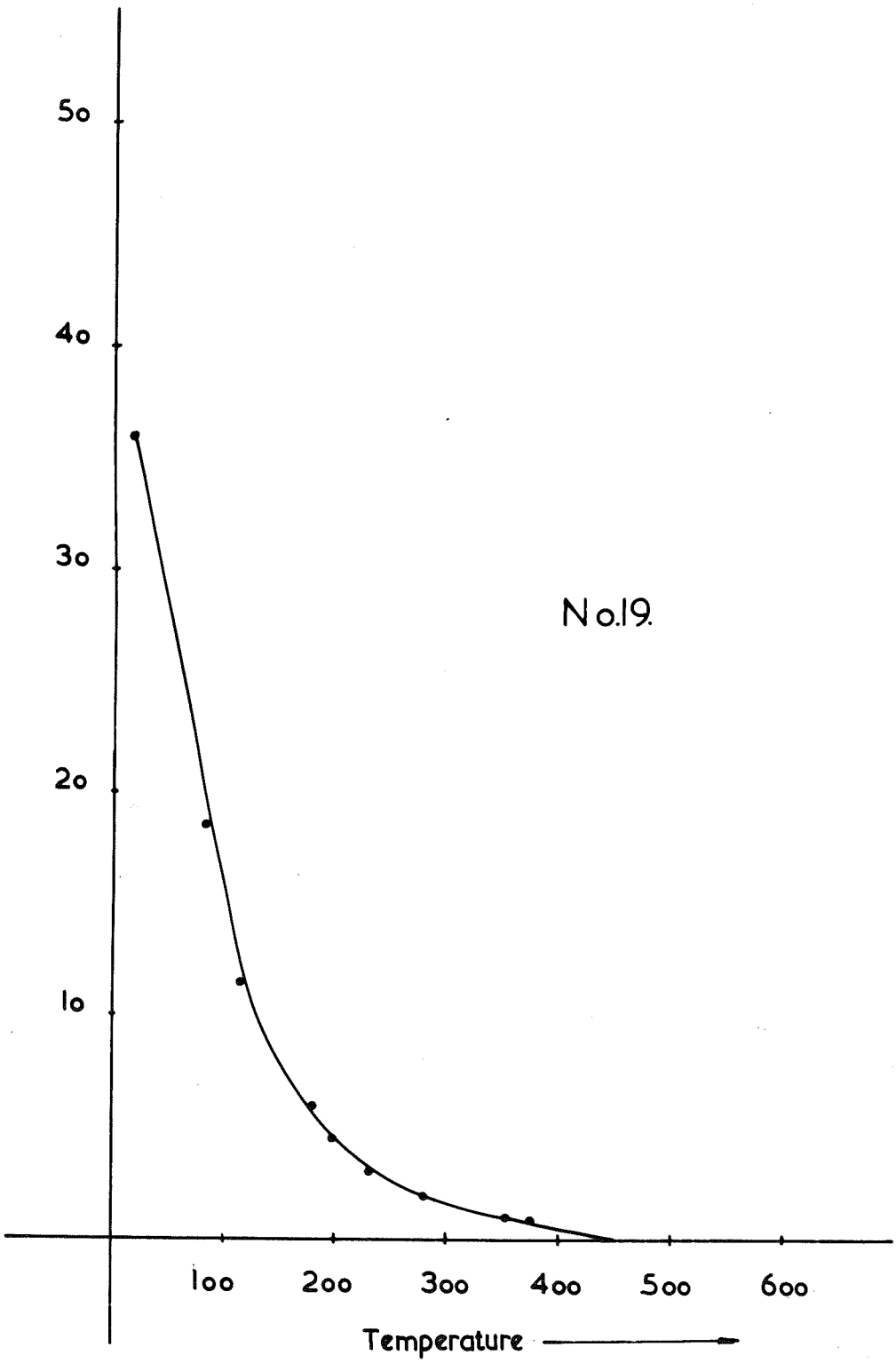

Figure 91.

SPECIMEN

No.19a

Cold temperature junction

= 15°C

E.M.F. (millivolts)	Temperature °C	Deflection
0	15	35
.2	50	31
.5	95	19
.8	140	11
2.3	300	1.5
2.7	340	1.0
3.1	380	.5

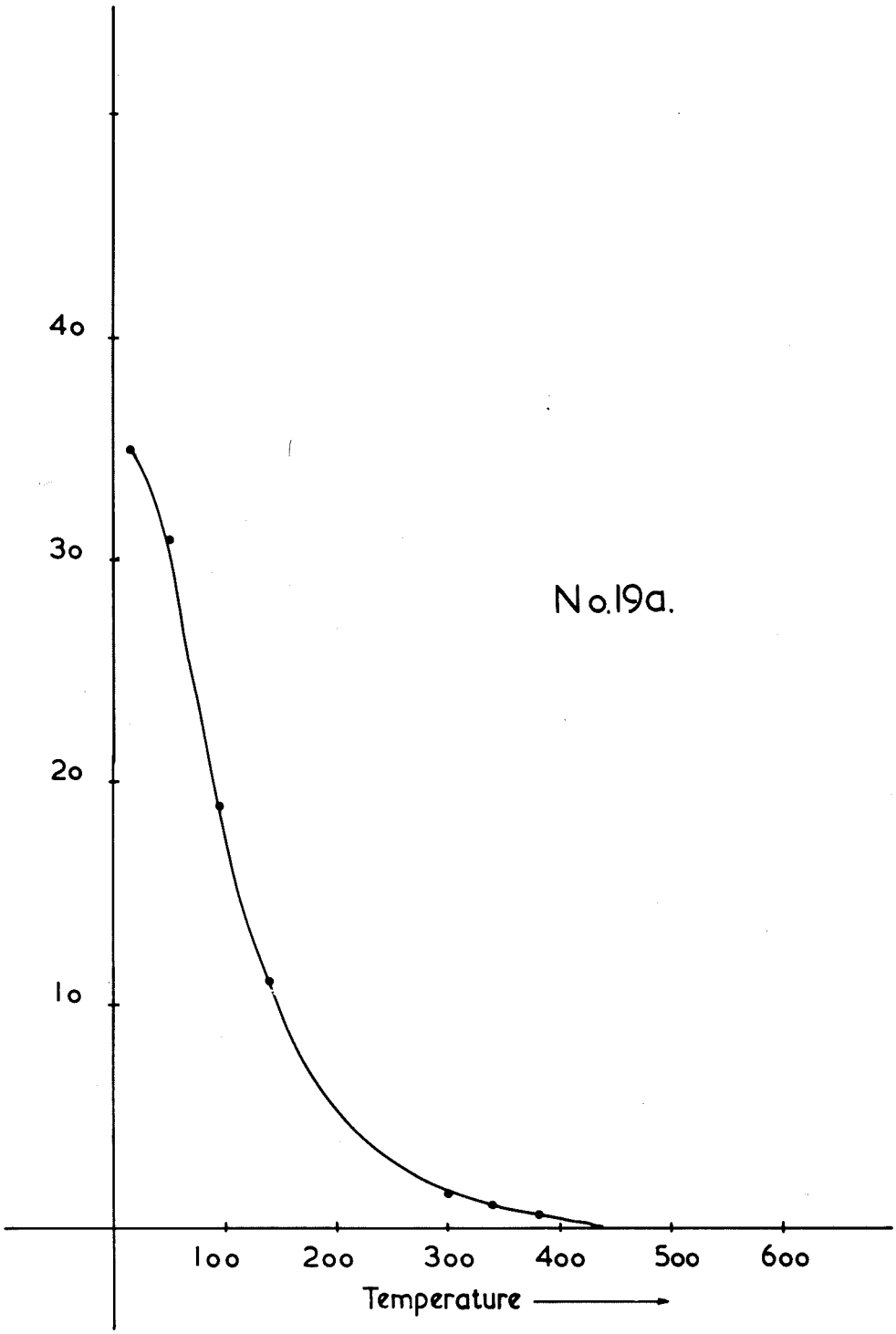

Figure.92.

SPECIMEN

No.20

Cold temperature junction

= 15°C

E.M.F. (millivolts)	Temperature °C	Deflection
0	15	
.2	55	40
.5	100	24
.8	140	12
1.1	175	8
1.5	215	5
1.75	245	4
2.40	310	2
2.90	360	1

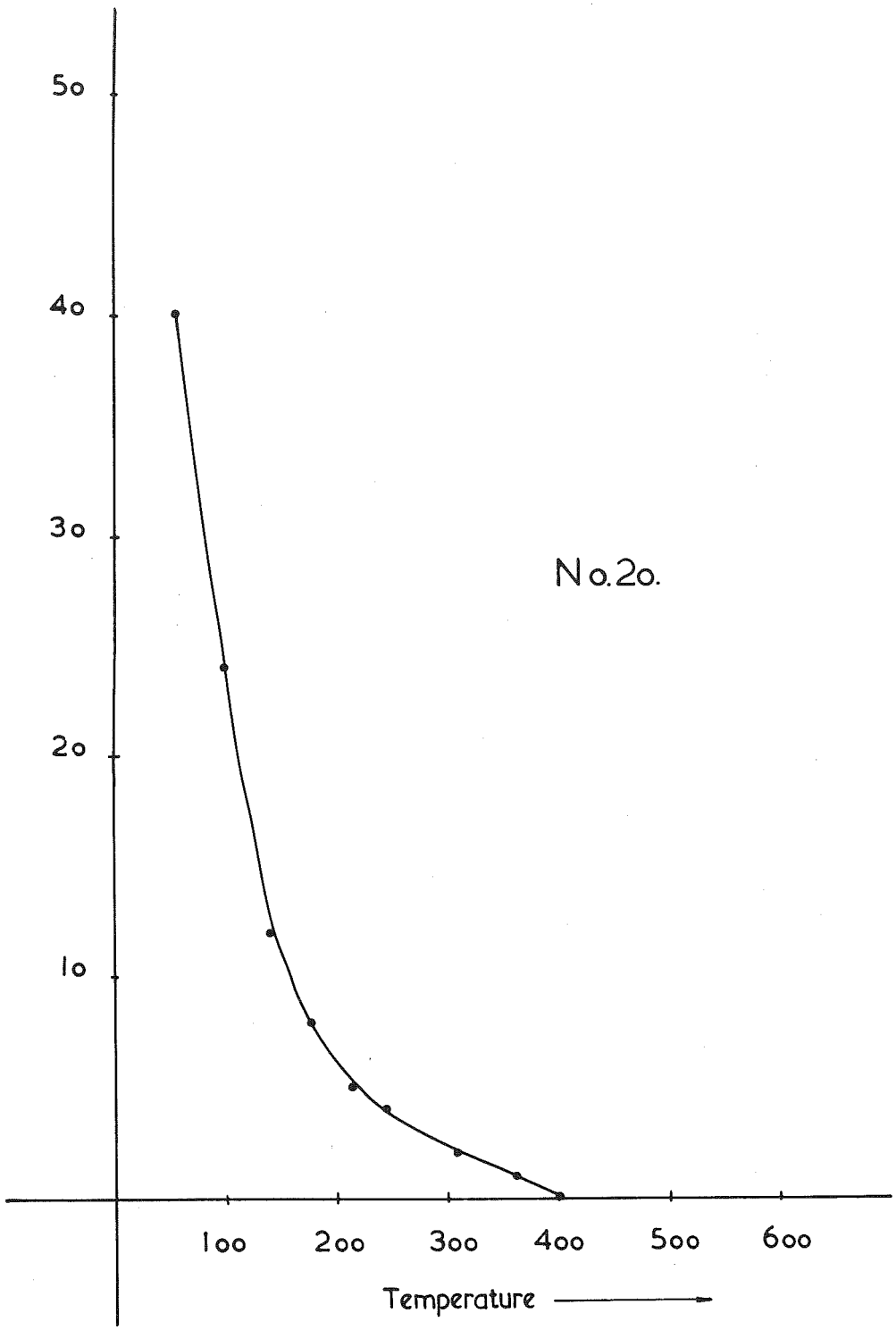

Figure.93.

SPECIMEN

No.21b

Cold temperature junction

= 15°C

E.M.F. (millivolts)	Temperature °C	Deflection
0	15	41
.25	60	40
.5	95	28
.7	125	22
1.0	165	17
1.1	175	15
1.8	250	9
1.9	260	8
2.2	290	6
2.4		
2.7	340	3.5
3.1	380	2

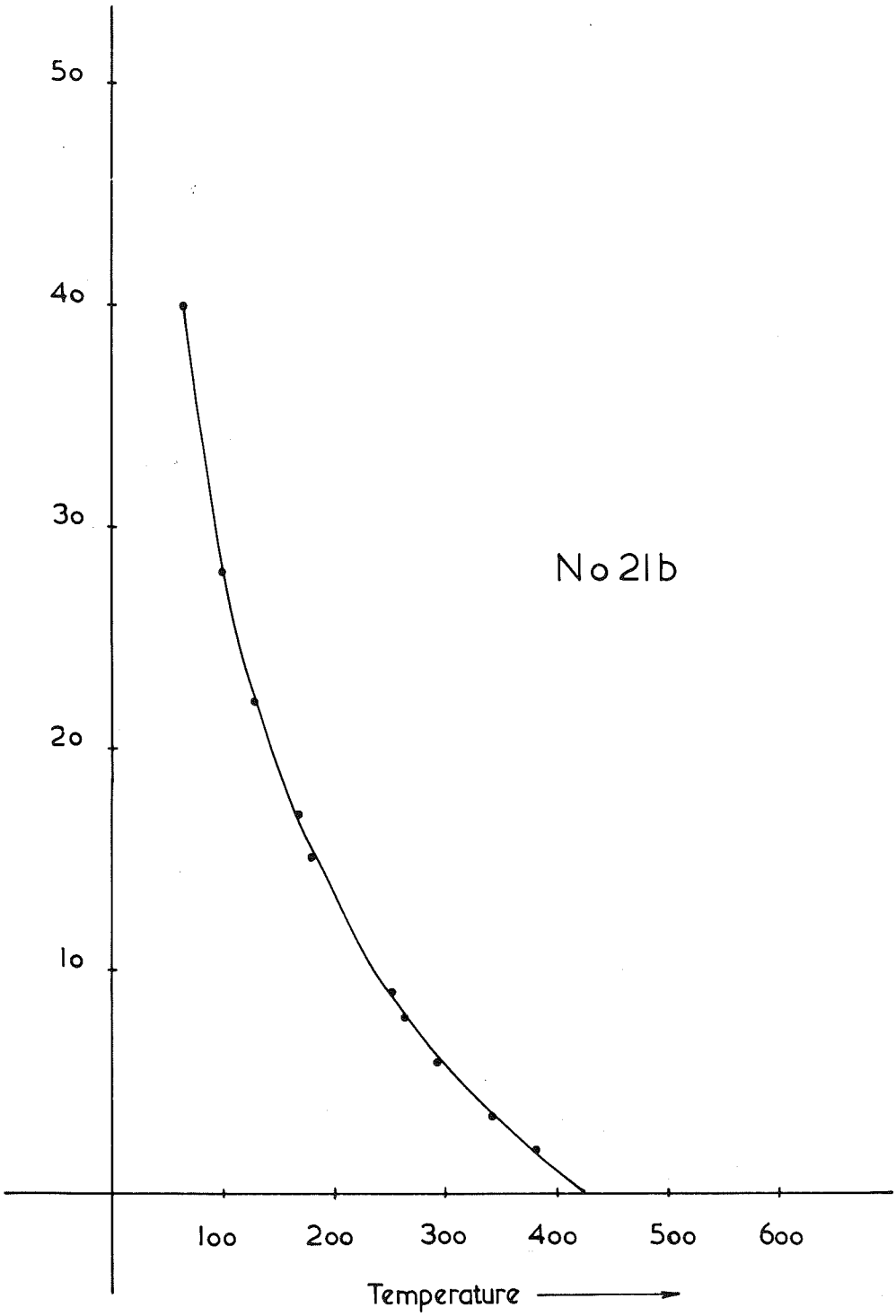

Figure.94.

SPECIMEN

No.25

Cold temperature junction

= 15°C

E.M.F. (millivolts)	Temperature °C	Deflection
.9	155	47.5
1.25	195	29
1.8	250	11
2.3	300	7
2.6	330	5
2.9	360	4
3.2	390	3
3.6	430	1

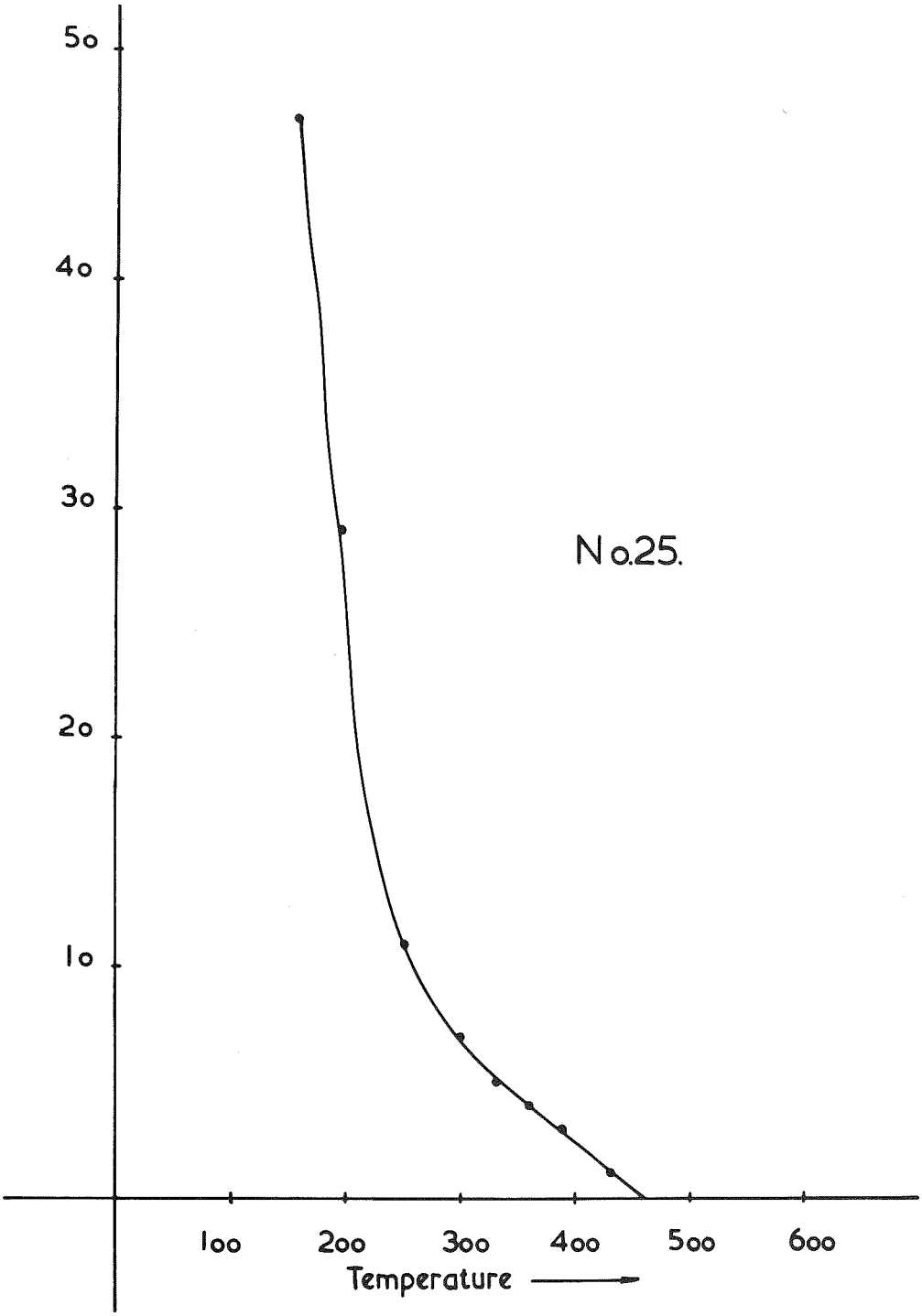

Figure.95.

SPECIMEN

No.26

Cold temperature junction

= 15°C

E.M.F. (millivolts)	Temperature °C	Deflection
0	15	47
.17	45	43.5
.31	70	37.5
.60	110	22
.70	125	18
1.00	165	10
1.30	200	6.5
1.70	240	4.0
2.20	290	2.5
2.70	340	1.5
3.05	375	1.0
3.25	395	.7
3.37	410	.5

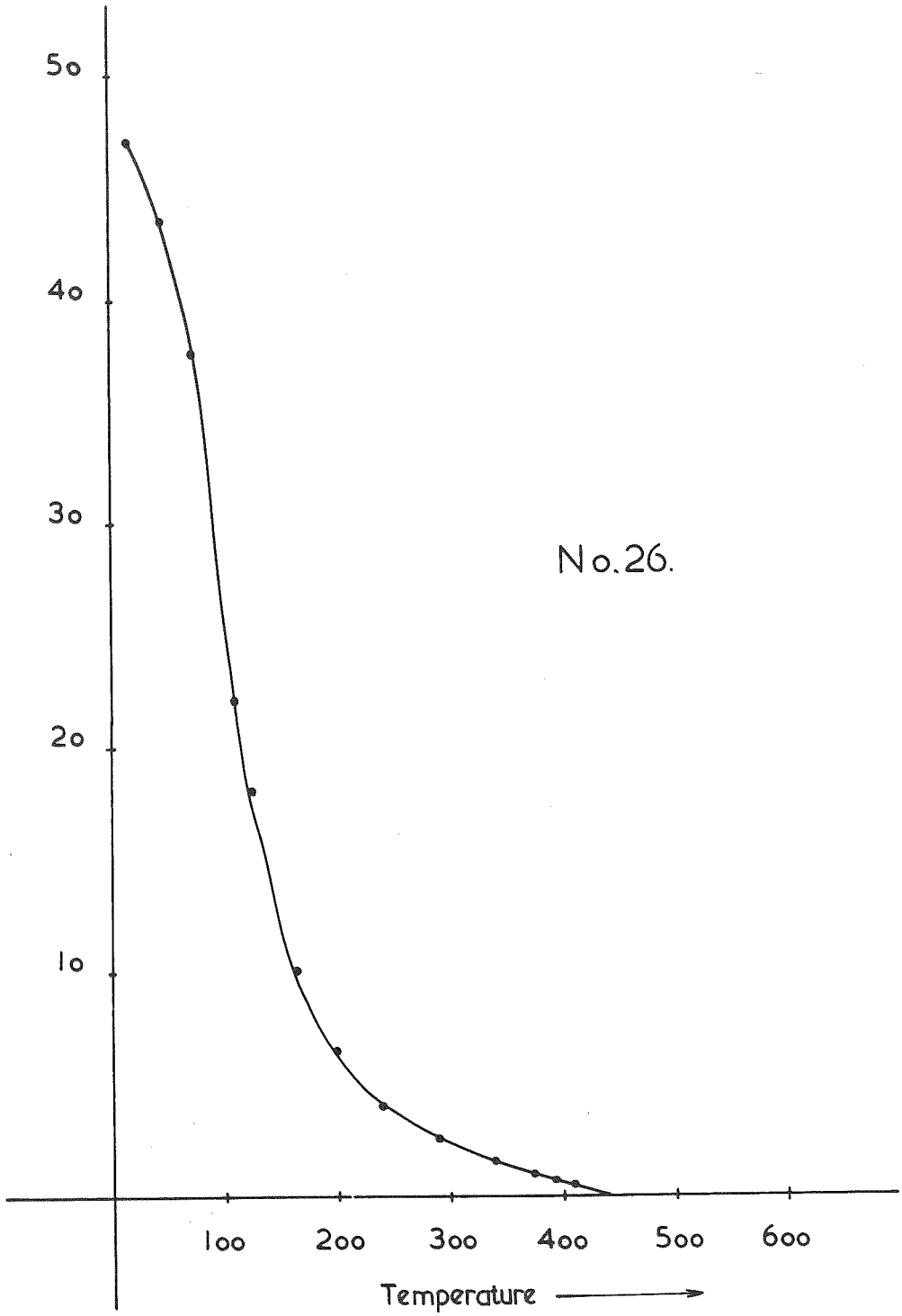

No. 26.

Figure. 96.

SPECIMEN

No.26a

Cold temperature junction

= 15°C

E.M.F. (millivolts)	Temperature °C	Deflection
.5	100	45
.8	140	21
1.1	180	10
1.6	240	6
2.15	285	4.5
2.65	335	3
2.90	360	2
3.25	395	1

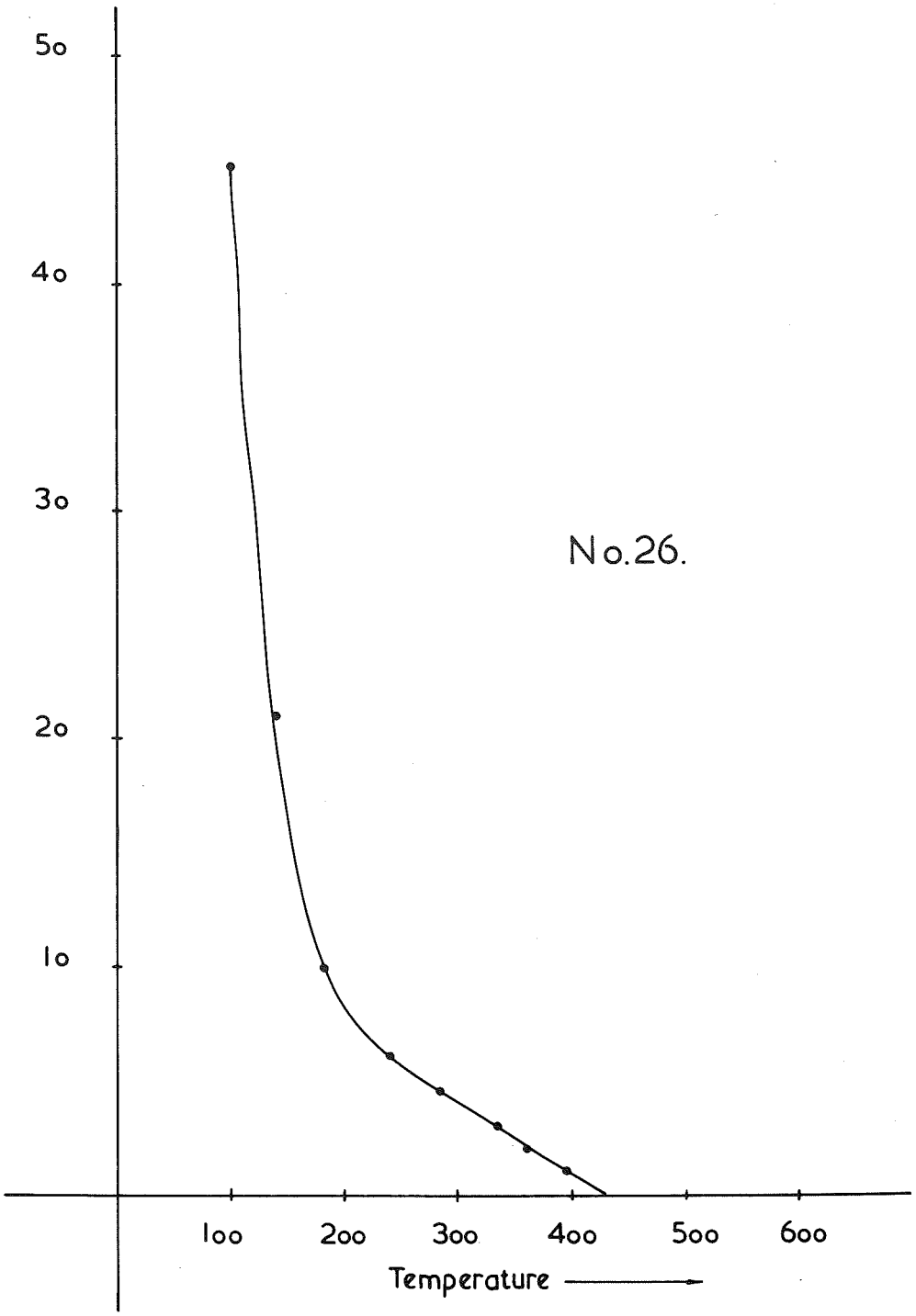

Figure 97.

SPECIMEN

No.31

Cold temperature junction

= 15°C

E.M.F. (millivolts)	Temperature °C	Deflection
.6	110	44.5
.75	135	26
.90	155	16.5
1.10	177	7.5
1.20	190	5.0
1.40	210	2.0
1.65	235	1.0
1.76	250	.5
1.85	255	.5

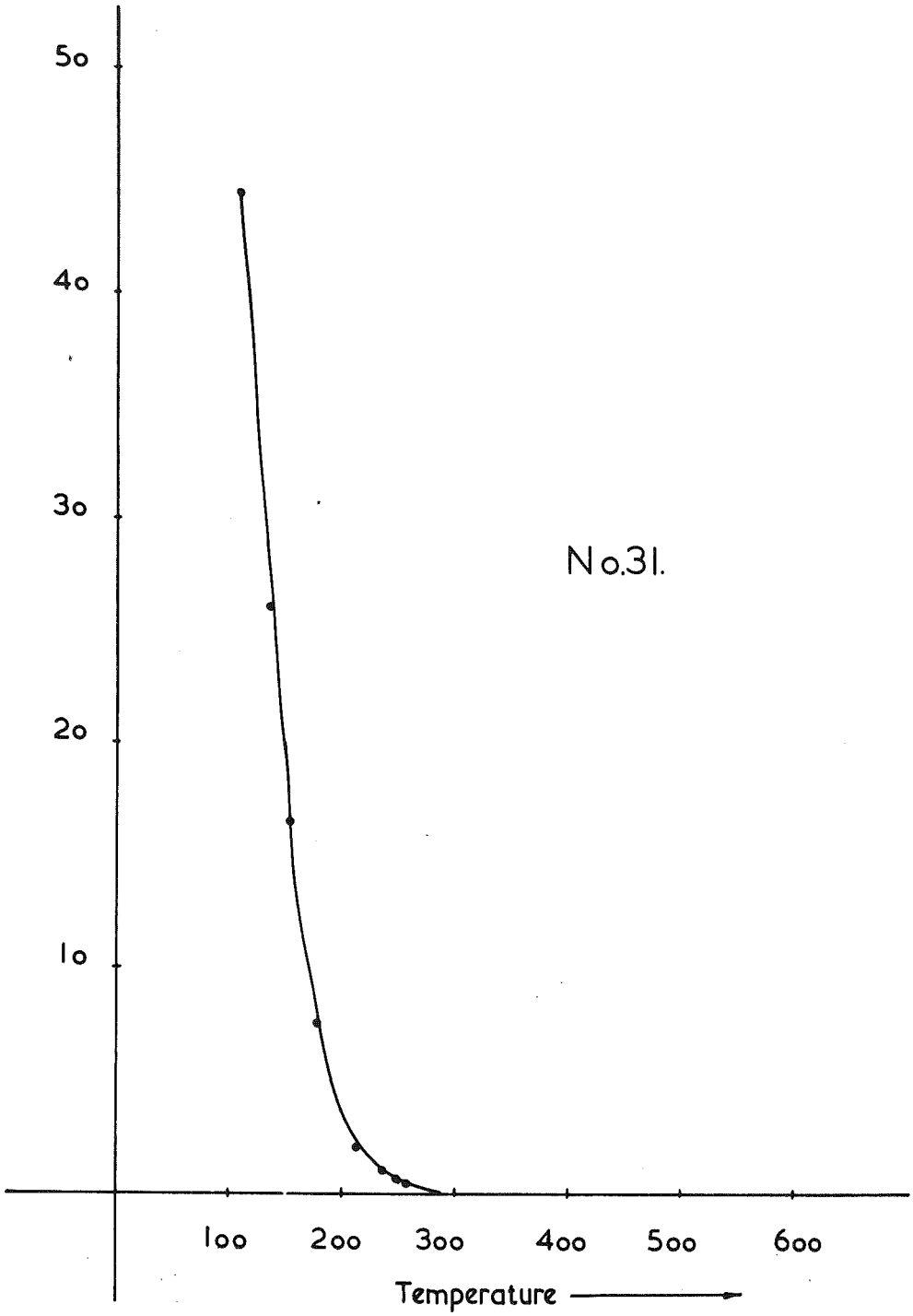

Figure .98.

SPECIMEN

No.33c

Cold temperature junction

= 15°C

E.M.F. (millivolts)	Temperature °C	Deflection
.2	70	31
.46	90	13
.60	110	9
.88	150	4.5
1.10	180	2.5
1.20	190	2.0
1.60	230	
1.70	240	.7
1.90	260	.5
2.10	280	.3

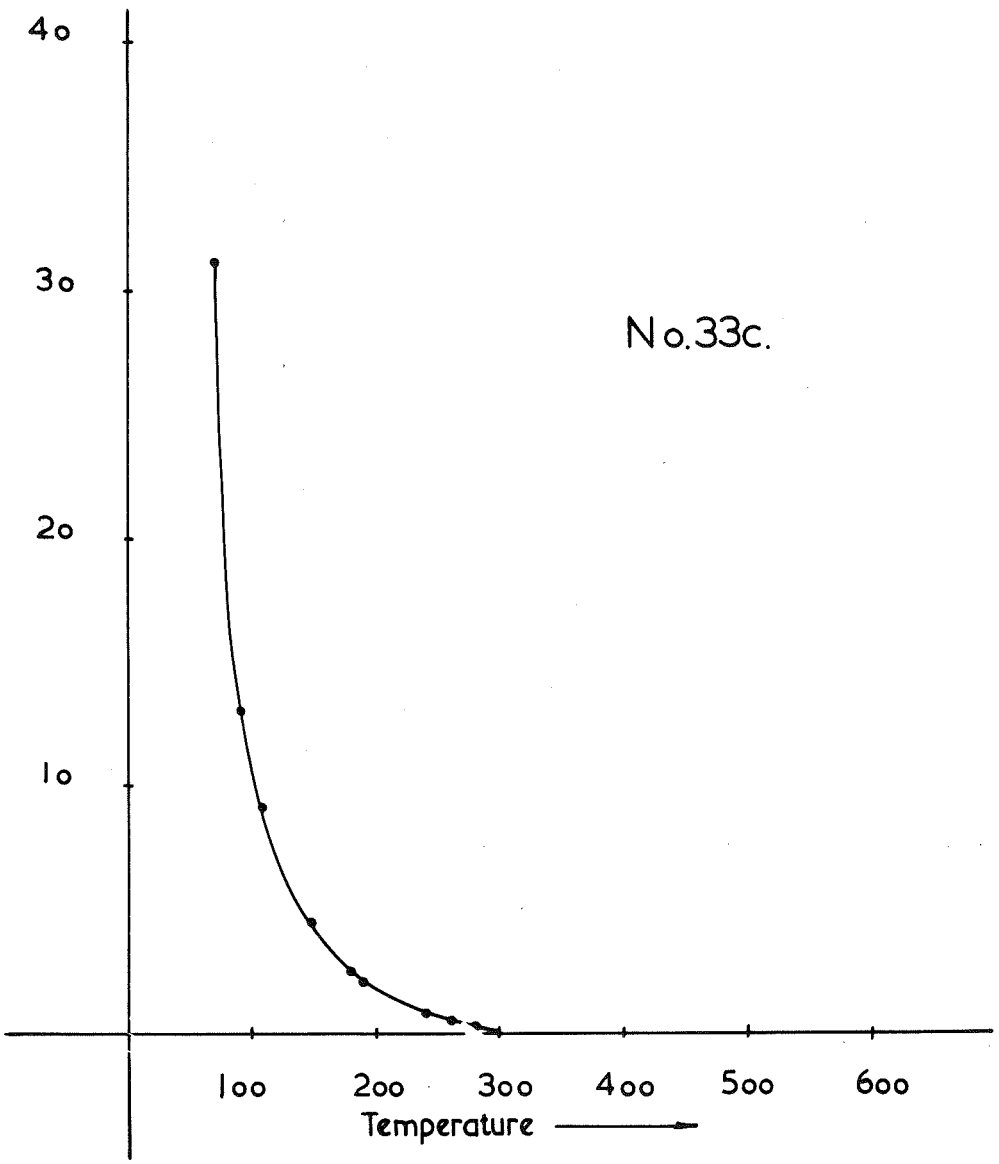

Figure.99.

SPECIMEN

No.36

Cold temperature junction

= 15°C

E.M.F. (millivolts)	Temperature °C	Deflection
.03	20	34
.2	55	26
.45	85	9.5
.55	105	7
.65	115	7
.8	140	6
1.1	175	5.5
1.45	210	5.0
1.9	260	4.5
2.5	320	4.0
3.4	410	3.0
4.5	515	1.0
5.0	560	1.0
5.15	570	.5

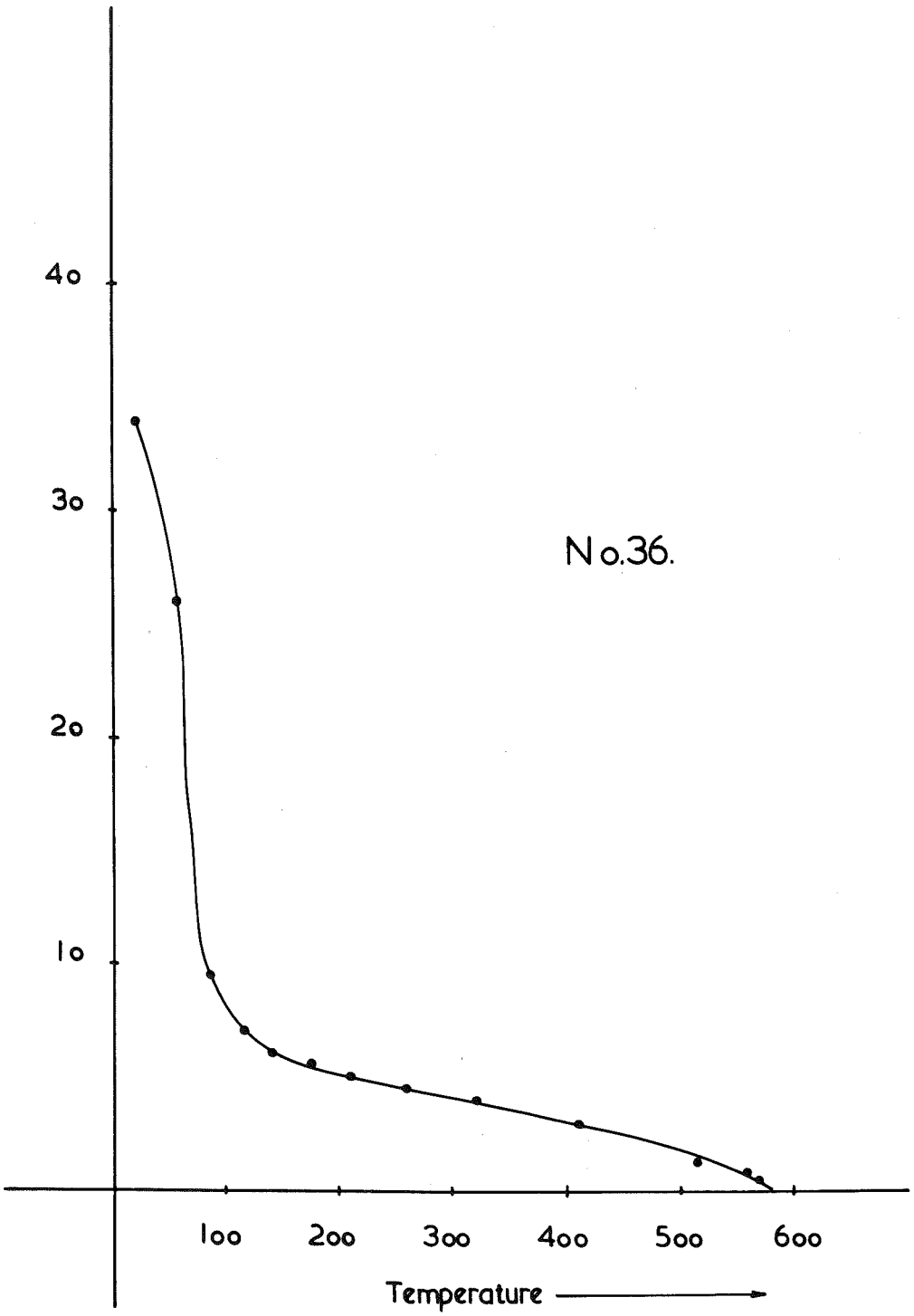

Figure.100.

SPECIMEN

No.38

Cold temperature junction

= 15°C

E.M.F. (Millivolts)	Temperature °C	Deflection
.2	50	32
.6	110	8
1.1	175	7
1.55	225	6
2.0	270	6
2.5	320	4.5
3.1	380	.5
4.0	465	.3
4.6	525	.2
4.8	540	1.5
4.9	550	1.5
5.1	565	1.0

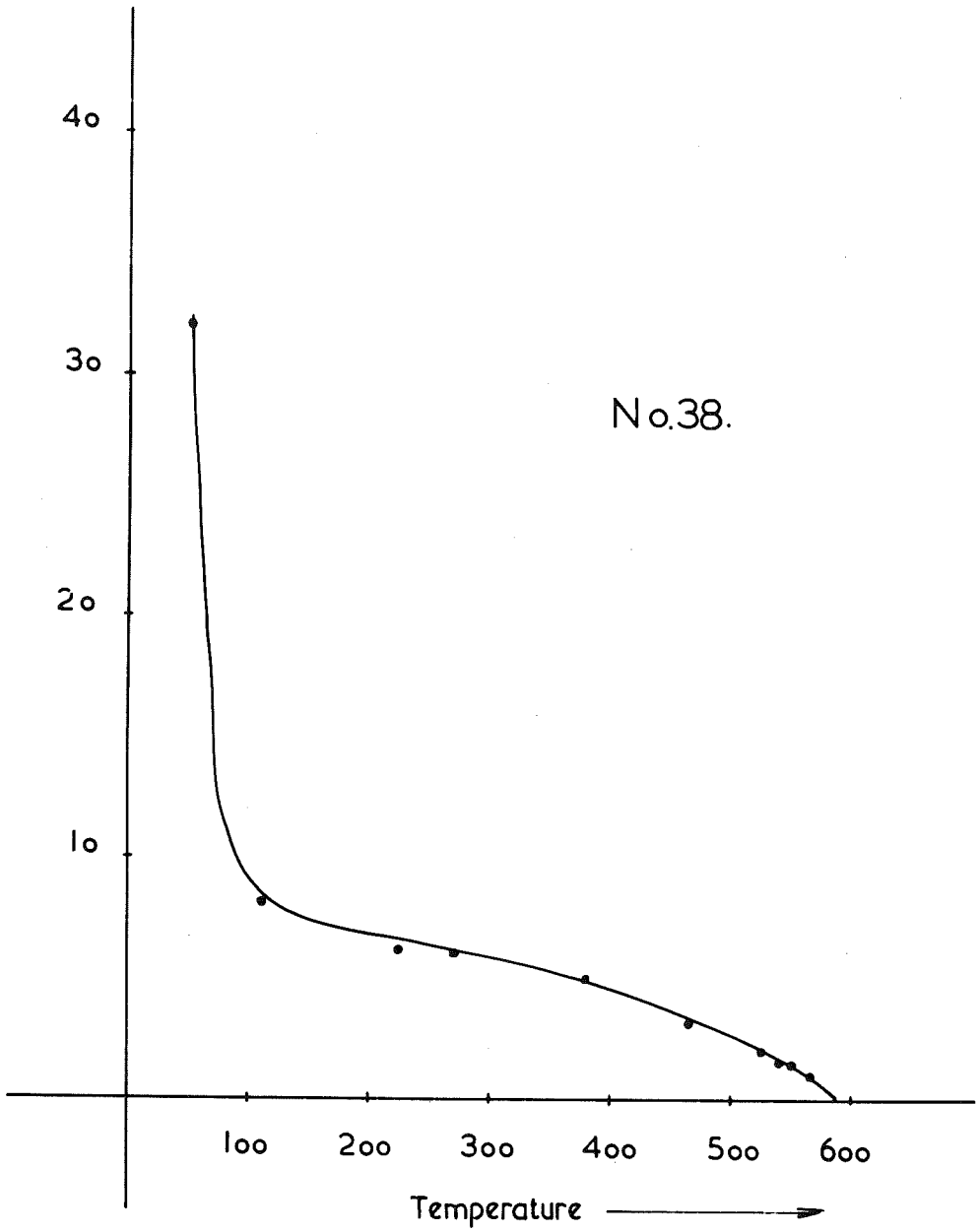

Figure 101

SPECIMEN

No.41

Cold temperature junction

= 15°C

E.M.F. (millivolts)	Temperature °C	Deflection
1.15	185	49
1.35	200	37
1.70	240	25
2.30	300	20
2.80	350	16
3.30	400	15
3.60	430	
3.80	450	14
4.10	475	11
4.35	500	10
4.80	540	9
5.00	560	5
5.10	565	4
5.20	575	3

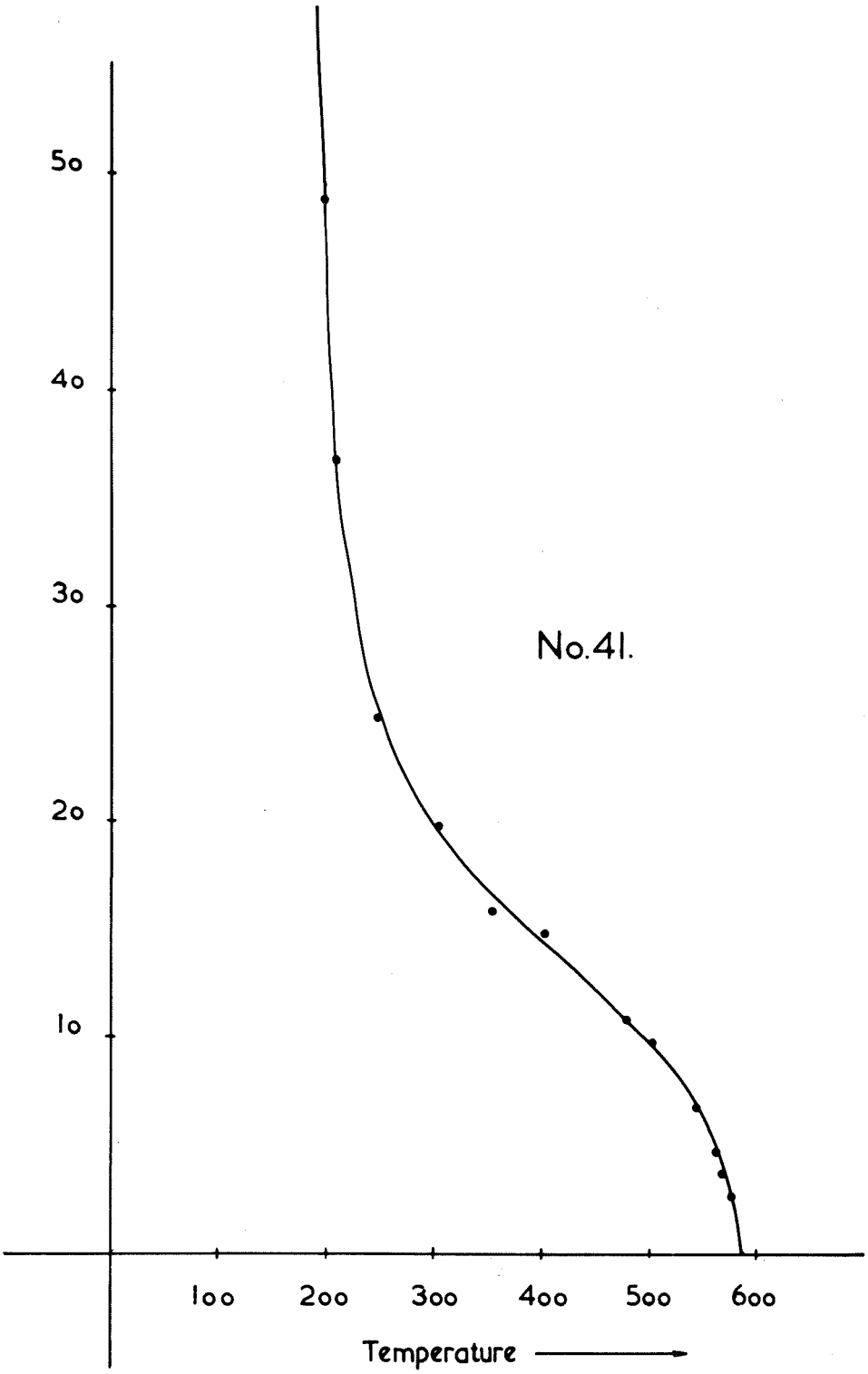

Figure.102.

SPECIMEN

No.41a

Cold temperature junction

= 15°C

E.M.F. (millivolts)	Temperature °C	Deflection
.7	125	44
1.5	225	30
2.0	270	22
3.2	380	10
4.0	460	7
4.5	510	4.5
4.9	550	2
5.1	565	1

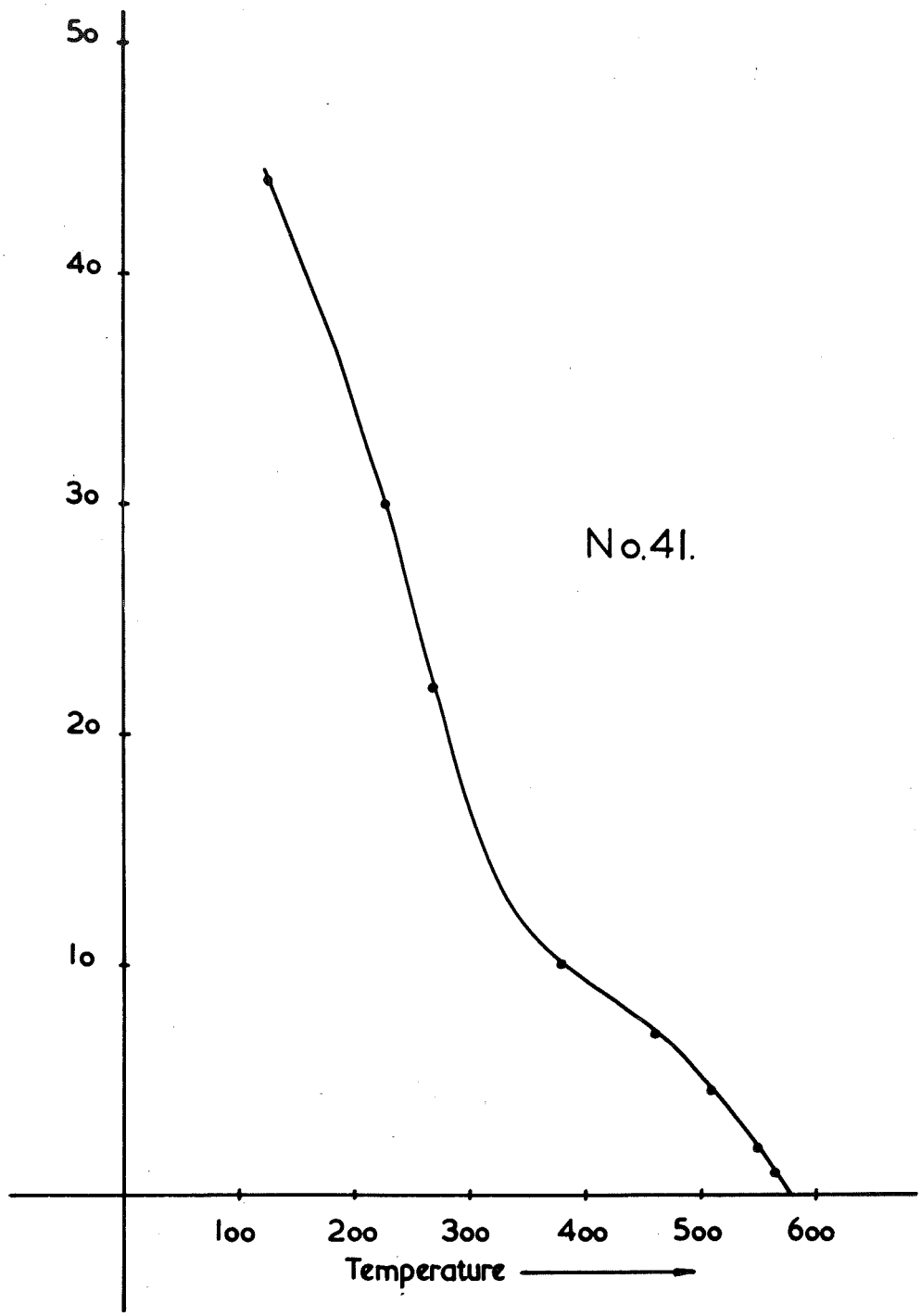

Figure 103.

2. Results obtained by the discontinuous method of thermal demagnetization.

SPECIMEN

Magnetite

Temperature °C	Moment c.g.s. units
15	4.5×10^{-3}
185	2.3×10^{-3}
380	1.4×10^{-3}
505	8.1×10^{-4}
540	6.0×10^{-4}
575	2.9×10^{-4}
635	1.5×10^{-4}

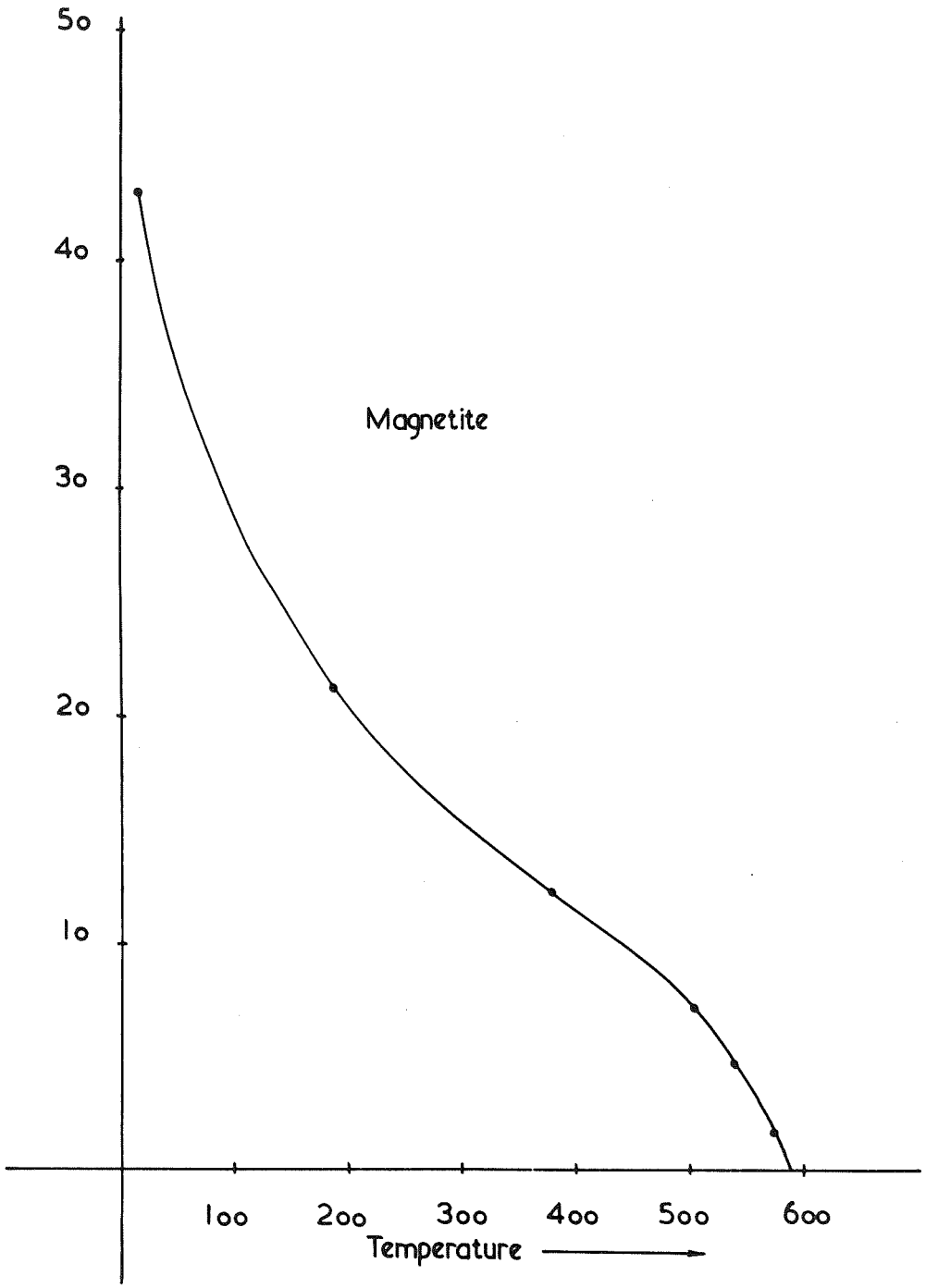

Figure.104.

SPECIMEN

No. 6ac

Temperature °C	Moment c.g.s. units
15	1.5×10^{-2}
110	7.4×10^{-3}
240	2.0×10^{-3}
330	1.2×10^{-3}
455	1.1×10^{-3}

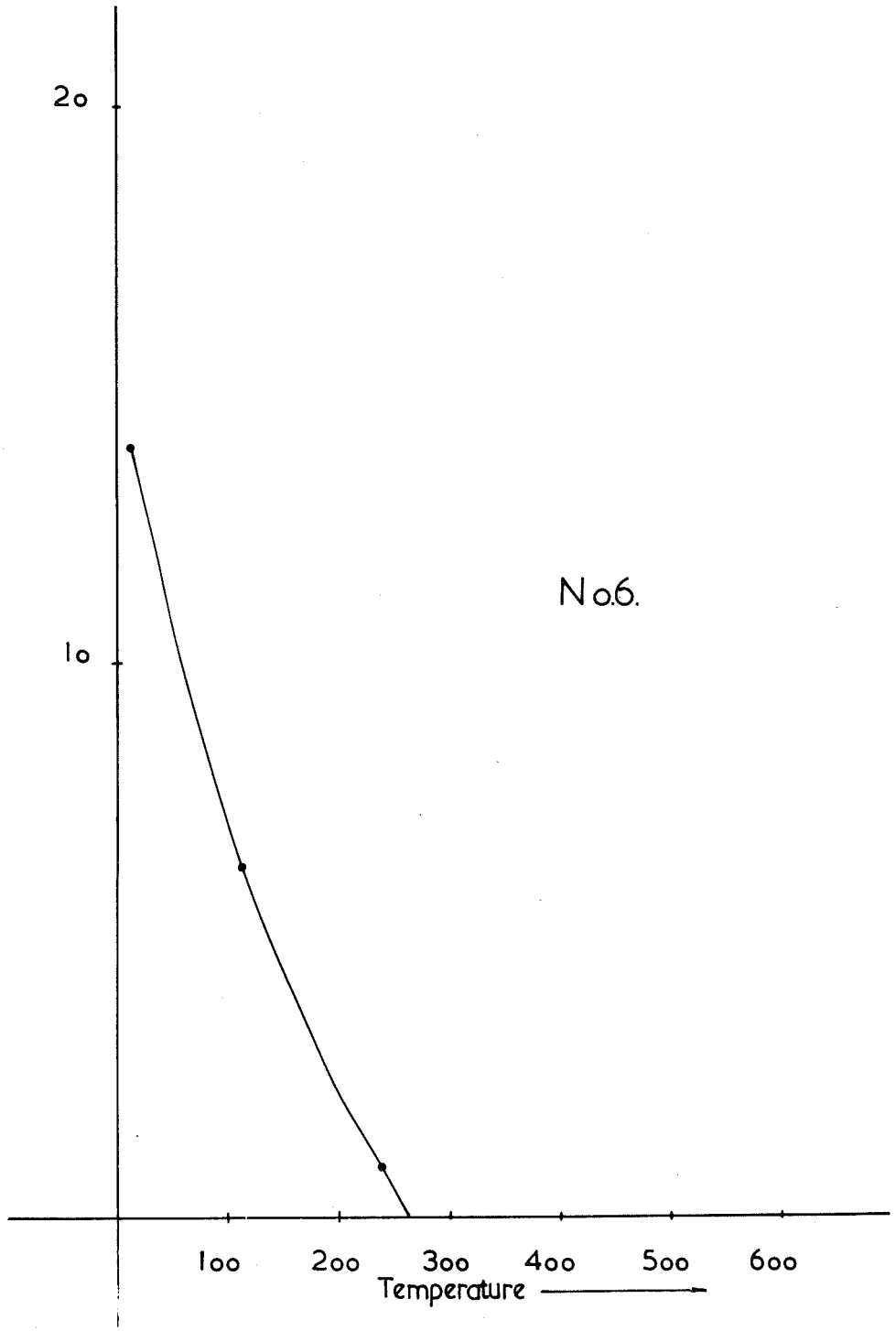

Figure.105.

SPECIMEN

No.33

Temperature ^{o}C	Moment c.g.s. units
15	3.3×10^{-2}
100	7.2×10^{-3}
185	6.3×10^{-3}
330	6.3×10^{-3}

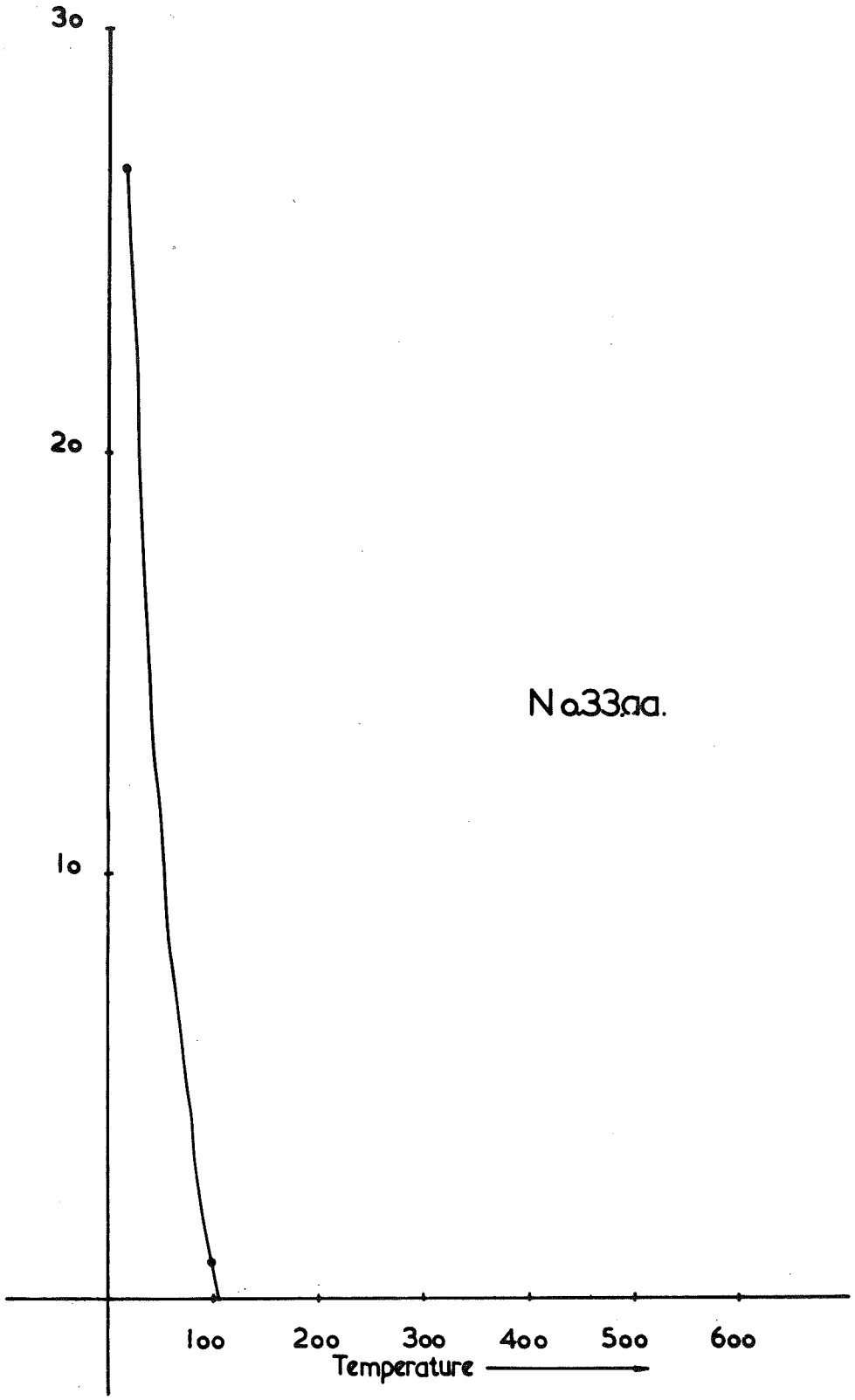

Figure.106.

SPECIMEN

36

Temperature ^{o}C	Moment c.g.s. units
15	2.7×10^{-2}
135	4.4×10^{-3}
290	3.4×10^{-3}
390	3.1×10^{-3}

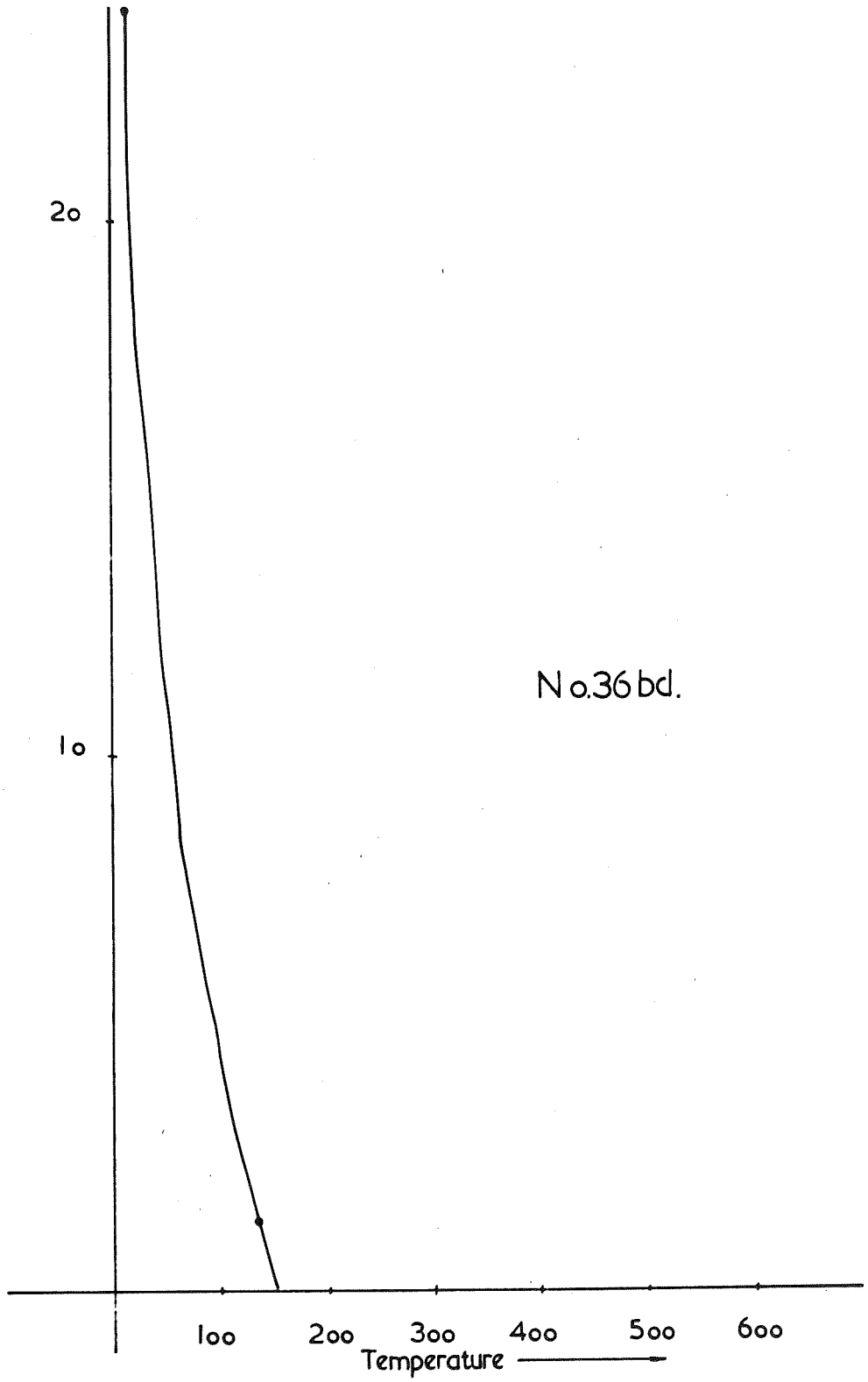

Figure.107.

SPECIMEN

No. 41ae

Temperature °C	Moment c.g.s. units
15°	2.98×10^{-2}
130	2.5×10^{-2}
280	9.5×10^{-3}
420	4.1×10^{-3}
515	4.5×10^{-3}

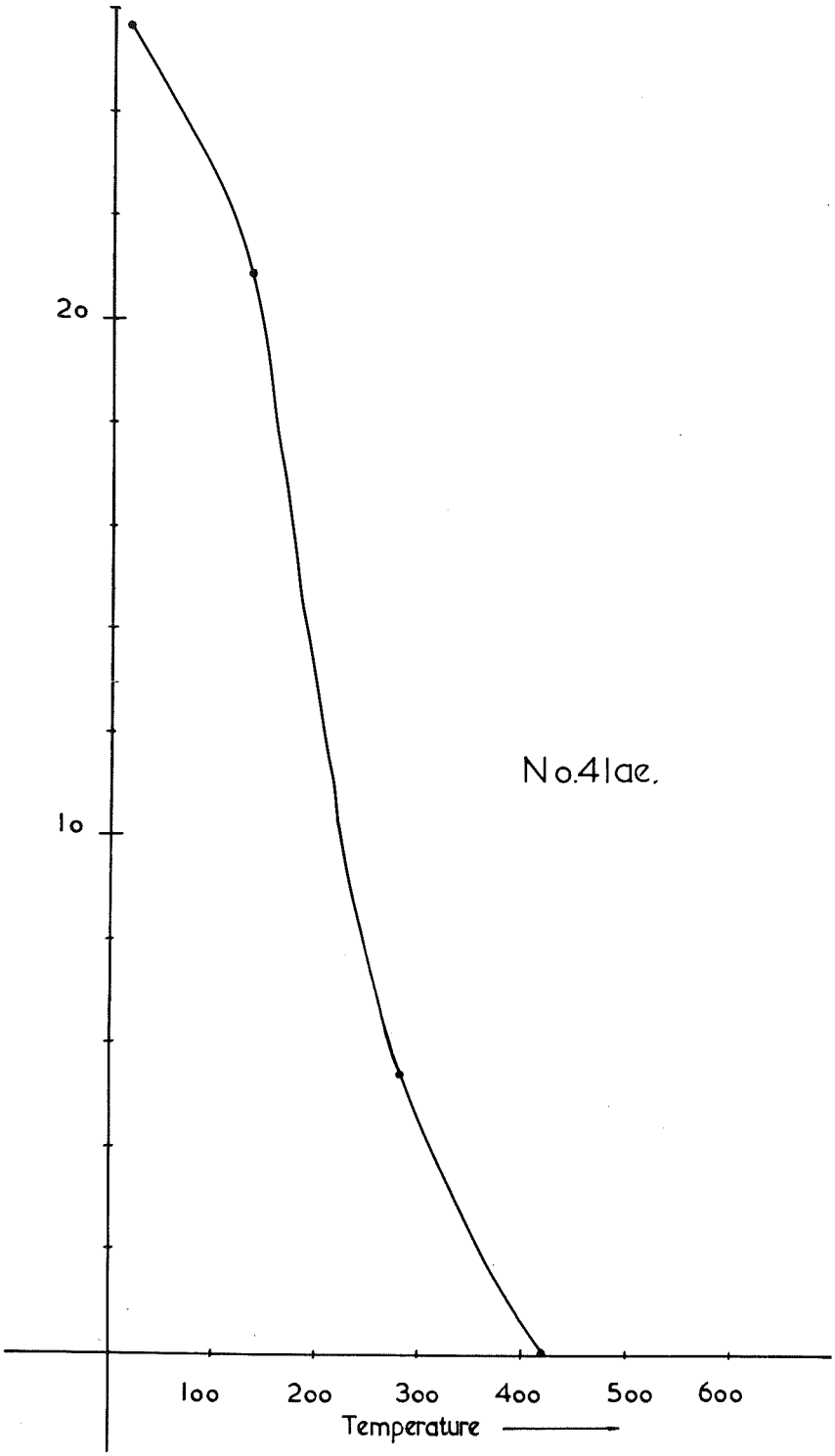

Figure.108.

3. Thermal demagnetization results from specimens taken at Drouin-South. The continuous method of demagnetization is used.

SPECIMEN

No. 2/35

Cold temperature junction
= 30°C

E.M.F. (millivolts)	Temperature °C	Deflection
0	30	
.1	50	39
.2	65	29
.4	95	20
.6	125	15
.85	160	9
1.1	190	5
1.6	215	2
		0

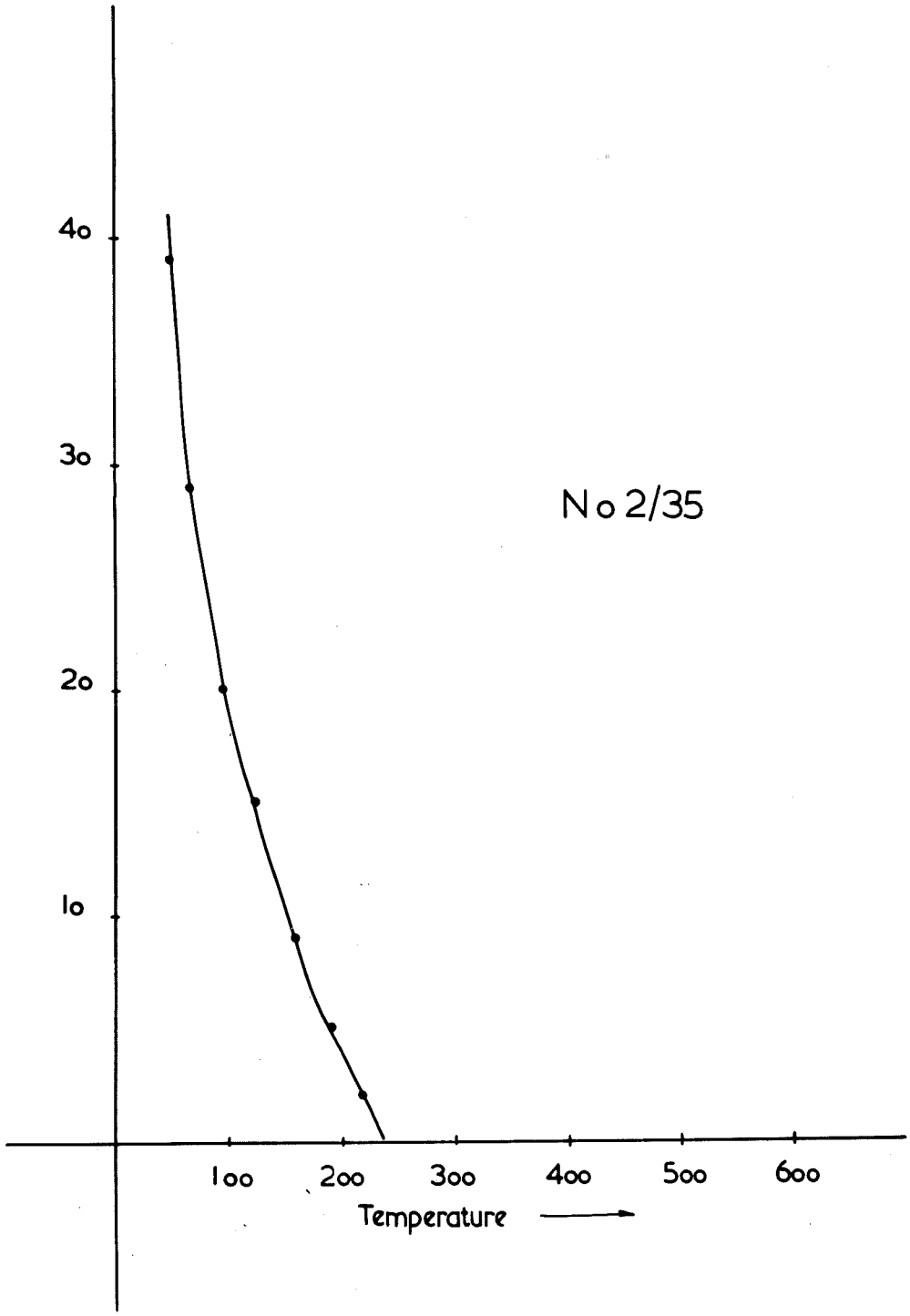

Figure.109.

SPECIMEN

No. 2/37

Cold temperature junction

= 30°C

E.M.F. (millivolts)	Temperature °C	Deflection
0	30	
.2	70	
.5	110	30
.7	140	25
.9	165	21
1.15	195	15
1.5	225	11
1.7	250	7
1.9	270	5
2.1	290	3
2.25	310	0

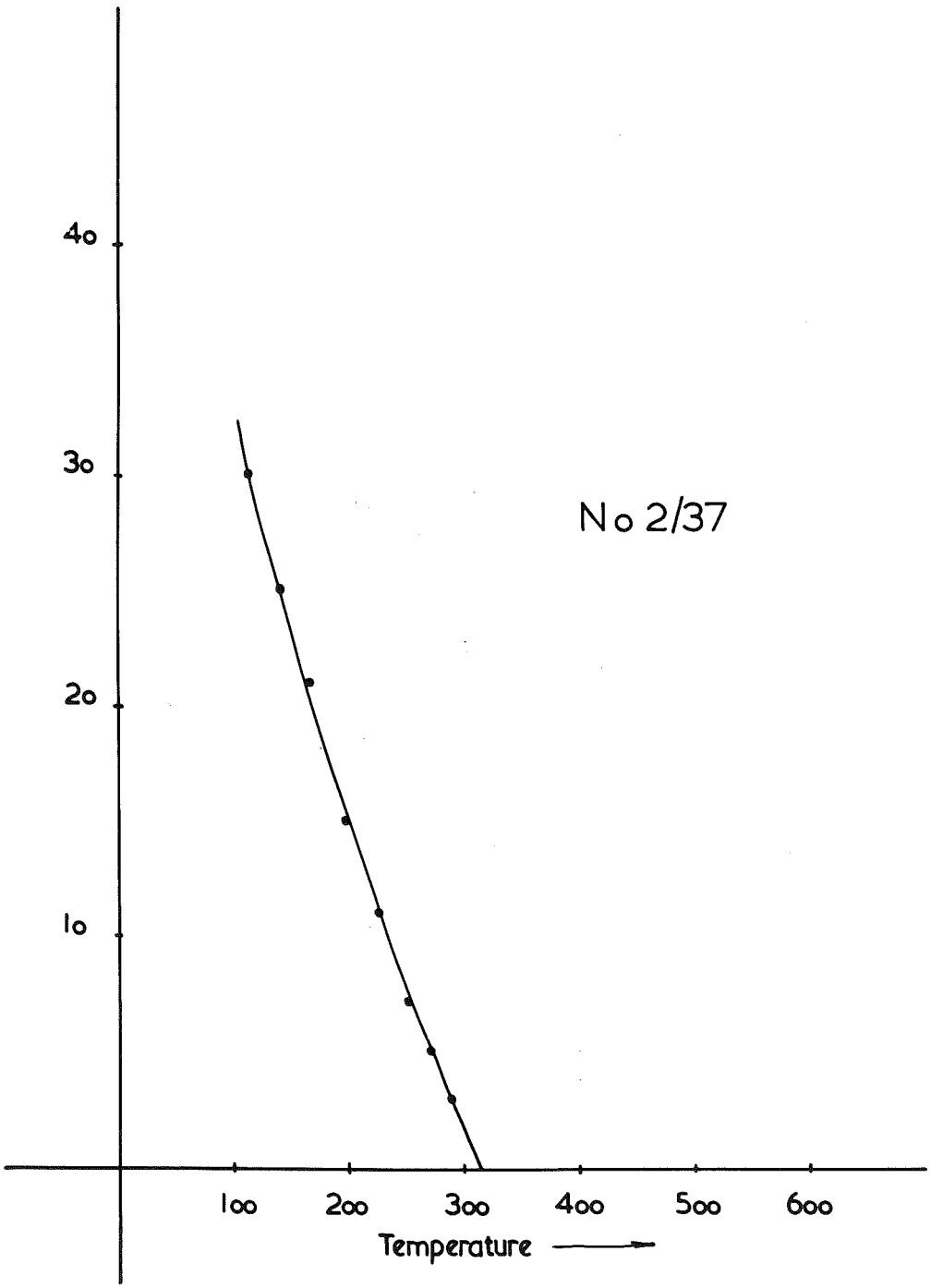

Figure.110.

SPECIMEN

No. 2/40

Cold temperature junction

= 30°C

E.M.F. (millivolts)	Temperature °C	Deflection
0	30	
.2	70	50
.3	80	36
.55	120	24
1.0	175	14
1.3	210	7
1.6	240	3
1.8	260	0

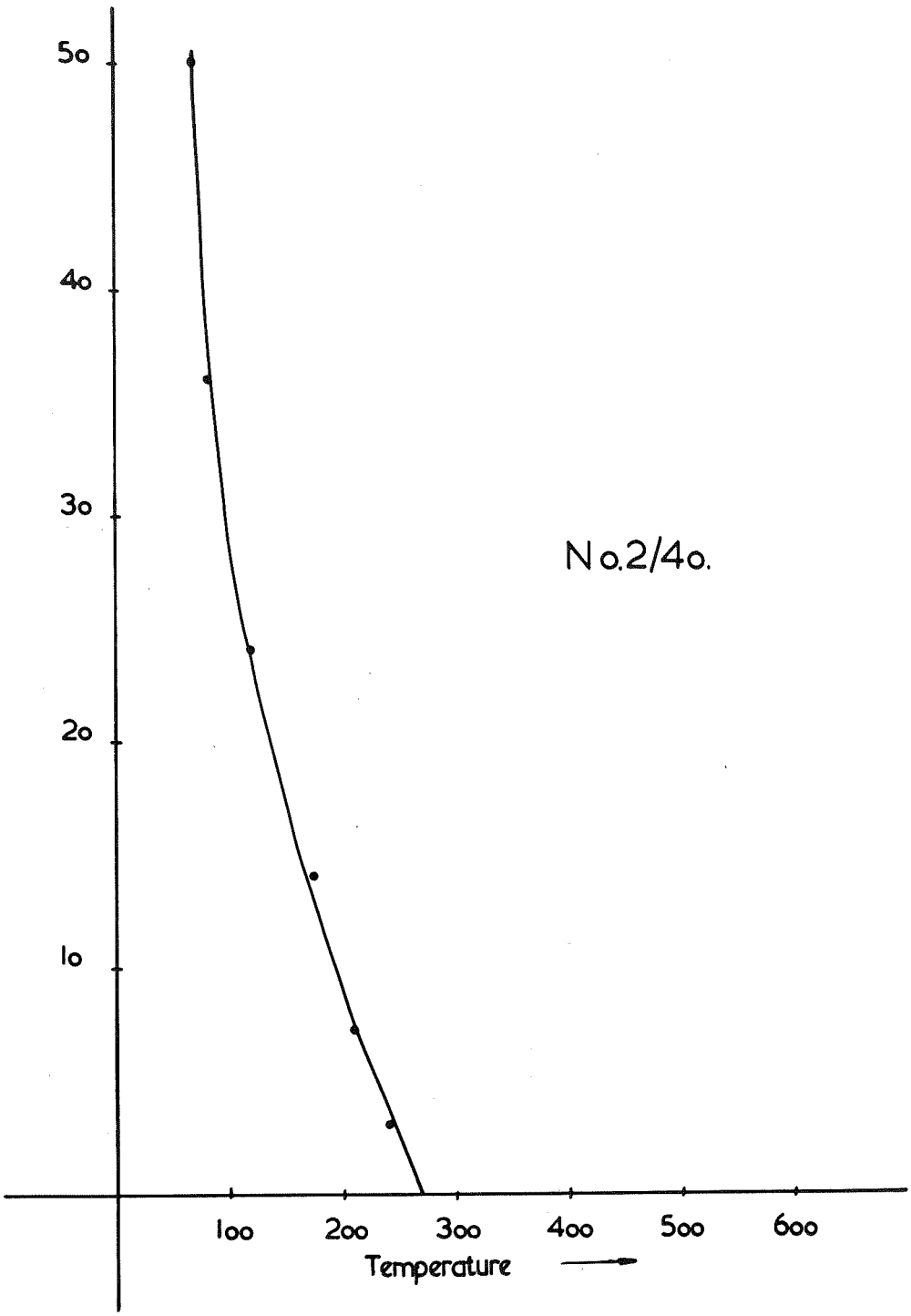

Figure.111.

SPECIMEN

No. 2/41

Cold temperature junction

= 30°C

E.M.F. (millivolts)	Temperature °C	Deflection
0	30	24
.2	70	18
.5	110	15
.8	155	14
1.1	190	12
1.5	225	10
2.0		
2.3	310	5
2.9	370	3
3.1	390	2
3.6	420	0

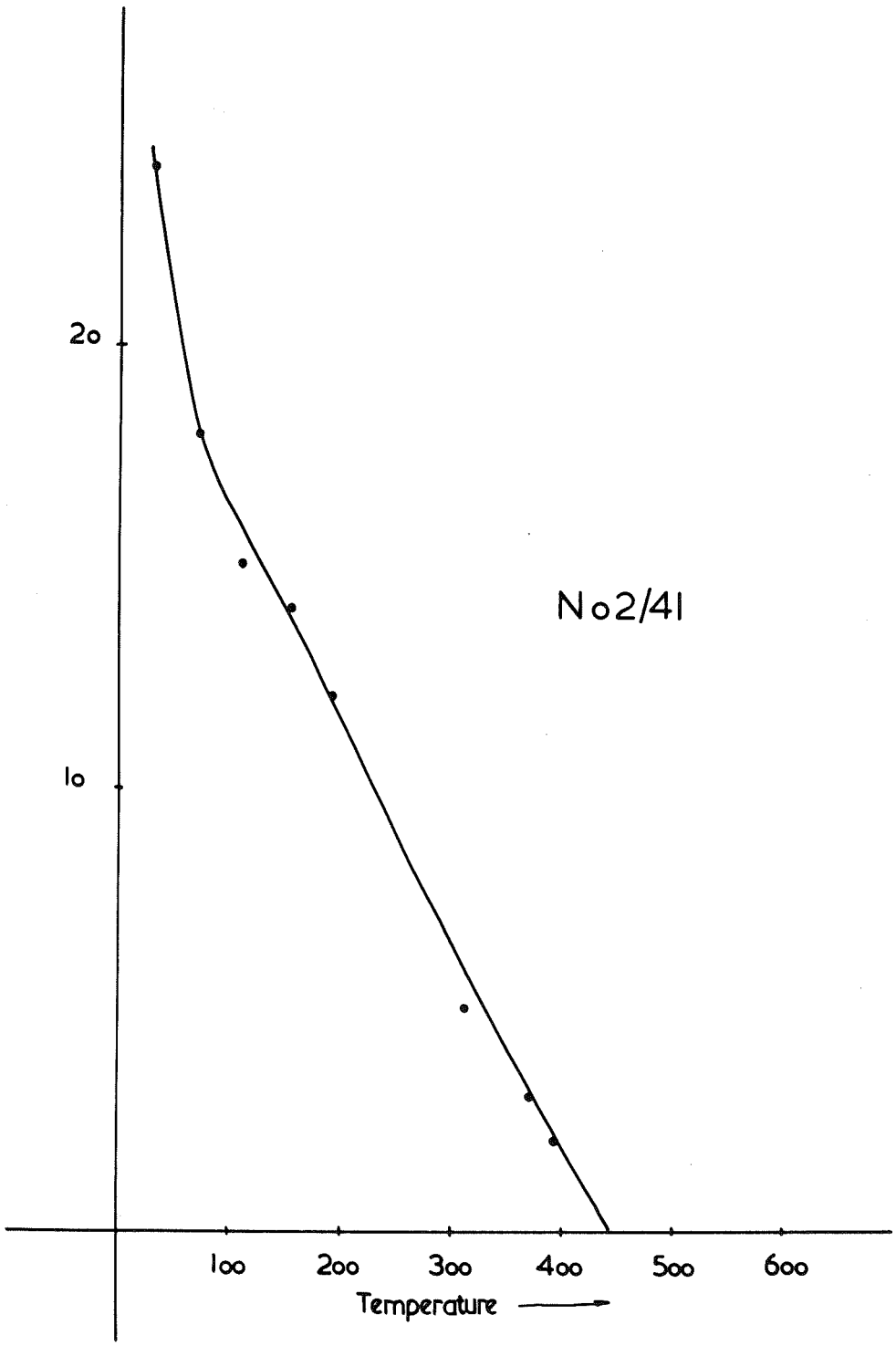

Figure.112.

SPECIMEN

No. 2/44

Cold temperature junction
= 30°C

E.M.F. (millivolts)	Temperature °C	Deflection
0	30	25
.3	80	19
.6	125	14
1.1	190	12
1.4	215	11
1.8	260	10
2.1	290	8½
2.4	320	7
2.8	360	6
3.2	400	5
3.6	435	3½
4.0	475	2
4.1	485	1

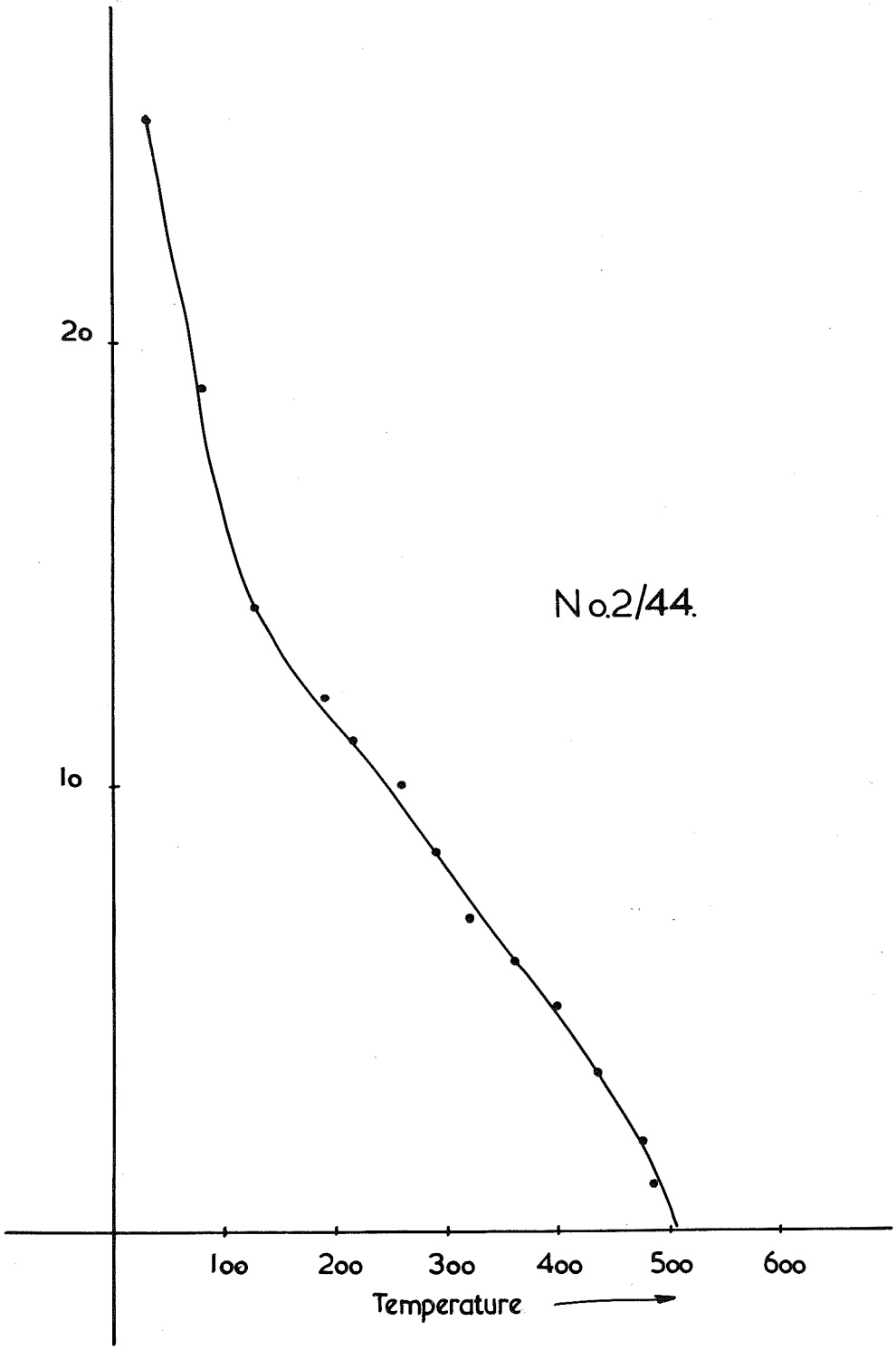

Figure.113.

SPECIMEN

No. 2/45

Cold temperature junction

= 30°C

E.M.F. (millivolts)	Temperature °C	Deflection
0	30	
.6	125	
.8	150	25
1.0	175	23
1.3	210	21
1.8	260	20
2.4	320	16
2.9	365	13
3.45	425	9
3.75	450	7
4.10	485	3

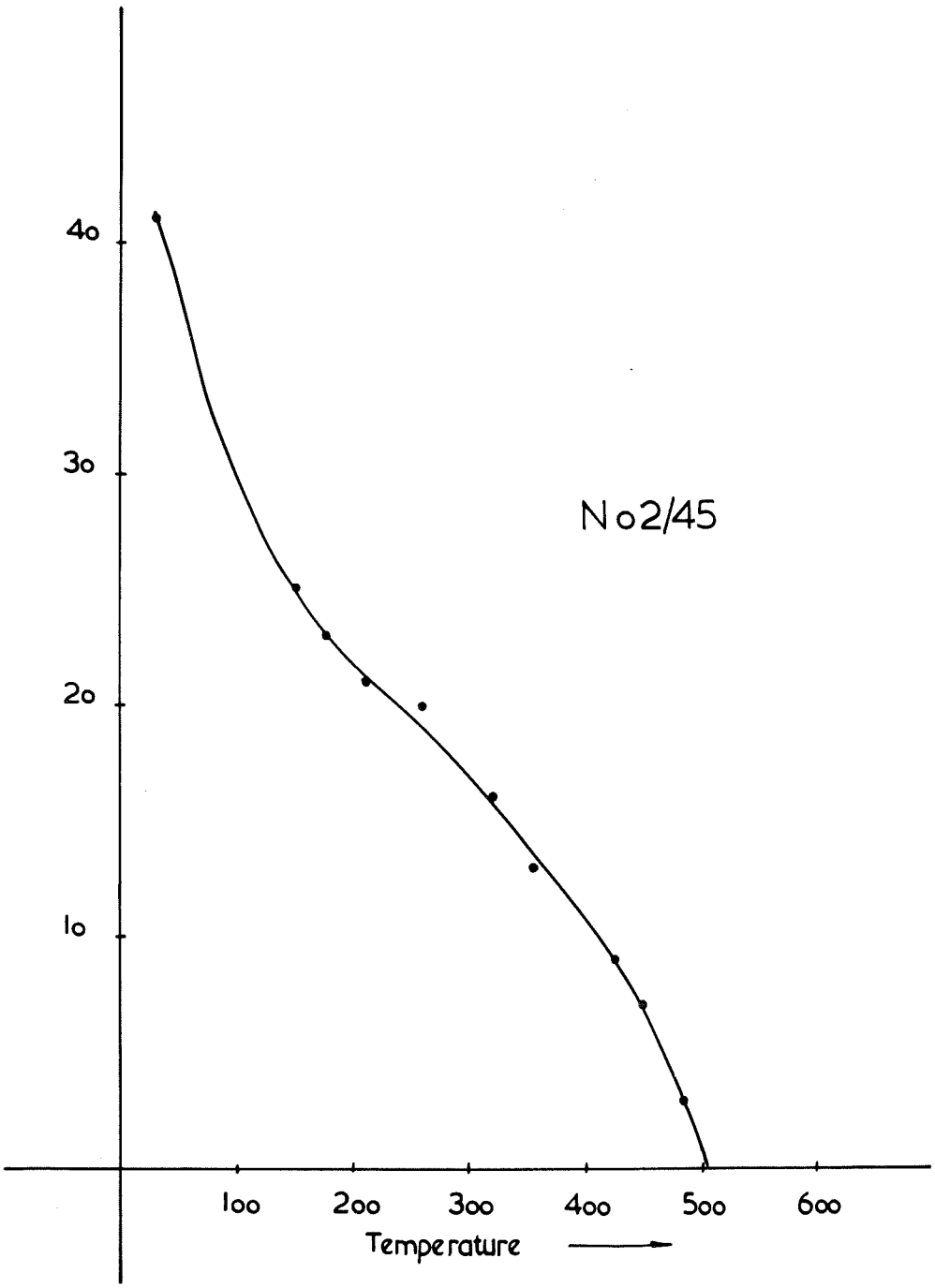

Figure 114.

SPECIMEN

No. 2/52

Cold temperature junction

= 30°C

E.M.F. (millivolts)	Temperature °C	Deflection
0		
.25	75	50
.4	95	47
.7	140	27
1.0	175	19
1.4	215	10
1.7	250	5
1.9	270	2

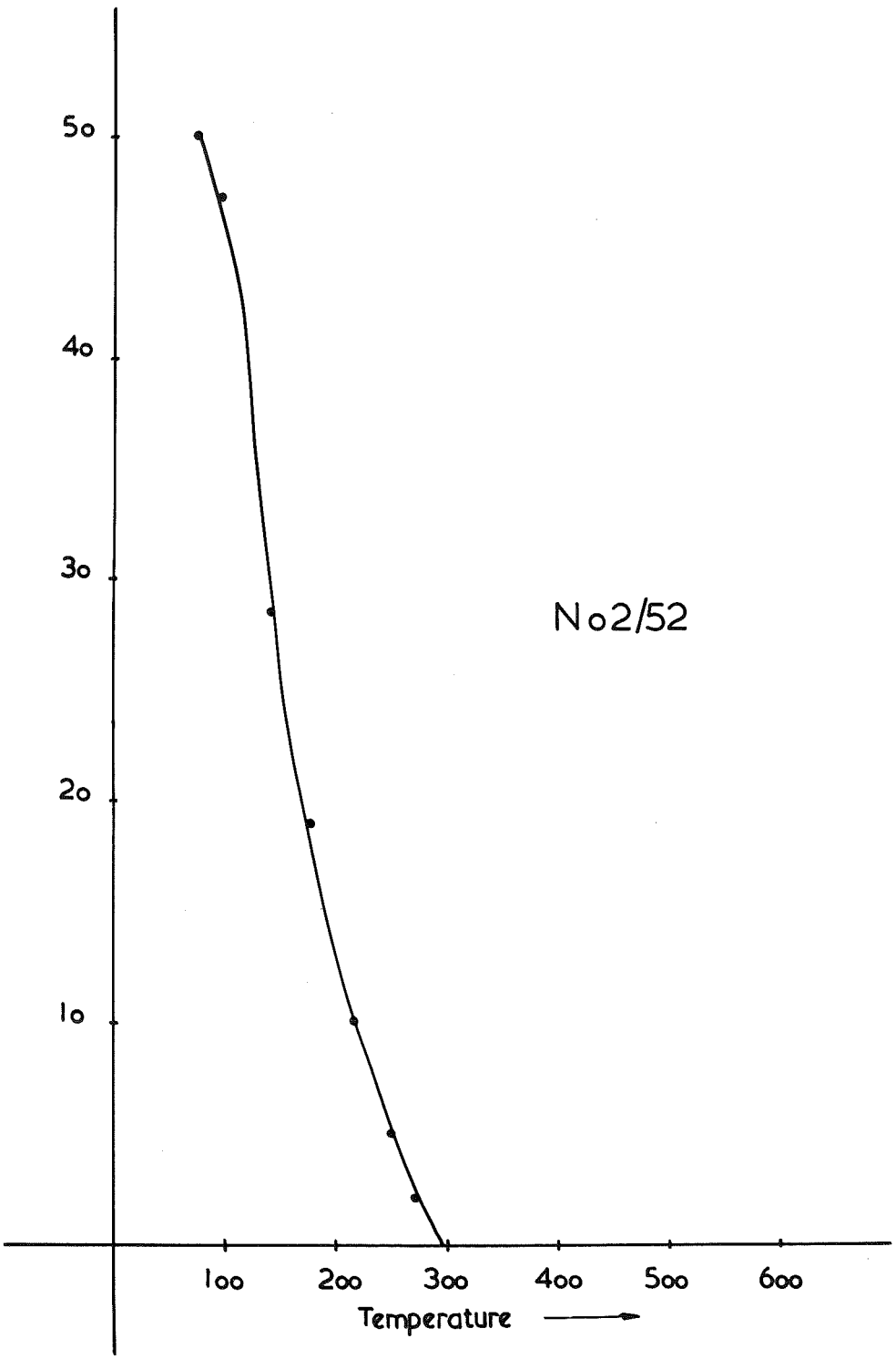

Figure.115.

SPECIMEN

No. 2/54

Cold temperature junction

= 30°C

E.M.F. (millivolts)	Temperature °C	Deflection
0		
.2	70	33
.5	110	22
.7	140	15
.9	165	12
1.1	190	9
1.45	225	4
1.6	240	2
1.8	260	0

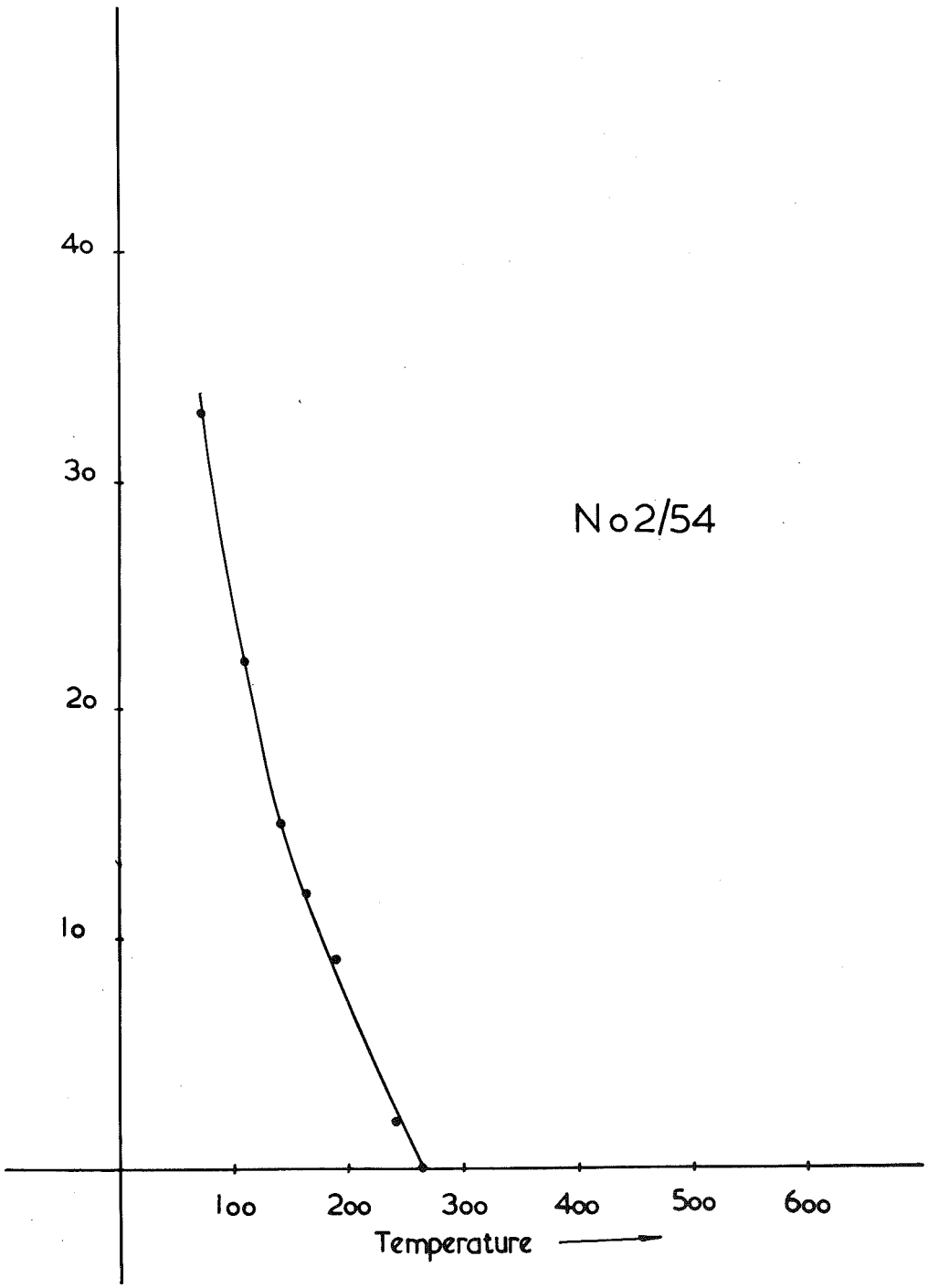

Figure.116.

SPECIMEN

No. 2/55

Cold temperature junction

= 30°C

E.M.F. (millivolts)	Temperature °C	Deflection
0	30	28
.2	70	20
.35	90	12
.45	100	8
.7	140	4
.95	170	3
1.2	200	1

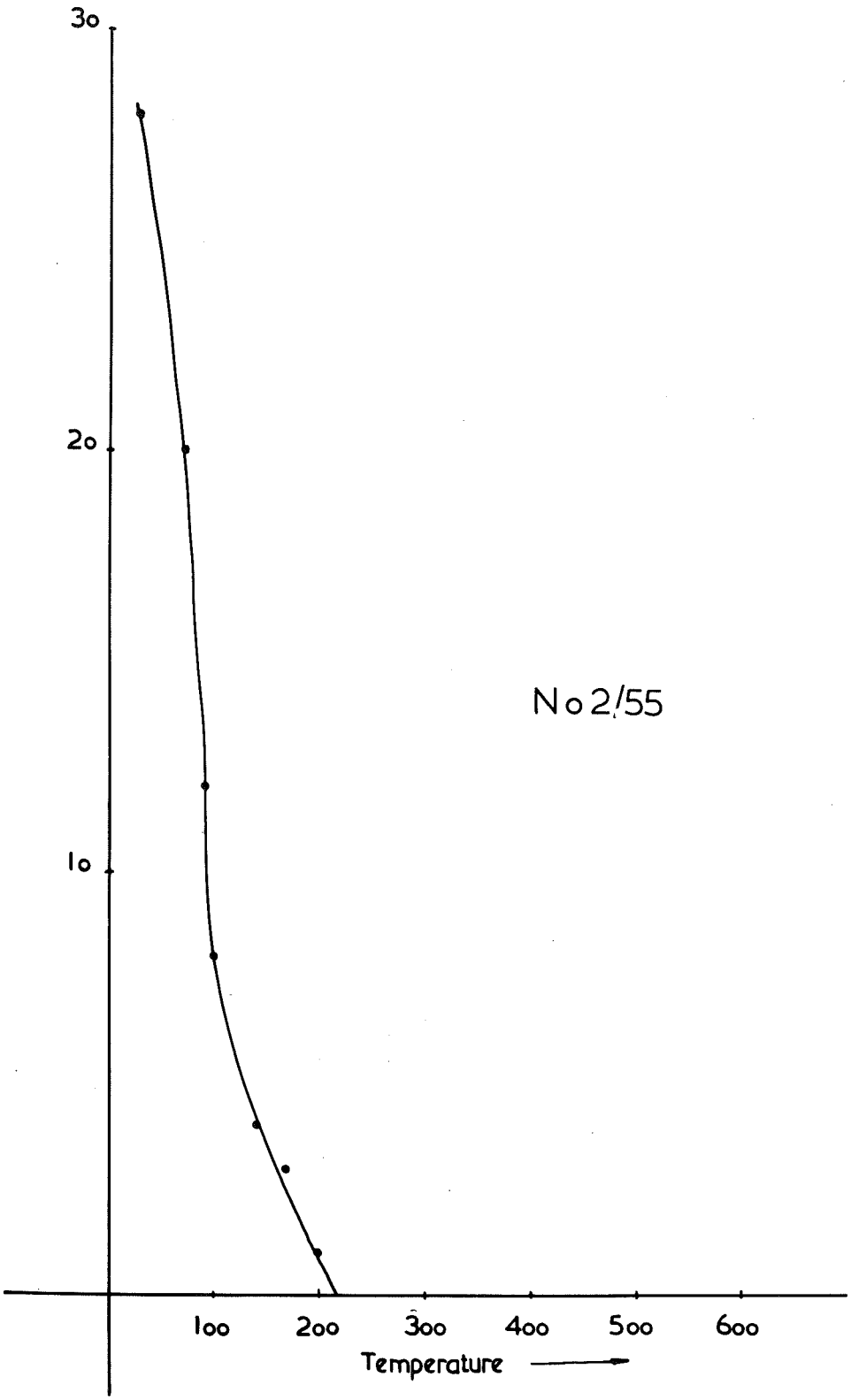

Figure.117

SPECIMEN

No. 2/56

Cold temperature junction

= 30°C

E.M.F. (millivolts)	Temperature °C	Deflection
0	30	48
.35	75	43
.5	125	30
.75	145	21
.9	165	17
1.6	235	6
2.0	280	3
2.5	330	0

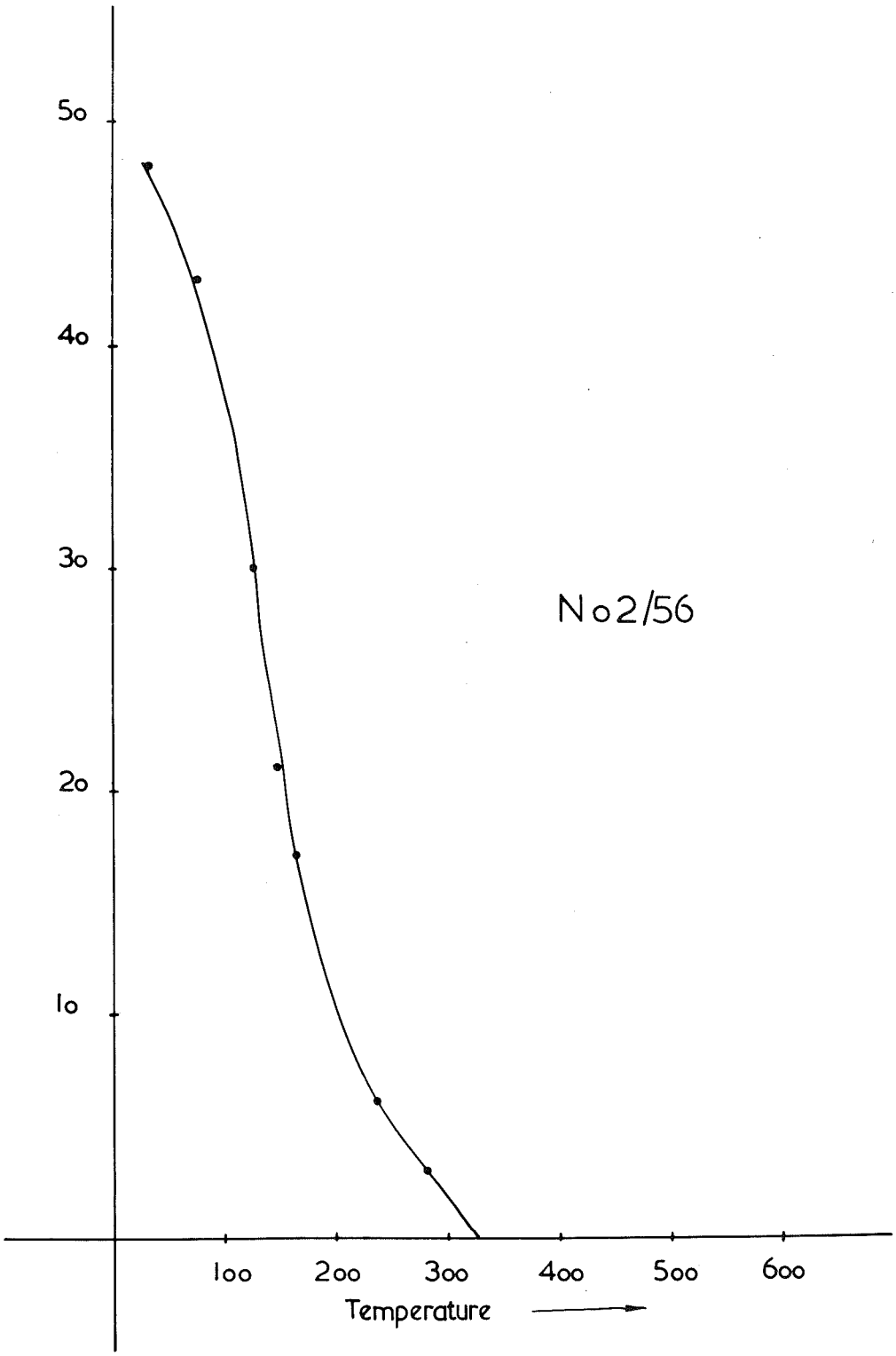

Figure.118.

SPECIMEN

2/58

Cold Temperature junction

= 30°C

E.M.F. (millivolts)	Temperature °C	Deflection
	55	60
	75	45
1.3	210	20
1.6	240	19
2.8	360	14
3.4	420	10
4.25	500	7
4.6	535	5
4.85	555	3

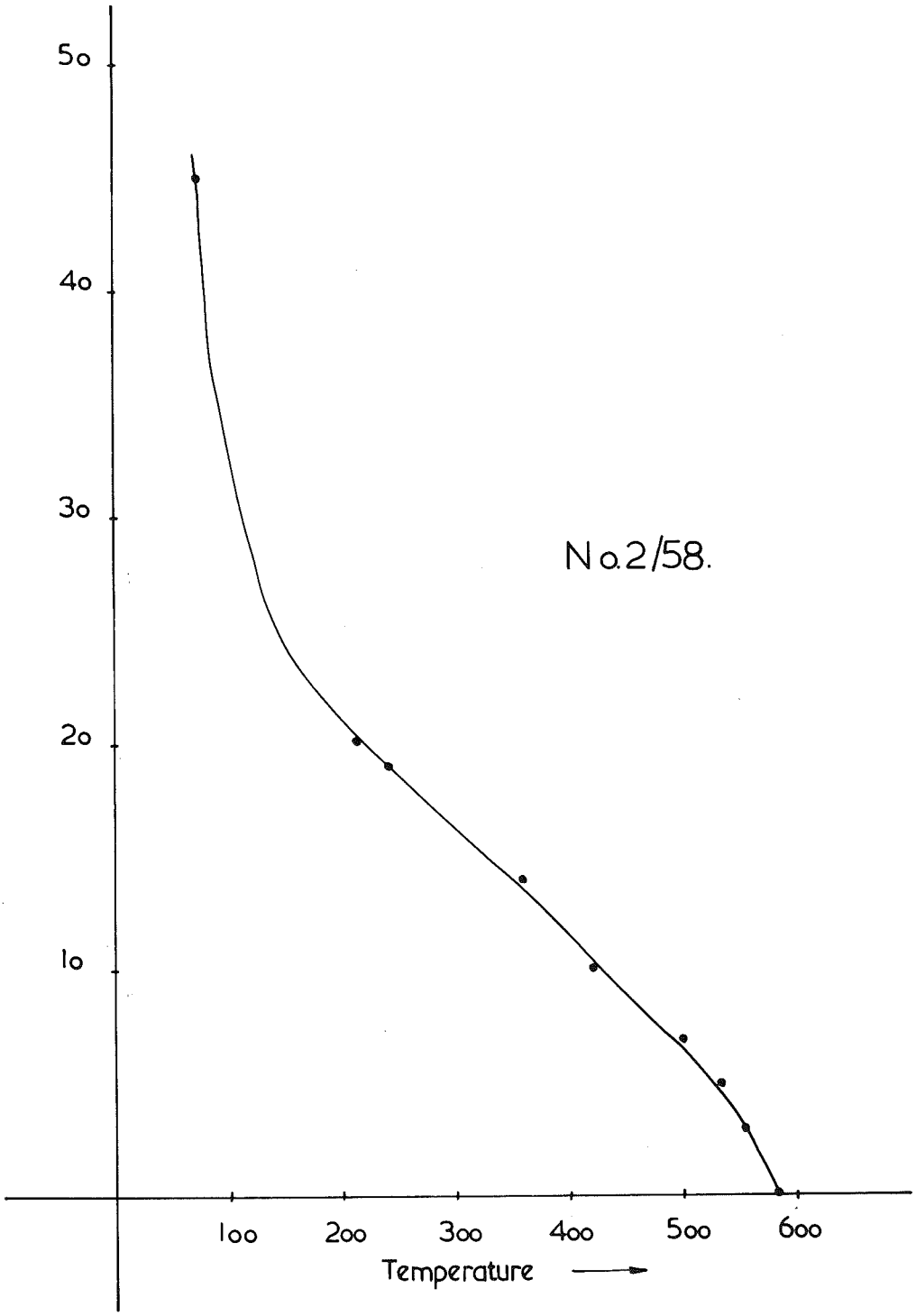

Figure .119

SPECIMEN

No.2/59

Cold temperature junction

= 30°C

E.M.F. (millivolts)	Temperature °C	Deflection
0		
.1	50	38
.2	70	31
.4	95	18
.5	110	16
.7	140	
1.2	200	10
1.5	225	9
2.05	285	8
2.20	300	7
2.60	340	6
3.1	380	4
3.3	410	2
3.6	435	0

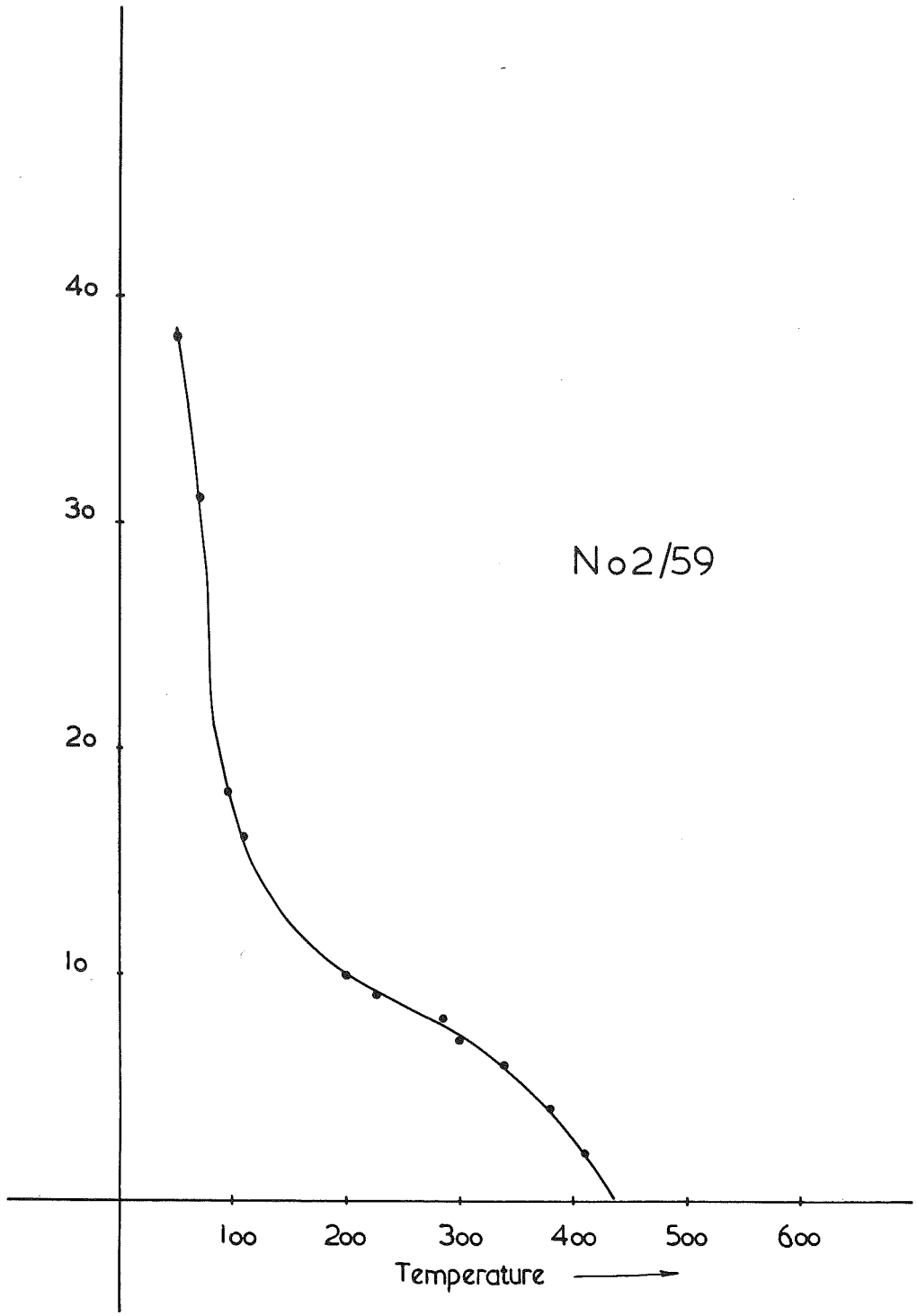

Figure. 120.

4. Thermal demagnetization curves for specimens from Merri Creek quarry. Continuous method of thermal demagnetization is used.

SPECIMEN

No. 2/21

Cold temperature junction
= 25°C

E.M.F. (millivolts)	Temperature °C	Deflection
0	25	46
.25	70	40
.45	100	35
.75	140	28
1.4	215	13
1.7	245	8
2.0	275	4
2.25	300	2

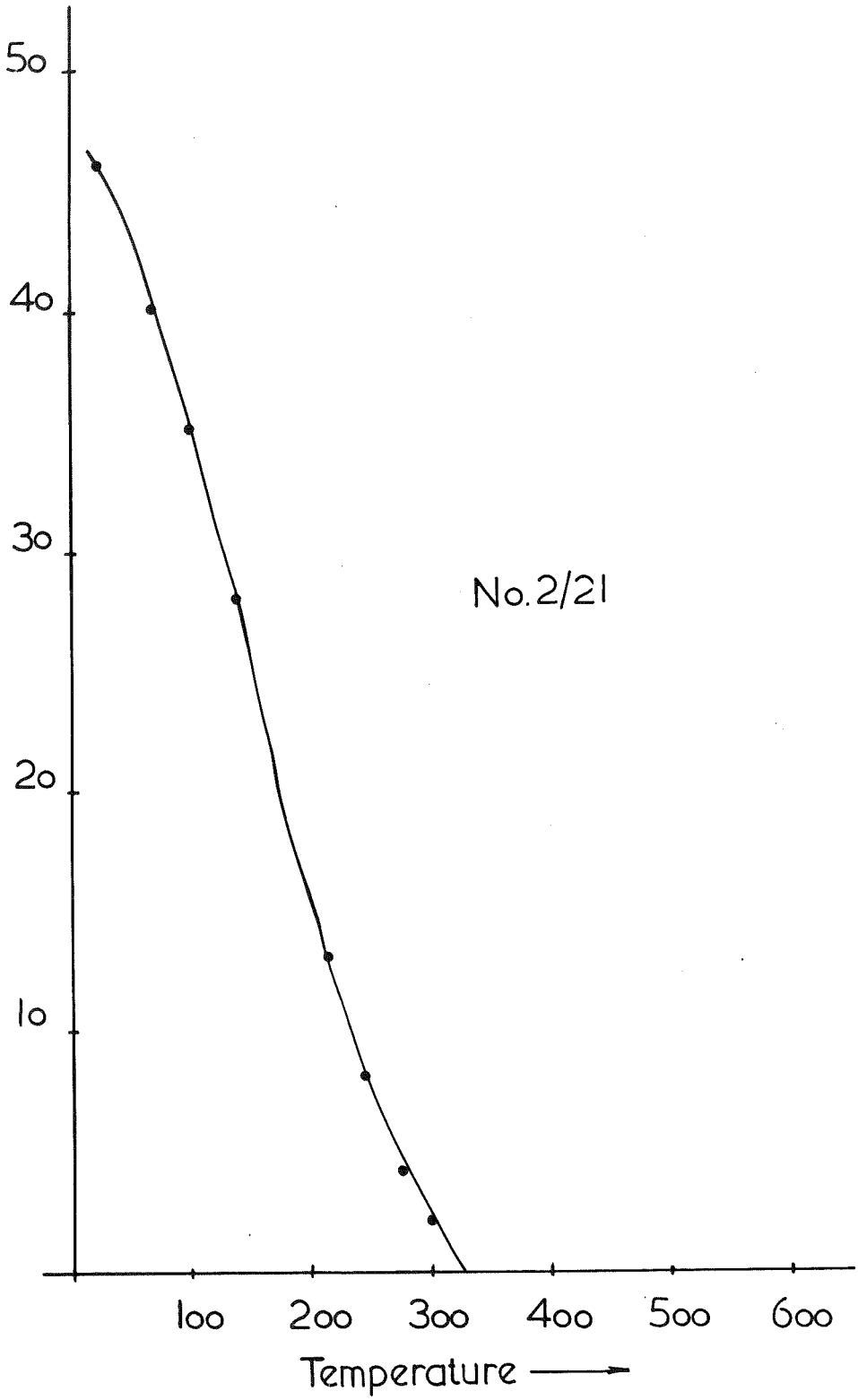

Figure. 121.

SPECIMEN

No. 2/29

Cold temperature junction

= 25°C

E.M.F. (millivolts)	Temperature °C	Deflection
.05	30	
.25	70	29
.5	100	27
.75	140	25
1.0	175	20
1.4	210	14
1.7	245	10
2.0	275	7
2.3	305	4
2.5	325	2

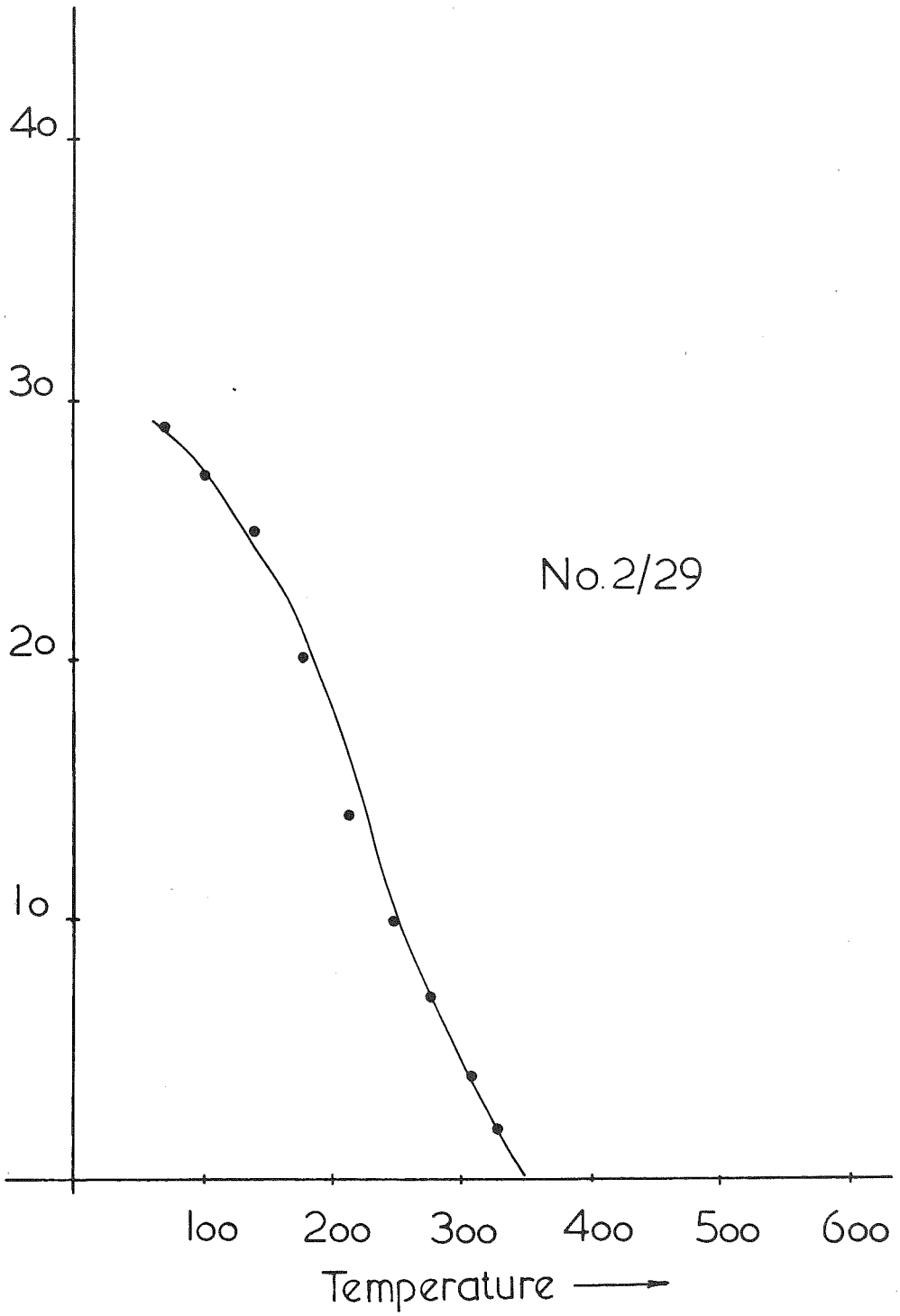

Figure. 122.

SPECIMEN

No. 2/34

Cold temperature junction

= 25°C

E.M.F. (millivolts)	Temperatur e °C	Deflection
0	25	0
.35	80	35
.6	115	33
.9	160	30
1.15	190	26
1.4	215	21
1.7	245	15
2.05	280	8
2.30	305	6
2.55	330	4
2.90	365	2

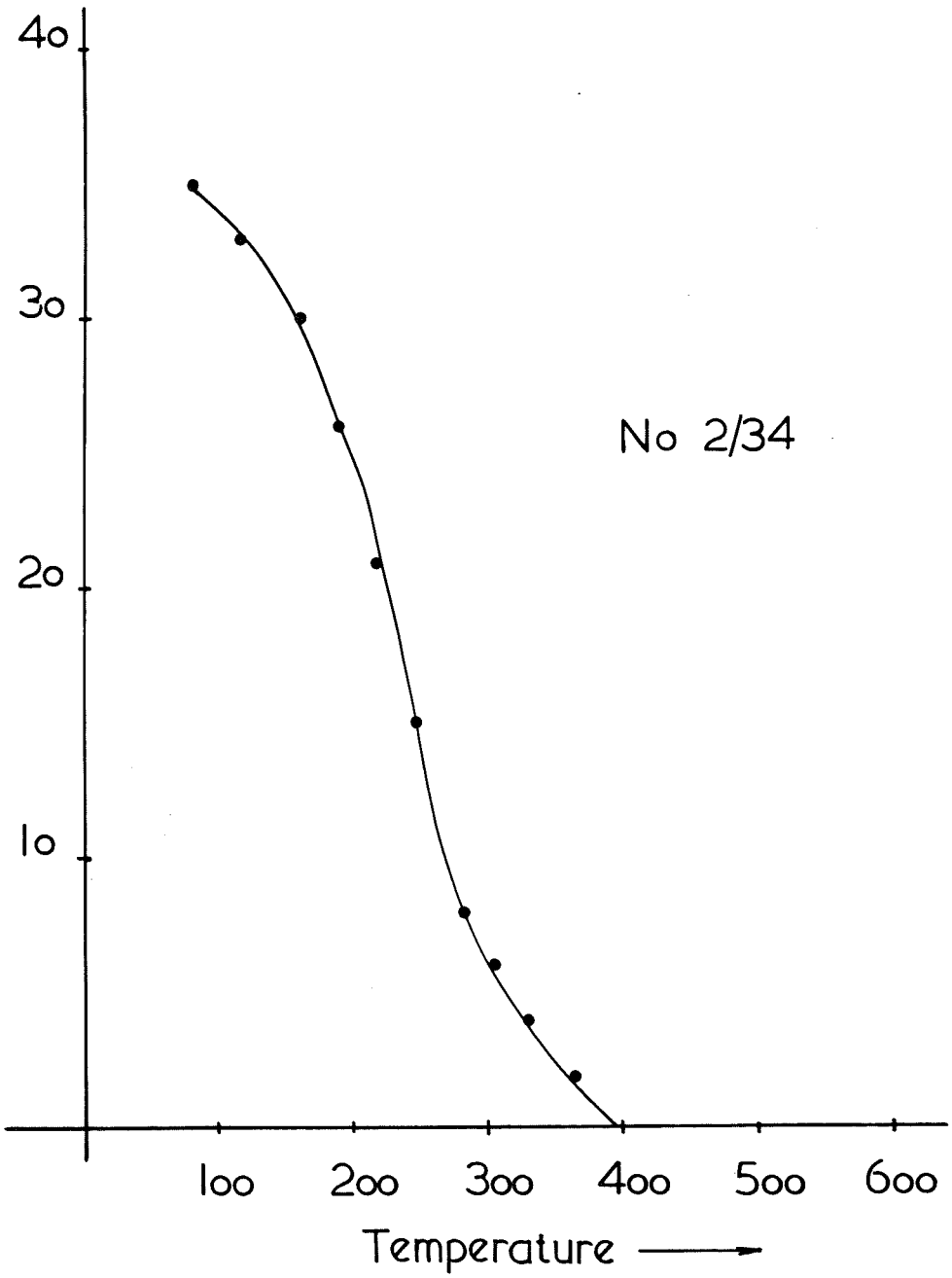

Figure .123.

5. The results of other thermal demagnetization experiments using the continuous method of thermal demagnetization.

SPECIMEN

No. 33c

E.M.F. (Millivolts)	Temperature °C	Deflection
.1	35	38
.3	70	20
.7	125	7
1.3	200	3
1.95	275	1

Remarks

Specimen heated in a vertical field of 1.12 oersted.

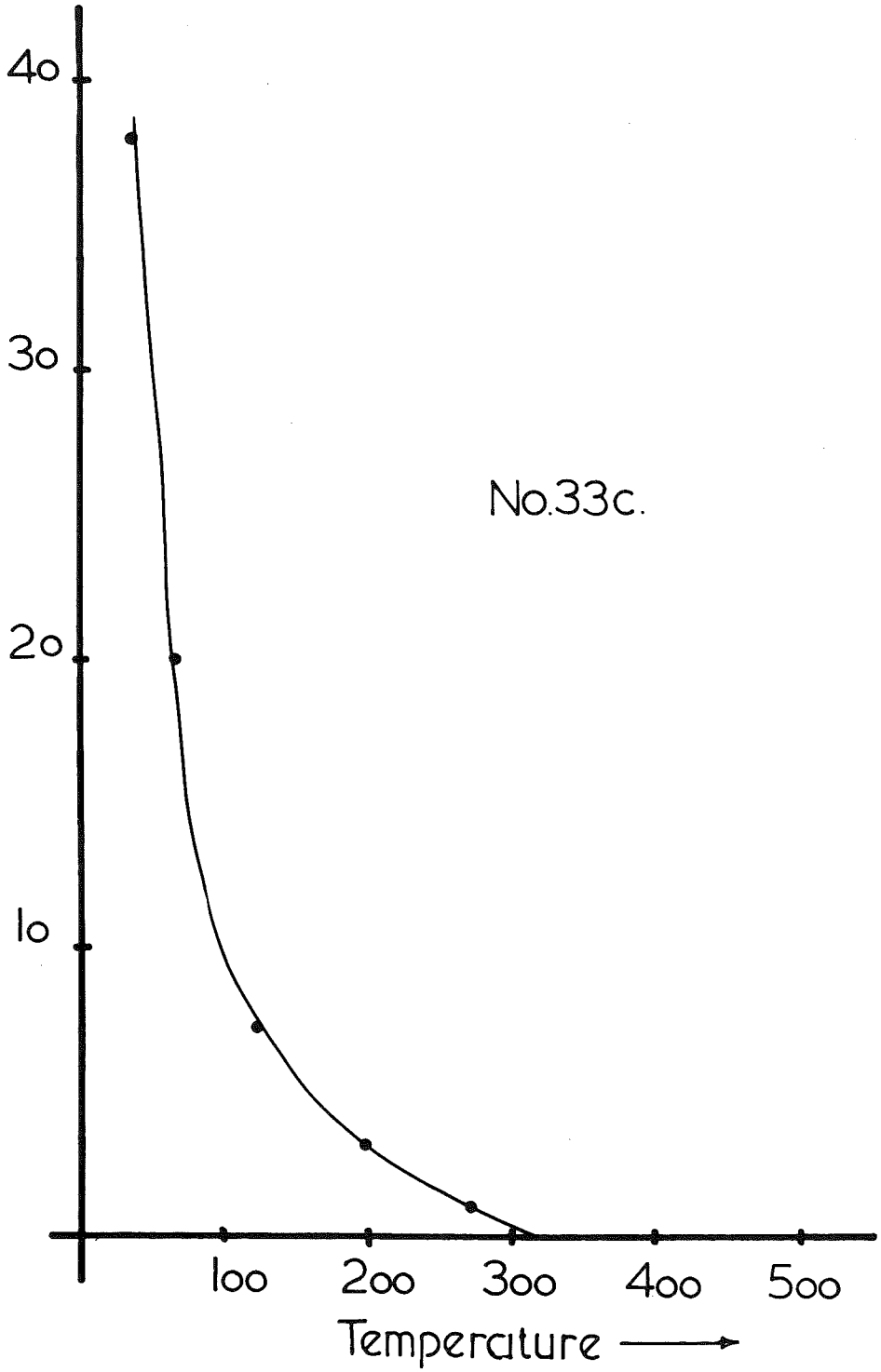

Figure .124.

SPECIMEN

No. 21a

Cold temperature junction

= 20°C

E.M.F. (millivolts)	Temperature °C	Deflection
0	20	44
.5	95	32
1.0	165	20
1.6	225	12
2.3	300	6½
2.8	350	4
3.3	400	1

Remarks

Specimen heated in a vertical field of 1.12 oersted.

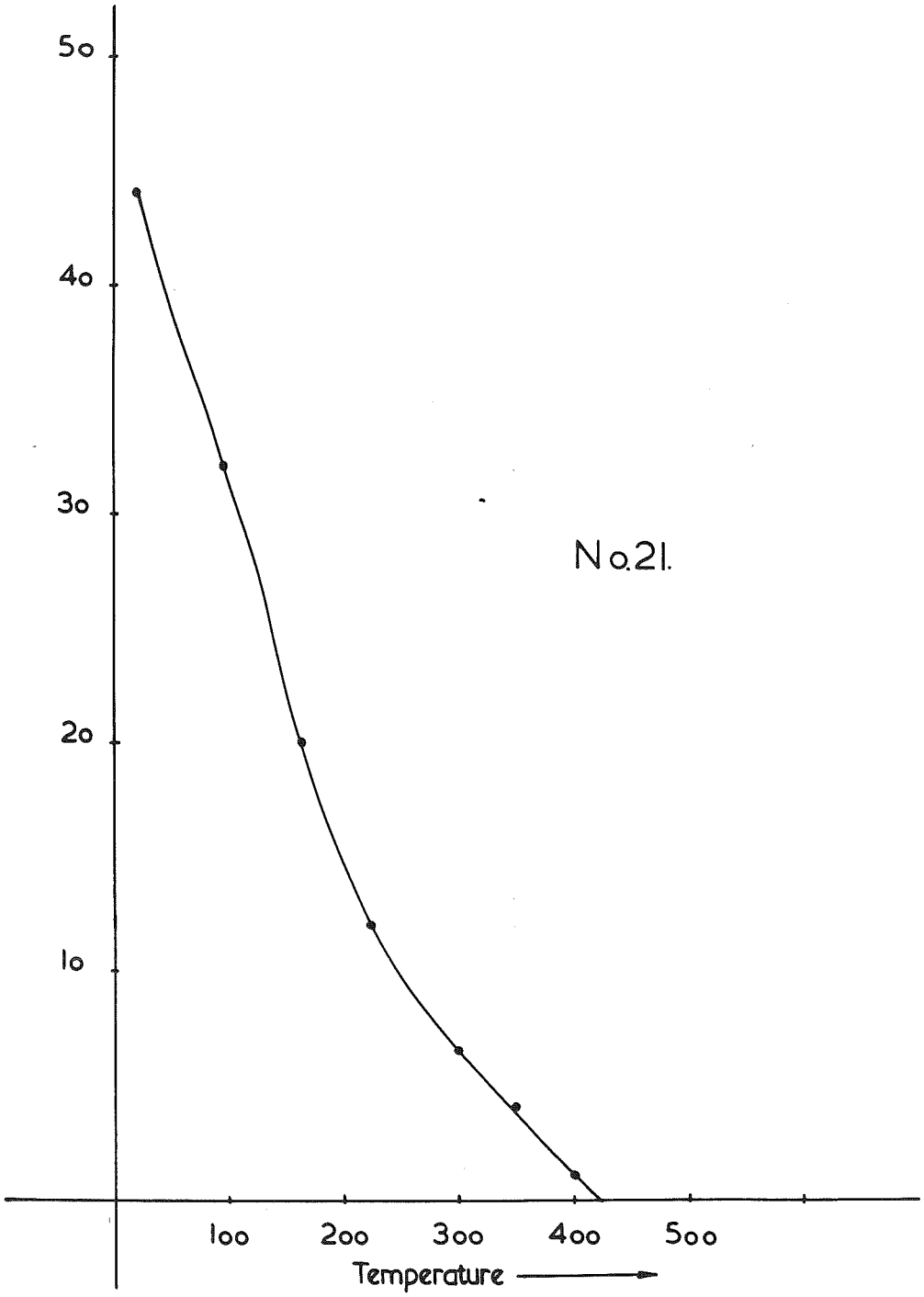

Figure .125.

SPECIMEN

No. 25

Cold temperature junction

= 20°C

E.M.F. (millivolts)	Temperature °C	Deflection
.55	100	41
1.0	165	22
1.6	225	9
2.6	330	3
3.0	380	1

Remarks

Specimen heated in a vertical field of 1.12 oersted.

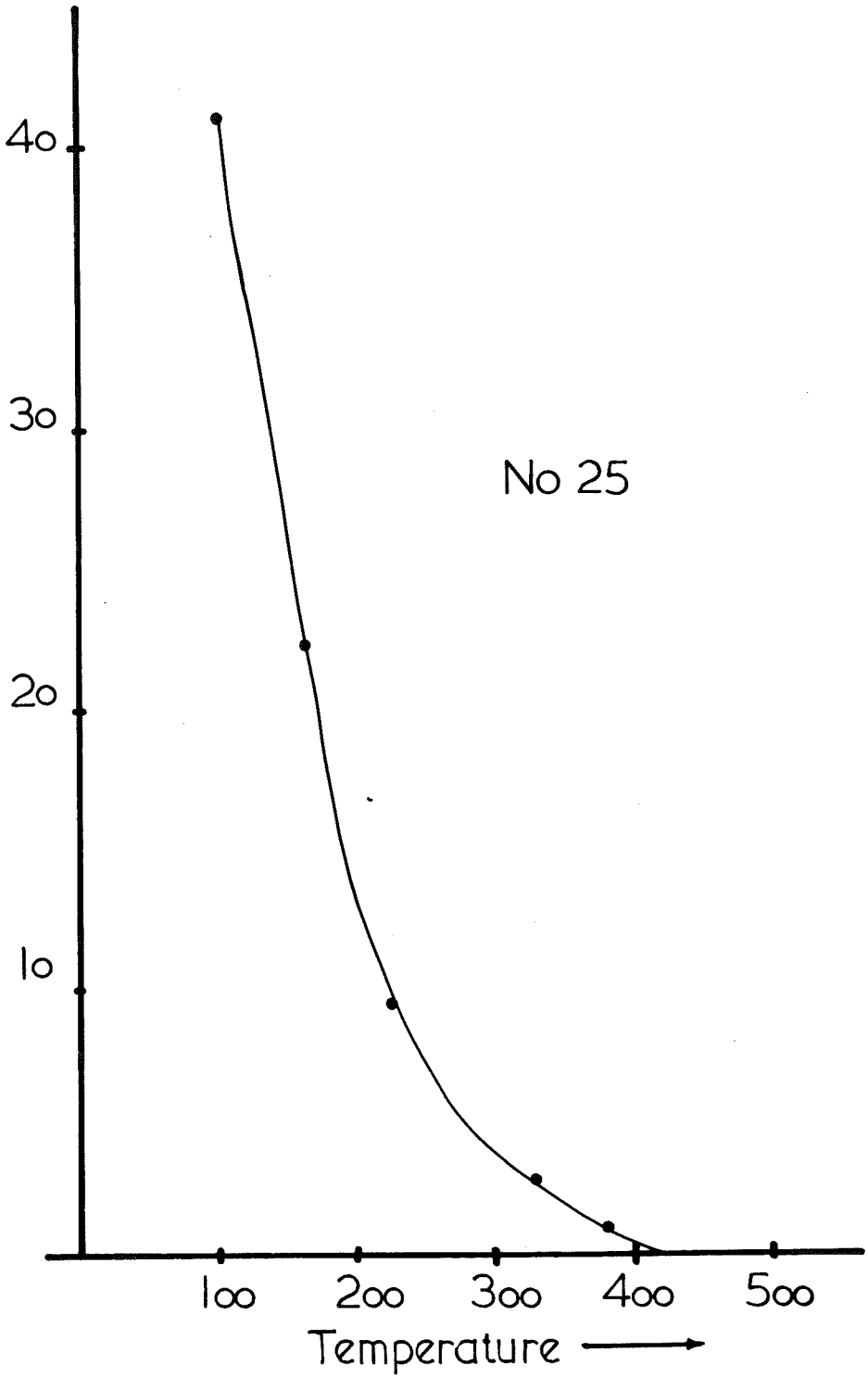

Figure .126.

SPECIMEN

No.6

Cold temperature junction

= 20°C

E.M.F. (millivolts)	Temperature °C	Deflection
1.4	205	46.5
1.6	230	29.5
1.8	255	23.5
2.01	272	17.0
2.15	285	15
2.52	320	10
3.10	380	4
3.30	400	3.5
3.44	415	3.0
3.50	420	3.0
3.70	440	2.5

Remarks

Specimen magnetized in 3,000 oersted.

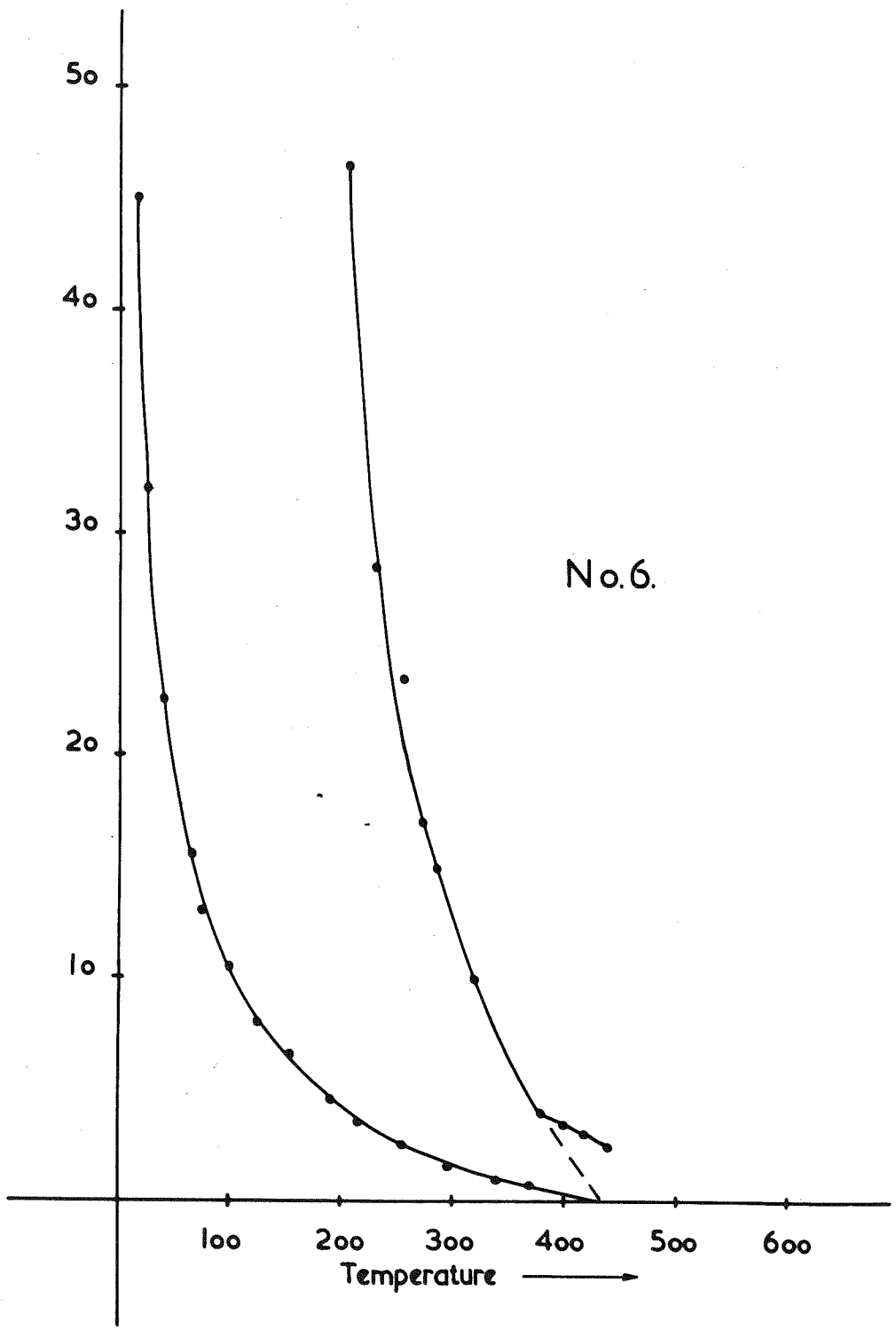

Figure 127.

SPECIMEN

No. 26

Cold temperature junction

= 20°C

E.M.F. (millivolts)	Temperature °C	Deflection
1.33	200	42
1.60	230	30
1.93	265	20.5
2.20	290	14.5
2.30	300	13.0
2.80	340	7.0
3.10	375	4.0
3.30	400	3.0
3.50	420	3.0
3.65	435	2.5

Remarks

Specimen magnetized in 3,000 oersted.

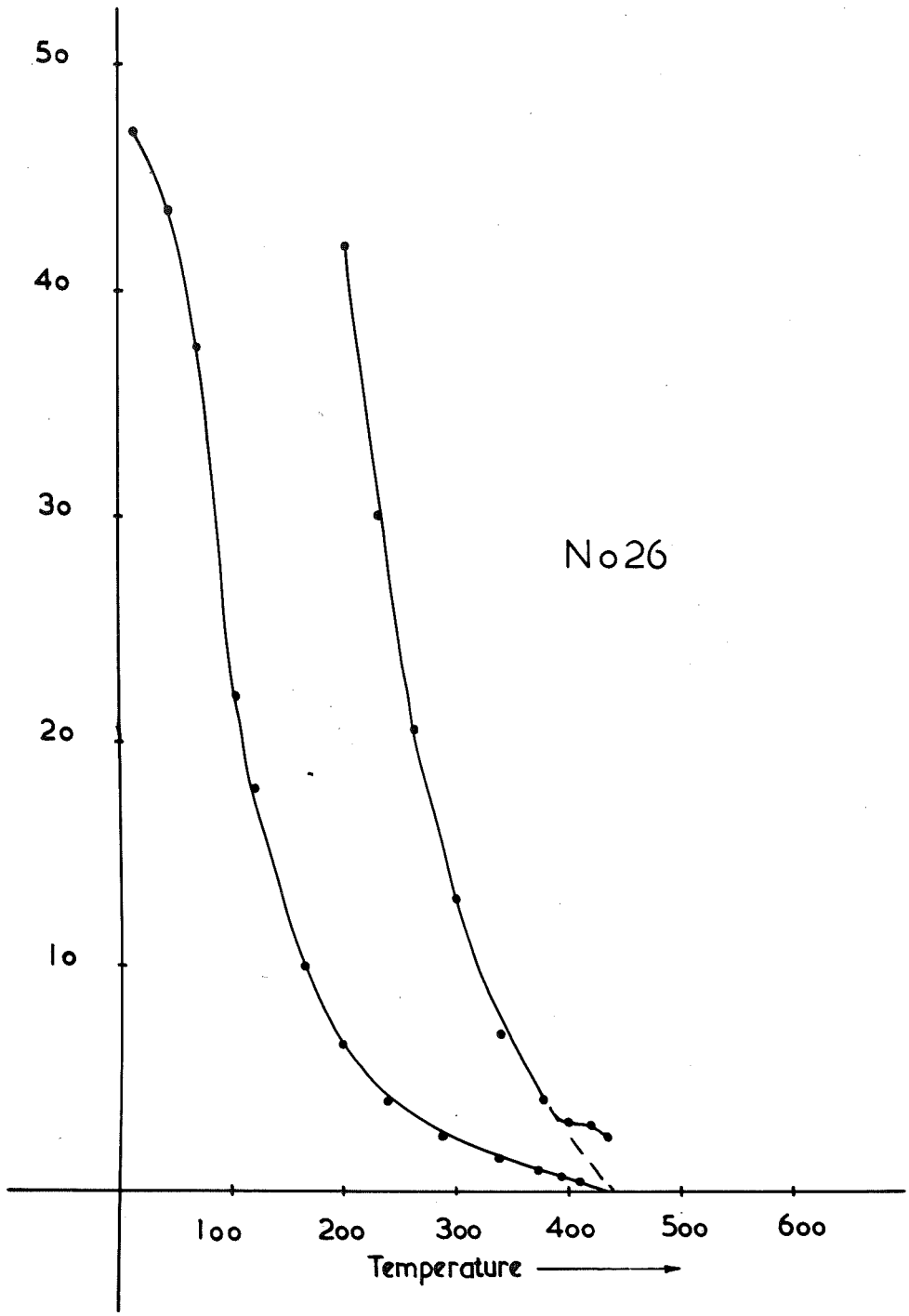

Figure.128.

APPENDIX 6

SPECIMEN		DIRECTION OF MAGNETIZATION RELATIVE TO HORIZONTAL		DIRECTION OF MAGNETIZATION RELATIVE TO BEDDING	
		D (M.N.)	I	D (M.N.)	I
TH 2	a	271	-20	270	-3
	b	264	-23	264	-3
	c	259	-4	259	-23
	d	271	-18	270	-1
	e	269	-22	268	-4
TH 3	a	17	76	82	40
	b	55	70	86	29
	c	96	52	99	4
	d	82	54	90	6
	e	54	76	89	32
TH 5	a	-79	8	-76	28
	b	-62	38	-45	54
	c	-57	7	-53	24
	d	-4	39	14	37
	e	-80	39	-74	60
M 5	d	54	66	91	-7
	a	32	84	102	1
	c	50	65	90	-6

(contd.).

Appendix 6 Page 2.

SPECIMEN	DIRECTION OF MAGNETIZATION RELATIVE TO HORIZONTAL		DIRECTION OF MAGNETIZATION RELATIVE TO BEDDING	
	D (M.N.)	I	D (M.N.)	I
M 6 d	107	50	107	-39
e	31	22	356	-30
c	74	14	44	-50
b	85	24	78	-54
a	14	16	36	7
M 7 a	164	-9	185	34
b	172	-2	195	27
c	166	-3	192	32
d	178	-6	192	22
e	157	25	230	38
M 8 a	22	-16	23	-34
b	28	-32	30	-50
e	287	-86	212	-74
c	101	-63	136	-71
d	102	-52	122	-52
M 9 d	130	18	120	36
c	132	14	126	30
b	75	50	53	46
a	83	61	50	56
M 10 a	142	28	131	30
b	80	52	67	28
c	84	64	63	42
d	62	8	60	-18
e	108	4	108	-6

(contd.)

Appendix 6. Page 3

SPECIMEN		DIRECTION OF MAGNETIZATION RELATIVE TO HORIZONTAL		DIRECTION OF MAGNETIZATION RELATIVE TO BEDDING	
		D (M.N.)	I	D (M.N.)	I
M 11	e	208	46	178	57
	d	208	38	185	50
	c	229	18	223	39
	b	201	20	190	31
	a	215	5	210	23
M 12	a	242	57	219	72
	b	237	40	222	55
	c	219	57	186	65
	d	234	45	217	60
M 13	d	170	-27	181	-24
	a	172	-29	176	-28
	b	187	-46	206	-35
	c	178	-53	204	-42

REFERENCES

1. AKIMOTO, S. (1957), Advances in Physics, 6, 23, 288.
2. AKIMOTO, S. (1951), Journal of Geomag. Geoelect., 3, 47.
3. AKIMOTO, S., KATSURA, T. and YOSHIDA, M., (1957), Journal of Geomag. Geoelect., 9, 165.
4. AKIMOTO, S. (1954), Journal of Geomag. Geoelect., 10, 69.
5. AKIMOTO, S. and KATSURA, T., (1958), Journal of Geomag. Geoelect., 10, 69.
6. BLACKETT, P.M.S. (1952), Phil.Trans., A, 245, 303.
7. CHAPMAN and BARTELS, (1940), Geomagnetism.
8. COLLINSON, D.W. et al. (1957), Phil.Trans., A, 250, 71.
9. CHEVALLIER, R. and PIERRE, J. (1932), Annals de Physic, 10, 18, 383.
10. CREER, K.M., (1954), Thesis.
11. FISHER, R.A., (1953), Proc.Roy.Soc., A, 217, 295.
12. GOTTSCHALK, V.H. (1953), Physics 6, 27.
13. GORTER, E.W., and SCHULKES, J.A., (1953), Phys.Rev., 90, 487.
14. HENRY, N.F.M., LIPSON, H. and WOOSTER, W.A., (1953), The Interpretation of X-ray diffraction photographs.
15. IRVING, E. and GREEN, R. (1957), Monthly Notices of the Royal Astronomical Society, Geophysical Supplement, 7, 6.
16. IRVING, E. et al. (1961), Phil.Mag., 6, 62, 225.
17. IRVING, E. et al. (1961), Journal of Geophysical Research, 66, 6, 1927.
18. KHAN, M.A. (1960), Geophysical Journal, 3, 45.
19. MAHONEY, D.J. (1931), Proc.Roy.Soc. Victoria, N.S., 43, 2, 123.
20. NEEL, L. (1955), Phil.Mag.Supplement, 4, 191.

References (contd.)

21. NAGATA, T., (1956), Rock Magnetism.

22. NICHOLS, G.D., (1955), Phil.Mag.Supplement, 4, 14, 113.

23. POUILLARD, E., (1950), Annals de Chemie, 5, 164.

24. PARRY, L.G., (1960), Journal of Geophysical Research, 65, 8, 24, 25.

25. STACEY, F.D., (1958), Phil.Mag., 3, 36, 1391.

26. STACEY, F.D., (1959), Journal of Scientific Instruments, 36, 355.

27. STACEY, F.D., (1959), Phil.Mag., 4, 41, 594.

28. UYEDA, S., (1958), Japanese Journal of Geophysics, 2,1,1.